

AD-A190 615

EFFECT OF FREESTREAM TURBULENCE ON A TWO DIMENSIONAL
CASCADE WITH DIFFER. (U) AIR FORCE INST OF TECH
WRIGHT-PATTERSON AFB OH SCHOOL OF ENGI.. S AD5AR

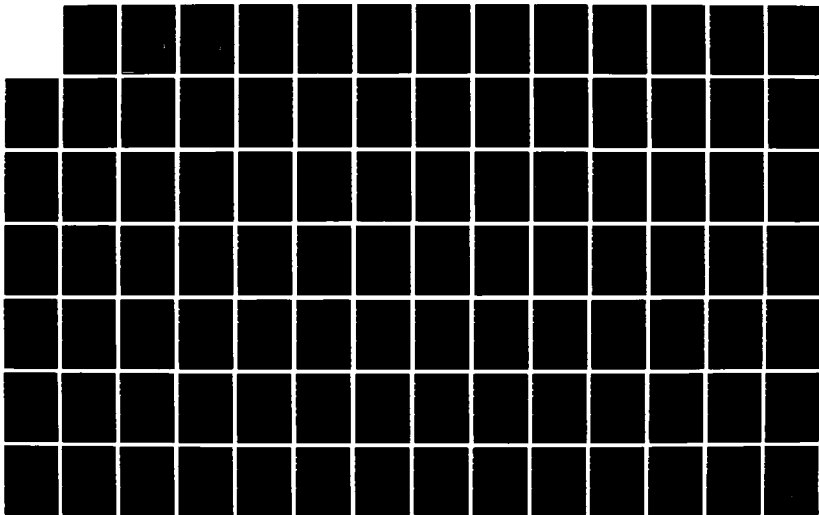
1/3

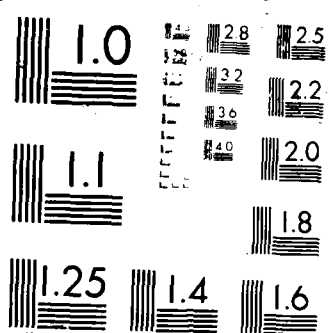
UNCLASSIFIED

MAR 88 AFIT/GAE/AA/88M-1

F/B 28/4

NL





AD-A190 615



DTIC FILE COPY

1

EFFECT OF FREESTREAM TURBULENCE ON
A TWO DIMENSIONAL CASCADE, WITH
DIFFERENT SURFACE ROUGHNESS, AT
HIGH REYNOLDS NUMBER

THESIS

SQN.LDR. (MAJ.) Salman Absar
Pakistan Air Force
AFIT/GAE/AA/88M-1

DTIC
ELECTE
MAR 3 1 1988
S
D

DISTRIBUTION STATEMENT A

Approved for public release
Distribution Unlimited

DEPARTMENT OF THE AIR FORCE

AIR UNIVERSITY

AIR FORCE INSTITUTE OF TECHNOLOGY

Wright-Patterson Air Force Base, Ohio

88 3 30 061

①

SQN.LDR. (MAJ.) Salman Absar
Pakistan Air Force
AFIT/GAE/AA/88M-1

DTIC
ELEC
MAR 31 1988
S
P

[illegible]

DTIC
COPY
UNRECEIVED
2

AFIT/GAE/AA/88M-1

EFFECT OF FREESTREAM TURBULENCE ON
A TWO DIMENSIONAL CASCADE, WITH DIFFERENT
SURFACE ROUGHNESS, AT HIGH REYNOLDS NUMBER

THESIS

Presented to the Faculty of the School of Engineering
of the Air Force Institute of Technology

Air University

In Partial Fulfillment of the
Requirement for the degree of
Master of Science in Aeronautical Engineering

SQN.LDR (MAJ.) Salman Absar

Pakistan Air Force

March 1988

Approved for public release; distribution unlimited

ACKNOWLEDGEMENT

Having almost completed my work, here at AFIT, I welcome this opportunity to reflect back and thank everyone who made it possible. I am grateful to God Almighty for giving me the opportunity, my teachers and my parents for contributing to my knowledge.

A very special thank you to Dr. William C. Elrod who guided me at every step, for whom no time was inappropriate and no questions irrelevant or insignificant. My thanks to lab supervisor Nick Yardich and his staff for giving constant support and enduring patiently, the noise of long test runs.

Finally, I would like to thank my wife whose support and constant encouragement kept me going through the many long hours.

Salman Absar

CONTENTS

Acknowledgement.....	ii
List of Figures.....	v
List of Tables.....	xviii
List of Symbols.....	xix
Abstract.....	xxii
I. Introduction.....	1
Objectives and Scope.....	2
II. Theory.....	4
Turbulence Intensity.....	4
Blade Surface Roughness.....	5
Pressure Loss Coefficient and Efficiency.....	5
Wake Velocity Profile.....	6
Boundary Layer.....	8
Blade Pressure Profile.....	11
III. Experimental Apparatus.....	12
Cascade Test Facility.....	12
Turbulence Generation System.....	12
Test Section.....	14
Boundary Layer Control.....	17
Instrumentation.....	17
Traversing Mechanism.....	19
Blade Roughness Configuration.....	22
Suction Surface Pressure Measurement.....	22
Data Acquisition and Analysis System.....	24
IV. Experimentation and Data Reduction.....	25
Turbulence Generation.....	26
Wake Study.....	26
Velocity Correction.....	30
Pressure Loss Coefficient.....	31
Blade Pressure Profile.....	31
Boundary Layer Study.....	32
V. Results and Discussion.....	34
Wake Survey.....	34
Suction Surface Pressure Distribution.....	47
Boundary Layer Study.....	51

VI. Conclusions and Recommendations.....	65
Conclusions.....	65
Recommendations.....	66
Appendix A: Component Listings.....	68
Appendix B: Hot Film Anemometer Calibration.....	69
Appendix C: Wake Survey Conf.#1.....	71
Appendix D: Wake Survey Conf.#2.....	80
Appendix E: Wake Survey Conf.#3.....	89
Appendix F: Boundary Layer Survey Conf.#1.....	98
Appendix G: Boundary Layer Survey Conf.#2.....	149
Appendix H: Boundary Layer Survey Conf.#3.....	202
Bibliography.....	255
Vita.....	257

List of Figures

<u>Figure</u>	<u>Page</u>
1. Schematic Representation of Boundary Layer and Wake Development.....	7
2. Matching Channel and Boundary Layer Profiles.....	9
3. General Schematic of the AFIT Cascade Test Facility....	13
4. Test Section.....	16
5. 'X' Wire Wake Probe Calibration Curve.....	20
6. Boundary Layer Probe Calibration Curve.....	21
7. Blade Profiles and Pressure Tap Arrangement.....	23
8. Turb. Intensity Center Blade L.E. Vicinity, with Turb. Generation.....	27
9. Turbulence Intensity with Turb. Generation.....	28
10. Representation of Wake and Boundary Layer Traverses....	29
11. Downstream Variation of Full Thickness Ratio Conf.#1...	35
12. Downstream Variation of Full Thickness Ratio Conf.#2...	36
13. Downstream Variation of Full Thickness Ratio Conf.#3...	37
14. Wake Velocity Recovery Conf.#1.....	39
15. Wake Velocity Recovery Conf.#2.....	40
16. Wake Velocity Recovery Conf.#2.....	41
17. Change in the Total Pressure Loss Coefficient Conf.#1..	44
18. Change in the Total Pressure Loss Coefficient Conf.#2..	45
19. Change in the Total Pressure Loss Coefficient Conf.#3..	46
20. Pressure Profile, Conf.#1, $Ra = 0.45$ micrometers.....	48
21. Pressure Profile, Conf.#2, $Ra = 12.10$ micrometers.....	49

22.	Pressure Profile, Conf.#3, $Ra = 18.30$ micrometers.....	50
23.	Boundary Layer Growth Suction Surface Conf.#1.....	56
24.	Boundary Layer Growth Suction Surface Conf.#2.....	57
25.	Boundary Layer Growth Suction Surface Conf.#3.....	58
26.	Boundary Layer Edge Velocity Along the Suction Surface Conf.#1.....	60
27.	Boundary Layer Edge Velocity Along the Suction Surface Conf.#2.....	61
28.	Boundary Layer Edge Velocity Along the Suction Surface Conf.#3.....	62
29.	Wake Velocity and Turbulence Intensity Profiles, Conf.#1, $x/c = 0.625$ (Low Turbulence).....	72
30.	Wake Velocity and Turbulence Intensity Profiles, Conf.#1, $x/c = 1.125$ (Low Turbulence).....	73
31.	Wake Velocity and Turbulence Intensity Profiles, Conf.#1, $x/c = 1.625$ (Low Turbulence).....	74
32.	Wake Velocity and Turbulence Intensity Profiles, Conf.#1, $x/c = 2.125$ (Low Turbulence).....	75
33.	Wake Velocity and Turbulence Intensity Profiles, Conf.#1, $x/c = 0.625$ (High Turbulence).....	76
34.	Wake Velocity and Turbulence Intensity Profiles, Conf.#1, $x/c = 1.125$ (High Turbulence).....	77
35.	Wake Velocity and Turbulence Intensity Profiles, Conf.#1, $x/c = 1.625$ (High Turbulence).....	78
36.	Wake Velocity and Turbulence Intensity Profiles, Conf.#1, $x/c = 2.125$ (High Turbulence).....	79
37.	Wake Velocity and Turbulence Intensity Profiles, Conf.#2, $x/c = 0.625$ (Low Turbulence).....	81
38.	Wake Velocity and Turbulence Intensity Profiles, Conf.#2, $x/c = 1.125$ (Low Turbulence).....	82

39.	Wake Velocity and Turbulence Intensity Profiles, Conf.#2, $x/c = 1.625$ (Low Turbulence).....	83
40.	Wake Velocity and Turbulence Intensity Profiles, Conf.#2, $x/c = 2.125$ (Low Turbulence).....	84
41.	Wake Velocity and Turbulence Intensity Profiles, Conf.#2, $x/c = 0.625$ (High Turbulence).....	85
42.	Wake Velocity and Turbulence Intensity Profiles, Conf.#2, $x/c = 1.125$ (High Turbulence).....	86
43.	Wake Velocity and Turbulence Intensity Profiles, Conf.#2, $x/c = 1.625$ (High Turbulence).....	87
44.	Wake Velocity and Turbulence Intensity Profiles, Conf.#2, $x/c = 2.125$ (High Turbulence).....	88
45.	Wake Velocity and Turbulence Intensity Profiles, Conf.#3, $x/c = 0.625$ (Low Turbulence).....	90
46.	Wake Velocity and Turbulence Intensity Profiles, Conf.#3, $x/c = 1.125$ (Low Turbulence).....	91
47.	Wake Velocity and Turbulence Intensity Profiles, Conf.#3, $x/c = 1.625$ (Low Turbulence).....	92
48.	Wake Velocity and Turbulence Intensity Profiles, Conf.#3, $x/c = 2.125$ (Low Turbulence).....	93
49.	Wake Velocity and Turbulence Intensity Profiles, Conf.#3, $x/c = 0.625$ (High Turbulence).....	94
50.	Wake Velocity and Turbulence Intensity Profiles, Conf.#3, $x/c = 1.125$ (High Turbulence).....	95
51.	Wake Velocity and Turbulence Intensity Profiles, Conf.#3, $x/c = 1.625$ (High Turbulence).....	96
52.	Wake Velocity and Turbulence Intensity Profiles, Conf.#3, $x/c = 2.125$ (High Turbulence).....	97
53.	Boundary Layer Velocity Profiles, Conf.#1 at 4.68% Chord (Low Turbulence).....	99
54.	Boundary Layer Turb. Intensity Profile Conf.#1 at 4.68% Chord (Low Turbulence).....	100

55.	Boundary Layer Velocity Profiles, Conf.#1 at 9.37%	
	Chord (Low Turbulence).....	101
56.	Boundary Layer Turb. Intensity Profiles Conf.#1 at 9.37%	
	Chord (Low Turbulence).....	102
57.	Boundary Layer Velocity Profiles, Conf.#1 at 25%	
	Chord (Low Turbulence).....	103
58.	Boundary Layer Turb. Intensity Profiles Conf.#1 at 25%	
	Chord (Low Turbulence).....	104
59.	Boundary Layer Velocity Profiles, Conf.#1 at 29.68%	
	Chord (Low Turbulence).....	105
60.	Boundary Layer Turb. Intensity Profiles Conf.#1 at 29.68%	
	Chord (Low Turbulence).....	106
61.	Boundary Layer Velocity Profiles, Conf.#1 at 34.37%	
	Chord (Low Turbulence).....	107
62.	Boundary Layer Turb. Intensity Profiles Conf.#1 at 34.37%	
	Chord (Low Turbulence).....	108
63.	Boundary Layer Velocity Profiles, Conf.#1 at 40.62%	
	Chord (Low Turbulence).....	109
64.	Boundary Layer Turb. Intensity Profiles Conf.#1 at 40.62%	
	Chord (Low Turbulence).....	110
65.	Boundary Layer Velocity Profiles, Conf.#1 at 45.31%	
	Chord (Low Turbulence).....	111
66.	Boundary Layer Turb. Intensity Profiles Conf.#1 at 45.31%	
	Chord (Low Turbulence).....	112
67.	Boundary Layer Velocity Profiles, Conf.#1 at 50%	
	Chord (Low Turbulence).....	113
68.	Boundary Layer Turb. Intensity Profiles Conf.#1 at 50%	
	Chord (Low Turbulence).....	114
69.	Boundary Layer Velocity Profiles, Conf.#1 at 65.62%	
	Chord (Low Turbulence).....	115
70.	Boundary Layer Turb. Intensity Profiles Conf.#1 at 65.62%	
	Chord (Low Turbulence).....	116

71.	Boundary Layer Velocity Profiles, Conf.#1 at 70.31% Chord (Low Turbulence).....	117
72.	Boundary Layer Turb. Intensity Profiles Conf.#1 at 70.31% Chord (Low Turbulence).....	118
73.	Boundary Layer Velocity Profiles, Conf.#1 at 75% Chord (Low Turbulence).....	119
74.	Boundary Layer Turb. Intensity Profiles Conf.#1 at 75% Chord (Low Turbulence).....	120
75.	Boundary Layer Velocity Profiles, Conf.#1 at 79.68% Chord (Low Turbulence).....	121
76.	Boundary Layer Turb. Intensity Profiles Conf.#1 at 79.68% Chord (Low Turbulence).....	122
77.	Boundary Layer Velocity Profiles, Conf.#1 at 84.37% Chord (Low Turbulence).....	123
78.	Boundary Layer Turb. Intensity Profiles Conf.#1 at 84.37% Chord (Low Turbulence).....	124
79.	Boundary Layer Velocity Profiles, Conf.#1 at 4.68% Chord (High Turbulence).....	125
80.	Boundary Layer Turb. Intensity Profiles Conf.#1 at 4.68% Chord (High Turbulence).....	126
81.	Boundary Layer Velocity Profiles, Conf.#1 at 9.37% Chord (High Turbulence).....	127
82.	Boundary Layer Turb. Intensity Profiles Conf.#1 at 9.37% Chord (High Turbulence).....	128
83.	Boundary Layer Velocity Profiles, Conf.#1 at 25% Chord (High Turbulence).....	129
84.	Boundary Layer Turb. Intensity Profiles Conf.#1 at 25% Chord (High Turbulence).....	130
85.	Boundary Layer Velocity Profiles, Conf.#1 at 29.68% Chord (High Turbulence).....	131
86.	Boundary Layer Turb. Intensity Profiles Conf.#1 at 29.68% Chord (High Turbulence).....	132

87.	Boundary Layer Velocity Profiles, Conf.#1 at 34.37%	
	Chord (High Turbulence).....	133
88.	Boundary Layer Turb. Intensity Profiles Conf.#1 at 34.37%	
	Chord (High Turbulence).....	134
89.	Boundary Layer Velocity Profiles, Conf.#1 at 40.62%	
	Chord (High Turbulence).....	135
90.	Boundary Layer Turb. Intensity Profiles Conf.#1 at 40.62%	
	Chord (High Turbulence).....	136
91.	Boundary Layer Velocity Profiles, Conf.#1 at 45.31%	
	Chord (High Turbulence).....	137
92.	Boundary Layer Turb. Intensity Profiles Conf.#1 at 45.31%	
	Chord (High Turbulence).....	138
93.	Boundary Layer Velocity Profiles, Conf.#1 at 50%	
	Chord (High Turbulence).....	139
94.	Boundary Layer Turb. Intensity Profiles Conf.#1 at 50%	
	Chord (High Turbulence).....	140
95.	Boundary Layer Velocity Profiles, Conf.#1 at 65.62%	
	Chord (High Turbulence).....	141
96.	Boundary Layer Turb. Intensity Profiles Conf.#1 at 65.62%	
	Chord (High Turbulence).....	142
97.	Boundary Layer Velocity Profiles, Conf.#1 at 70.31%	
	Chord (High Turbulence).....	143
98.	Boundary Layer Turb. Intensity Profiles Conf.#1 at 70.31%	
	Chord (High Turbulence).....	144
99.	Boundary Layer Velocity Profiles, Conf.#1 at 75%	
	Chord (High Turbulence).....	145
100.	Boundary Layer Turb. Intensity Profiles Conf.#1 at 75%	
	Chord (High Turbulence).....	146
101.	Boundary Layer Velocity Profiles, Conf.#1 at 79.68%	
	Chord (High Turbulence).....	147

102.	Boundary Layer Turb. Intensity Profiles Conf.#1 at 79.68% Chord (High Turbulence).....	148
103.	Boundary Layer Velocity Profiles, Conf.#2 at 4.68% Chord (Low Turbulence).....	150
104.	Boundary Layer Turb. Intensity Profiles Conf.#2 at 4.68% Chord (Low Turbulence).....	151
105.	Boundary Layer Velocity Profiles, Conf.#2 at 9.37% Chord (Low Turbulence).....	152
106.	Boundary Layer Turb. Intensity Profiles Conf.#2 at 9.37% Chord (Low Turbulence).....	153
107.	Boundary Layer Velocity Profiles, Conf.#2 at 25% Chord (Low Turbulence).....	154
108.	Boundary Layer Turb. Intensity Profiles Conf.#2 at 25% Chord (Low Turbulence).....	155
109.	Boundary Layer Velocity Profiles, Conf.#2 at 29.68% Chord (Low Turbulence).....	156
110.	Boundary Layer Turb. Intensity Profiles Conf.#2 at 29.68% Chord (Low Turbulence).....	157
111.	Boundary Layer Velocity Profiles, Conf.#2 at 34.37% Chord (Low Turbulence).....	158
112.	Boundary Layer Turb. Intensity Profiles Conf.#2 at 34.37% Chord (Low Turbulence).....	159
113.	Boundary Layer Velocity Profiles, Conf.#2 at 40.62% Chord (Low Turbulence).....	160
114.	Boundary Layer Turb. Intensity Profiles Conf.#2 at 40.62% Chord (Low Turbulence).....	161
115.	Boundary Layer Velocity Profiles, Conf.#2 at 45.31% Chord (Low Turbulence).....	162
116.	Boundary Layer Turb. Intensity Profiles Conf.#2 at 45.31% Chord (Low Turbulence).....	163

117.	Boundary Layer Velocity Profiles, Conf.#2 at 50%	
	Chord (Low Turbulence).....	164
118.	Boundary Layer Turb. Intensity Profiles Conf.#2 at 50%	
	Chord (Low Turbulence).....	165
119.	Boundary Layer Velocity Profiles, Conf.#2 at 65.62%	
	Chord (Low Turbulence).....	166
120.	Boundary Layer Turb. Intensity Profiles Conf.#2 at 65.62%	
	Chord (Low Turbulence).....	167
121.	Boundary Layer Velocity Profiles, Conf.#2 at 70.31%	
	Chord (Low Turbulence).....	168
122.	Boundary Layer Turb. Intensity Profiles Conf.#2 at 70.31%	
	Chord (Low Turbulence).....	169
123.	Boundary Layer Velocity Profiles, Conf.#2 at 75%	
	Chord (Low Turbulence).....	170
124.	Boundary Layer Turb. Intensity Profiles Conf.#2 at 75%	
	Chord (Low Turbulence).....	171
125.	Boundary Layer Velocity Profiles, Conf.#2 at 79.68%	
	Chord (Low Turbulence).....	172
126.	Boundary Layer Turb. Intensity Profiles Conf.#2 at 79.68%	
	Chord (Low Turbulence).....	173
127.	Boundary Layer Velocity Profiles, Conf.#2 at 84.37%	
	Chord (Low Turbulence).....	174
128.	Boundary Layer Turb. Intensity Profiles Conf.#2 at 84.37%	
	Chord (Low Turbulence).....	175
129.	Boundary Layer Velocity Profiles, Conf.#2 at 4.68%	
	Chord (High Turbulence).....	176
130.	Boundary Layer Turb. Intensity Profiles Conf.#2 at 4.68%	
	Chord (High Turbulence).....	177
131.	Boundary Layer Velocity Profiles, Conf.#2 at 9.37%	
	Chord (High Turbulence).....	178

132.	Boundary Layer Turb. Intensity Profiles Conf.#2 at 9.37%	
	Chord (High Turbulence).....	179
133.	Boundary Layer Velocity Profiles, Conf.#2 at 25%	
	Chord (High Turbulence).....	180
134.	Boundary Layer Turb. Intensity Profiles Conf.#2 at 25%	
	Chord (High Turbulence).....	181
135.	Boundary Layer Velocity Profiles, Conf.#2 at 29.68%	
	Chord (High Turbulence).....	182
136.	Boundary Layer Turb. Intensity Profiles Conf.#2 at 29.68%	
	Chord (High Turbulence).....	183
137.	Boundary Layer Velocity Profiles, Conf.#2 at 34.37%	
	Chord (High Turbulence).....	184
138.	Boundary Layer Turb. Intensity Profiles Conf.#2 at 34.37%	
	Chord (High Turbulence).....	185
139.	Boundary Layer Velocity Profiles, Conf.#2 at 40.62%	
	Chord (High Turbulence).....	186
140.	Boundary Layer Turb. Intensity Profiles Conf.#2 at 40.62%	
	Chord (High Turbulence).....	187
141.	Boundary Layer Velocity Profiles, Conf.#2 at 45.31%	
	Chord (High Turbulence).....	188
142.	Boundary Layer Turb. Intensity Profiles Conf.#2 at 45.31%	
	Chord (High Turbulence).....	189
143.	Boundary Layer Velocity Profiles, Conf.#2 at 50%	
	Chord (High Turbulence).....	190
144.	Boundary Layer Turb. Intensity Profiles Conf.#2 at 50%	
	Chord (High Turbulence).....	191
145.	Boundary Layer Velocity Profiles, Conf.#2 at 65.62%	
	Chord (High Turbulence).....	192
146.	Boundary Layer Turb. Intensity Profiles Conf.#2 at 65.62%	
	Chord (High Turbulence).....	193

147.	Boundary Layer Velocity Profiles, Conf.#2 at 70.31% Chord (High Turbulence).....	194
148.	Boundary Layer Turb. Intensity Profiles Conf.#2 at 70.31% Chord (High Turbulence).....	195
149.	Boundary Layer Velocity Profiles, Conf.#2 at 75% Chord (High Turbulence).....	196
150.	Boundary Layer Turb. Intensity Profiles Conf.#2 at 75% Chord (High Turbulence).....	197
151.	Boundary Layer Velocity Profiles, Conf.#2 at 79.68% Chord (High Turbulence).....	198
152.	Boundary Layer Turb. Intensity Profiles Conf.#2 at 79.68% Chord (High Turbulence).....	199
153.	Boundary Layer Velocity Profiles, Conf.#2 at 84.37% Chord (High Turbulence).....	200
154.	Boundary Layer Turb. Intensity Profiles Conf.#2 at 84.37% Chord (High Turbulence).....	201
155.	Boundary Layer Velocity Profiles, Conf.#3 at 4.68% Chord (Low Turbulence).....	203
156.	Boundary Layer Turb. Intensity Profiles Conf.#3 at 4.68% Chord (Low Turbulence).....	204
157.	Boundary Layer Velocity Profiles, Conf.#3 at 9.37% Chord (Low Turbulence).....	205
158.	Boundary Layer Turb. Intensity Profiles Conf.#3 at 9.37% Chord (Low Turbulence).....	206
159.	Boundary Layer Velocity Profiles, Conf.#3 at 25% Chord (Low Turbulence).....	207
160.	Boundary Layer Turb. Intensity Profiles Conf.#3 at 25% Chord (Low Turbulence).....	208
161.	Boundary Layer Velocity Profiles, Conf.#3 at 29.68% Chord (Low Turbulence).....	209
162.	Boundary Layer Turb. Intensity Profiles Conf.#3 at 29.68% Chord (Low Turbulence).....	210

163.	Boundary Layer Velocity Profiles, Conf.#3 at 34.37%	
	Chord (Low Turbulence).....	211
164.	Boundary Layer Turb. Intensity Profiles Conf.#3 at 34.37%	
	Chord (Low Turbulence).....	212
165.	Boundary Layer Velocity Profiles, Conf.#3 at 40.62%	
	Chord (Low Turbulence).....	213
166.	Boundary Layer Turb. Intensity Profiles Conf.#3 at 40.62%	
	Chord (Low Turbulence).....	214
167.	Boundary Layer Velocity Profiles, Conf.#3 at 45.31%	
	Chord (Low Turbulence).....	215
168.	Boundary Layer Turb. Intensity Profiles Conf.#3 at 45.31%	
	Chord (Low Turbulence).....	216
169.	Boundary Layer Velocity Profiles, Conf.#3 at 50%	
	Chord (Low Turbulence).....	217
170.	Boundary Layer Turb. Intensity Profiles Conf.#3 at 50%	
	Chord (Low Turbulence).....	218
171.	Boundary Layer Velocity Profiles, Conf.#3 at 65.62%	
	Chord (Low Turbulence).....	219
172.	Boundary Layer Turb. Intensity Profiles Conf.#3 at 65.62%	
	Chord (Low Turbulence).....	220
173.	Boundary Layer Velocity Profiles, Conf.#3 at 70.31%	
	Chord (Low Turbulence).....	221
174.	Boundary Layer Turb. Intensity Profiles Conf.#3 at 70.31%	
	Chord (Low Turbulence).....	222
175.	Boundary Layer Velocity Profiles, Conf.#3 at 75%	
	Chord (Low Turbulence).....	223
176.	Boundary Layer Turb. Intensity Profiles Conf.#3 at 75%	
	Chord (Low Turbulence).....	224
177.	Boundary Layer Velocity Profiles, Conf.#3 at 79.68%	
	Chord (Low Turbulence).....	225

178.	Boundary Layer Turb. Intensity Profiles Conf.#3 at 79.68% Chord (Low Turbulence).....	226
179.	Boundary Layer Velocity Profiles, Conf.#3 at 84.37% Chord (Low Turbulence).....	227
180.	Boundary Layer Turb. Intensity Profiles Conf.#3 at 84.37% Chord (Low Turbulence).....	228
181.	Boundary Layer Velocity Profiles, Conf.#3 at 4.68% Chord (High Turbulence).....	229
182.	Boundary Layer Turb. Intensity Profiles Conf.#3 at 4.68% Chord (High Turbulence).....	230
183.	Boundary Layer Velocity Profiles, Conf.#3 at 9.37% Chord (High Turbulence).....	231
184.	Boundary Layer Turb. Intensity Profiles Conf.#3 at 9.37% Chord (High Turbulence).....	232
185.	Boundary Layer Velocity Profiles, Conf.#3 at 25% Chord (High Turbulence).....	233
186.	Boundary Layer Turb. Intensity Profiles Conf.#3 at 25% Chord (High Turbulence).....	234
187.	Boundary Layer Velocity Profiles, Conf.#3 at 29.68% Chord (High Turbulence).....	235
188.	Boundary Layer Turb. Intensity Profiles Conf.#3 at 29.68% Chord (High Turbulence).....	236
189.	Boundary Layer Velocity Profiles, Conf.#3 at 34.37% Chord (High Turbulence).....	237
190.	Boundary Layer Turb. Intensity Profiles Conf.#3 at 34.37% Chord (High Turbulence).....	238
191.	Boundary Layer Velocity Profiles, Conf.#3 at 40.62% Chord (High Turbulence).....	239
192.	Boundary Layer Turb. Intensity Profiles Conf.#3 at 40.62% Chord (High Turbulence).....	240
193.	Boundary Layer Velocity Profiles, Conf.#3 at 45.31% Chord (High Turbulence).....	241

194.	Boundary Layer Turb. Intensity Profiles Conf.#3 at 45.31% Chord (High Turbulence).....	242
195.	Boundary Layer Velocity Profiles, Conf.#3 at 50% Chord (High Turbulence).....	243
196.	Boundary Layer Turb. Intensity Profiles Conf.#3 at 50% Chord (High Turbulence).....	244
197.	Boundary Layer Velocity Profiles, Conf.#3 at 65.62% Chord (High Turbulence).....	245
198.	Boundary Layer Turb. Intensity Profiles Conf.#3 at 65.62% Chord (High Turbulence).....	246
199.	Boundary Layer Velocity Profiles, Conf.#3 at 70.31% Chord (High Turbulence).....	247
200.	Boundary Layer Turb. Intensity Profiles Conf.#3 at 70.31% Chord (High Turbulence).....	248
201.	Boundary Layer Velocity Profiles, Conf.#3 at 75% Chord (High Turbulence).....	249
202.	Boundary Layer Turb. Intensity Profiles Conf.#3 at 75% Chord (High Turbulence).....	250
203.	Boundary Layer Velocity Profiles, Conf.#3 at 79.68% Chord (High Turbulence).....	251
204.	Boundary Layer Turb. Intensity Profiles Conf.#3 at 79.68% Chord (High Turbulence).....	252
205.	Boundary Layer Velocity Profiles, Conf.#3 at 84.37% Chord (High Turbulence).....	253
206.	Boundary Layer Turb. Intensity Profiles Conf.#3 at 84.37% Chord (High Turbulence).....	254

List of Tables

<u>Table</u>	<u>Page</u>
I. Blade Roughness Configuration.....	22
II. Total Pressure Loss Coefficient.....	42
III. Boundary Layer Parameters With Low Freestream Turbulence.	53
IV. Boundary Layer Parameters With High Freestream Turbulence.	54

LIST OF SYMBOLS

<u>Symbol</u>	<u>Name</u>	<u>Units</u>
A	Area	in ²
c	Chord length	in
Cp	Pressure coefficient	
Eo	Anemometer voltage	volts
γ	Ratio of specific heats	
Ks	Equivalent sand roughness	micrometers
Kt	Thermal conductivity	BTU/sec-ft-°R
N	Number of data points	
Nu	Nusselt number	
P	Pressure	lbf/in ²
\bar{P}	Mass averaged pressure	lbf/in ²
ΔP	Change in pressure	lbf/in ²
Ra	Arithmetic average roughness	micrometers
Rc	Cable resistance	ohms
Re	Reynolds number	
Rw	Anemometer wire resistance	ohms
R3	Anemometer bridge resistance	ohms
T	Temperature	°R
Tm	Mean temperature	°R
Tw	Wire temperature	°R
Tu	Turbulence intensity	

<u>Symbol</u>	<u>Name</u>	<u>Units</u>
V	Velocity	ft/sec
δ	Thickness	in
w	Pressure loss coefficient	
ρ	Density	lbm/ft ³

SubscriptsName

BL	Boundary layer
e	Edge
inv	Inviscid
m	Measured
Min	Minimum
rms	Root mean square
t	Total
th	Theoretical
o	Freestream
1	inlet
2	exit

Acronyms

CTF	Cascade Test Facility
DC	Direct Current
HP	Hewlett Packard
NACA	National Advisory Committee on Aeronautics
RMS	Root Mean Square
TSI	Thermal Systems Incorporated

ABSTRACT

The present study shows the effects of high freestream turbulence on the performance of a two dimensional cascade. The cascade consisted of seven NACA 65-A506 airfoils with two inches chord. Experiments were carried out at flow Reynolds number per foot in excess of two and a half million. Flow turbulence intensity of 7% was generated upstream of the cascade. Blades with three different categories of surface roughness were studied.

High freestream turbulence results in a decrease in total pressure loss coefficient in the cascade and an increase in the total pressure loss coefficient in the wake. The results also show an increase in pressure coefficient, over the suction surface, independent of the amount of surface roughness. The boundary layer thickness, after 50% chord, increases substantially, with an increase in freestream turbulence. This effect is aggravated with higher surface roughness. The effects of high freestream turbulence on boundary layer edge velocity are sensitive to local surface roughness. With low surface roughness, the boundary layer edge velocity increase with freestream turbulence. The results indicate an opposite effect when local surface roughness is increased.

EFFECT OF FREESTREAM TURBULENCE ON A
TWO DIMENSIONAL CASCADE, WITH DIFFERENT
SURFACE ROUGHNESS, AT HIGH REYNOLDS NUMBER

I. INTRODUCTION

Present day economics have placed very strict requirements on efficiency of aircraft powerplants. As this efficiency is largely dependent on rotating parts, that is, compressors and turbines, these have to be studied and analyzed more carefully. The airflow through these is complex therefore difficult to simulate and analyze theoretically. Although---"major efforts over the last few years have tended to--- concentrate on generation of powerful analysis techniques for cascades, it is desirable to have a correlation between theoretical and experimental results" (1:259).

The cascade test facility already set up at the Air Force Institute of Technology has been used to collect data on cascades for various test conditions. However, the reliability of cascades in predicting performance of turbomachinery has been debatable. One of the methods of improving reliability of this data is to establish cascade inlet conditions as similar to a compressor as possible. It has been found that in a six stage compressor, the turbulence intensity varies from 2% to about 6% from the first to the sixth stage (2:255). It is therefore

considered necessary to create similar turbulence upstream of the cascade. This will not only give more realistic data but will also permit comparison of cascade performance with low and high freestream turbulence.

Objectives and scope: The objectives of this study are

1. To create sufficient turbulence intensity upstream of the cascade, so as to simulate compressor conditions.
2. To study the effect of this upstream turbulence on cascade performance.

The first aim is to have a physical disturbance in the flow path so as to result in the required turbulence. To study the effect of this turbulence, it is very important that no other flow parameter (e.g., mass flow, etc.) be changed.

The parameters required for comparison are

- (i) Pressure loss coefficient.
- (ii) Wake velocity and turbulence intensity profiles.
- (iii) Center blade boundary layer profile and its thickness.
- (iv) Pressure distribution over the center blade.

Variation of the above parameters was studied for a cascade with NACA 65-A506 aerofoils. Three different categories of surface roughness were used and data for each of these analyzed. This was done in a manner to assure repeatability in results and allow

determination of the effect of surface roughness on compressor blade performance in cascade.

II. THEORY

The independent variables for this compressor cascade investigation are freestream turbulence intensity and surface roughness. Variables upon which cascade flow performance is based are pressure loss coefficient, wake velocity profile, center blade suction surface boundary layer profile and thickness, and center blade suction surface pressure distribution.

Turbulence intensity: The degree of the turbulence or turbulence intensity in a flow is given by

$$Tu = V_{rms}/V_2 \quad (1)$$

where V_{rms} denotes the RMS and V_2 denotes the mean flow velocity. The RMS voltage output of an anemometer and its DC voltage are proportional to V_{rms} and V_2 respectively.

As predicted by Schlichting and Das, "it may be expected that in the lower range of Reynolds number ($Re < 2 \times 10^5$) the flow will be largely influenced by the turbulence of the freestream. This is in contrast to the flow about isolated aerofoils at high Reynolds number ($Re > 10^6$) where the turbulence, because of its large scale, does not play any part "(2:254). The Reynolds number at which the turbulence effect was studied in this investigation was $Re = 4.5 \times 10^5$ ($Re/ft. = 2.7 \times 10^6$).

Blade Surface Roughness: The blades used in this study were the same as used by Poulin (3:23). Roughness definition and its method of calculation has been described by Poulin, Williams and Tanis (3:90, 4:49, 5:54).

Pressure Loss Coefficient and Efficiency: Flow through a cascade, like flow through compressor and turbine blades, is very sensitive to irreversibility in the flow process. Irreversibility effects are due to blade friction, vortex formation and secondary losses. These cause a loss in the stage efficiency which is given as

Stage Efficiency = $1 - \frac{\Delta P / \frac{1}{2} \rho v_1^2}{\Delta P_{th} / \frac{1}{2} \rho v_1^2}$ (13:381) where ΔP is actual total pressure loss, ΔP_{th} is the theoretical pressure rise, v_1 is the inlet velocity and ρ is the density. The term $\Delta P / \frac{1}{2} \rho v_1^2$ is also called total pressure loss coefficient. This loss coefficient is also related to cycle efficiency (2:247). Therefore, the non dimensional total pressure loss coefficient w , across a two dimensional cascade, best describes the losses. It is defined by the equation

$$w = \frac{P_{t1} - \overline{P_{t2}}}{\frac{1}{2} \rho v_1^2} \quad (2)$$

where P_{t1} is the mass averaged total pressure at the cascade exit (from centerline of the flow adjacent to the blade). In order to calculate the mass averaged total pressure $\overline{P_{t2}}$, in the exit plane, the total pressure at each of the 133 measuring points is

calculated by

$$P_{t_2} = P \left[1 + \frac{v_2^2}{2C_p T_2} \right]^{\gamma-1/\gamma} \quad (3)$$

The mass averaged total pressure is calculated by the equation

$$\overline{P_{t_2}} = \frac{\int P_{t_2} \rho v_2 dA}{\int \rho v_2 dA} \quad (7:14) \quad (4)$$

Wake Velocity profile: The interaction of blade surfaces with the flow, forms boundary layers. These boundary layers join at the trailing edge to form a wake. "A mixing process takes place so that as we go downstream, a homogeneous flow field results after sufficient distance behind the cascade. This is shown in Fig. 1. The mixing process generates additional losses, which amount to about 20% of the total losses" (8:311, 315). In their analysis of a low speed two dimensional cascade, Lieblein and Roudebush state "Inasmuch as loss in the total pressure is involved in mixing process, the ultimate total pressure at a station far downstream where conditions become uniform will be less than at the blade trailing edge. The difference in total pressure far downstream and at the trailing edge is referred to as mixing loss. As the wake is reenergized downstream of the blade, the velocity profile in the wake changes. ----- The rate at which a blade wake is reenergized depends to some extent upon such additional factors as initial state of the wake, freestream turbulence level, Reynolds number and Mach number " (7:5, 6).

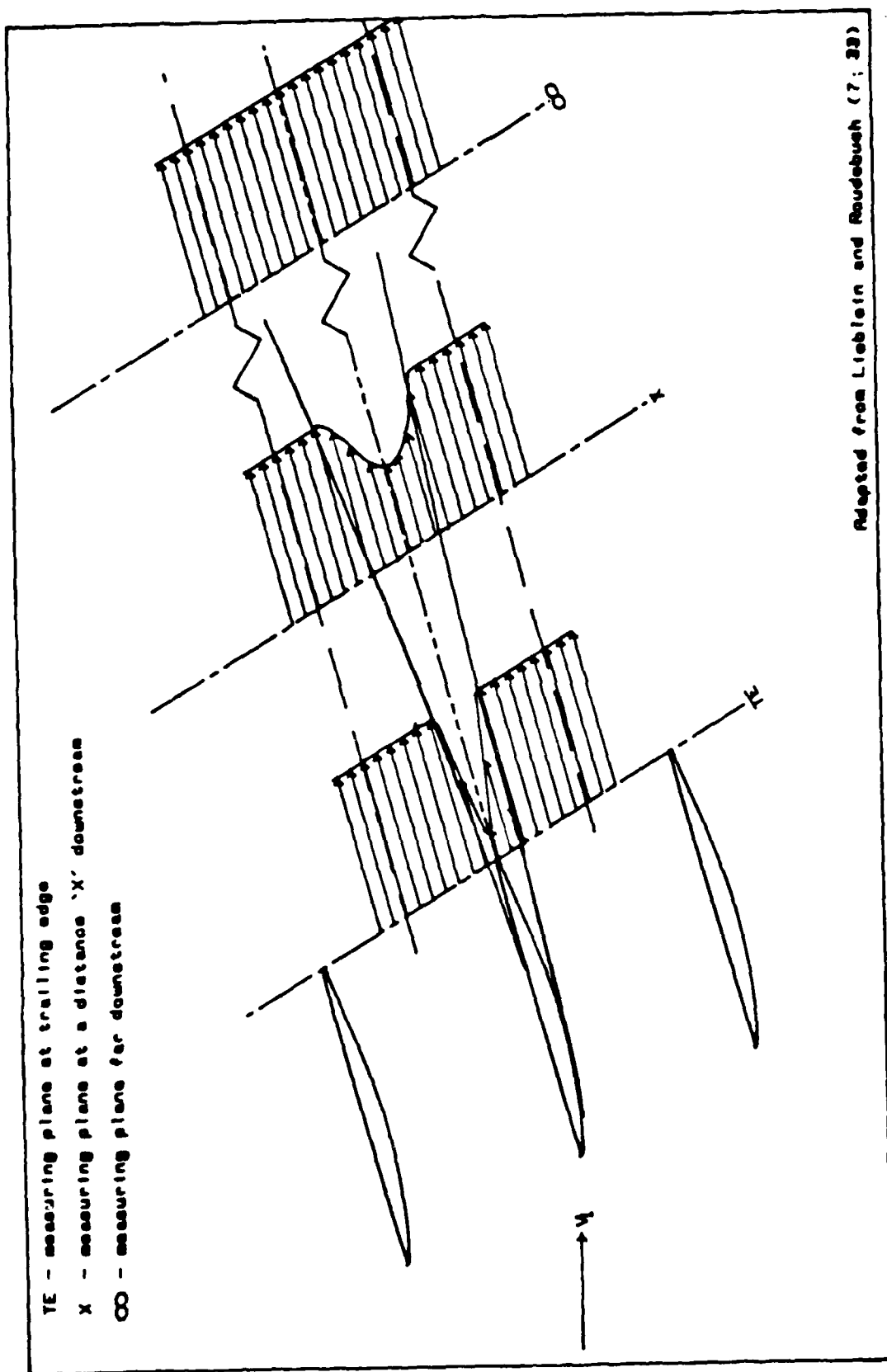


Fig. 1. Schematic Representation of Boundary Layer and Wake Development

From these remarks, it is obvious that rate of wake mixing is important in determining wake losses. The rate of wake mixing can be determined by two parameters

- (i) Change in the ratio of wake minimum velocity to freestream velocity, V_{min}/V_o at various positions along the wake flow. As determined by Lieblein and Roudebush (7:6-7) this ratio may be given by

$$V_{min}/V_o = 1 - a(x/c + b)^{-1/2} \quad (5)$$

where a and b are constants whose value have been experimentally found to be 0.13 and 0.025 respectively.

- (ii) Change in wake flow thickness, which is defined arbitrarily to be the width of the wake as established by the points where $V/V_o = 0.99$ (7:15). (V = velocity at any point in that plane and V_o is the freestream velocity in that plane)

Boundary Layer: The velocity boundary layer can be described in terms of viscous effects which produce a no slip condition at the surface. It is the layer within which the fluid velocity changes from zero at the surface to the freestream velocity. Its thickness therefore is the perpendicular distance from the surface to the point at which approximate freestream velocity is

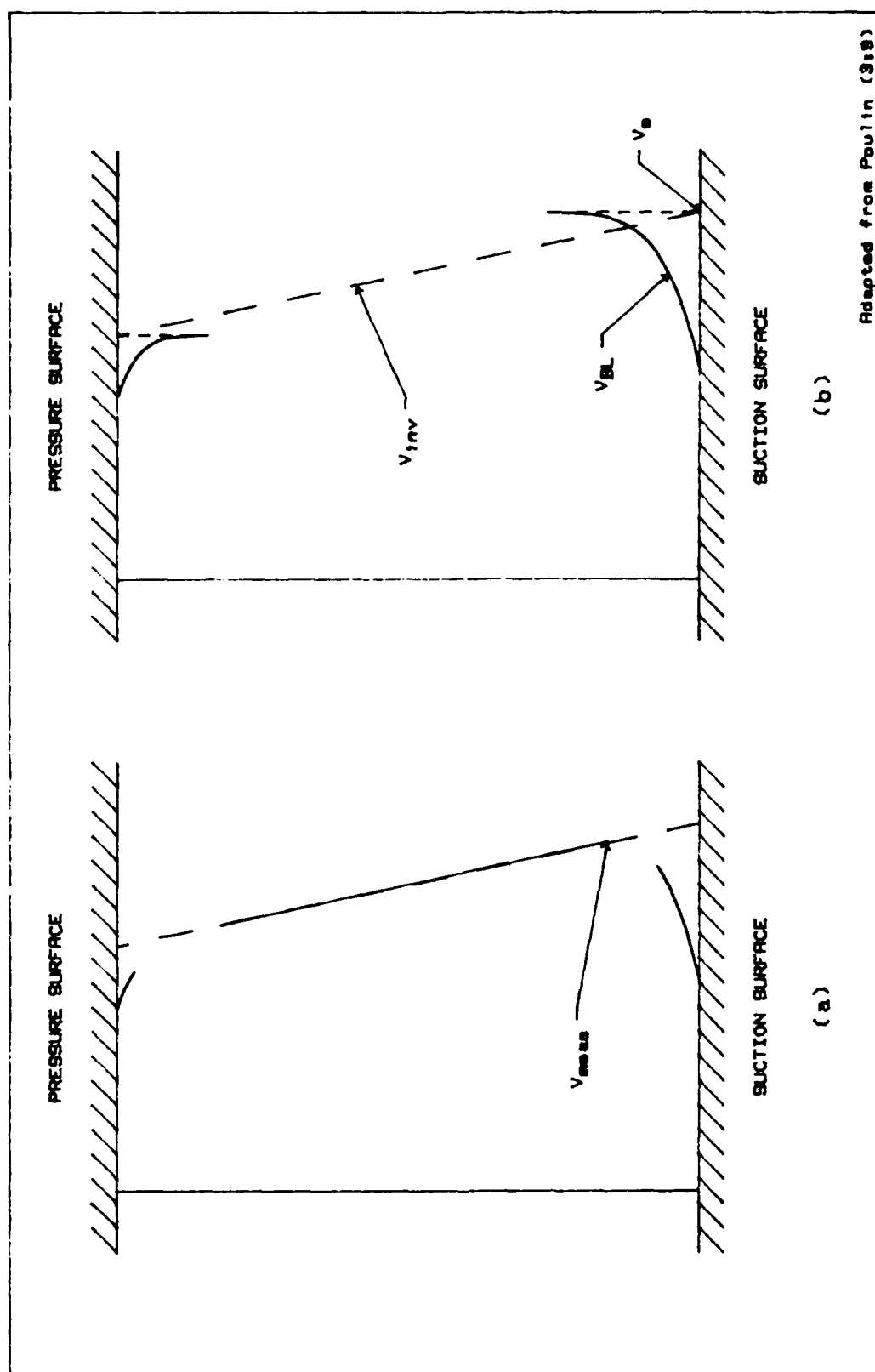


Fig. 2. Matching Channel and Boundary Layer Profiles

surface to the point at which approximate freestream velocity is attained. In a cascade, determination of boundary layer thickness and velocity over blade surface becomes difficult because of the influence of adjacent blades. "The normal pressure gradient that exists between the suction surface of one blade and pressure surface of the other creates a velocity profile as shown in Fig. 2(a). As a result, boundary layer edge velocity and thickness are difficult to determine" (3:4). To overcome this, Deutsch and Zierke (9:8) used the principle of composite matching, according to which the measured profile is a composite one, consisting of three regions: an inner region dominated by viscous effects, an inviscid region where normal pressure gradient acts, and a region in between the two, where inviscid / viscid flows interact. The measured velocity can therefore be written as

$$V_m = V_{BL} + V_{inv} - V_e \quad (6)$$

where V_m = measured velocity

V_{BL} = boundary layer velocity

V_{inv} = inviscid velocity

V_e = edge velocity

Also, the measured velocity at wall should go to zero. With no slip condition fluid flow, V_{BL} must be equal to zero. This means that V_{inv} at the wall equals V_e .

"An extrapolated quadratic curve was used by Deutsch and Zierke to fit a statistical number of points in the inviscid

region and to determine V_{inv} at the wall. The number of points included in the curve fit was determined by locating a range of points beyond the maximum velocity point where the calculated wall velocity was constant. $N/2 \pm N/4$ points provide the optimum curve fit, where N is the number of points from the maximum velocity position to the outer edge of the velocity profile" (4:21).

The same method with slight modification was used by Poulin (3:40). This was adopted to determine boundary layer velocity profile and boundary layer thickness. Fig. 2(b) shows the two distinct regions of composite velocity profile.

Blade Pressure profile: The pressure distribution over the blade suction surface is obtained by measuring static pressure at discrete points along the surface. This is then expressed in terms of a nondimensional pressure coefficient ' C_p '.

$$C_p = (P - P_1) / \frac{1}{2} \rho V_1^2 \quad (7)$$

where

P = Measured static pressure

P_1 = Inlet static pressure

ρ = Inlet density

V_1 = Inlet velocity

III. EXPERIMENTAL APPARATUS

Cascade Test Facility: This experimental investigation was conducted on the cascade test facility (CTF) located at the Air Force Institute of Technology, School of Engineering. A schematic diagram of the facility is shown in Fig. 3. It consists of a forty horsepower centrifugal blower with a discharge rating of 3000 cubic feet per minute at a flow pressure of 1.666 pounds per square inch (gauge). The air intake is ducted to take outside air at constant temperature. Recirculated room air can also be used if required. A series of screen wire and electrostatic air cleaners have been provided upstream of the blower. Air from the blower passing through a nine foot long diffuser, is directed into a stilling tank where, after being radially diffused, it passes through a filtering / flow straightening arrangement. The air exits the stilling tank and passes through a turbulence generating arrangement, which can be switched on / off as required. The air flow then enters a two by seven inch test section. At this point the flow has a Reynolds number per foot about two and a half million. Its turbulence intensity depending upon whether the turbulence generation is off or on, varies from less than 2% to approximately 7%. A detailed description of the CTF is given by Allison (10).

Turbulence Generation System: One of the main objectives of

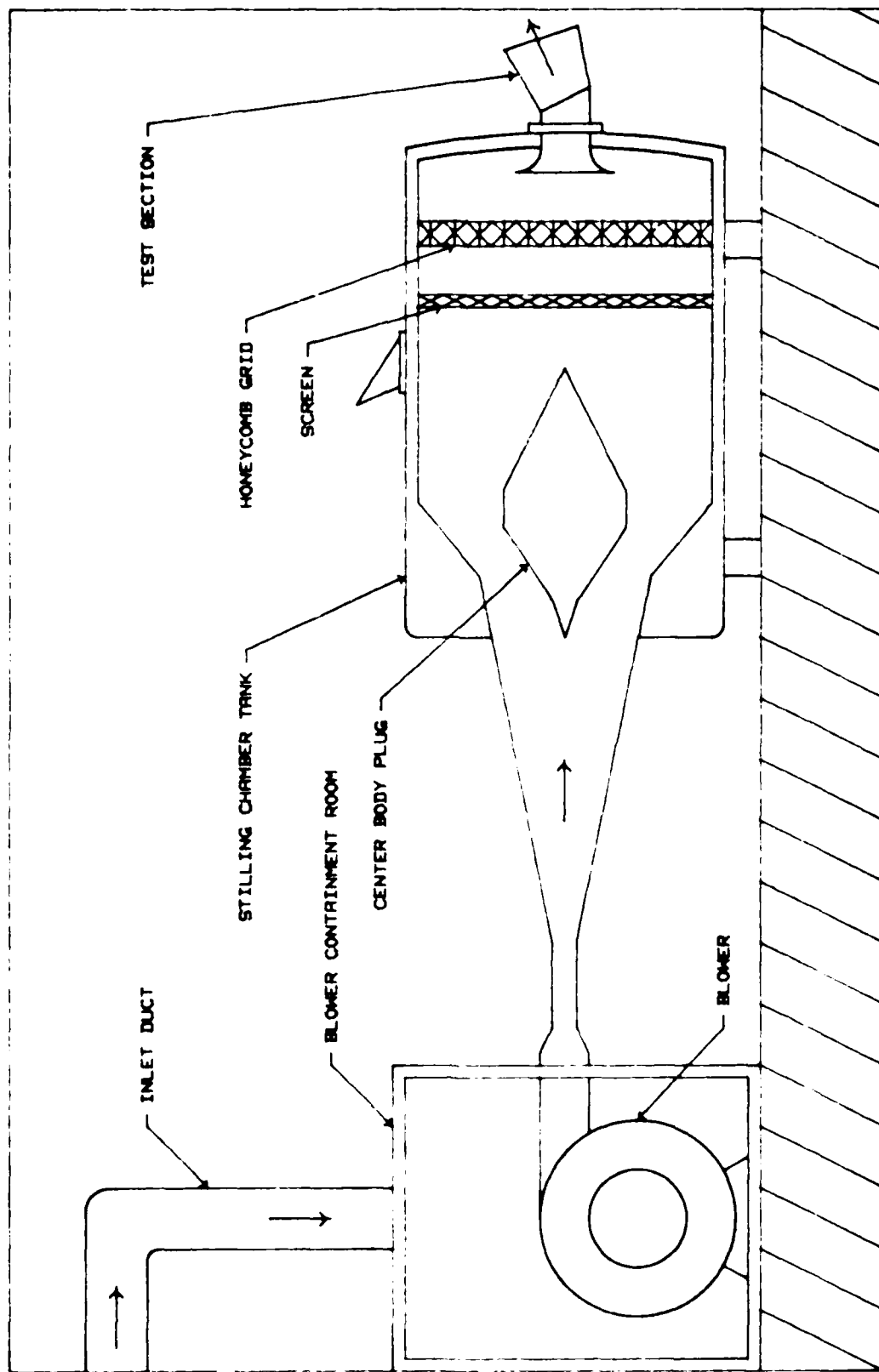


Fig. 3. General Schematic of the AFIT Cascade Test Facility

this investigation is to create turbulence intensity upstream of the cascade, similar to that observed in the last stages of an axial flow compressor. Also the compressor blade performance in a cascade is to be compared with and without this turbulence generation. It is therefore necessary to have a turbulence generation system which will not alter any other flow parameter. This is achieved by installing an aluminum plate $3/4$ inch thick, ahead of the test section. This plate has the same flow area as the test section. Sixteen $1/16$ inch holes have been drilled in the plate, perpendicular to the test section centerline, seven on each side and one each on top and bottom. These are interconnected through a manifold, which is also connected to four $1/4$ inch holes on the outside. These four holes are the air inlets connected to a source having 100 psi(g) pressure. The air is ducted from the source through a sufficiently large diameter pipe so as not to choke the flow. This secondary air is blown into the main air stream through the $1/16$ inch holes. The total pressure change in the main air flow, caused by this is less than 2%. It is however sufficient to cause turbulence intensity of the main flow to increase from less than 2% to about 7%. In this report, the turbulence intensity of the flow has been referred to as low and high turbulence, depending on the state of turbulence generation.

Test Section: The CTF test section is configured with seven

NACA 65-A506 aerofoils. According to Moe (11:5), the profile of these blades is similar to that found in the latter stages of a high pressure compressor. The blade setting is the same as used by Poulin (3:17). To simulate an infinite cascade, the outer blades are half imbedded in the test section wall. The blades are set at a row angle of 31 degrees, a stagger angle of 16 degrees and an angle of attack of 15 degrees. The blade turning angle is 19 degrees. Each blade has a two inch chord and an aspect ratio of 1. The solidity of 1.5 is due to a blade separation of 1.3333 inches.

Test section diagram is shown in Fig. 4. There are six static ports at the cascade inlet. As these are in the same plane, they are used to confirm uniformity of flow at the inlet and to get an average inlet static pressure reading. The exit channel has two plexiglass side walls and adjustable top and bottom walls. The top and bottom walls each have four static pressure ports in the direction of the flow. These, along with the top and bottom walls are used to adjust the exit area as required, to establish uniform conditions entering and leaving the cascade. One of the plexiglass side walls has four rows of static pressure ports. These are 1.25 inches, 2.25 inches, 3.25 inches, and 4.25 inches, behind the trailing edge of the cascade. They are used to measure static pressure at the planes where wake survey is done.

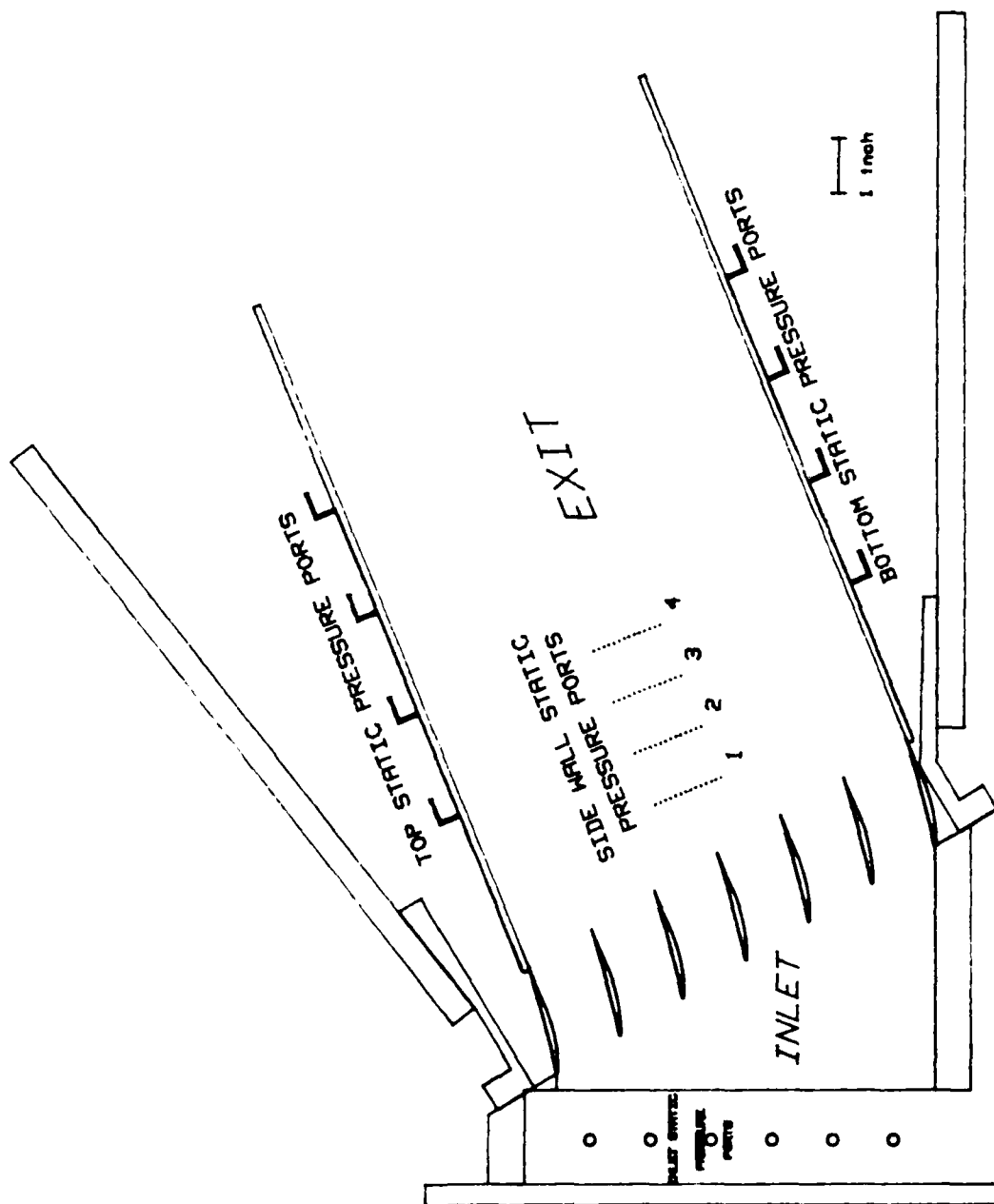


Fig. 4. Test section

Boundary Layer Control: To get a two dimensional flow, a boundary layer control mechanism has been installed. This consists of a side wall suction which continuously draws off the boundary layer from the side walls before the flow reaches the blades. Moe (11:47) determined that with appropriate suction applied, two dimensional flow was established at the center span (about 2/3rd width of the blade) of an aerofoil in a cascade.

Instrumentation: In this study, pressure, velocity and temperature at various locations, are measured. This is done with pressure transducers, thermocouples and two types of hot film anemometers. A traversing mechanism is provided to position anemometer probes at different locations. A complete listing these instruments is given in Appendix A. Measurements are taken at the following points

- (i) Pressure and temperature readings are taken from the stilling tank with a pressure transducer and a thermocouple.
- (ii) Static pressure readings are taken at the cascade entrance plane with a pressure transducer.
- (iii) Static pressure readings are taken at 38 points on the suction surface of the center blade with a scanivalve pressure transducer system.

(iv) Velocity and turbulence intensity of the flow are measured over the blade surface with a boundary layer anemometer probe mounted on the traversing system.

(v) Static pressure is measured at four exit planes with a pressure transducer.

(vi) Exit plane velocity measurements are taken at four planes with a 'X' wire anemometer probe mounted on the traversing mechanism.

Additionally, eighteen water manometers are installed with the CTF to monitor the balancing of inlet and exit plane pressures.

The pressure transducers were calibrated over their operating ranges with a linear curve fit used to convert output voltages to pressures. The copper / constantan thermocouple voltage output is converted to temperatures with the help of data acquisition software (12:3.78, 3.85).

For the velocity and turbulence intensity data, two Thermal System International (TSI) Model 1050 anemometers are used. These are connected to TSI Model 1241-10 'X' configuration hot film probe. One of the same anemometers is connected to a TSI

Model 1218-20 hot film boundary layer probe for boundary layer measurements. The anemometer system was calibrated using a modified TSI Model 1125 calibrator. The probes were calibrated at a range of temperature which varied from 20 degrees to 50 degrees F above the ambient temperature. The complete procedure has been given by Poulin, Williams and Tanis (3:81-89, 4:11, 5:7). The procedure for data reduction was modified for more accurate velocity data by adding probe wire resistance. The procedure is given in Appendix B. Calibration curves were obtained, examples of which are shown in Figs. 5 and 6. With the use of X wire probe, both magnitude and direction of velocity and turbulence intensity can be measured.

Traversing Mechanism: This equipment is designed to position the anemometer probe at a number of points for velocity and turbulence intensity measurements. It consists of two motors which move the probe in X (parallel to the chord) and Y (perpendicular to blade surface) directions. Manual movement in Z (parallel to blade span) direction is also possible. The X and Y direction movement are integrated to the data acquisition system through an encoder. A position indicator provides accurate information of probe location with respect to a reference point. Accurate location of the initial reference point is very important to make precise use of this system.

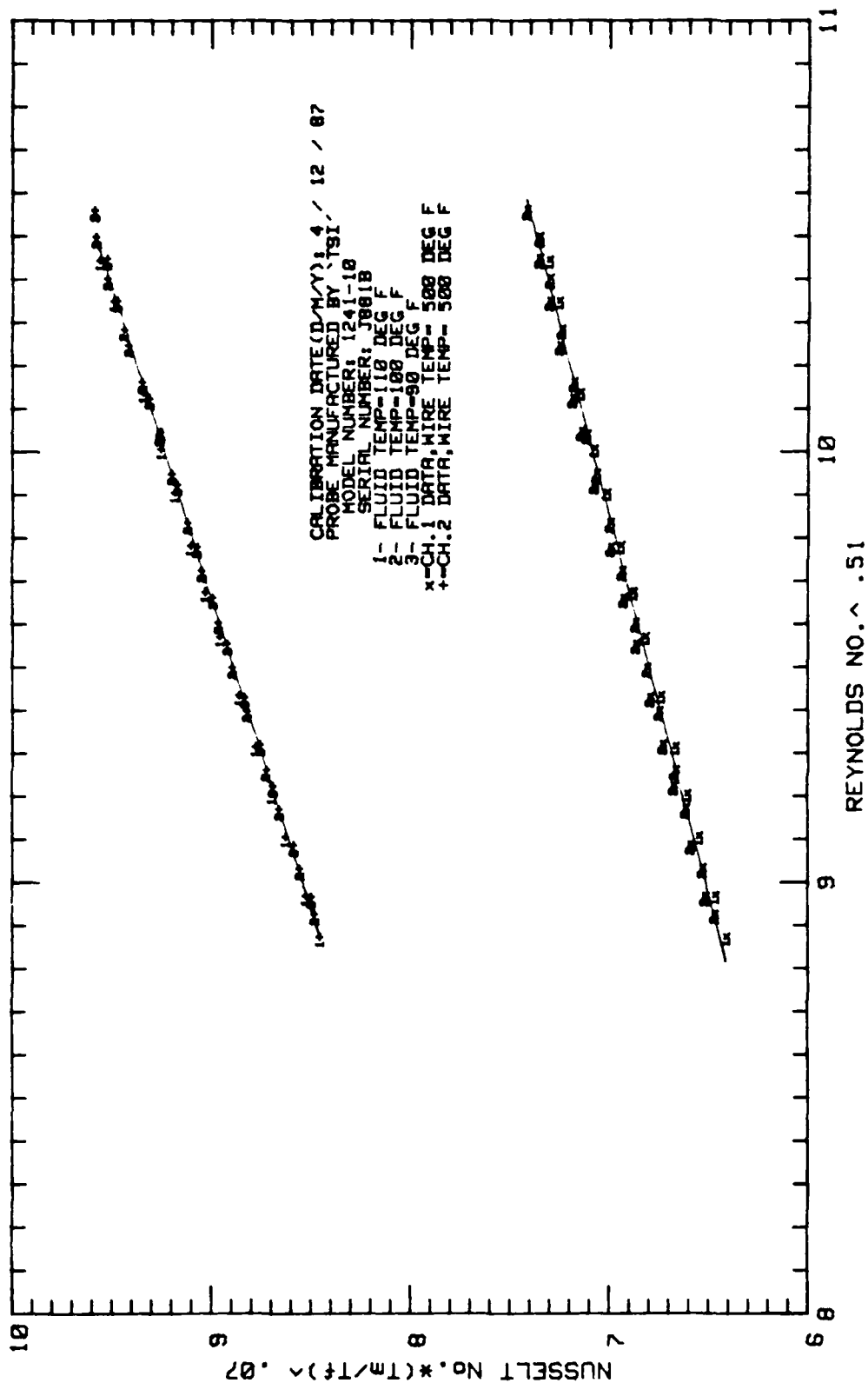


Fig. 5. 'X' Wire Wake Probe Calibration Curve

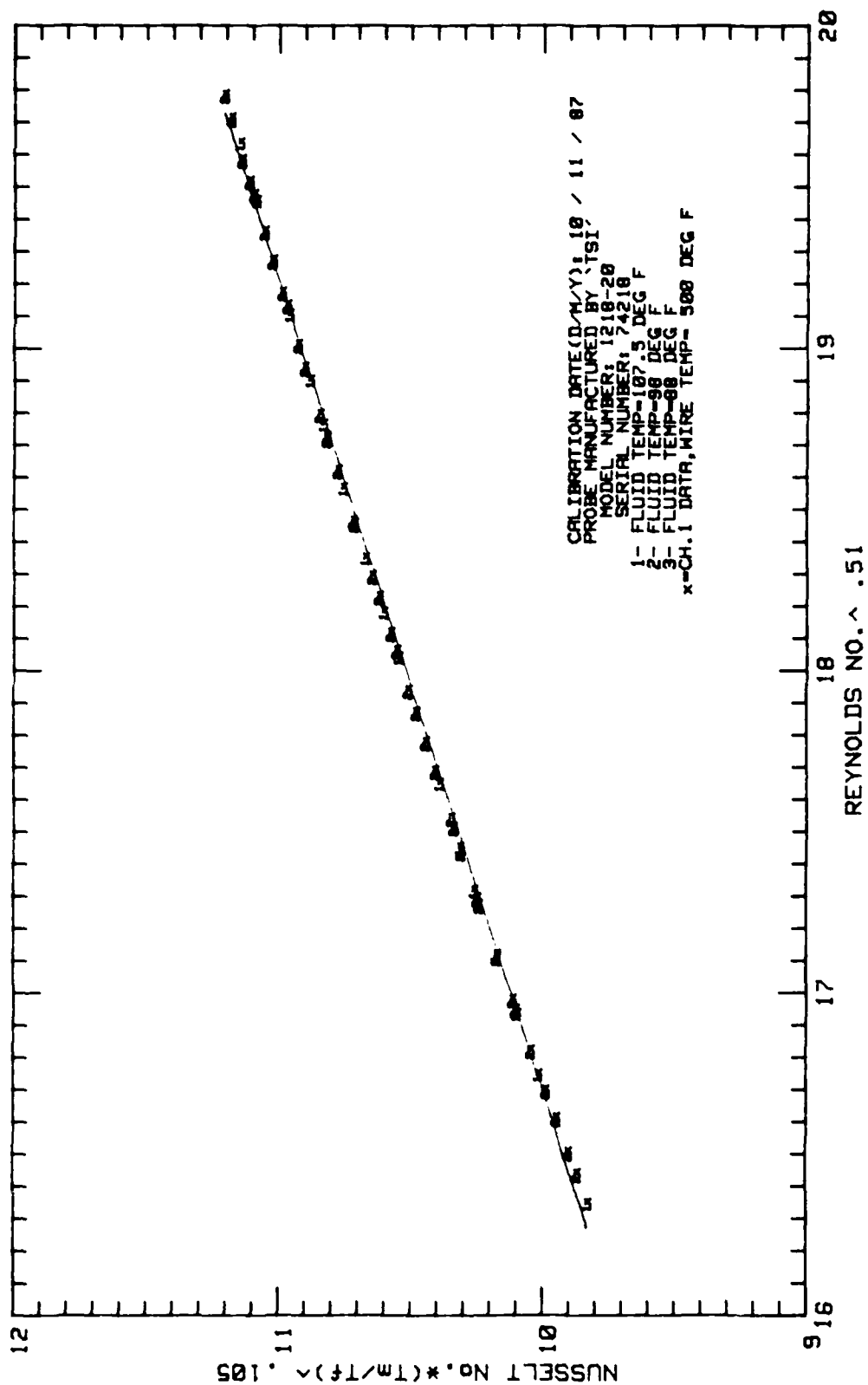


Fig.6. Boundary Layer Probe Calibration Curve

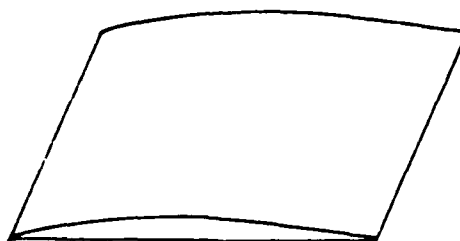
Blade Roughness Configuration: The aerofoils used are NACA 65-506 with three different roughness categories. One is the original smooth casting while the other two have different grades of emery paper bonded on the suction surface. The emery paper is placed in the mold so as to preserve the blade surface contour. The roughness begins a sixteenth of an inch from the leading edge and extends to the 25% chord point. Further details of roughness measurements are given by Poulin (3:25). Roughness values for the three configurations are given in Table I.

TABLE I.

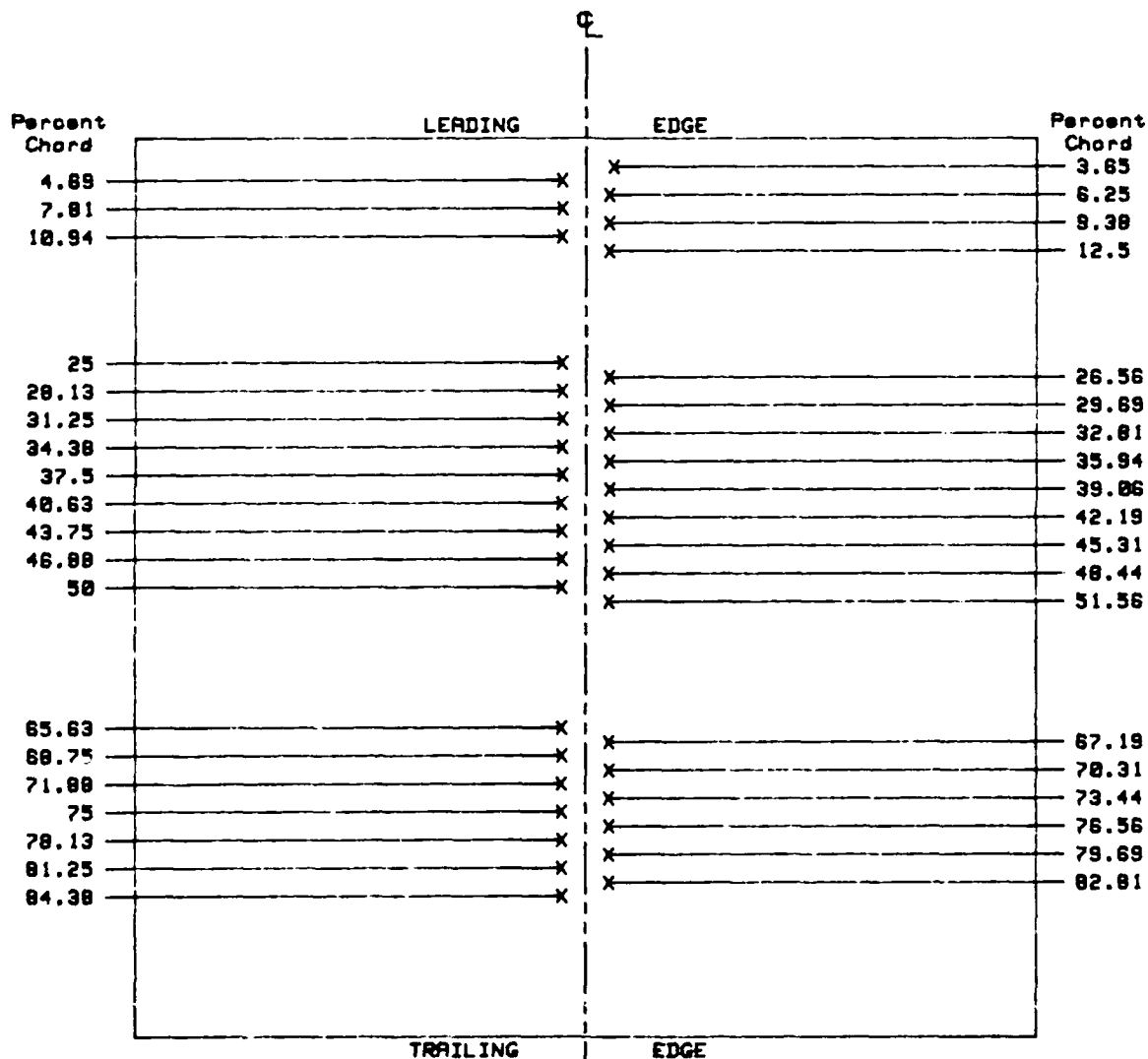
Blade Roughness Configurations

<u>Conf#</u>	<u>Ra,mic m</u>	<u>Ks,mic m</u>
1	0.45	2.79
2	12.10	75.00
3	18.30	113.00

Suction Surface Pressure Measurement: The center blade on all three configurations is instrumented with 38 static pressure ports over the suction surface. These are alternately offset a sixteenth of an inch to either right or left of the center. Holes have been drilled from either end of the blades to join the taps. Metal tubing with 0.22 inch outer diameter are inserted in these holes. The pressure taps are further connected to 38 lines



NACA 85-A506 Profile



Top view of center blade, looking down at the suction surface, showing pressure tap locations (X) and tube arrangement.

Fig. 7. Blade Profile and Pressure Tap Arrangement

on the scanivalve measuring system. Pressure measurement can be made by manually operating the scanivalve controller and monitoring the position display. For automatic pressure readings, the system is controlled by HP 9845B computer software. The pressure tap arrangement is shown in Fig. 7.

Data Acquisition & Analysis System: All measurements taken at the CTF are monitored by HP 3052A Data Acquisition System, which is controlled through HP 9845B computer software. These measurements are recorded as raw data on HP 9845B computer system. All components of this are listed in Appendix A. HP 9845B computer software also controls the movement of the traversing mechanism. Data is converted to engineering units later through other programs, and used in performance analysis.

IV. EXPERIMENTATION AND DATA REDUCTION

The experiments conducted during this study were divided into four stages.

1. Turbulence generation.
2. Study of effects of turbulence in the wake.
3. Study of effects of turbulence upon pressure profile on the blade.
4. Study of turbulence effect on boundary layer profile and thickness.

After stage one was successfully completed, stages two, three and four were accomplished for the three different blade configurations.

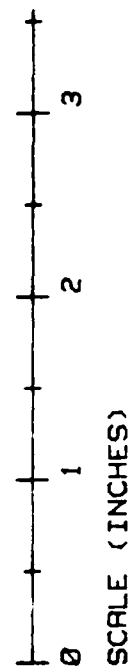
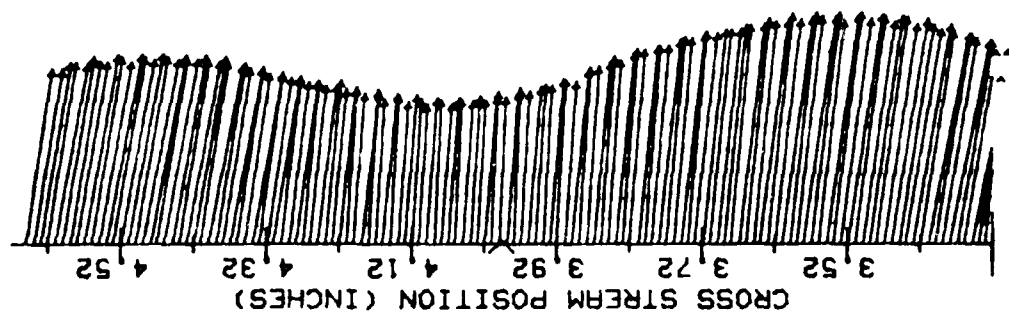
The CTF was allowed to warm up to flow operating temperatures and was balanced before taking any measurements. The balanced conditions were reached when static pressure ports along the top and bottom walls at the exit of the test section were indicating approximate ambient pressure. Also, the inlet pressure ports were at constant pressure across the channel. These established a two dimensional flow (3:29). With turbulence generation on, the exit pressure readings changed slightly, however the test section was not rebalanced again.

Turbulence Generation: The turbulence generation device described in Chapter III was integrated with the CTF. RMS and DC voltage measurements were taken of the output signal from a 'X' wire anemometer probe placed in the flow. This was done with the turbulence generation device on, but without installing any cascade. A 1.33 inches traverse, perpendicular to the chord, was carried out where the leading edge of the center blade was supposed to be. The voltages were converted to flow and RMS velocities using the calibration curve. Turbulence intensity at each point was then calculated using Equation (1). The profile is shown in Fig. 8. Another similar traverse was done over the whole section, at the same position. The turbulence intensity profile for this is shown in Fig. 9.

The effect of blowing secondary air into the main stream was checked by installing a pitot tube in the flow. Total pressure readings were taken at several positions with and without secondary air being injected in the flow. The change in total pressure with this air blowing was less than 2%.

Wake Study: For each of the cascade configurations, four wake traverses were carried out. These were done both with low and high freestream turbulence, 1.25 inches, 2.25 inches, 3.25 inches and 4.25 inches behind the trailing edge of the center blade. Each traverse covered a vertical distance of 1.33 inches,

TURBULENCE INTENSITY AROUND
CENTER BLADE LEADING EDGE, CASCADE NOT INSTALLED



— % TURB INT SCALE= 5.00 % / INCH

Fig. 8. Turb. Intensity Center Blade L.E. Vicinity, With Turb. Generation

TURBULENCE INTENSITY AT CASCADE LEADING
EDGE, CASCADE NOT INSTALLED

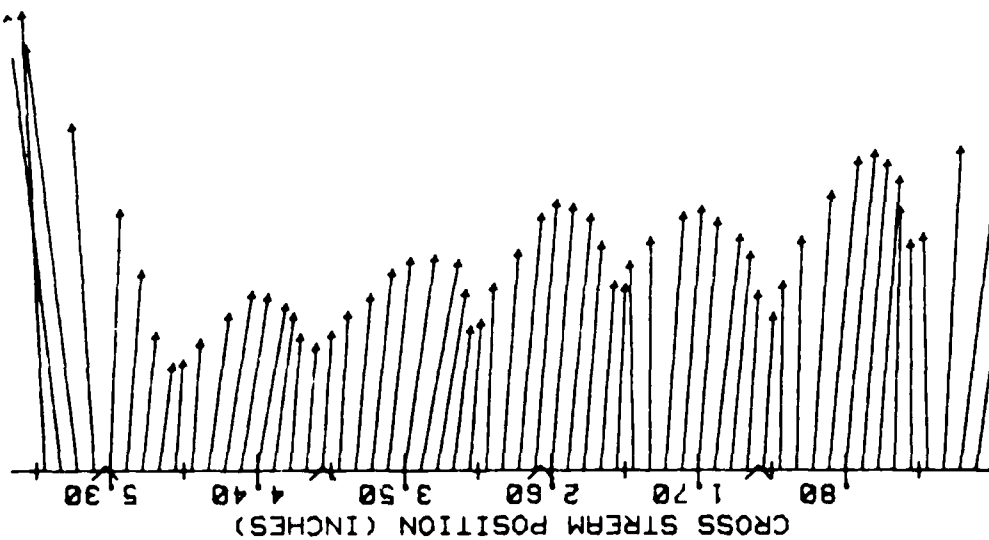


Fig.9. Turbulence Intensity With Turb. Generation

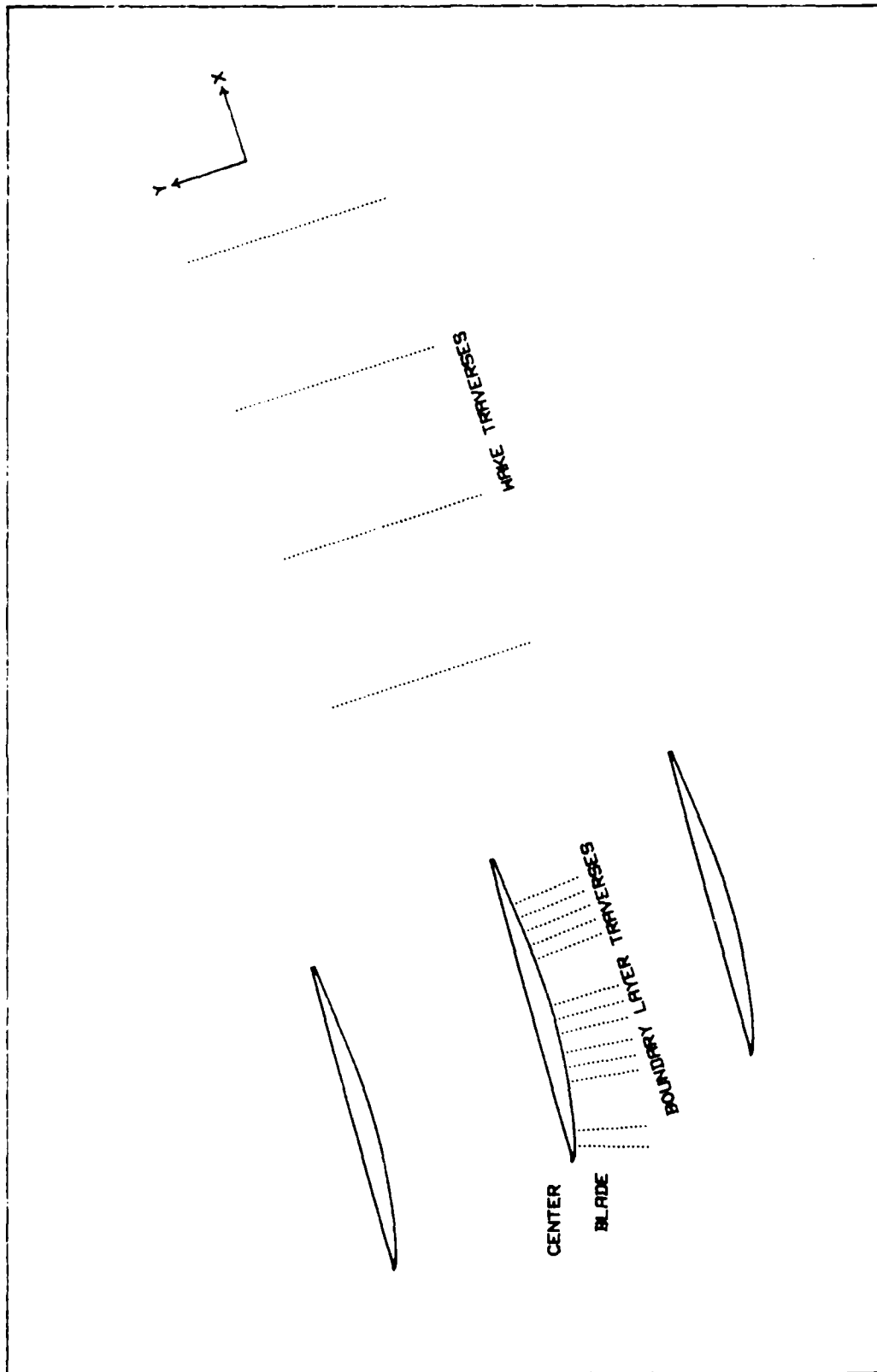


Fig.10. Representation of Wake and Boundary Layer Traverses

half on each side of the blade chord. The location of each traverse is shown in Fig. 10. 133 data points were taken in each traverse. Using the anemometer calibration curve, these were reduced to wake velocities, from which turbulence intensities were also calculated using Equation (1). These profiles are shown in Appendices C, D, and E. Pressure and temperature measurements at points described earlier, were also taken during all the traverses.

Velocity Correction: The anemometer voltage output was converted to velocity using probe sensor calibration curve. This was compared with the isentropic velocity calculated from total and static pressure measurements. It was found that the experimentally measured velocity was approximately 5% higher. In previous studies on this CFF (3, 4, 5, 11) this error had been about 7% to 10%. This has been reduced because of incorporating the cable resistance in the calibration and data reduction procedure. The cause of this error, as explained by Poulin (3:30) and Tanis (5:14-15) is thought to be related to variation in heat transfer rate due to humidity. The problem was overcome by applying continuity condition upstream and downstream of the flow and obtaining a correction factor for velocity (5:15-16, 11:12).

Pressure Loss Coefficient: As pointed out earlier, this quantifies the total loss through a cascade and is given by Equation (2). The total pressure upstream of the cascade is the pressure inside the stilling tank, this was measured. Cascade inlet static pressure was measured and from these two the dynamic pressure calculated. To calculate mass averaged total pressure Equation (3) and (4) were used.

As stated by Poulin (3:33) and Moe (11:16), the area integrals in Equation (4) can be reduced to single integrals because of the two dimensional flow. These integrals were evaluated numerically on HP 9845A computer, using the available data. The pressure loss coefficient for all three configurations, with and without turbulence is given in Chapter V, Table II.

Blade Pressure Profile: The scanivalve pressure monitoring system was used to get a pressure profile over the blade suction surface. Static pressure was measured for all roughness and turbulence configurations. The positions at which these measurements were taken are shown previously in Fig. 7. The pressure coefficient, C_p , for each point was calculated using Equation (7). These were plotted against their locations. The plots are given in Chapter V, Figs. 20, 21, and 22.

Boundary Layer Study: Hot film boundary layer probe, TSI Model 1218-20, was used for this part of the investigation. RMS and DC voltages were recorded for traverses perpendicular to the blade surface, with the CTF operating. These measurements were taken at thirteen different chord locations shown in Fig. 10. Each of the thirteen traverses were done for all three surface roughness configurations, with low and high freestream turbulence. These started 0.03 inches above the blade surface. Most of these included sixty points 0.005 inch apart. However, for the last four chord locations, with high turbulence and surface roughness, ninety points per traverse were required.

The voltages obtained were converted to flow and RMS velocities with the calibration curves. This gave the velocity profile for the measured velocity (V_m). The mean edge velocity was calculated by the scheme given by Deutsch and Zierke (9:8-9) which has also been used by Williams (4:20) and Poulin (3:39-40) in similar studies. Using Equation (6), the boundary layer velocity profile was calculated for each traverse. The boundary layer thickness, δ_{BL} , was determined at a distance from the surface where

$$V = 0.99 V_e \quad (8)$$

The edge velocity corresponding to this thickness was then taken as the actual edge velocity.

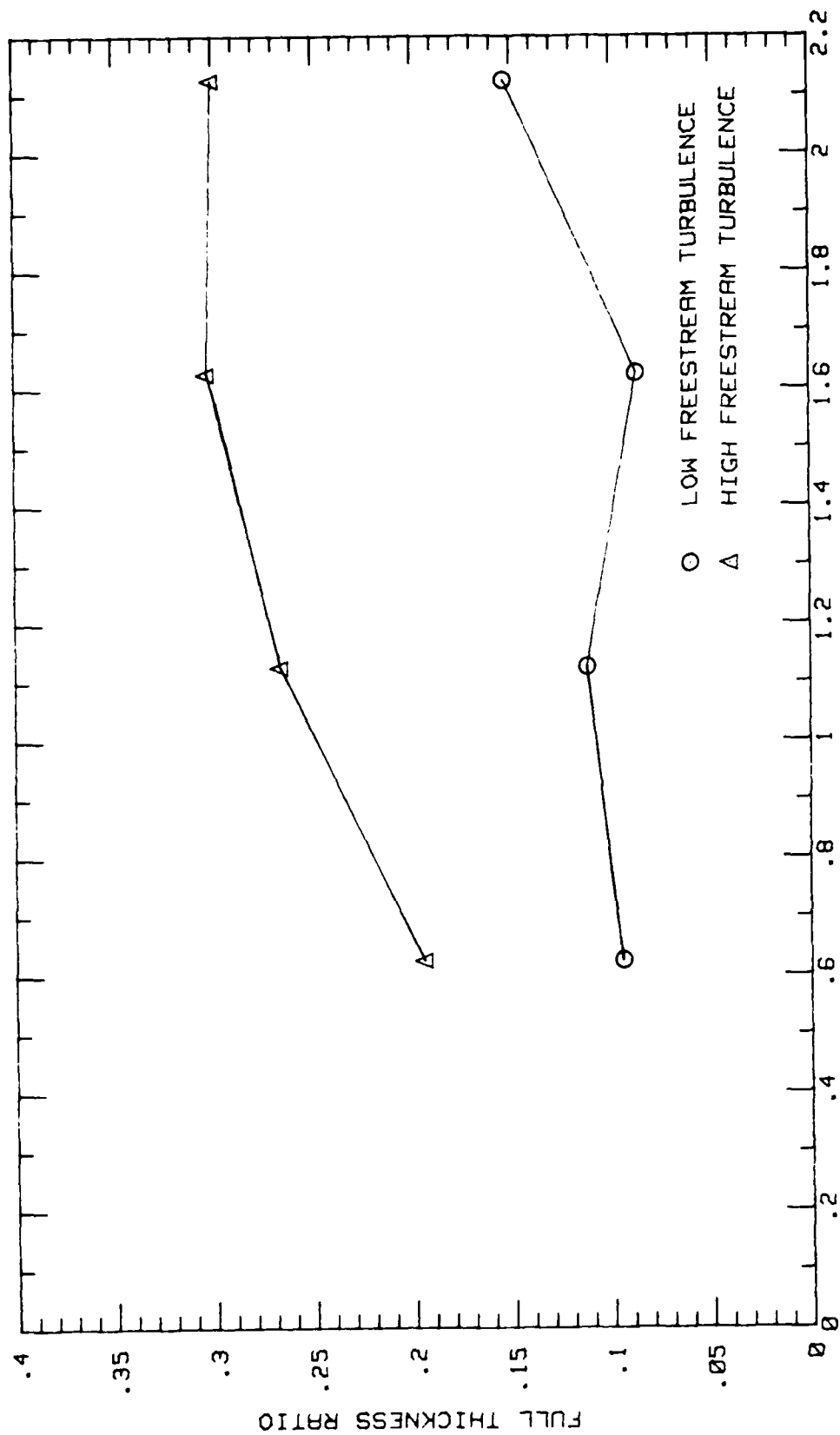
The turbulence intensity was calculated from the measured flow and RMS velocities using Equation (1). As quoted by Poulin (3:41) "Deutsch and Zierke (9:9) pointed out that the turbulence intensity will be higher than freestream turbulence till approximately $y=1.25\delta_{BL}$ ". This gave an approximate value of δ_{BL} , to compare with that determined from velocity measurements. The velocity profile plots and turbulence intensity profile plots for all traverses are given in Appendices F, G, and H.

V. RESULTS AND DISCUSSION

This investigation involved study of the same blade profile with three different configurations characterized by surface roughness. The roughness parameter R_a is given by the average value of deviation from the center line over a particular sampling length. Each of the three configurations was studied with low and high freestream turbulence. The areas of interest were the wake, the pressure profile over the suction surface and the boundary layer.

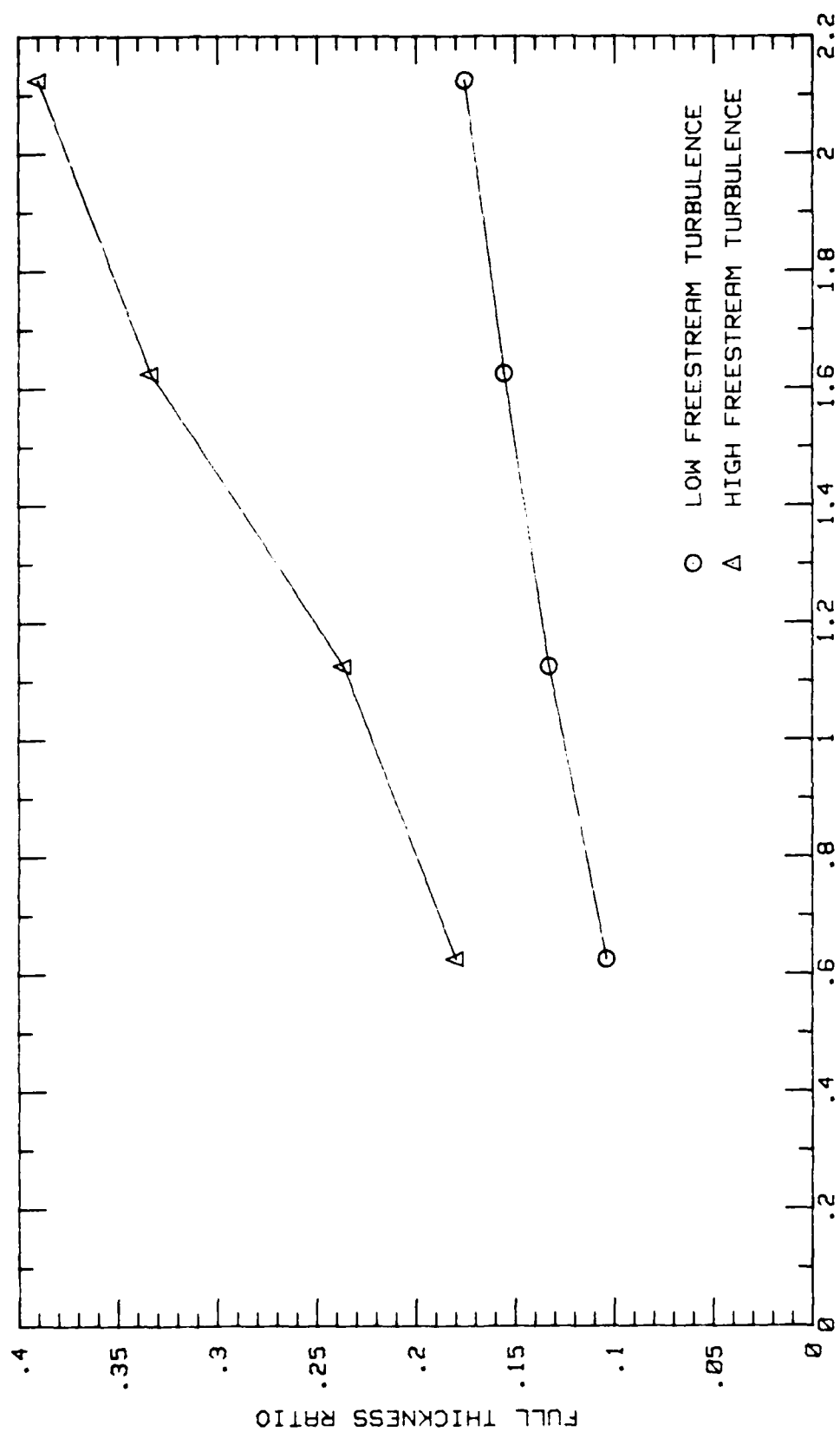
Wake Survey: For the two levels of freestream turbulence, data was obtained in the wake. This has been plotted in the form of velocity and turbulence intensity profiles. The results are given in Appendices C, D and E, corresponding to configurations 1, 2, and 3 respectively.

From the figures (App. C, D, & E), it can be seen that the wake velocity profiles are similar to those predicted by Lieblein and Roudebush (14:33) and reproduced as Fig. 1. A comparison of the profiles indicate that the trough in the wake velocity is spread more for profiles with increased freestream turbulence. This implies that the 'wake flow thickness' should increase with freestream turbulence. The wake flow thickness should increase with freestream turbulence. The wake flow thickness was



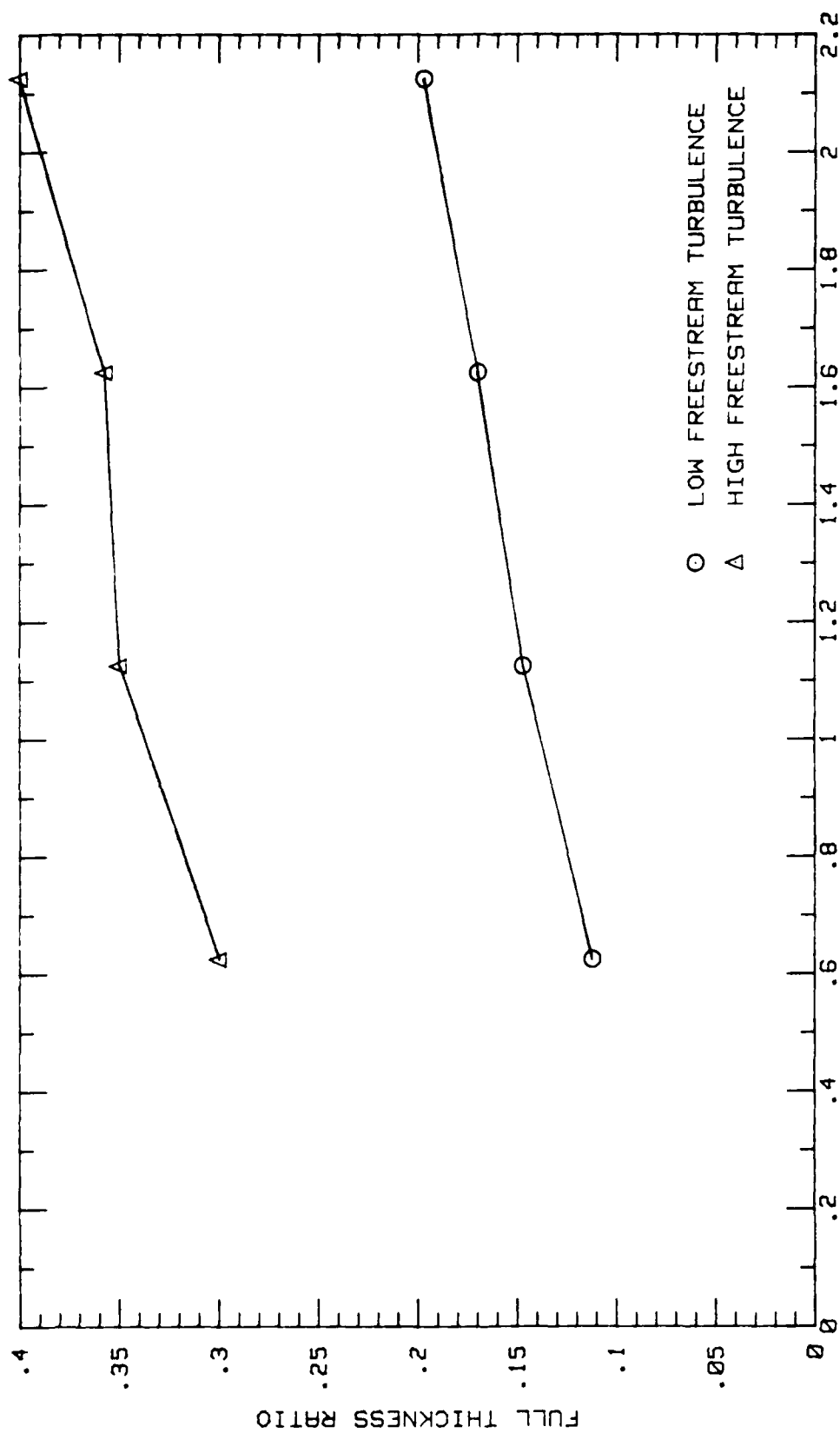
DIMENSIONLESS DISTANCE DOWNSTREAM OF TRAILING EDGE, x/c

Fig. 11. Downstream Variation of Full Thickness Ratio Conf#1



DIMENSIONLESS DISTANCE DOWNSTREAM OF TRAILING EDGE, x/c

Fig. 12. Downstream Variation of Full Thickness Ratio Conf#2



DIMENSIONLESS DISTANCE DOWNSTREAM OF TRAILING EDGE, x/c

Fig. 13. Downstream Variation of Full Thickness Ratio Conf#3

calculated and is given as full thickness ratio (δ/c) versus distance downstream, in Figs. 11, 12, and 13. These confirm the observation just made. Full thickness ratio is more than doubled with increased freestream turbulence. It may be noted that there was a discontinuity in the velocity profile of smooth airfoils for the traverse at 3.25 inches behind trailing edge, at both low and high turbulence (Figs. 31 and 35). This was not there in the case of rough blades. No explanation for this was found. As it was repeatable, it is probable that the cause was some slight defect in test section exit.

The velocity ratio V_{min}/V_o is plotted in Figs. 14, 15, and 16. The theoretical equation given by Lieblein and Roudebush is also plotted for comparison. The slope of the line joining data points on these plots is indicative of the rate at which wake is energized. As can be seen V_{min}/V_o with high freestream turbulence, is lower than for the case with low freestream turbulence, for points at the same location. The difference decreases for locations further downstream from the cascade. Thus plots of data with higher turbulence have a greater slope. This trend is similar for all three roughness configurations, although the effect decreases with increased roughness. From this and the fact that wake full thickness is larger with high turbulence, it may be concluded that the mixing rate in the wake of a cascade increases with increase of freestream turbulence.

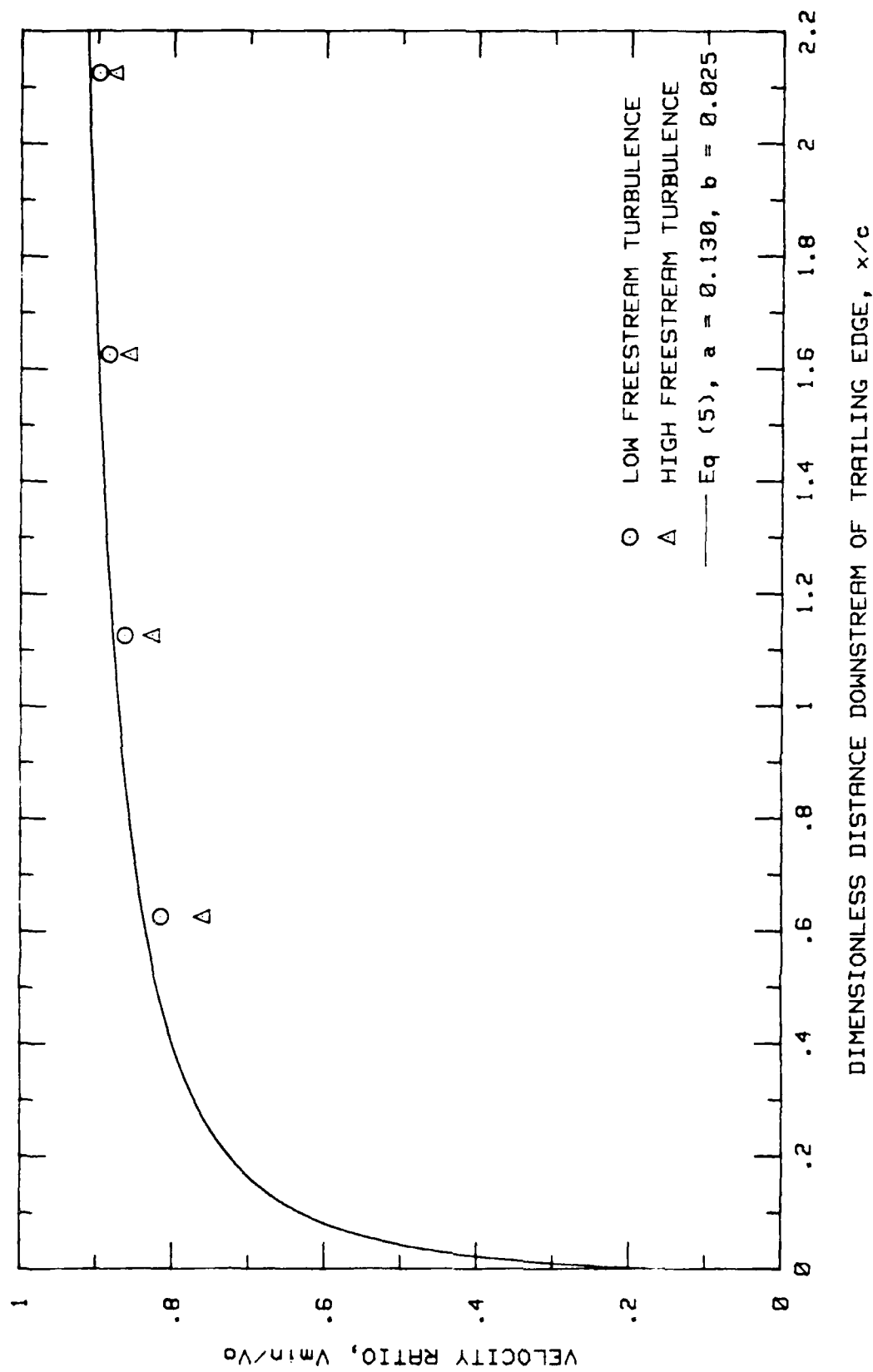


Fig. 14. Wake Velocity Recovery Conf#1

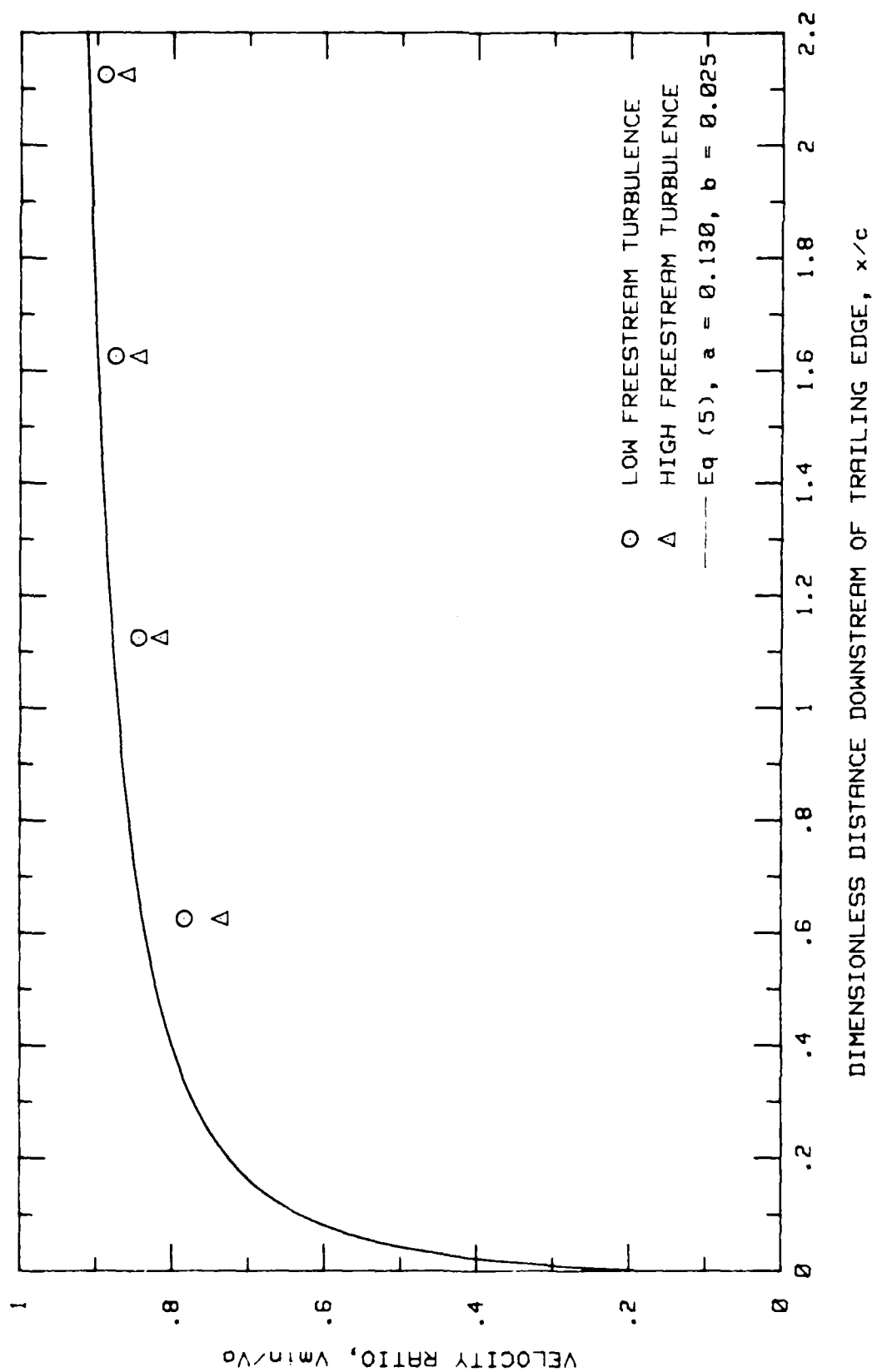


Fig. 15. Wake Velocity Recovery Conf#2

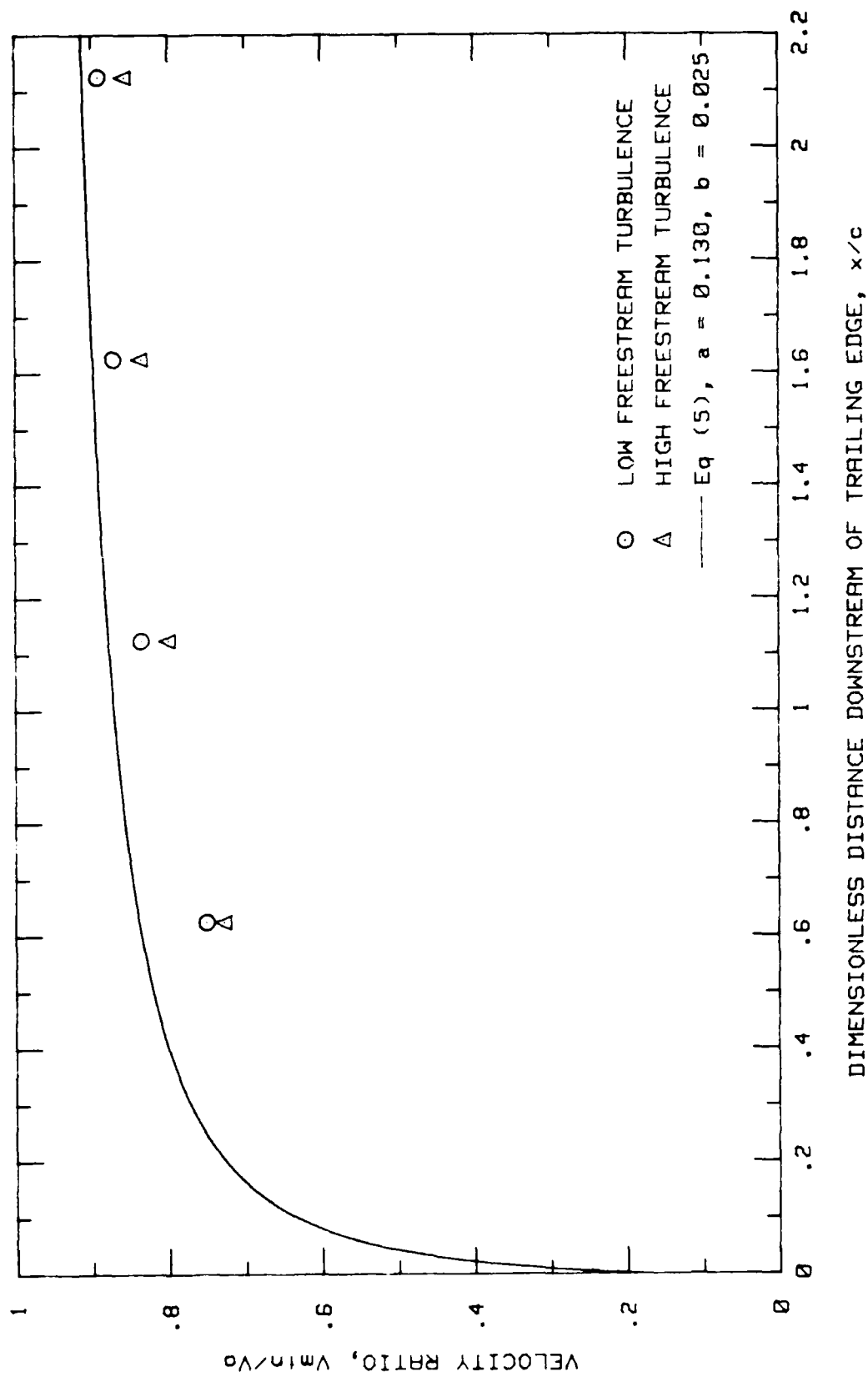


Fig. 16. Wake Velocity Recovery Conf#2

TABLE II.

Total Pressure Loss Coefficient

Investi- gator	Conf#	Turb. State	x/c			
			0.625	1.125	1.625	2.125
Absar	1	Low	0.0667	0.0798	0.0716	0.0837
Absar	1	High	0.0540	0.0685	0.0757	0.0826
Absar	2	Low	0.0671	0.0755	0.0811	0.0844
Absar	2	High	0.0419	0.0635	0.0840	0.0940
Absar	3	Low	0.0882	0.0965	0.0982	0.1013
Absar	3	High	0.0671	0.0819	0.0925	0.1017
Poulin	1	Low	0.0641	0.0780	0.0659	0.0663
Poulin	2	Low	0.0729	0.0770	0.0750	0.0770
Poulin	3	Low	0.0808	0.0895	0.0877	0.0896

The total pressure loss coefficient, w , as defined earlier, was calculated. This is given for each traverse in Table II. For low freestream turbulence, these had also been calculated by Poulin (3:68), his results have also been tabulated for comparison. This coefficient was also plotted at each traverse location; these plots are given in Figs. 17, 18, and 19 for configuration 1, 2, and 3 respectively. These show that at the first traverse location, 1.25 inches behind the trailing edge, pressure loss coefficient is reduced when freestream turbulence is increased for all three configurations. This reduction varies from 18% to 25%. Further downstream, about 4 inches from the trailing edge, the pressure loss coefficient, for both levels of turbulence, is the same. The trend is similar for all three configurations, although the increase is slightly more for conf. #2. This leads to the conclusion that the rate of increase of pressure loss coefficient in the wake increases with freestream turbulence. As stated earlier, higher mixing rate will lead to higher wake losses downstream.

To summarize it, can be said that the pressure loss coefficient just behind the cascade was found to be much lower at the high value of turbulence investigated. However, the rate of wake mixing was much higher with high turbulence, causing higher wake losses. This resulted in the pressure loss coefficient

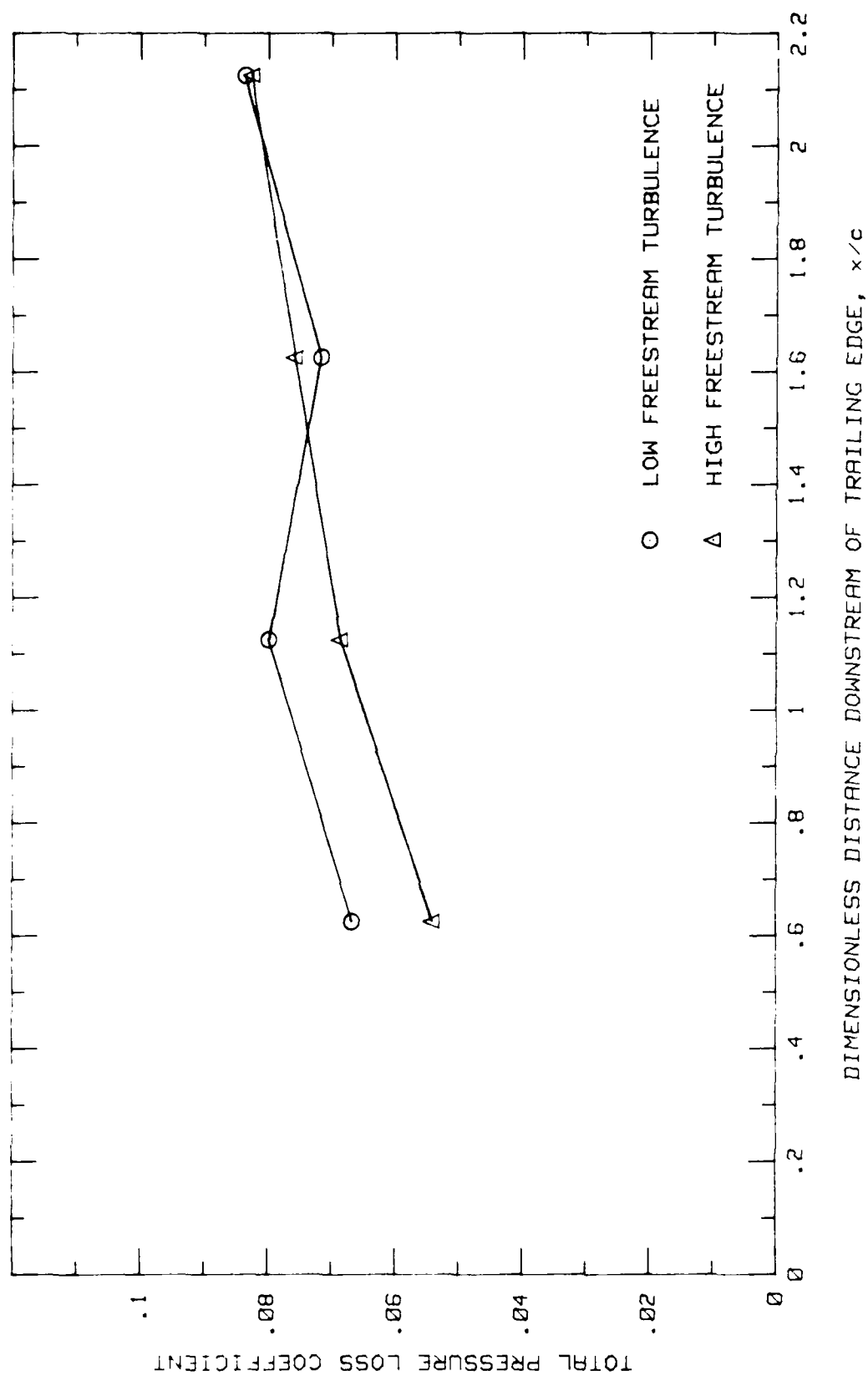


Fig. 17. Change in the Total Pressure Loss Coefficient CONF#1

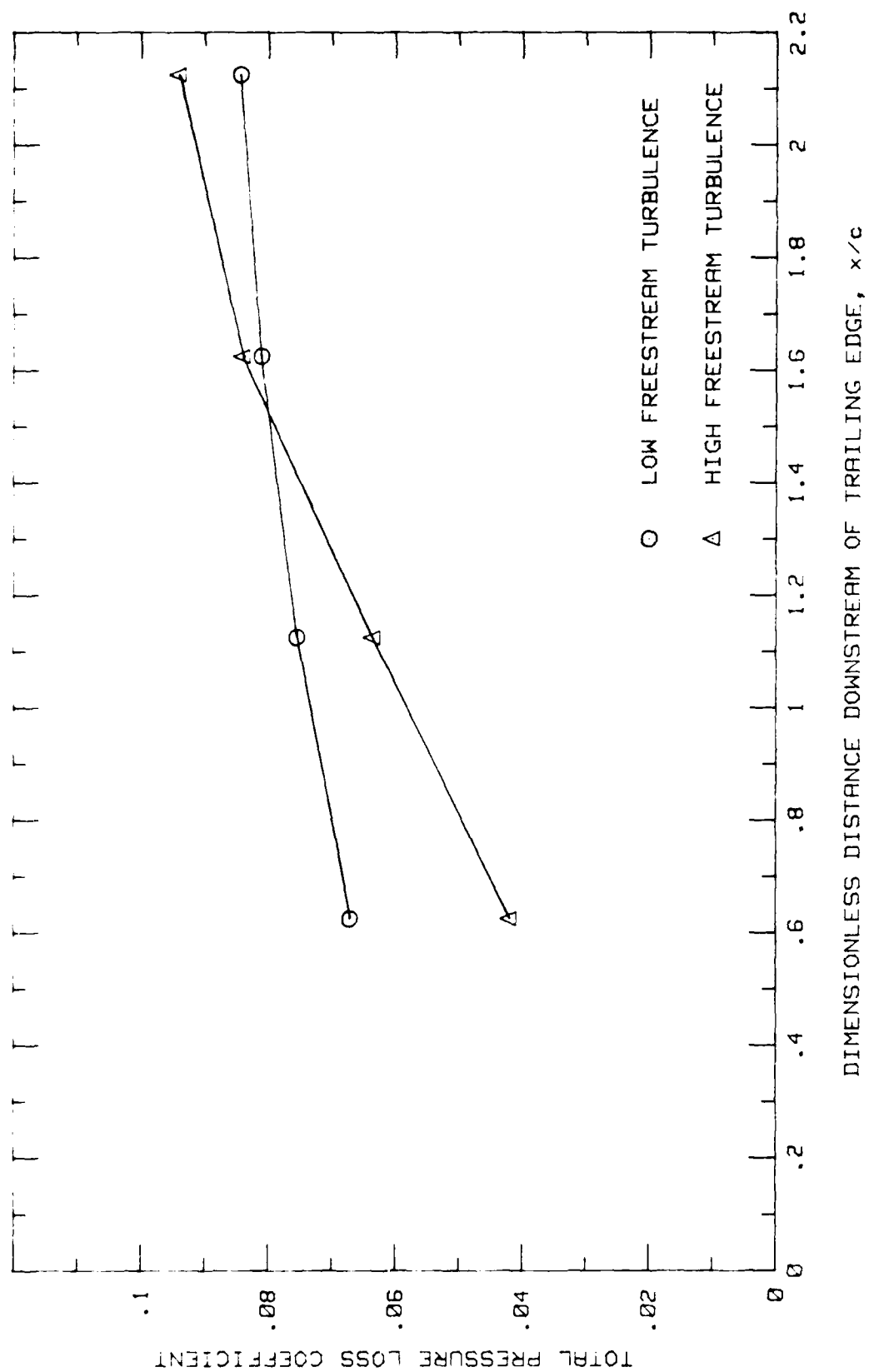


Fig. 18. Change in the Total Pressure Loss Coefficient CONF#2

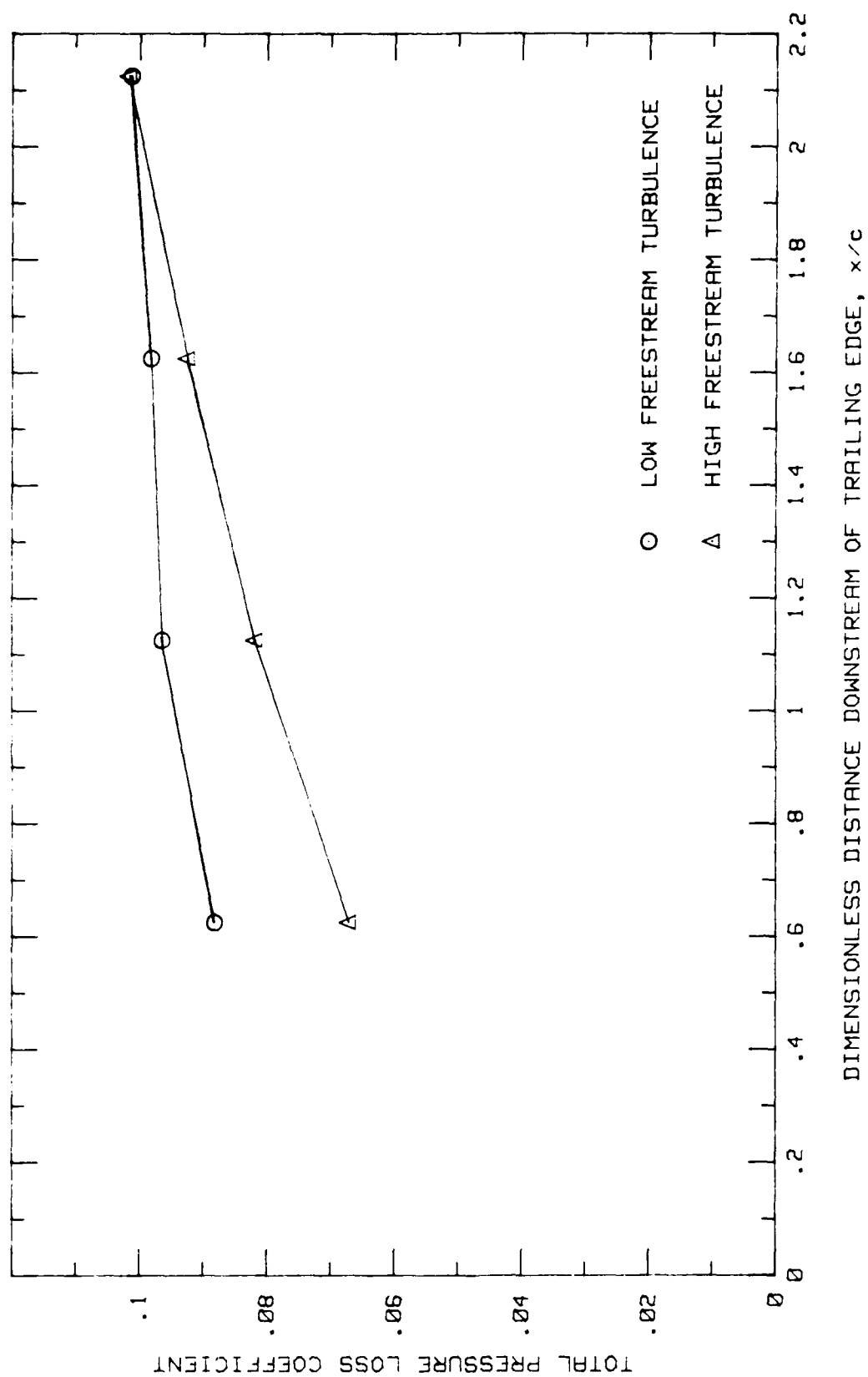


Fig. 19. Change in the Total Pressure Loss Coefficient CONF#3

becoming almost the same about 4 inches behind the trailing edge. No data was taken further down stream but the velocity profiles at the 4.25 inches traverse position indicate that wake mixing is almost completed. Therefore, the loss coefficients at 4.25 inches are representative of the combined total pressure loss in the cascade and due to mixing.

Suction Surface Pressure Distribution: Static pressure at each of the 38 locations on the suction surface of the center blade was measured. These pressures were converted to pressure coefficients, C_p , as described in Equation (7). Three sets of measurements were taken for each configuration, at low and high turbulence. The repeat readings were almost the same for any one set of conditions, indicating consistency of flow through CTF.

For every configuration and turbulence condition, a mean C_p at each location on the suction surface, was calculated. These have been plotted in Figs. 20, 21, and 22 for configuration 1, 2, and 3 respectively. The pressure distribution for all three configurations at low turbulence was the same as observed by Poulin (3:43-45). As observed previously, there is a definite fluctuation in pressure coefficients between 25 and 42 percent chord, for the two configurations with roughness. Poulin (3:46) attributed this to the method of roughness application. Increased turbulence does not change this behavior.

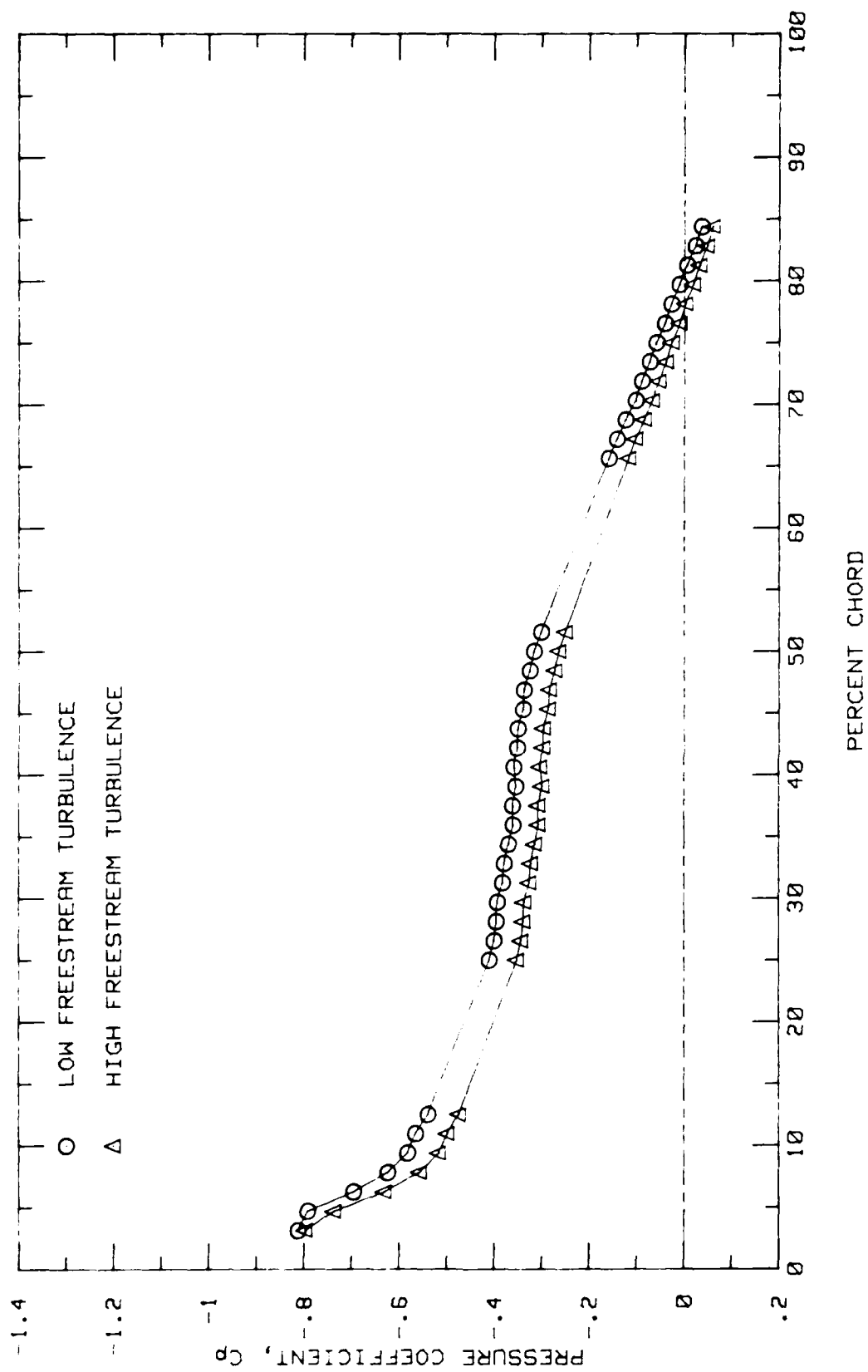


Fig. 20. Pressure Profile, Conf. #1, $Ra = 0.45$ micrometers

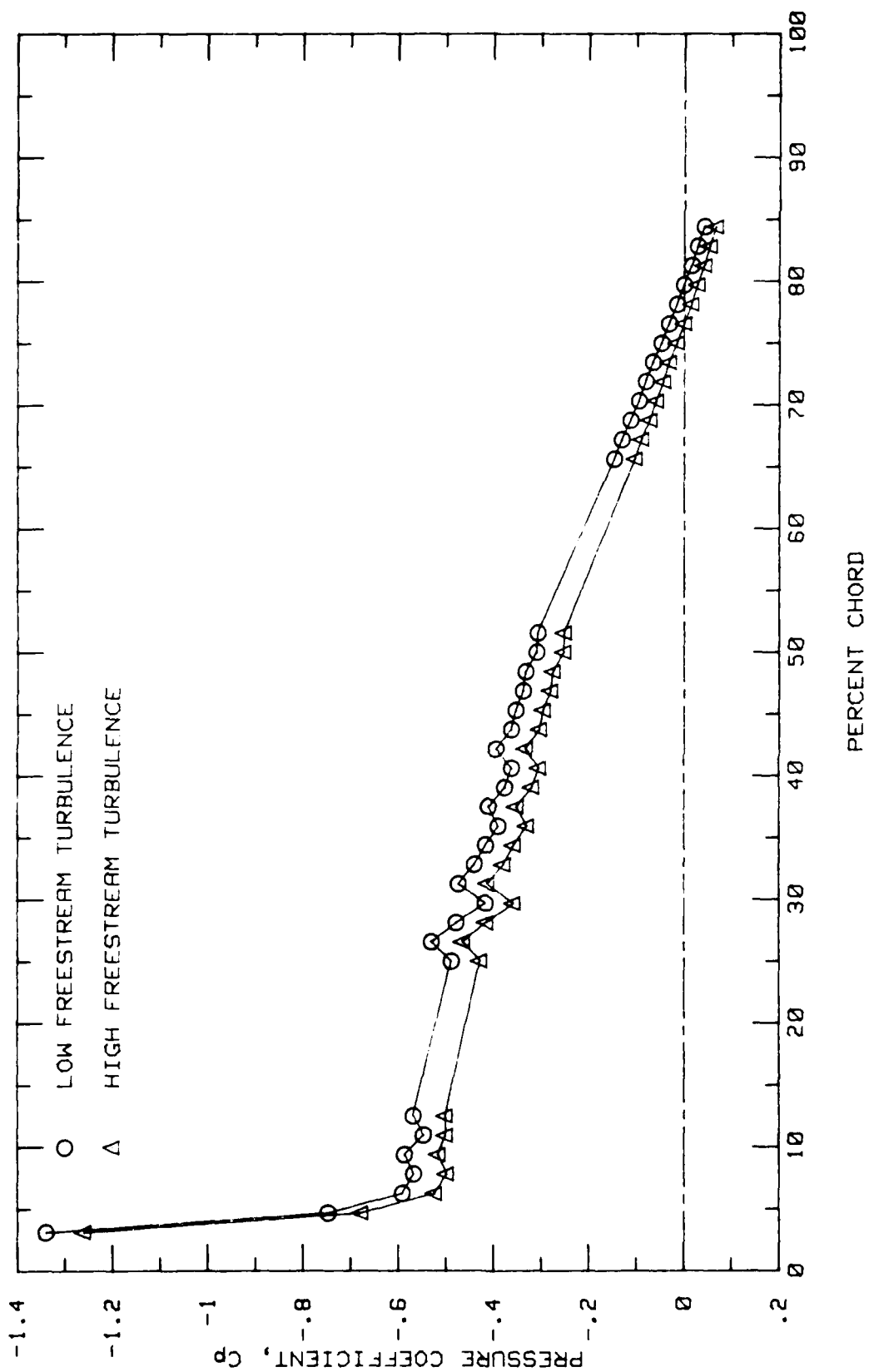


Fig. 21. Pressure Profile, Conf. #2, $Re = 12.10$ micrometers

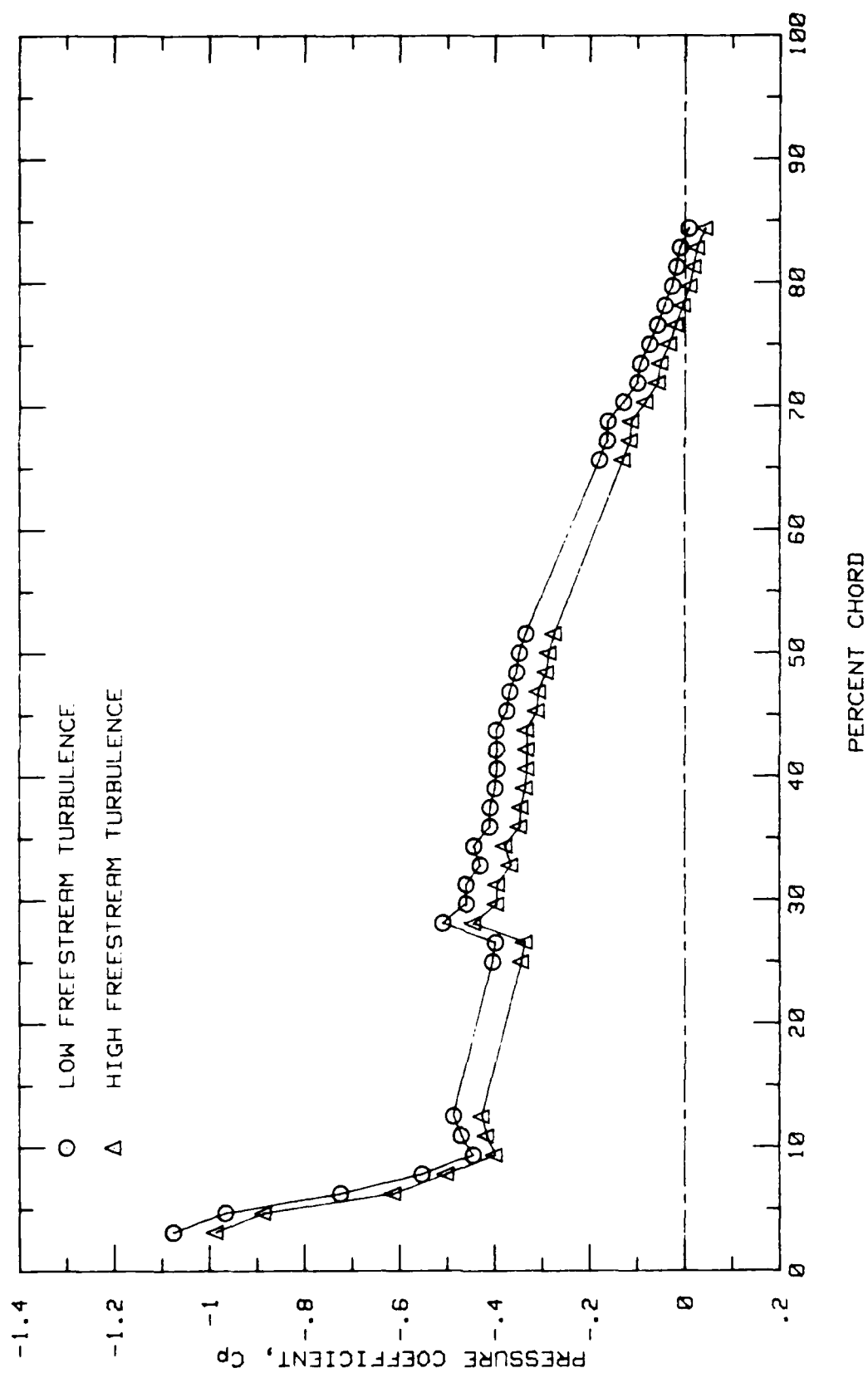


Fig. 22. Pressure Profile, Conf. #3, $Re = 18.30$ micrometers

A comparison of the two C_p profiles for the suction surface of smooth blades reveal that the pressure coefficient increases with freestream turbulence. This increase is consistent over the whole blade surface. On most of the surface C_p increases by about 12 to 15 percent. This corresponds to an increase in static pressure of about 10%. This behavior is similar in case of rough blades.

It can therefore be concluded that static pressure over the suction surface of a blade in a cascade increases with freestream turbulence. This effect remains the same irrespective of the amount of surface roughness. It may be noted that similar effects of turbulence have been observed by Evans (14:3), who conducted his experiments on a one foot chord cascade. In his experiment, turbulence intensity of 3.14% and 5.2% was produced by 1 and 2 inch wire grids.

Boundary Layer Study: As described earlier, the study of boundary layer involved determination of flow velocity and turbulence intensity profiles. These were used to calculate boundary layer velocity profiles, boundary layer thickness and edge velocity along the suction surface at thirteen different chord locations.

Using a boundary layer anemometer probe, data was obtained at

4.688, 9.375, 25.00, 29.68, 34.375, 40.625, 45.313, 50.00, 65.625, 70.313, 75.00, 79.688, and 84.375 percent chord. From the method described in Chapter IV, flow velocity and turbulence intensity profiles were determined. The boundary layer velocity and turbulence intensity profiles are given in Appendices F, G, and H for configurations 1, 2, and 3 respectively. Table III gives the numerical values of edge velocity, boundary layer thickness and turbulence intensity boundary layer thickness for all three configurations at low freestream turbulence. Table IV gives the same with high freestream turbulence.

TABLE III.

Boundary Layer Parameters
With Low Freestream Turbulence

Conf #	% Chord	Ve ft/sec	δ_{BL} ins.	Tu _{BL} ins.
1	4.688	648.04	0.0337	0.0352
	9.375	630.61	0.0370	0.0392
	25.000	606.62	0.0401	0.0407
	29.688	605.08	0.0386	0.0372
	34.375	600.58	0.0392	0.0394
	40.625	595.02	0.0418	0.0414
	45.313	589.38	0.0393	0.0388
	50.000	583.01	0.0387	0.0385
	65.625	552.02	0.0458	0.0425
	70.313	545.14	0.0712	0.0482
	75.000	532.53	0.0544	0.0537
	79.688	520.93	0.0582	0.0543
	84.375	511.13	0.0691	0.0615
2	4.688	657.66	-----	-----
	9.375	638.71	-----	-----
	25.000	618.989	0.0340	0.0332
	29.688	611.83	0.0352	0.0324
	34.375	605.71	0.0354	0.0345
	40.625	596.13	0.0375	0.0357
	45.313	590.15	0.0377	0.0344
	50.000	580.09	0.0381	0.0372
	65.625	548.34	0.0381	0.0372
	70.313	538.03	0.0452	0.0428
	75.000	528.45	0.0509	0.0484
	79.688	519.87	0.0606	0.0521
	84.375	492.54	0.0449	0.0556
3	4.688	658.44	-----	-----
	9.375	626.73	0.0311	-----
	25.000	615.24	0.0400	0.0411
	29.688	614.60	0.0427	0.0416
	34.375	608.87	0.0431	0.0425
	40.625	598.74	0.0416	0.0414
	45.313	592.64	0.0415	0.0406
	50.000	584.31	0.0431	0.0427
	65.625	554.72	0.0520	0.0499
	70.313	544.16	0.0571	0.0547
	75.000	537.27	0.0662	0.0592
	79.688	525.74	0.0688	0.0628
	84.375	503.91	0.0634	0.0675

TABLE IV.

Boundary Layer Parameters
With High Freestream Turbulence

Conf #	% Chord	Ve ft/sec	δ_{BL} ins.	Tu _{BL} ins.
1	4.688	673.21	-----	-----
	9.375	657.15	0.0319	0.0323
	25.000	629.02	0.0443	0.0429
	29.688	623.71	0.0464	0.0431
	34.375	614.47	0.0425	0.0426
	40.625	612.04	0.0509	0.0484
	45.313	608.30	0.0521	0.0452
	50.000	599.58	0.0517	0.0397
	65.625	567.36	0.0844	0.0450
	70.313	555.52	0.1104	0.05042
	75.000	545.26	0.1267	0.0584
	79.688	534.44	0.1636	0.06363
	84.375	-----	-----	-----
2	4.688	675.22	-----	-----
	9.375	654.00	-----	-----
	25.000	633.98	0.0305	0.0377
	29.688	625.83	0.0570	0.0397
	34.375	621.10	0.0578	0.0422
	40.625	612.08	0.0678	0.0464
	45.313	607.49	0.0715	0.0472
	50.000	598.98	0.0827	0.0502
	65.625	567.96	0.1357	0.0629
	70.313	558.28	0.1493	0.0689
	75.000	555.40	0.1993	0.1367
	79.688	541.42	0.2072	0.1455
	84.375	535.26	0.2469	0.1564
3	4.688	655.27	-----	-----
	9.375	623.98	-----	-----
	25.000	611.16	0.0319	-----
	29.688	612.33	0.0367	-----
	34.375	608.58	0.0575	-----
	40.625	599.59	0.0598	0.0437
	45.313	594.59	0.0689	0.0443
	50.000	587.50	0.0651	0.0465
	65.625	570.40	0.1044	0.0838
	70.313	558.72	0.1463	0.0975
	75.000	548.33	0.1735	0.1098
	79.688	538.28	0.2062	0.1237
	84.375	540.80	0.3013	0.1338

A comparison of boundary layer thickness for the two levels of freestream turbulence, for each of the three configurations, is made in Figs. 23, 24, and 25. These show that the boundary layer thickness increases substantially and rapidly, with freestream turbulence, after 50% chord. This behavior is similar for all three configurations, however the rate and the amount of change is proportional to the amount of surface roughness. For the first half of the blade surface, any changes in boundary layer thickness are relatively small and inconsistent from configuration to configuration. In case of smooth blade, these changes ahead of 50% chord are negligible. For configuration #2, the boundary layer thickness with increased turbulence is higher from the forward most data point, but the rate of increase is negligible till about 40% chord. For configuration #3, the boundary layer thickness is slightly less with increased turbulence till about 30% chord, from where it starts increasing. This inconsistency in thickness change of the boundary layer, with high freestream turbulence, for the forward area can be attributed to the error in positioning of the boundary layer probe. The probe is set at a distance of 0.03 inches above the blade surface by manually moving the traversing mechanism. The accuracy of this is ± 0.005 inches, additionally, the diameter of anemometer wire is 0.002 inches. These combined can give an error of 0.012 inches. The boundary layer thickness in the front

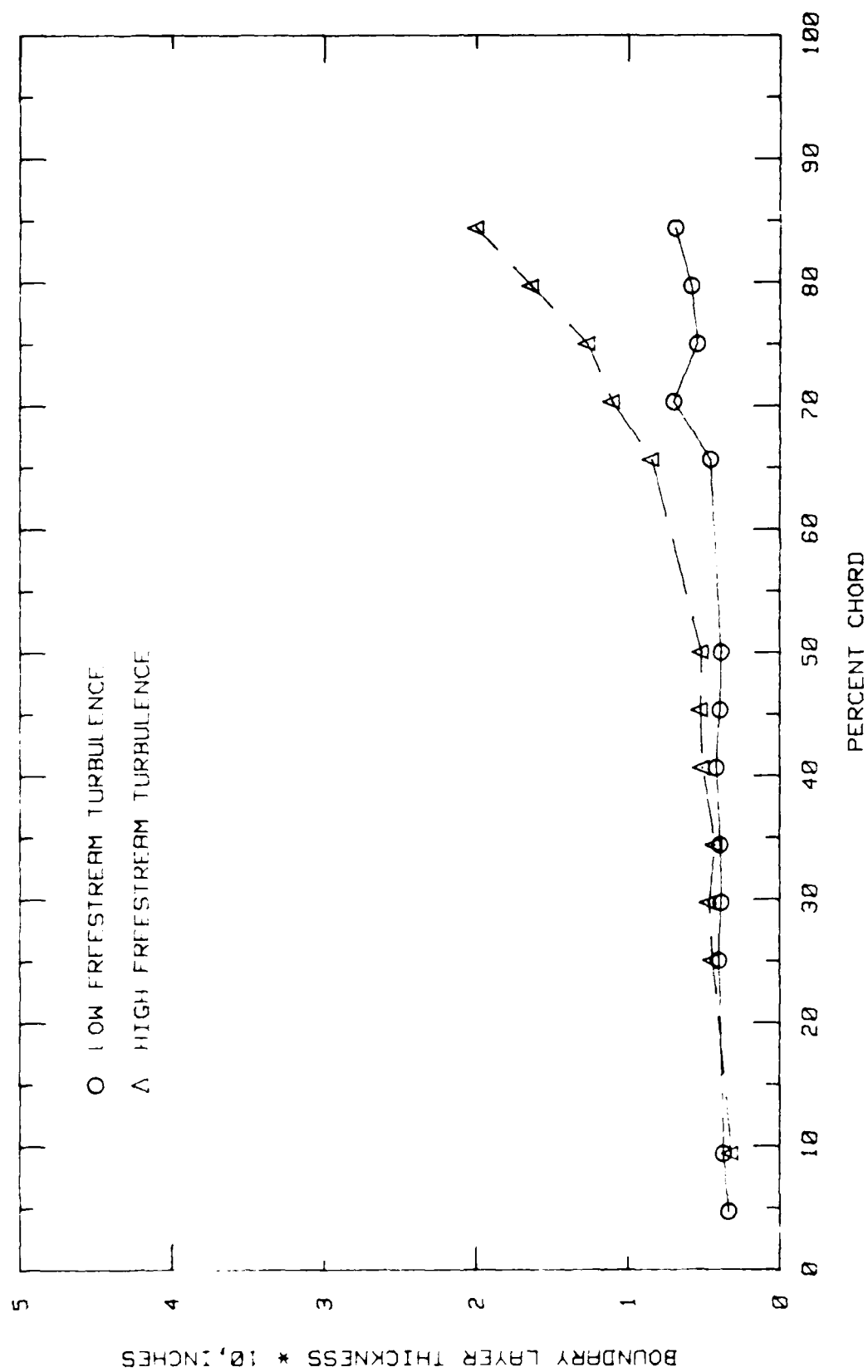


Fig. 23 Boundary Layer Growth Suction Surface Conf#1

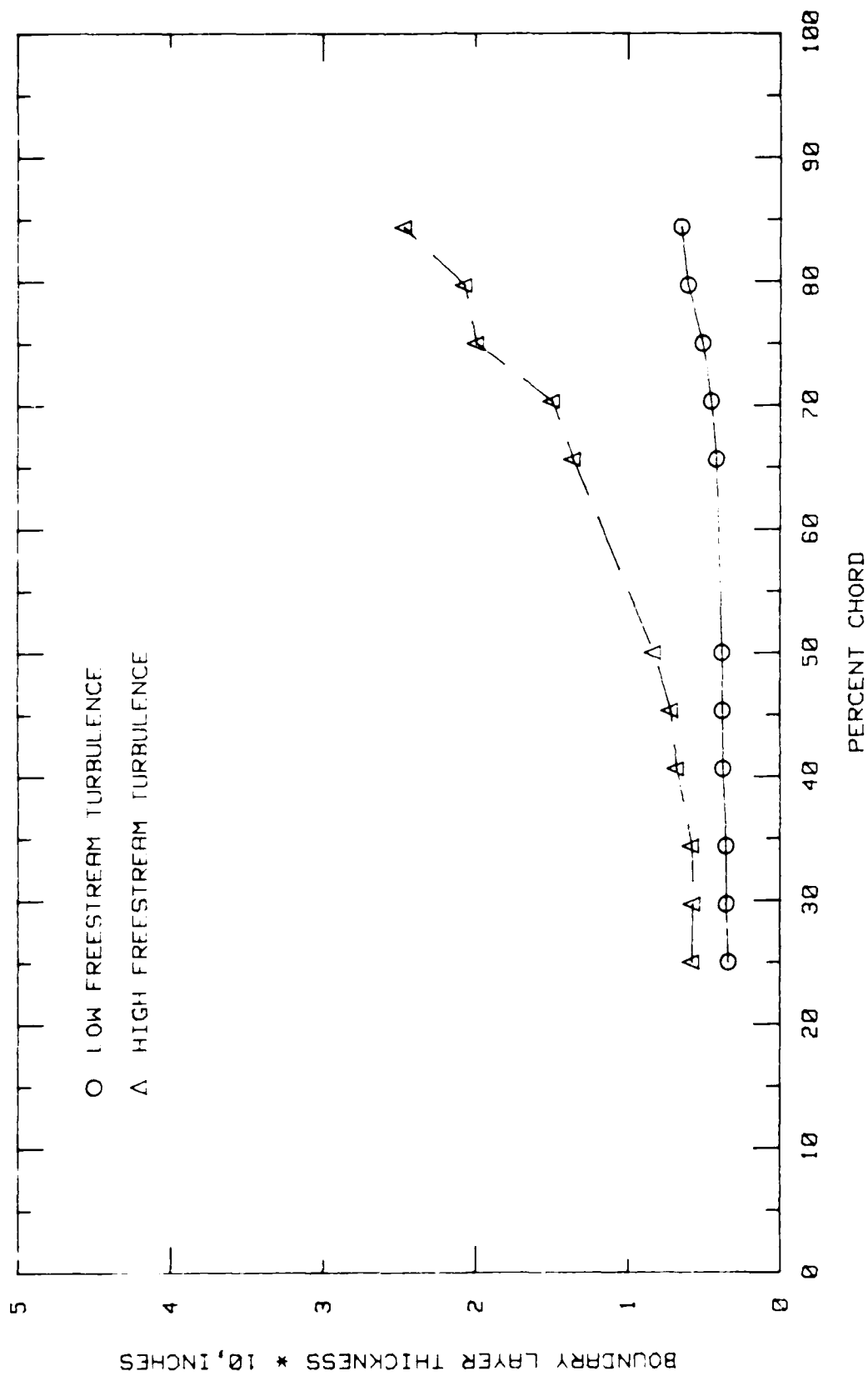


Fig. 24. Boundary Layer Growth Suction Surface Conf#2

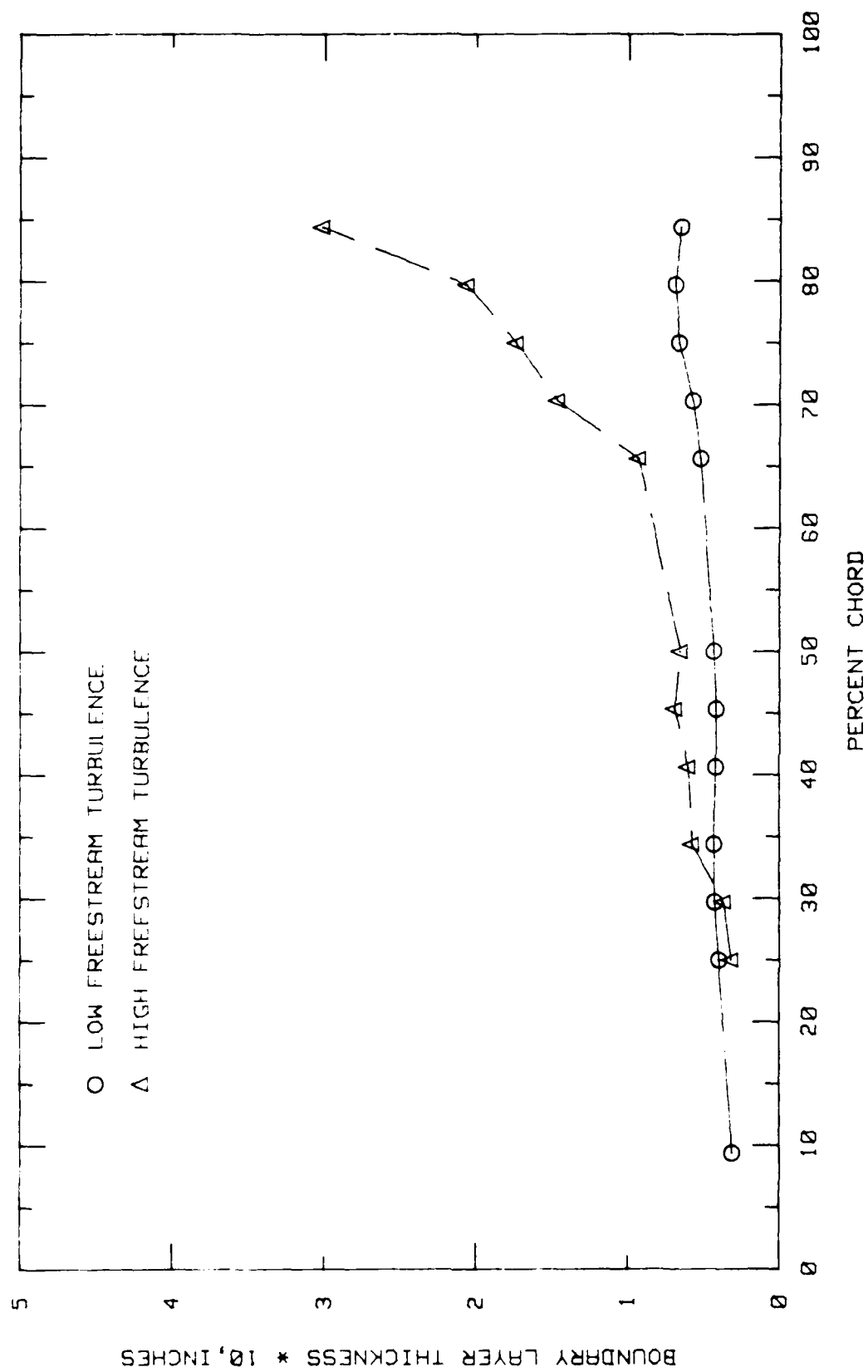


Fig. 25 Boundary Layer Growth Suction Surface Conf#3

region is about 0.03 inches, this positioning error can therefore be greater than 1/3rd of the boundary layer thickness in forward region.

With the exception of smooth blades with low freestream turbulence, boundary layer could not be detected at 4.688% chord. This indicates that the boundary layer thickness at this point is less than 0.03 inches for all other cases. Also, for configuration #1, boundary layer at 84.375% chord could not be determined because of maximum traverse limitation at that time. This point was therefore extrapolated. Later for the other configurations, this was resolved by increasing the number of points per traverse in the trailing edge region.

Boundary layer thickness with low freestream turbulence was compared with the same obtained by Poulin (3:51), the results were similar. Therefore, this method was considered valid for determining the influence of freestream turbulence on boundary layer thickness.

To compare the boundary layer edge velocity at two levels of turbulence, dimensionless edge velocity (V_e/V_1) was plotted. These plots for configurations 1, 2, and 3 are given in Figs. 26, 27, and 28 respectively. It is observed that with increase of freestream turbulence, there is an increase in edge velocity

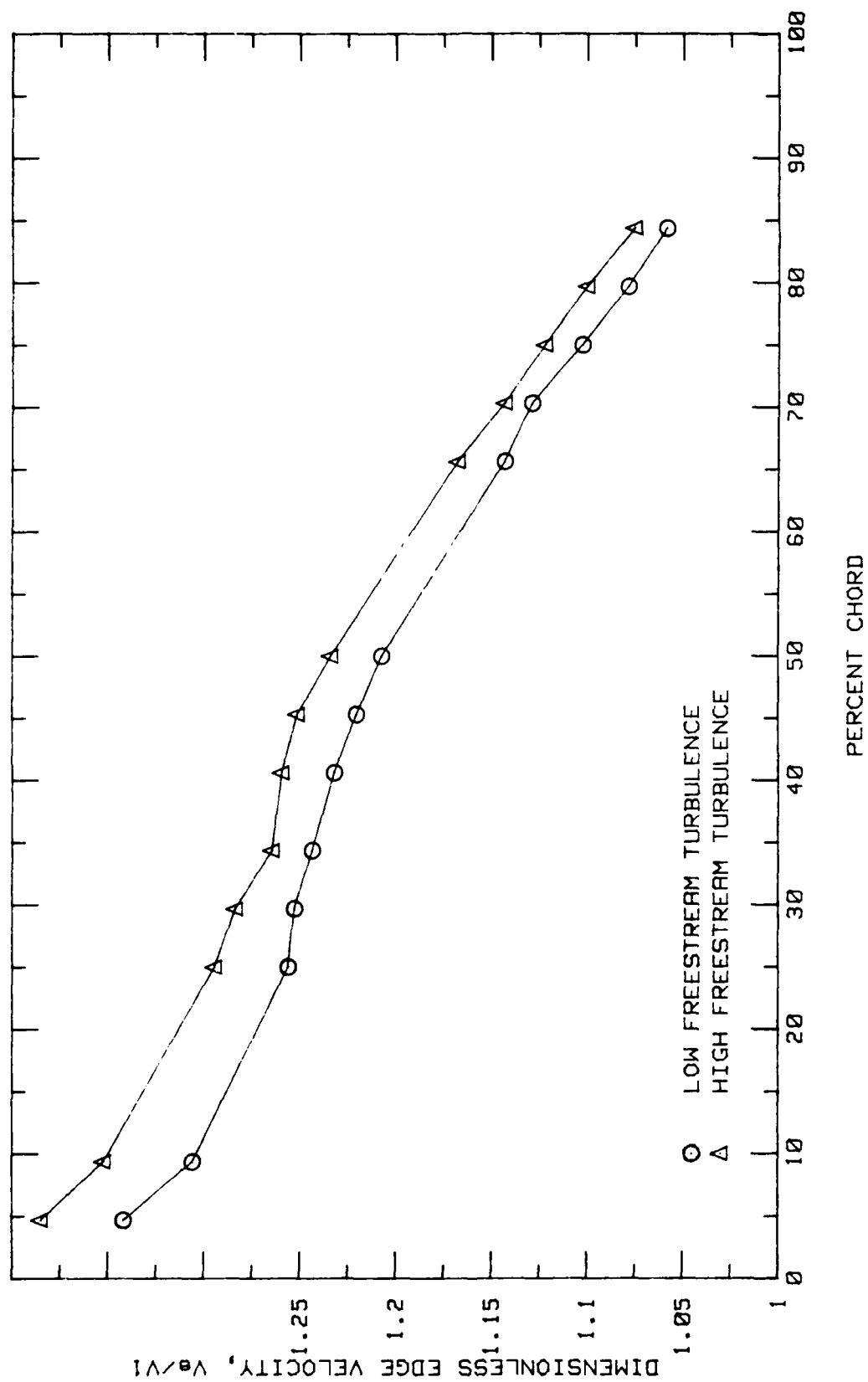


Fig.26. Boundary Layer Edge Velocity Along the Suction Surface Conf#1

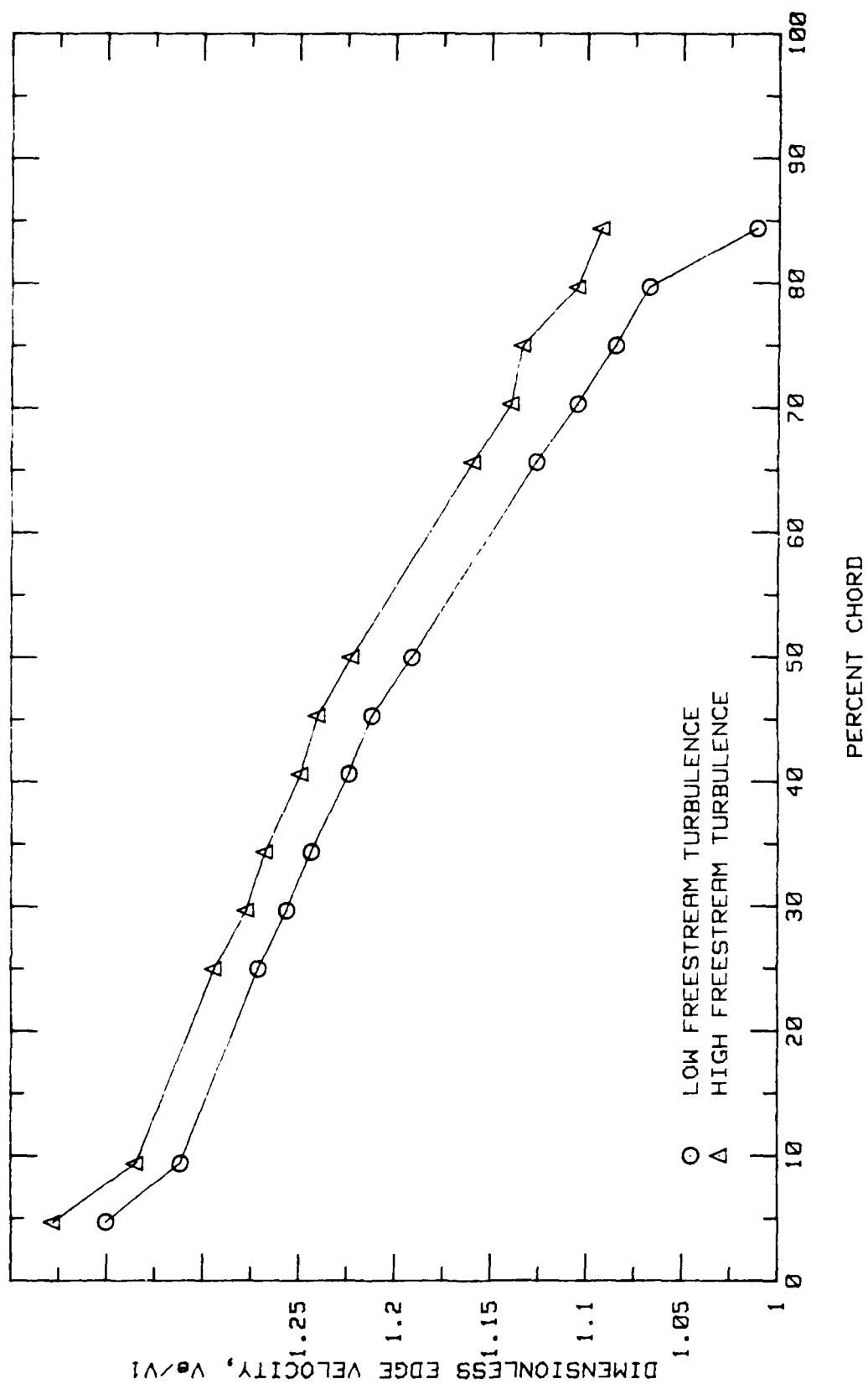


Fig.27. Boundary Layer Edge Velocity Along the Suction Surface Conf#2

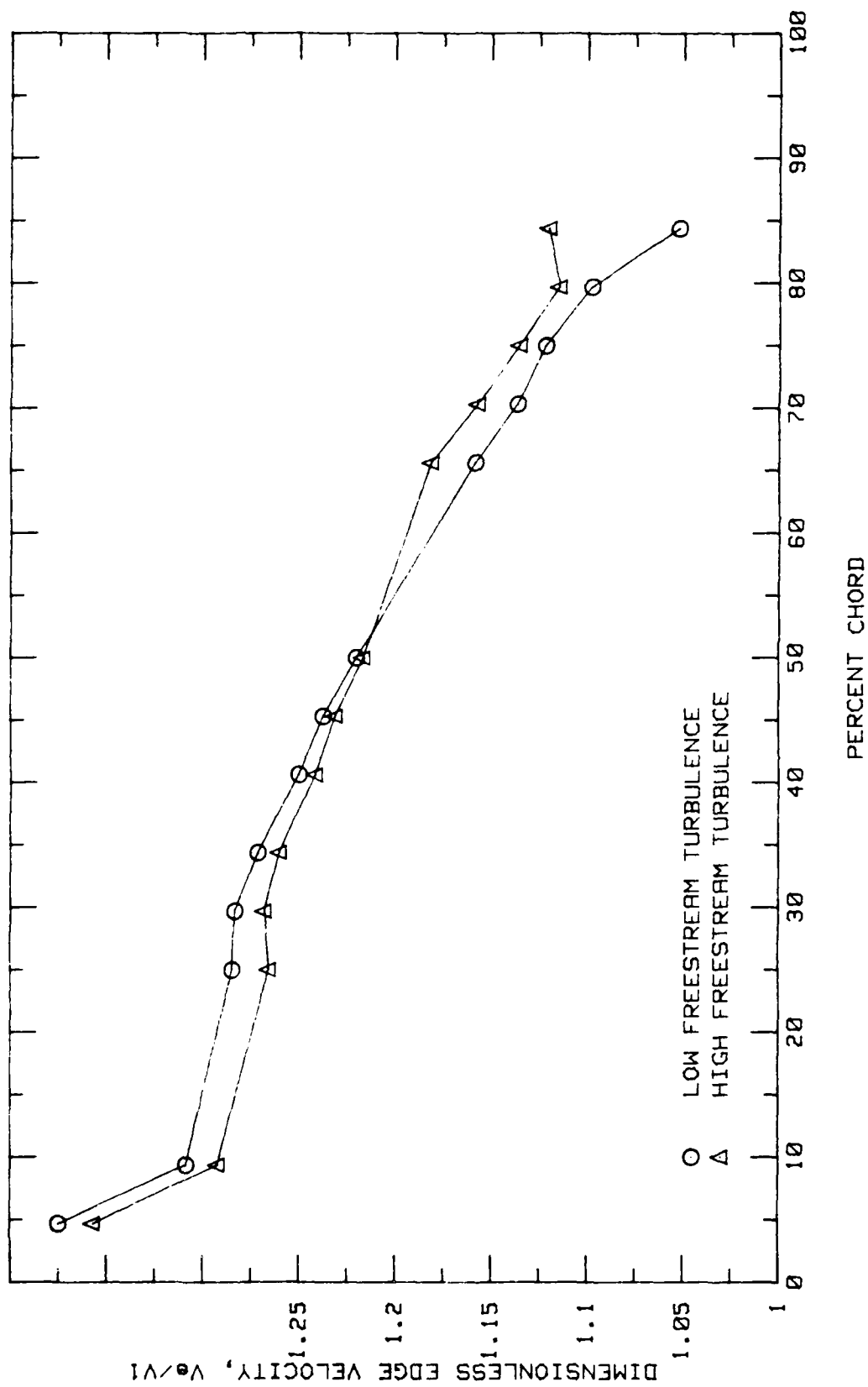


Fig.28. Boundary Layer Edge Velocity Along the Suction Surface Conf#3

for all three configurations behind 50% chord. The amount of increase in this region is similar for all three configurations. This behavior can be correlated with the increase in boundary layer thickness in this area. An increase in boundary layer would restrict the flow area, therefore to maintain the same mass flow rate, the velocity would increase.

The change in edge velocity from leading edge to 50% chord varies with each configuration. For conf. #1, the edge velocity in this region, with increase of freestream turbulence, increases more than it does in the rear half. For conf. #2, there is an increase in the velocity of forward portion, but less than the increase that occurs for the rear portion. In case of conf. #3, the edge velocity reduces with freestream turbulence for the front half of the blade. It almost seems that with an increase in surface roughness, the response of boundary layer to freestream turbulence, reduces. It may be noted that surface roughness has been incorporated starting 1/16th of the inch behind leading edge and extends to 25% chord. No definite explanation for this response of boundary layer edge velocity in the forward half portion of the blade can be given. This effect of surface roughness is confined to the area in the immediate vicinity of the roughness. It would be interesting to study this behavior with roughness over the entire suction surface.

The observations made in boundary layer study can be summed up by stating that the boundary layer thickness and its growth rate, in the rear half of the blade, increased with increase of freestream turbulence. The edge velocity in this region also increased. In the forward half of the blade, the effect of turbulence on boundary layer thickness was negligible. The edge velocity in this region changed depending upon the local surface roughness. The data obtained in this investigation is not enough to elaborate upon this aspect.

VI. CONCLUSIONS AND RECOMMENDATIONS

Conclusions: This study was mainly concerned with determining the effects of high freestream turbulence on a two dimensional cascade, at high Reynolds number. As a result of this investigation, the following conclusions can be made.

- (i) The total pressure loss coefficient in a cascade decreases with increase of freestream turbulence.
- (ii) Total pressure loss coefficient in the wake of a cascade increases, with increased freestream turbulence, because of high mixing losses.
- (iii) The combined effect of cascade losses and wake losses make the total pressure loss coefficient almost same for both low and high freestream turbulence. This trend seems to be independent of blade surface roughness. However, surface roughness increases the total pressure loss coefficient.
- (iv) Pressure coefficient (or static pressure) at each point on the blade suction surface, increases with an increase in freestream turbulence. This trend remains same with high surface roughness.

- (v) Any changes in boundary layer thickness, with high freestream turbulence, from leading edge to 50% chord, are negligible. This is similar for all three roughness configurations.
- (vi) From 50% chord till the trailing edge, high freestream turbulence causes the boundary layer thickness to increase very rapidly. This behavior is strengthened with an increase in surface roughness.
- (vii) The boundary layer edge velocity increases with an increase in freestream turbulence for blades with less surface roughness. When the surface roughness is increased, this behavior is changed in the immediate vicinity of high surface roughness.

Recommendations: Results of this investigation indicate that the effects of freestream turbulence upon boundary layer edge velocity change with local surface roughness. A confirmation of this effect is possible with blades having roughness over the whole suction surface. This investigation may be of interest in future.

It is also recommended that the pressure loss coefficient further downstream, where the wake mixing has been completed, may

be investigated. This is required to confirm the total pressure loss and the effect of freestream turbulence on it.

This study was limited to one particular blade setting. As suggested previously by Poulin (3:79), it may be of interest to modify the test section to allow for variation of angle of attack and angle of incidence.

Finally, there are two areas where the numerical values of the data are in doubt. Firstly, velocity readings from the anemometer are about 5% higher than those calculated by static pressure measurements, secondly, the boundary layer thickness can have an error of ± 0.006 inches due to initial positioning of the probe. The possibility of eliminating these errors may be studied.

APPENDIX A: Component Listing

<u>Component</u>	<u>Type/Model#</u>
Pressure Transducers	
Tank Total Pressure	Statham PM60TC
Test Section Inlet Static	Statham P6TC
Test Section Exit Static	Statham P6TC
Ambient Pressure	CEC 4-326
Bridge Balance	Type 8-108
DC Power Supply	HP 6205C
Scanivalve System	
Pressure Transducer	PDCR 23D
Scanivalve	48S9-3003
Controller	CTLR 2/S2-S6
Scanner Position Display	J102/J104
Thermocouples	
Copper-Constantan	Omega T-type
quantity 4	
Traversing Mechanism	
Motors quantity 2	North American
	Phillips part
	no. K82952-M
	Astrosystems
Encoder Transducer qty. 2	MT28-1/10
Hot Film Anemometer System	
Anemometers quantity 2	TSI Model 1050
Monitor and Power Supply	TSI Model 1051-6
Oscilloscope	B&K Model 1570A
Boundary layer hot film probe	TSI Model 1218-20
X-configuration hot film probe	TSI Model 1241-10
Boundary Layer Probe Support	TSI Model 1150-18
X-configuration Probe Supp.	TSI Model 1155-18
Calibrator (modified)	TSI Model 1125
Transformer	General Radio Co.
	Type 50B
Data Acquisition System	
Computer	HP 3052A
Disk Drives quantity 2	HP 9845B
Channel Scanner	HP 9885M, 9885S
Digital Voltmeter	HP 3495A
Printer	HP 3455A
Plotter	HP 9871A, 2934A
	HP 9872S

APPENDIX B: Hot Film Anemometer Calibration

The calibration technique used was first developed by Rivir and Vonada (3:81). Basically this is a heat transfer problem in which, variation of Nusselt number with Reynolds number, is calibrated. Subsequently, in actual experiments, Nusselt number is calculated from measurements, and the corresponding Reynolds number is obtained from calibration curve.

King developed an empirical relation for this problem.

$$Nu = A + B Re^n$$

This is known as King's law. Nu is the Nusselt number, A and B are the intercept and slope of the calibration curve, Re is the Reynolds number and n a constant depending upon the Reynolds number. As the freestream temperature varies a lot from the wire temperature, this equation has been modified to get a correction for fluid properties in freestream (3:82). The modified equation is

$$Nu(T_m/T_o) = B Re^n$$

where $T_m = (T_w + T_o)/2$, T_w is the temperature of the wire and T_o is the temperature of freestream.

The calibration procedure used in this study is exactly the same as adopted by Poulin (3:83-88). This

calibration was done for a range of temperature from 100°F to 125°F in warm weather and from 85°F to 110°F in cooler weather. For greater accuracy, the resistance of the cable connecting the anemometer to the probe was also included. This modified the Nusselt number equation as follows

$$Nu(T_m/T_o)^m = \frac{E_o^2 R_w}{K_t \gamma (R_3 + R_w + R_c)^2 (T_w - T_o)}$$

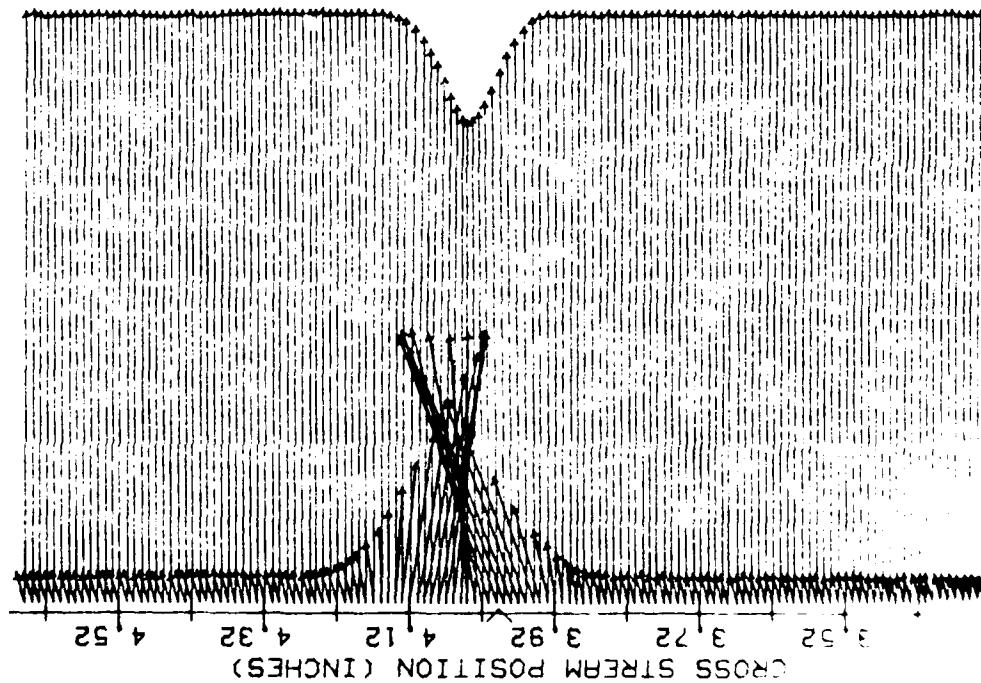
where E_o = Voltage output of the anemometer
 R_w = Resistance of the probe
 R_3 = Bridge resistance (3:87)
 R_c = Cable resistance
 K_t = Thermal conductivity of the flow

APPENDIX C

Wake Survey: Configuration #1

LOW AND HIGH FREESTREAM TURBULENCE

VANE WAKE: CONF. NO.1, EVAL. NO.1 LOW TURB.
 TRAVERSE NO. 1.00 AT 1.25 INCHES



Wake Velocity and Turbulence Intensity Profiles, Conf. #1, $x/c = 0.625$

AD-A190 615

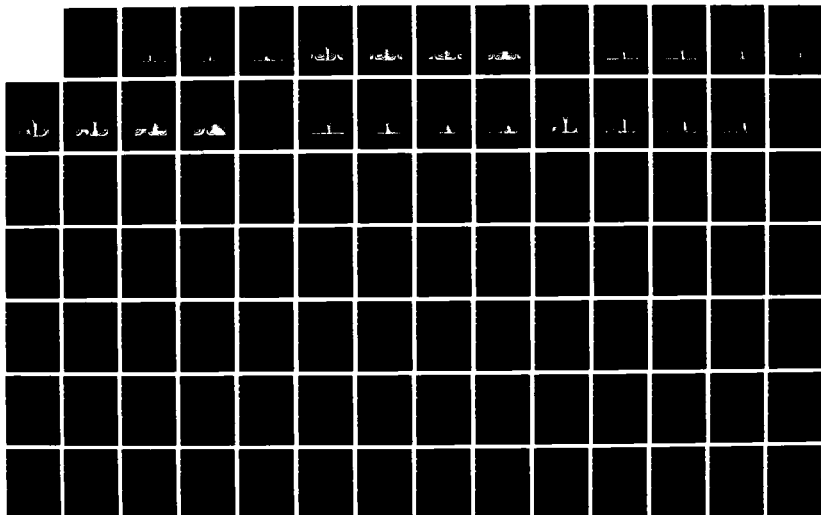
EFFECT OF FREESTREAM TURBULENCE ON A TWO DIMENSIONAL
CASCADE WITH DIFFER. (U) AIR FORCE INST OF TECH
WRIGHT-PATTERSON AFB OH SCHOOL OF ENGI.. S ADAR
MAR 88 AFIT/GAE/AA/88H-1

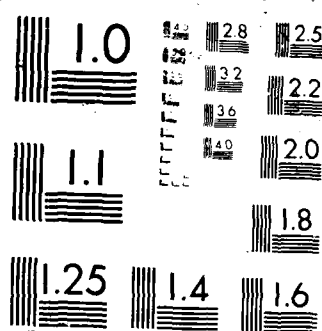
2/3

UNCLASSIFIED

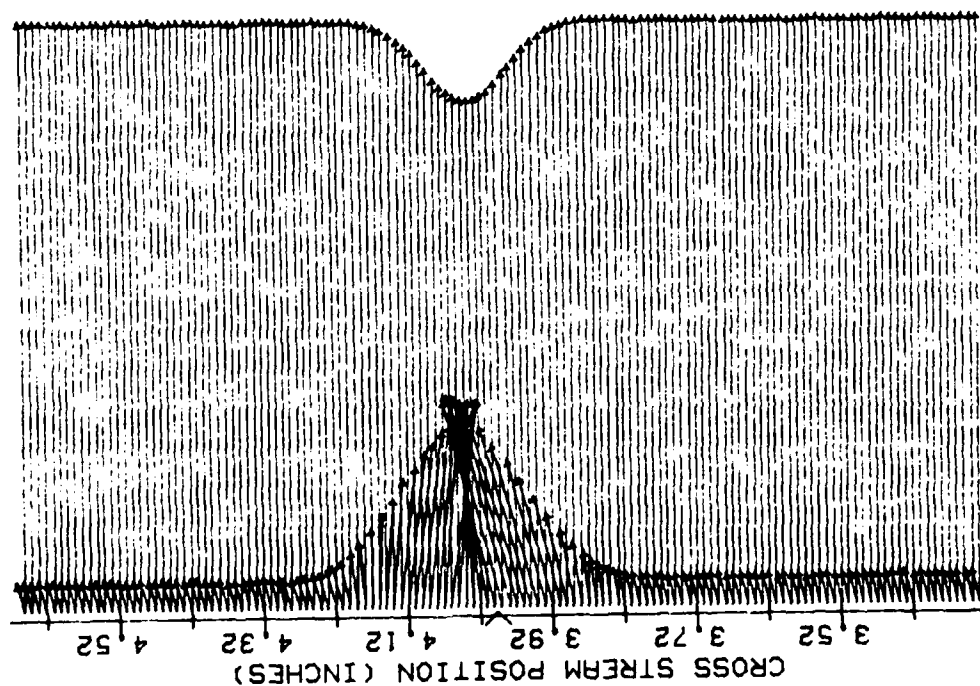
F/O 20/4

NL





VANE WAKE: CONF. NO.1, EVAL. NO.1 LOW TURB.
 TRAVERSE NO. 2.00 AT 2.25 INCHES



SCALE (INCHES)

— VEL. SCALE=150.00 (FT/SEC)/INCH
 - - - % TURB INT SCALE= 5.00 % /INCH

Fig. 30. Wake Velocity and Turbulence Intensity Profiles, Conf. #1, $x/c = 1.125$

VANE WAKE: CONF. NO.1, EVAL. NO.1 LOW TURB.
 TRAVERSE NO. 3.00 AT 3.25 INCHES

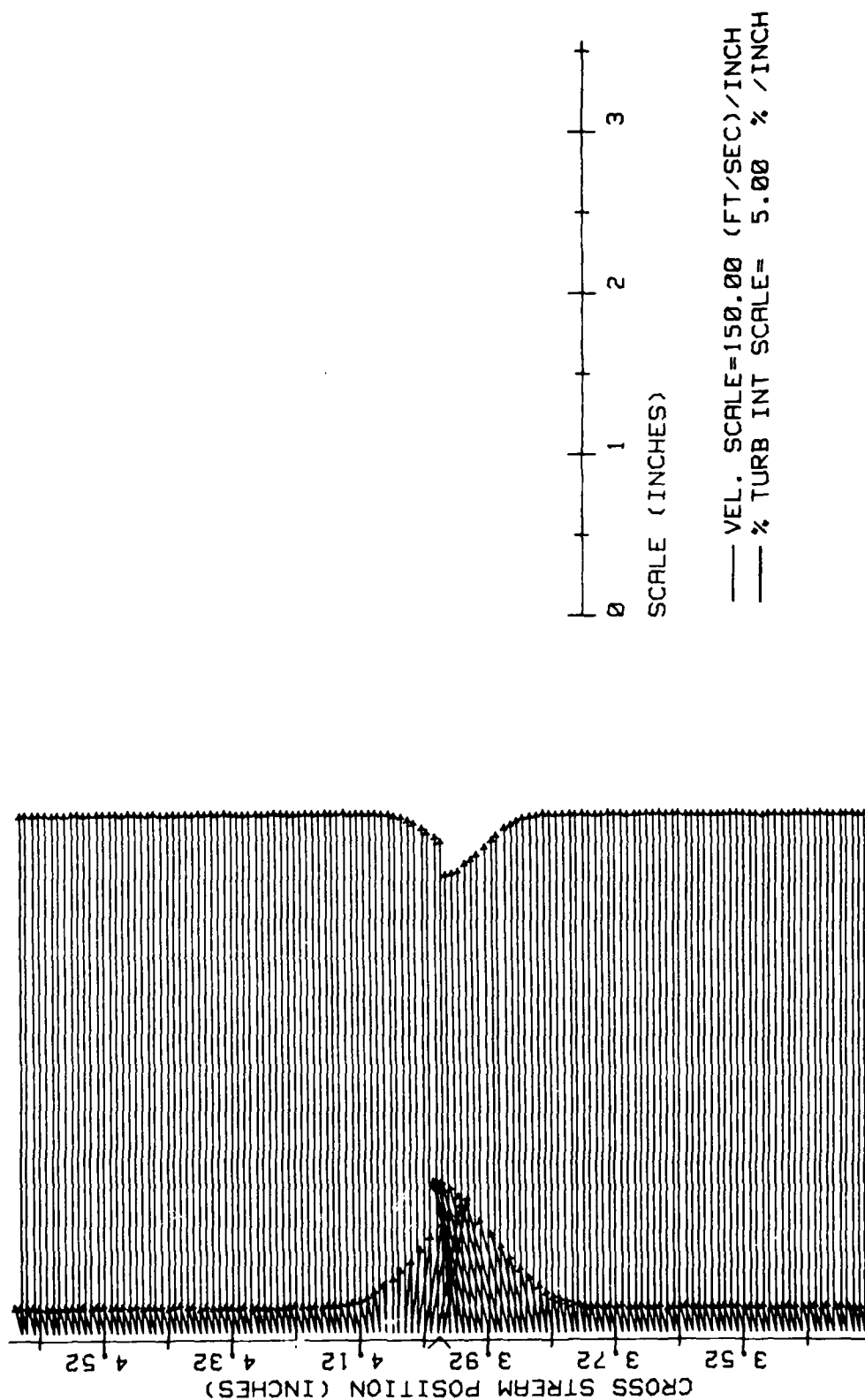


Fig. 31. Wake Velocity and Turbulence Intensity Profiles, Conf. #1, $x/c = 1.625$

VANE WAKE: CONF. NO.1, EVAL. NO.1 LOW TURB.
TRAVERSE NO. 4.00 AT 4.25 INCHES

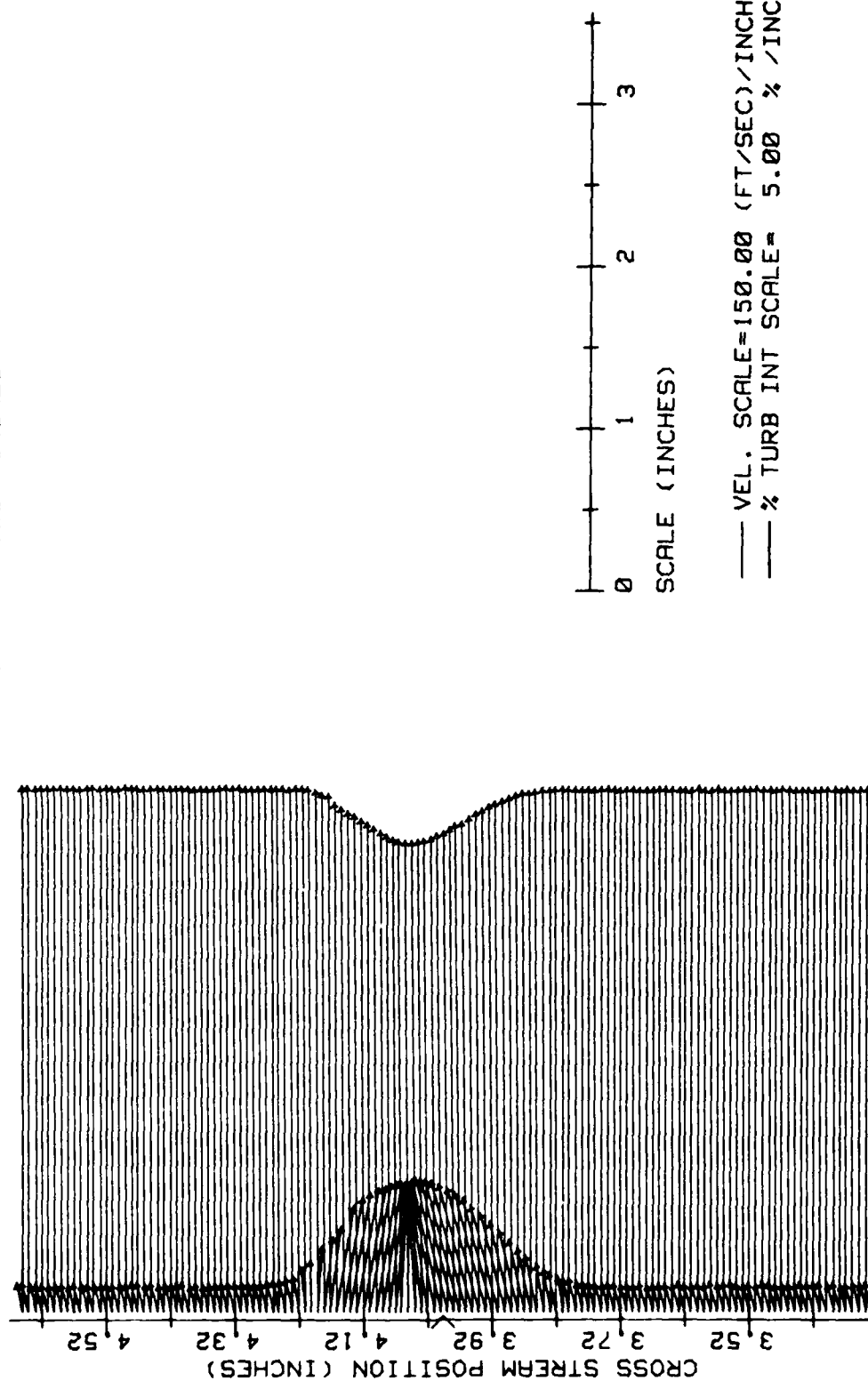
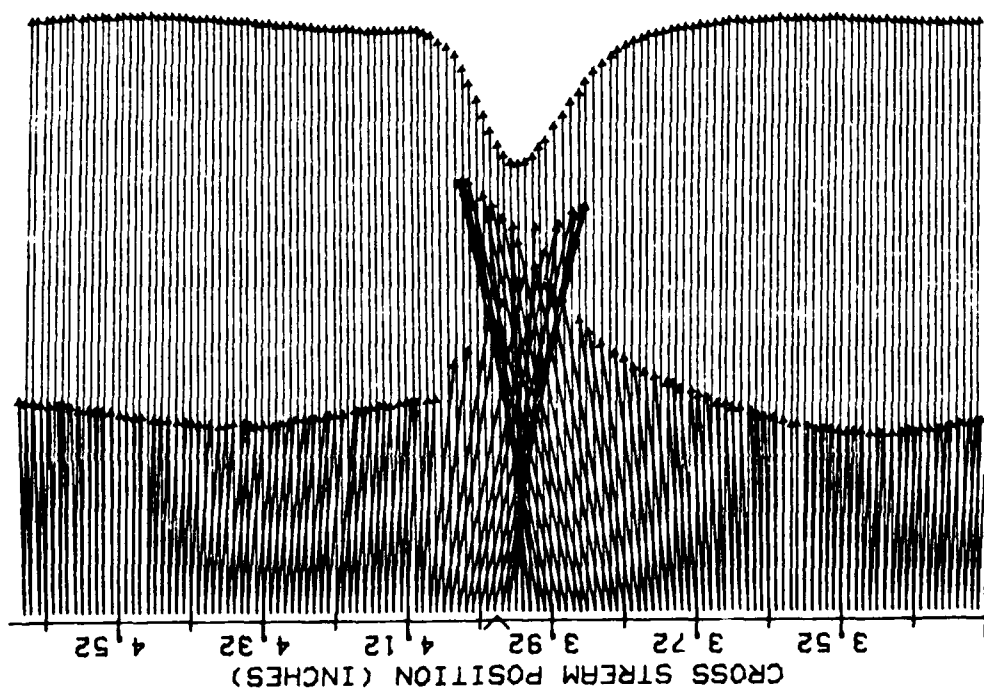


Fig. 32. Wake Velocity and Turbulence Intensity Profiles, Conf. #1, $x/c = 2.125$

VANE WAKE: CONF. 1, EVAL. NO. 1 HIGH TURB.
 TRAVERSE NO. 1.00 AT 1.25 INCHES



SCALE (INCHES)

0 1 2 3

— VEL. SCALE=150.00 (FT/SEC)/INCH
 - - - % TURB INT SCALE= 5.00 % /INCH

Fig. 33. Wake Velocity and Turbulence Intensity Profiles, Conf. #1, $x/c = 0.625$

VANE WAKE: CONF. #1, EVAL. NO.1 HIGH TURB.
TRAVERSE NO. 2.00 AT 2.25 INCHES

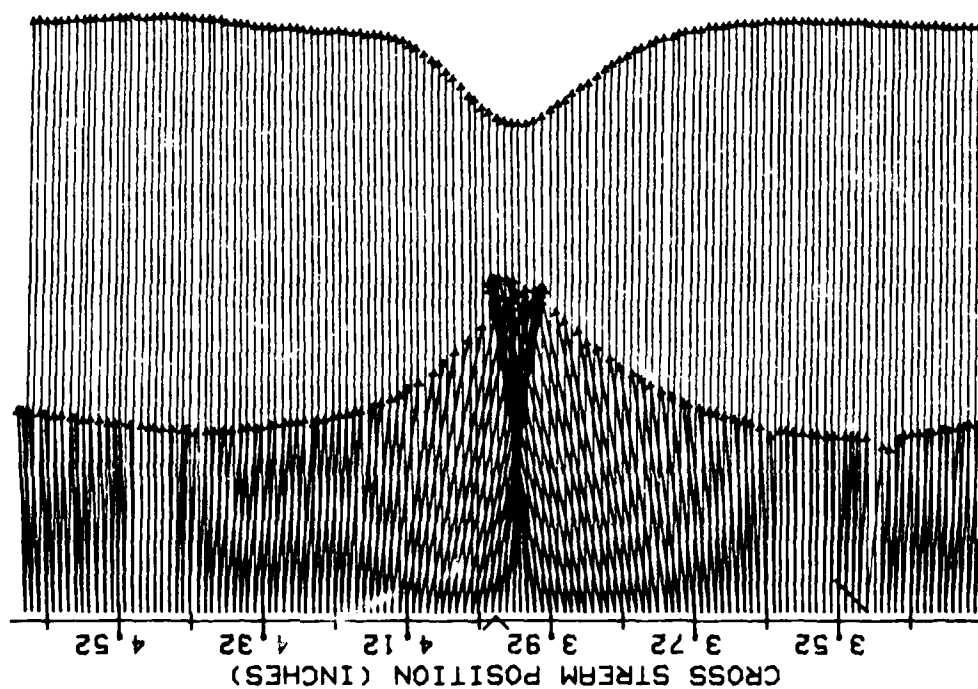
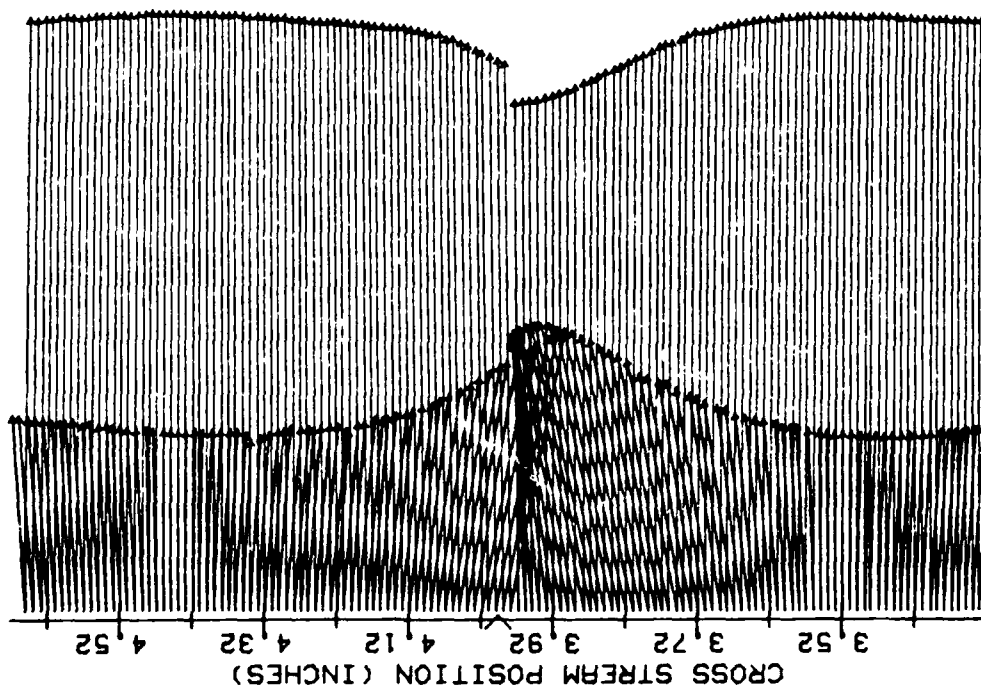


Fig. 34. Wake Velocity and Turbulence Intensity Profiles, Conf. #1, $x/c = 1.125$

VANE WAKE: CONF. #1, EVAL. NO.1 HIGH TURB.
 TRAVERSE NO. 3.00 AT 3.25 INCHES



SCALE (INCHES)

0 1 2 3

— VEL. SCALE=150.00 (FT/SEC)/INCH
 - - - % TURB INT SCALE= 5.00 % /INCH

Fig. 35. Wake Velocity and Turbulence Intensity Profiles, Conf. #1, $x/c = 1.625$

VANE WAKE: CONF. #1, EVAL. NO. 1 HIGH TURB.
 TRAVERSE NO. 4.00 AT 4.25 INCHES

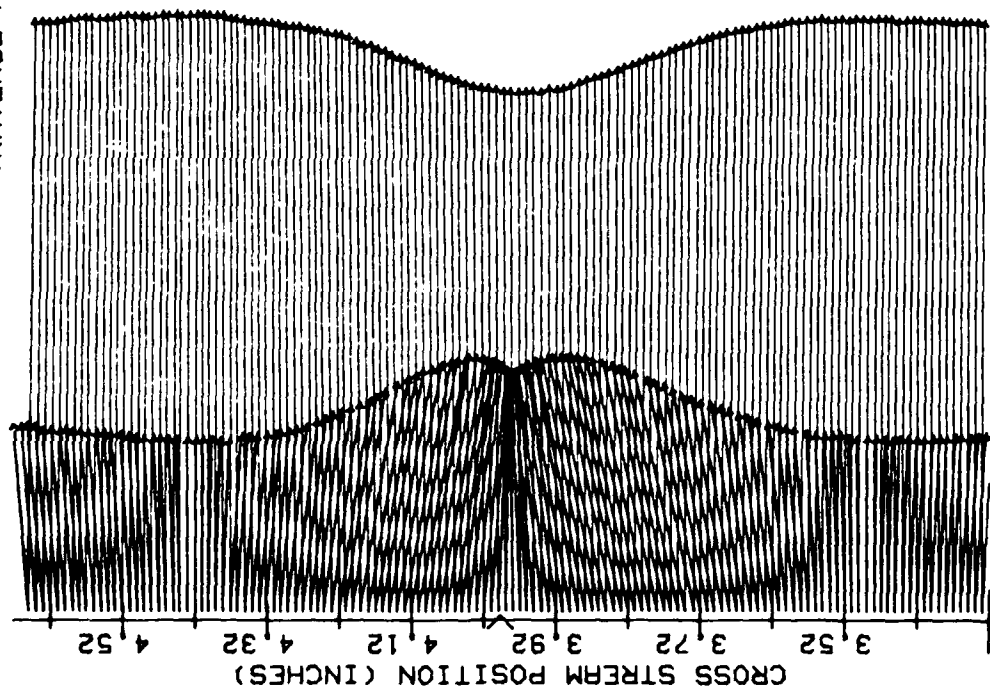


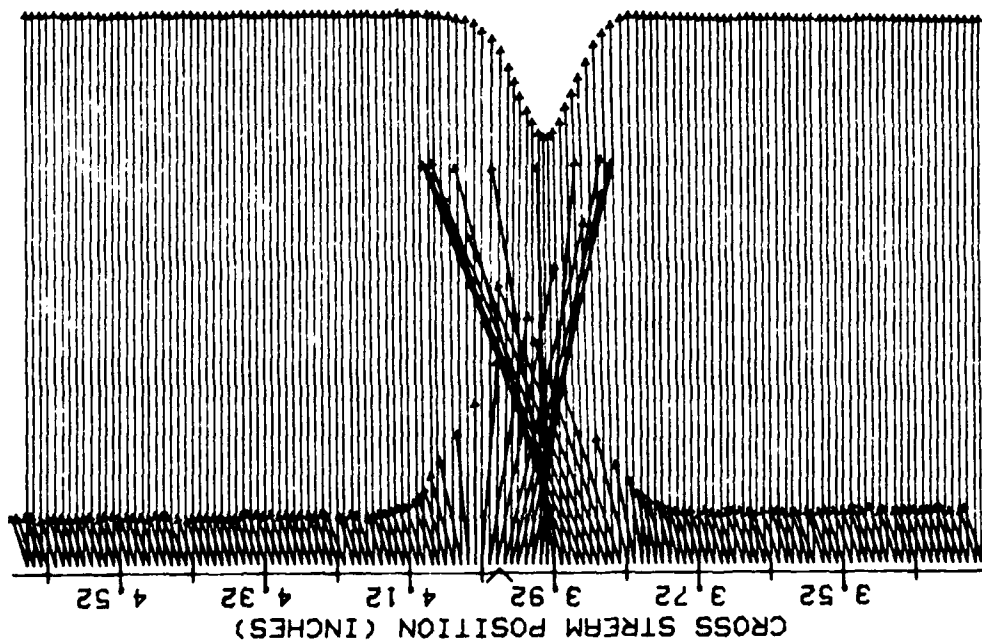
Fig. 36. Wake Velocity and Turbulence Intensity Profiles, Conf. #1, $x/c = 2.125$

APPENDIX D

Wake Survey: Configuration #2

LOW AND HIGH FREESTREAM TURBULENCE

VANE WAKE: CONF. 2, EVAL. NO. 1 LOW TURB.
 TRAVERSE NO. 1.00 AT 1.25 INCHES



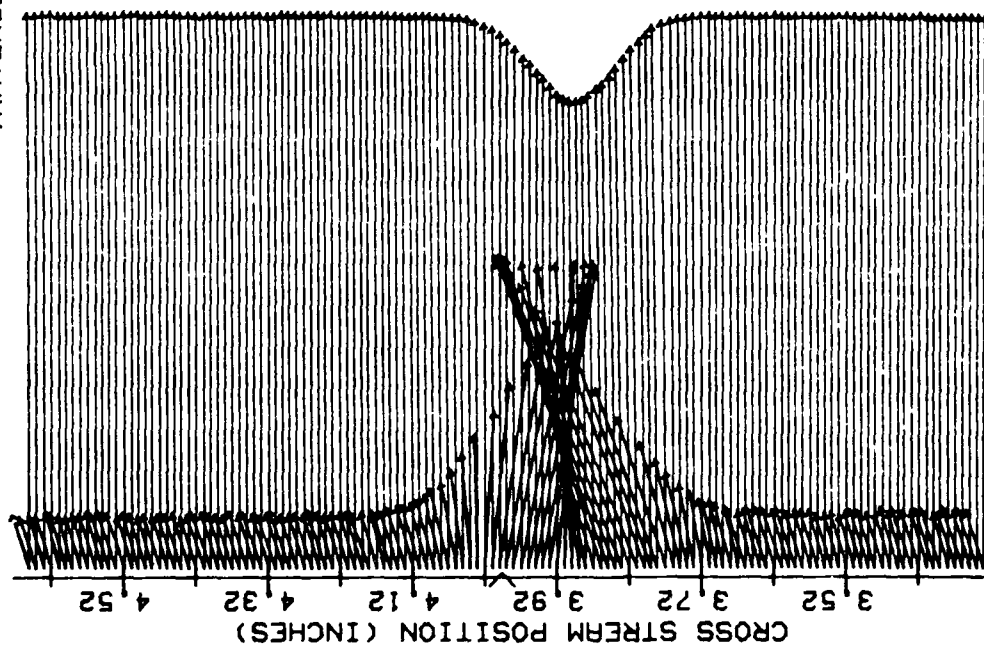
SCALE (INCHES)

0 1 2 3

— VEL. SCALE=150.00 (FT/SEC)/INCH
 - - - % TURB INT SCALE= 5.00 % /INCH

Fig. 37. Wake Velocity and Turbulence Intensity Profiles, Conf. #2, $x/c = 0.625$

VANE WAKE: CONF.2, EVAL. NO.1 LOW TURB.
 TRAVERSE NO. 2.00 AT 2.25 INCHES



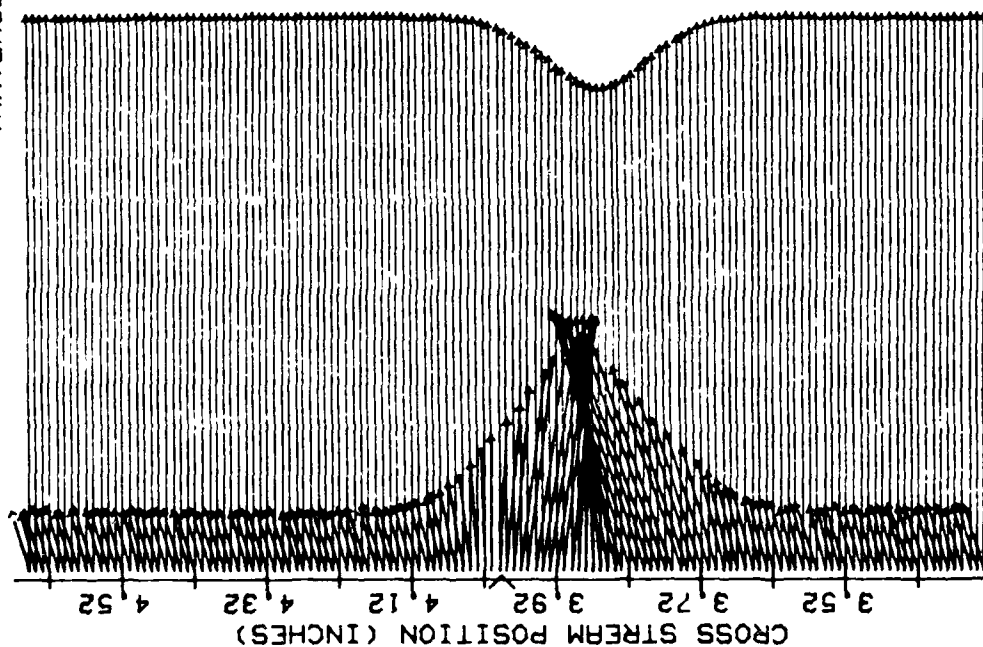
SCALE (INCHES)

0 1 2 3

— VEL. SCALE=150.00 (FT/SEC)/INCH
 - - - % TURB INT SCALE= 5.00 % /INCH

Fig. 38. Wake Velocity and Turbulence Intensity Profiles, Conf. #2, $x/c = 1.125$

VANE WAKE: CONF. 2, EVAL. NO. 1 LOW TURB.
TRAVERSE NO. 3.00 AT 3.25 INCHES



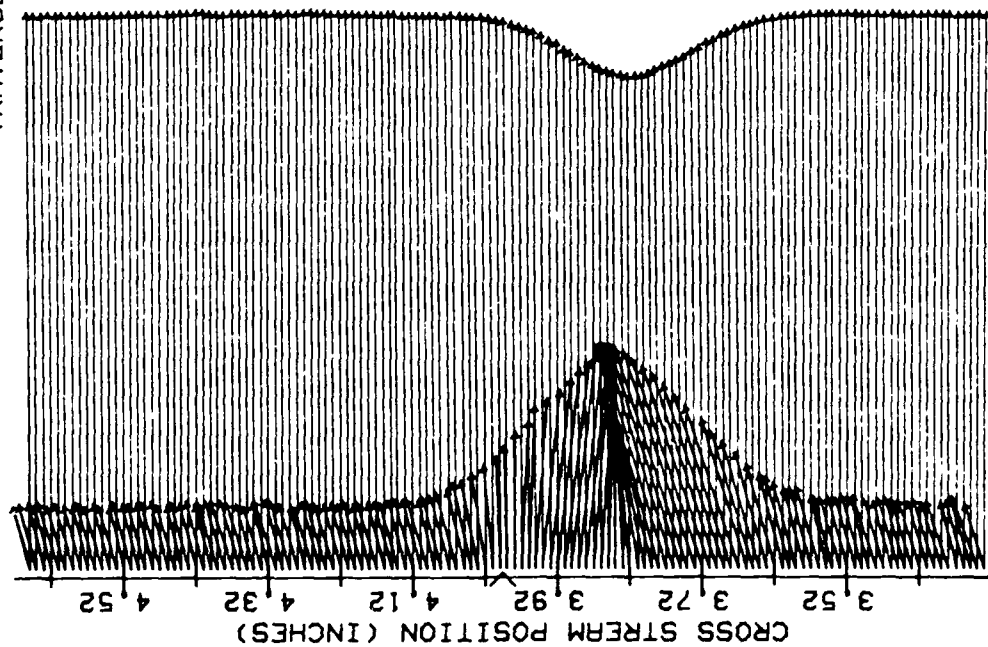
SCALE (INCHES)

0 1 2 3

— VEL. SCALE=150.00 (FT/SEC)/INCH
- - % TURB INT SCALE= 5.00 % /INCH

Fig. 39. Wake Velocity and Turbulence Intensity Profiles, Conf. #2, $x/c = 1.625$

VANE WAKE: CONF. 2, EVAL. NO. 1 LOW TURB.
TRAVERSE NO. 4.00 AT 4.25 INCHES



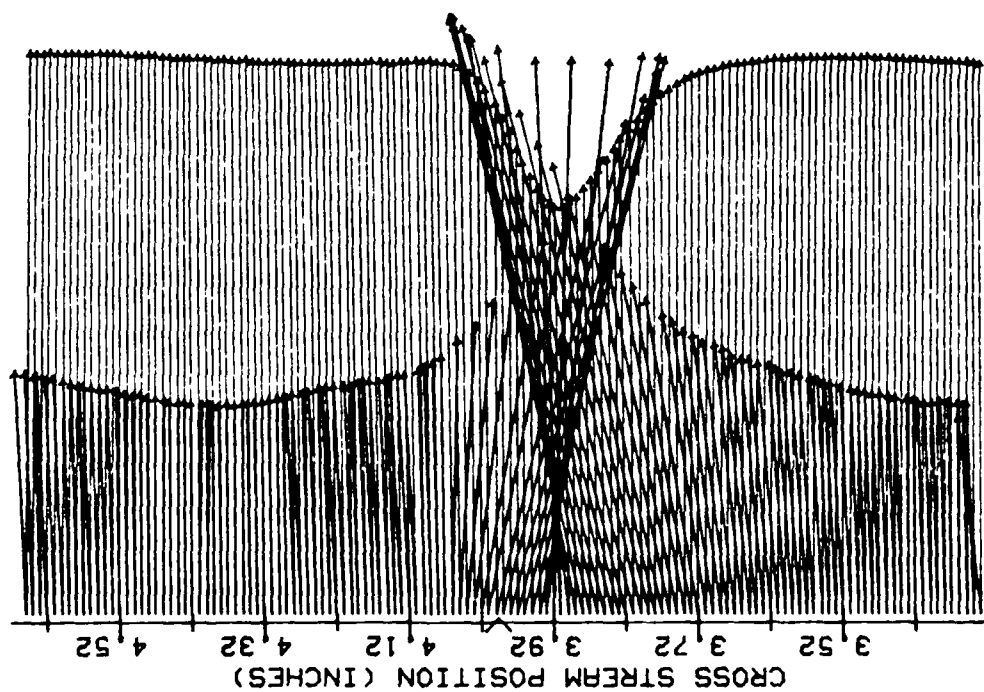
SCALE (INCHES)

0 1 2 3

— VEL. SCALE=150.00 (FT/SEC)/INCH
— % TURB INT SCALE= 5.00 % /INCH

Fig. 40. Wake Velocity and Turbulence Intensity Profiles, Conf. #2, $x/c = 2.125$

VANE WAKE: CONF. NO.2, EVAL. NO.1 HIGH TURB.
TRAVERSE NO. 1.00 AT 1.25 INCHES



SCALE (INCHES)

0 1 2 3

— VEL. SCALE=150.00 (FT/SEC)/INCH
- - - % TURB INT SCALE= 5.00 % /INCH

Fig. 41. Wake Velocity and Turbulence Intensity Profiles, Conf. #2, $x/c = 0.625$

VANE WAKE: CONF. NO.2, EVRL. NO.1 HIGH TURB.
 TRAVERSE NO. 2.00 AT 2.25 INCHES

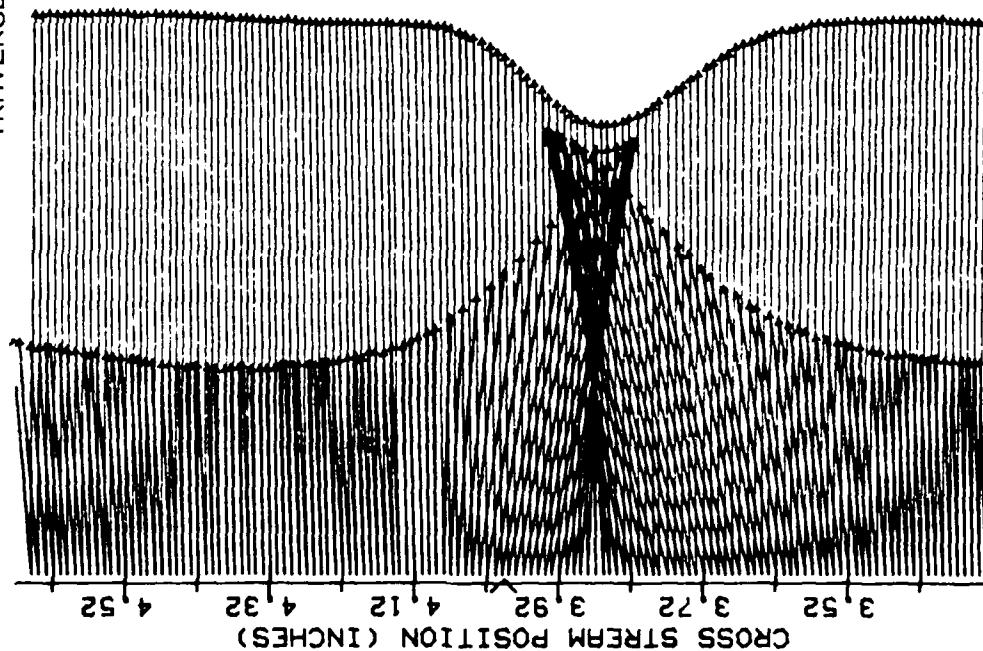
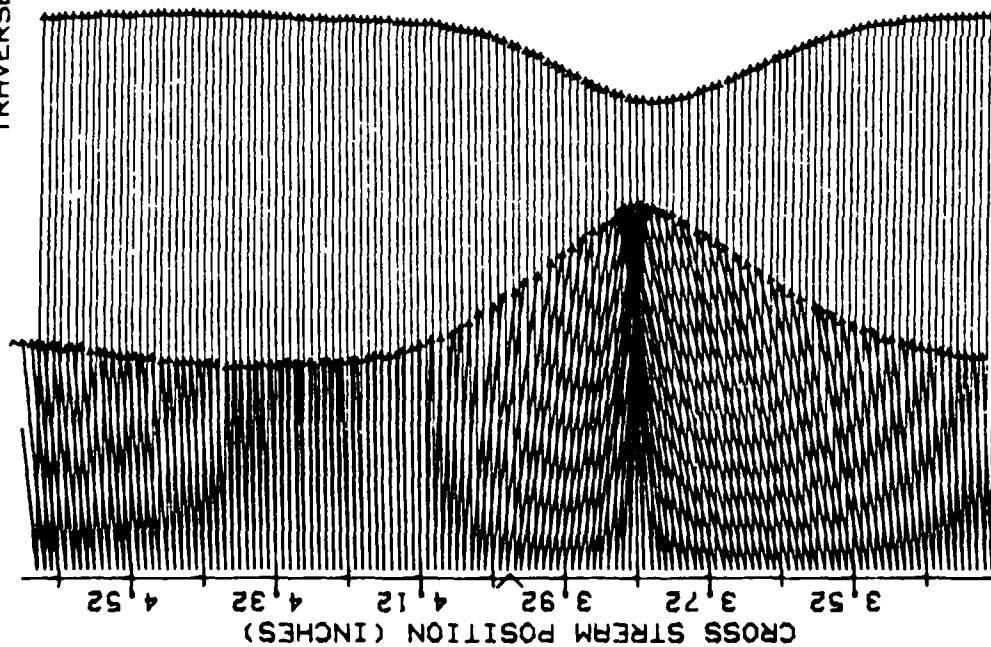


Fig. 42. Wake Velocity and Turbulence Intensity Profiles, Conf. #2, $x/c = 1.125$

VANE WAKE: CONF. NO.2, EVAL. NO.1 HIGH TURB.
 TRAVERSE NO. 3.00 AT 3.25 INCHES

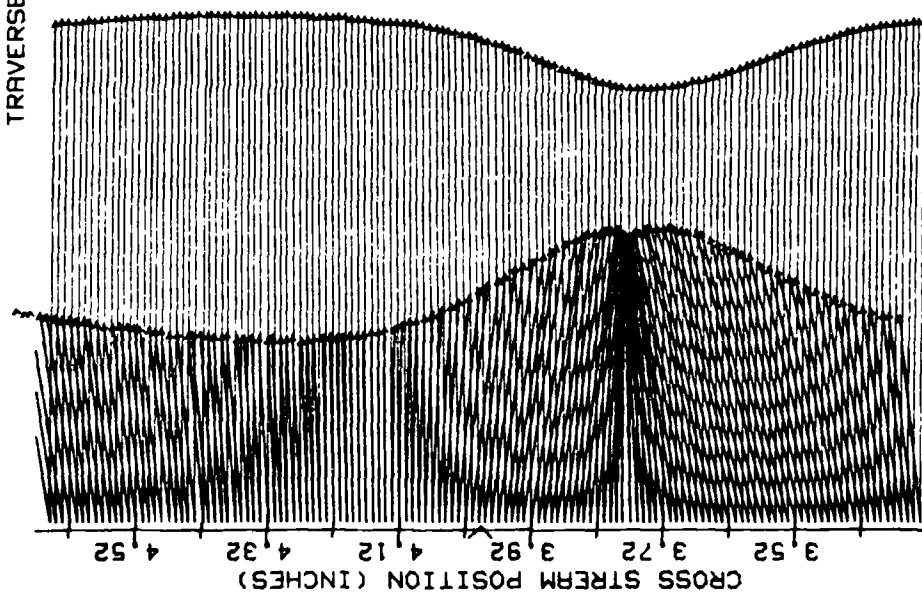


SCALE (INCHES)
 0 1 2 3

— VEL. SCALE=150.00 (FT/SEC)/INCH
 - - - % TURB INT SCALE= 5.00 % /INCH

Fig. 43. Wake Velocity and Turbulence Intensity Profiles, Conf. #2, $x/c = 1.625$

VANE WAKE: CONF. NO.2, EVAL. NO.1 HIGH TURB.
 TRAVERSE NO. 4.00 AT 4.25 INCHES



0 1 2 3
 SCALE (INCHES)

— VEL. SCALE=150.00 (FT/SEC)/INCH
 --- % TURB INT SCALE= 5.00 % /INCH

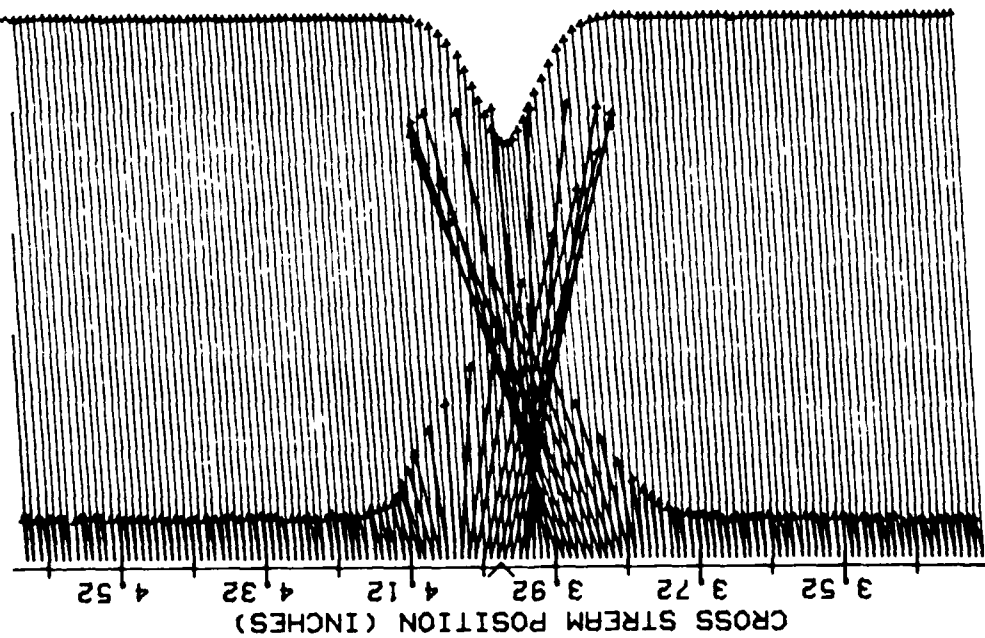
Fig. 44. Wake Velocity and Turbulence Intensity Profiles, Conf. #2, $x/c = 2.125$

APPENDIX E

Wake Survey: Configuration #3

LOW AND HIGH FREESTREAM TURBULENCE

VANE WAKE: CONF. NO.3, EVAL. NO.2 LOW TURB.
 TRAVERSE NO. 1.00 AT 1.25 INCHES

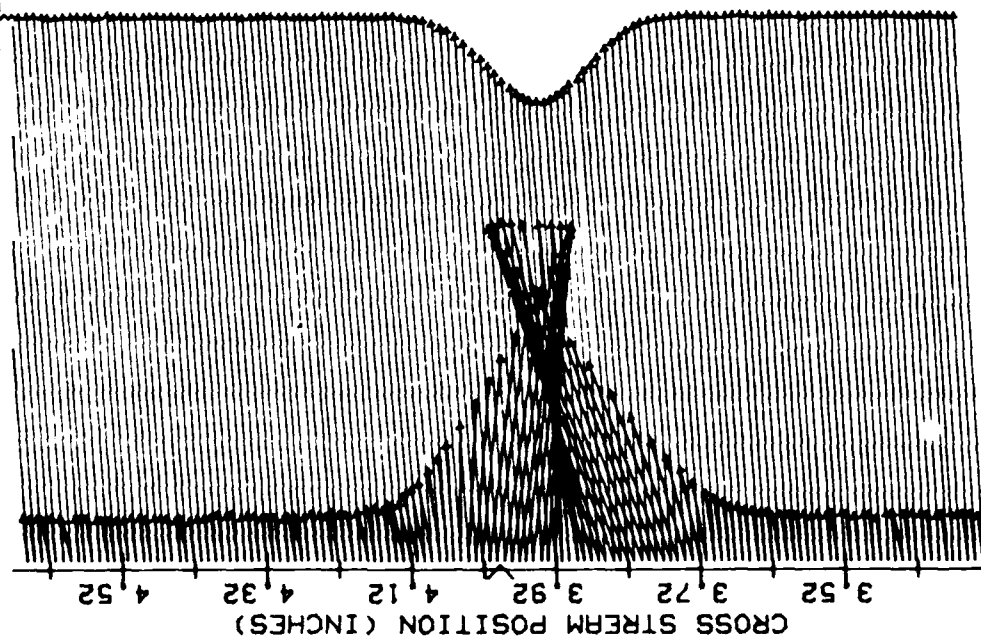


SCALE (INCHES)

— VEL. SCALE=150.00 (FT/SEC)/INCH
 - - - % TURB INT SCALE= 5.00 % /INCH

Fig. 45. Wake Velocity and Turbulence Intensity Profiles, Conf. #3, $x/c = 0.625$

VANE WAKE: CONF. NO.3, EVAL. NO.2 LOW TURB.
TRAVERSE NO. 2.00 AT 2.25 INCHES

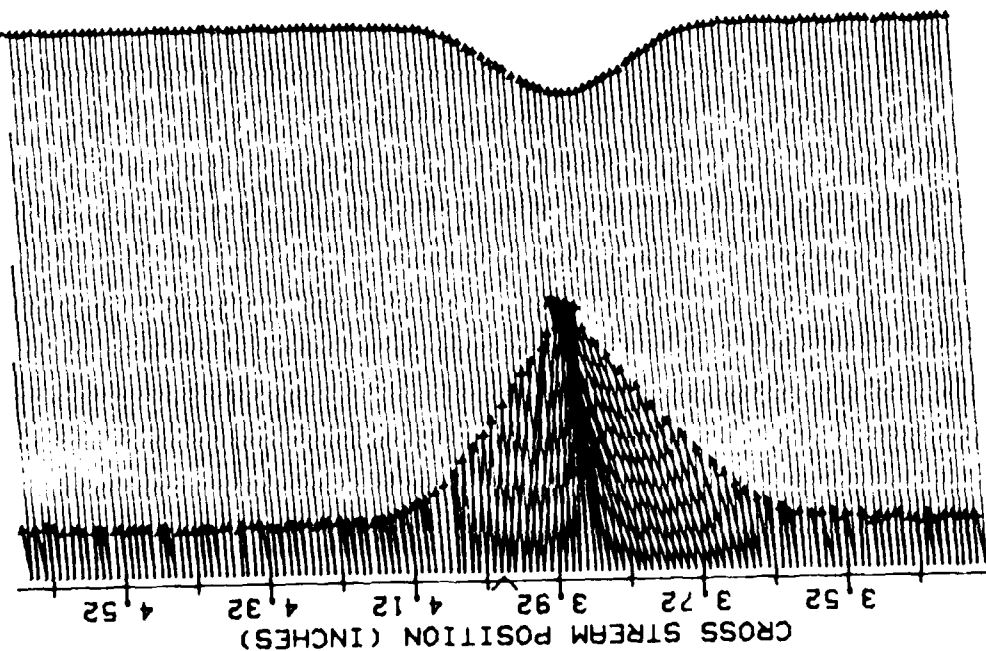


SCALE (INCHES)

— VEL. SCALE=150.00 (FT/SEC)/INCH
- - - % TURB INT SCALE= 5.00 % /INCH

Fig. 46. Wake Velocity and Turbulence Intensity Profiles, Conf. #3, $x/c = 1.125$

VANE WAKE: CONF. NO. 3, EVAL. NO. 2 LOW TURB.
 TRAVERSE NO. 3.00 AT 3.25 INCHES

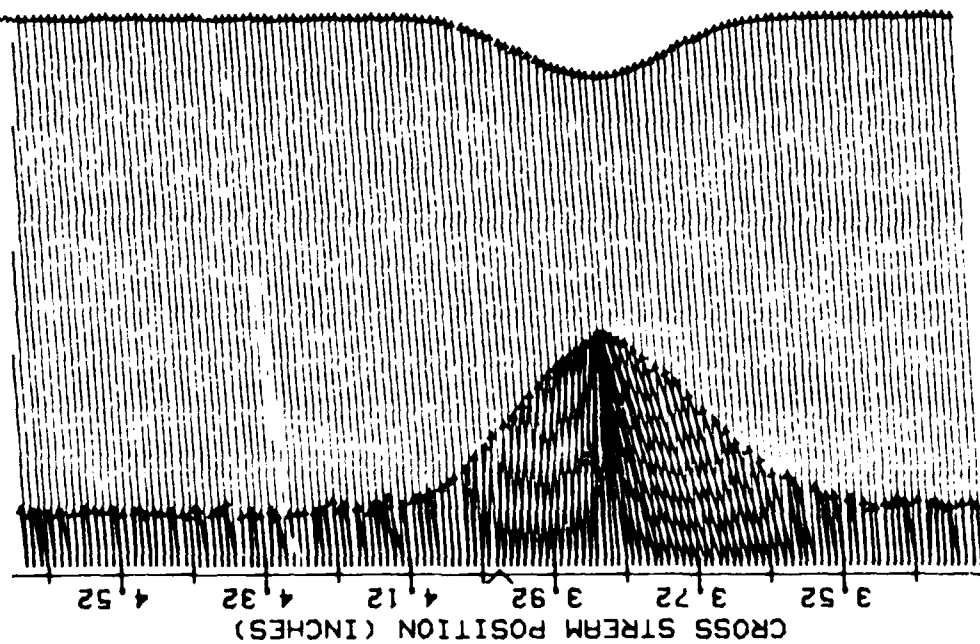


SCALE (INCHES)
 0 1 2 3

— VEL. SCALE=150.00 (FT/SEC)/INCH
 - - - % TURB INT SCALE= 5.00 % /INCH

Fig. 47. Wake Velocity and Turbulence Intensity Profiles, Conf. #3, $x/c = 1.625$

VAINE WAKE: CONF. NO. 3, EVAL. NO. 2 LOW TURB.
 TRAVERSE NO. 4.00 AT 4.25 INCHES



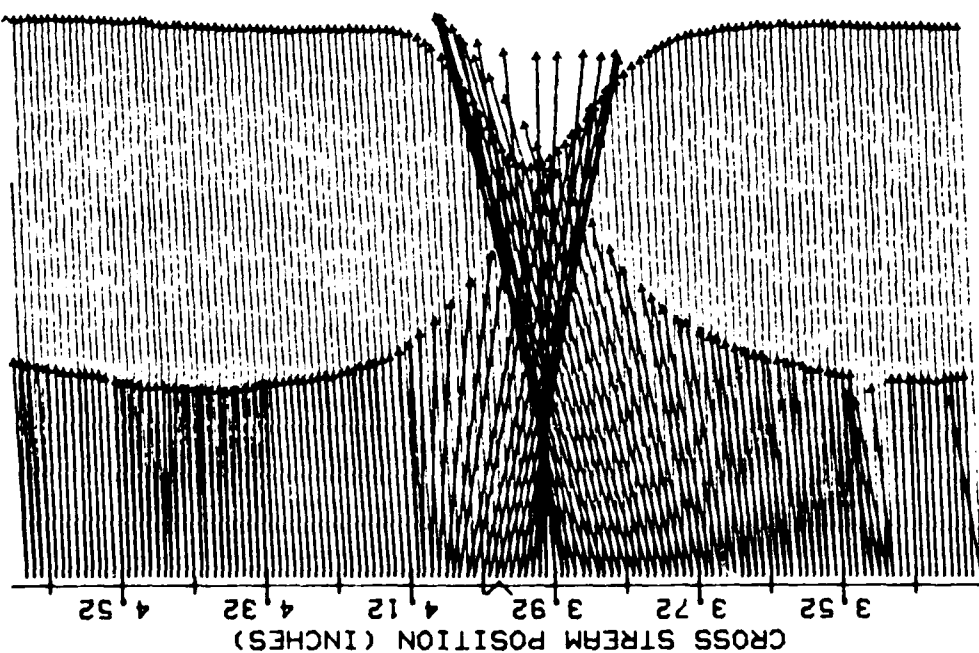
SCALE (INCHES)

0 1 2 3

— VEL. SCALE=150.00 (FT/SEC)/INCH
 - - - % TURB INT SCALE= 5.00 % /INCH

Fig. 48. Wake Velocity and Turbulence Intensity Profiles, Conf. #3, $x/c = 2.125$

VANE WAKE: CONF. NO.3, EVAL. NO.2 HIGH TURB.
TRAVERSE NO. 1.00 AT 1.25 INCHES



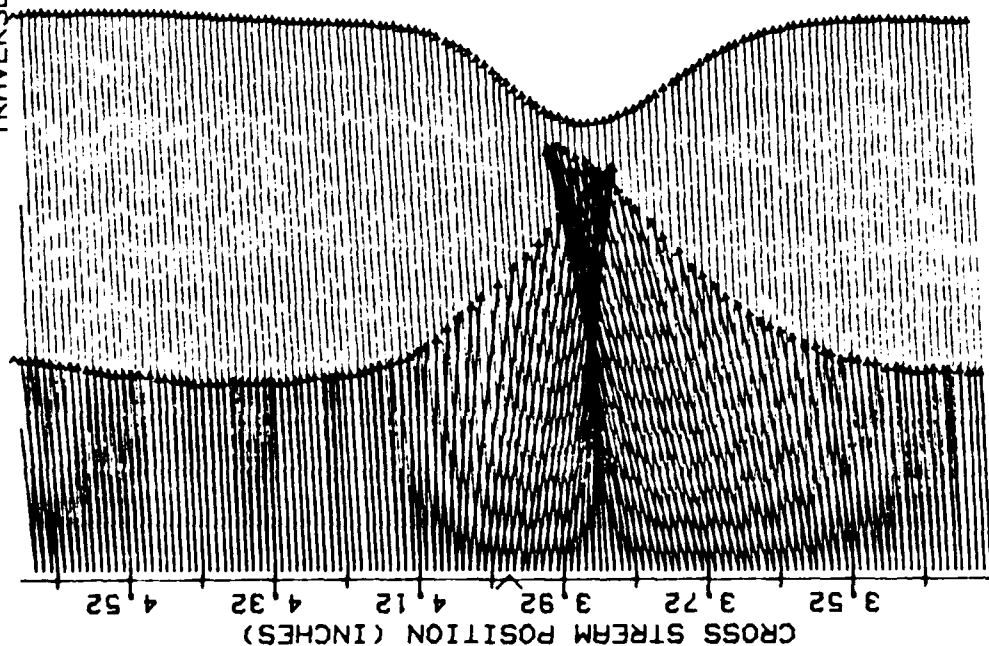
SCALE (INCHES)

0 1 2 3

— VEL. SCALE=150.00 (FT/SEC)/INCH
- - - % TURB INT SCALE= 5.00 % /INCH

Fig. 49. Wake Velocity and Turbulence Intensity Profiles, Conf. #3, $x/c = 0.625$

VANE WAKE: CONF. NO.3, EVAL. NO.2 HIGH TURB.
 TRAVERSE NO. 2.00 AT 2.25 INCHES

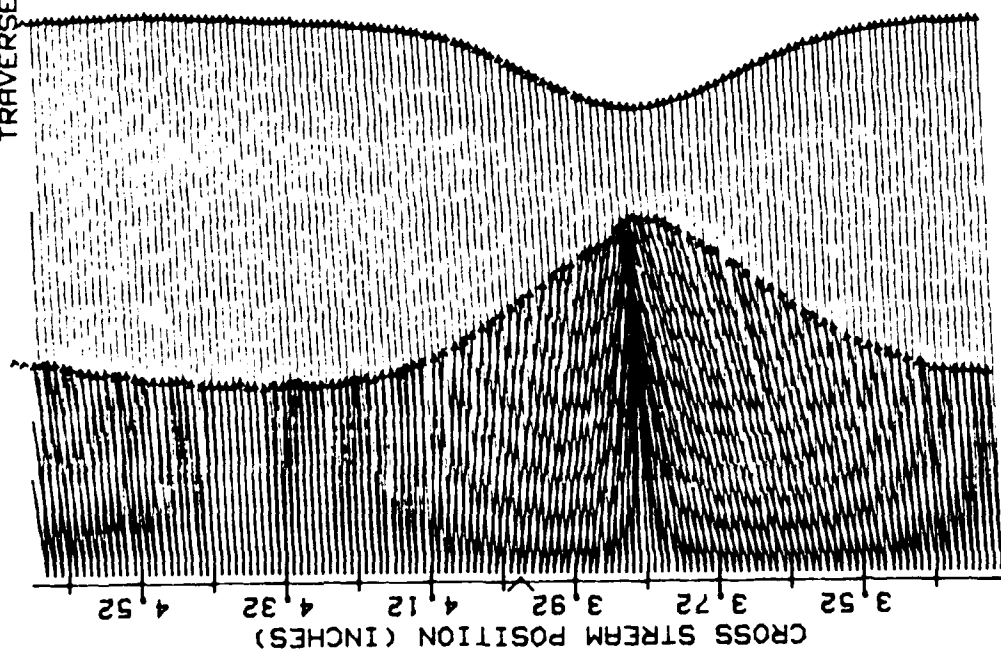


0 1 2 3
 SCALE (INCHES)

— VEL. SCALE=150.00 (FT/SEC)/INCH
 - - - % TURB INT SCALE= 5.00 % /INCH

Fig. 50. Wake Velocity and Turbulence Intensity Profiles, Conf. #3, $x/c = 1.125$

VANE WAKE: CONF. NO. 3, EVAL. NO. 2 HIGH TURB.
TRAVERSE NO. 3.00 AT 3.25 INCHES

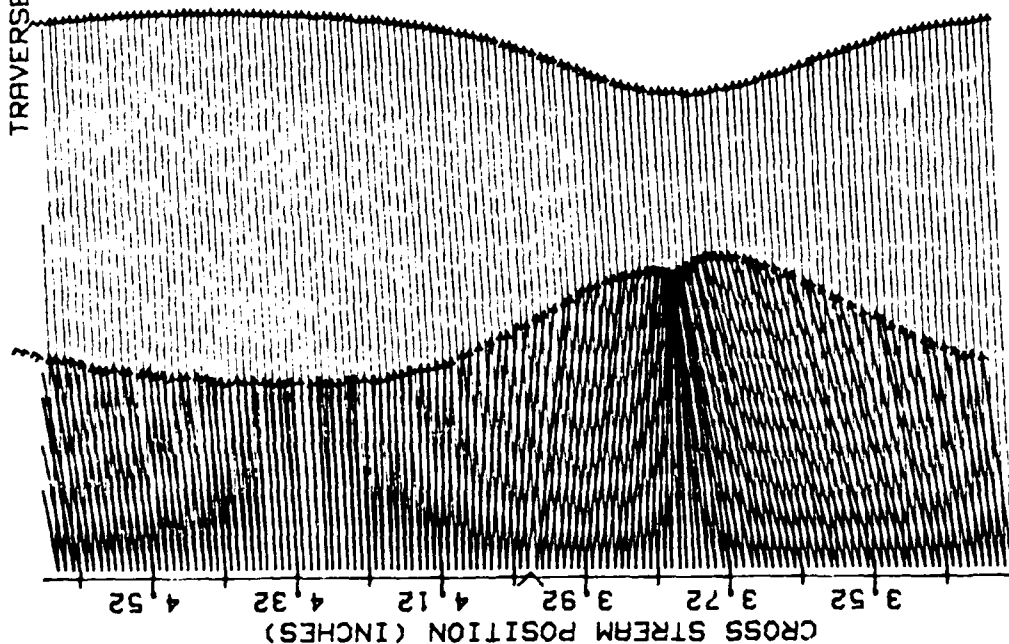


SCALE (INCHES)

— VEL. SCALE=150.00 (FT/SEC)/INCH
- - - % TURB INT SCALE= 5.00 % /INCH

Fig. 51. Wake Velocity and Turbulence Intensity Profiles, Conf. #3, $x/c = 1.625$

VANE WAKE: CONF. NO.3, EVAL. NO.2 HIGH TURB.
TRAVERSE NO. 4.00 AT 4.25 INCHES



SCALE (INCHES)

— VEL. SCALE=150.00 (FT/SEC)/INCH
- - - % TURB INT SCALE= 5.00 % /INCH

Fig. 52. Wake Velocity and Turbulence Intensity Profiles, Conf. #3, $x/c = 2.125$

APPENDIX F

Boundary Layer Velocity & Turbulence Intensity Profiles

Configuration #1, Low and High Freestream Turbulence

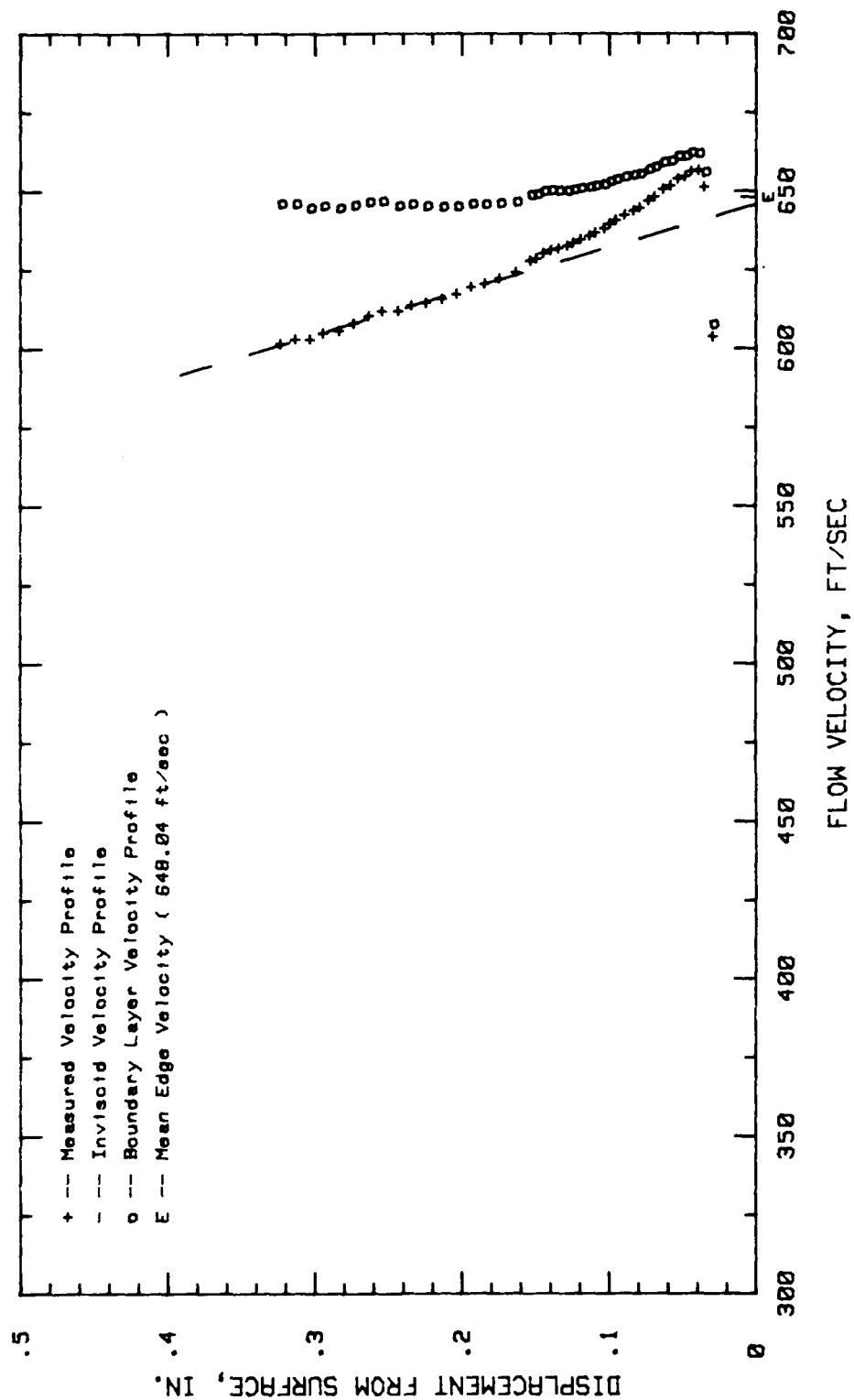


Fig.53.Boundary Layer Velocity Profiles, Conf.#1 at 4.68% Chord LOW TURB.

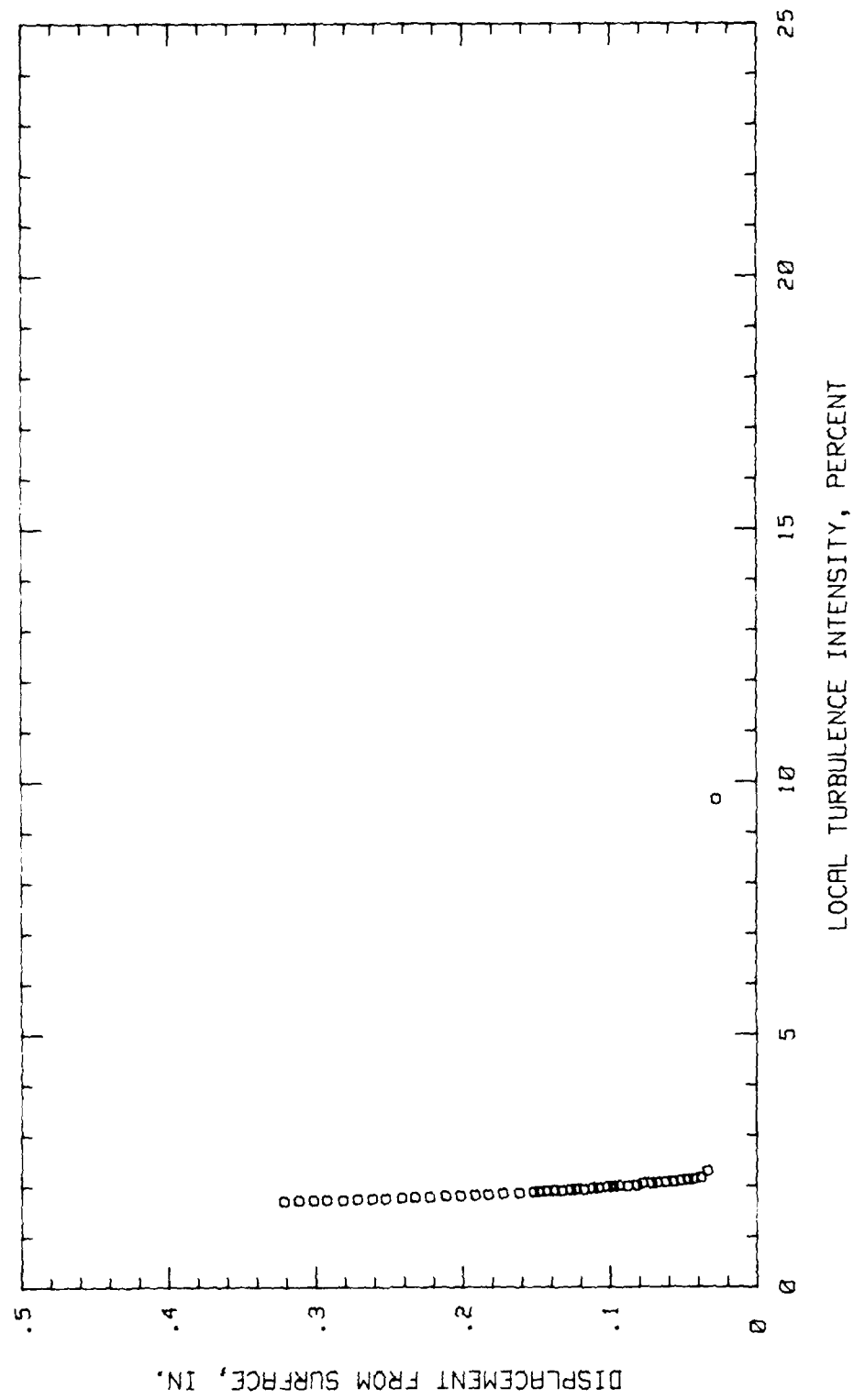


Fig. 54. Boundary Layer Turb. Intensity Profile, Conf. #1 at 4.68% Chord LOW TURB.

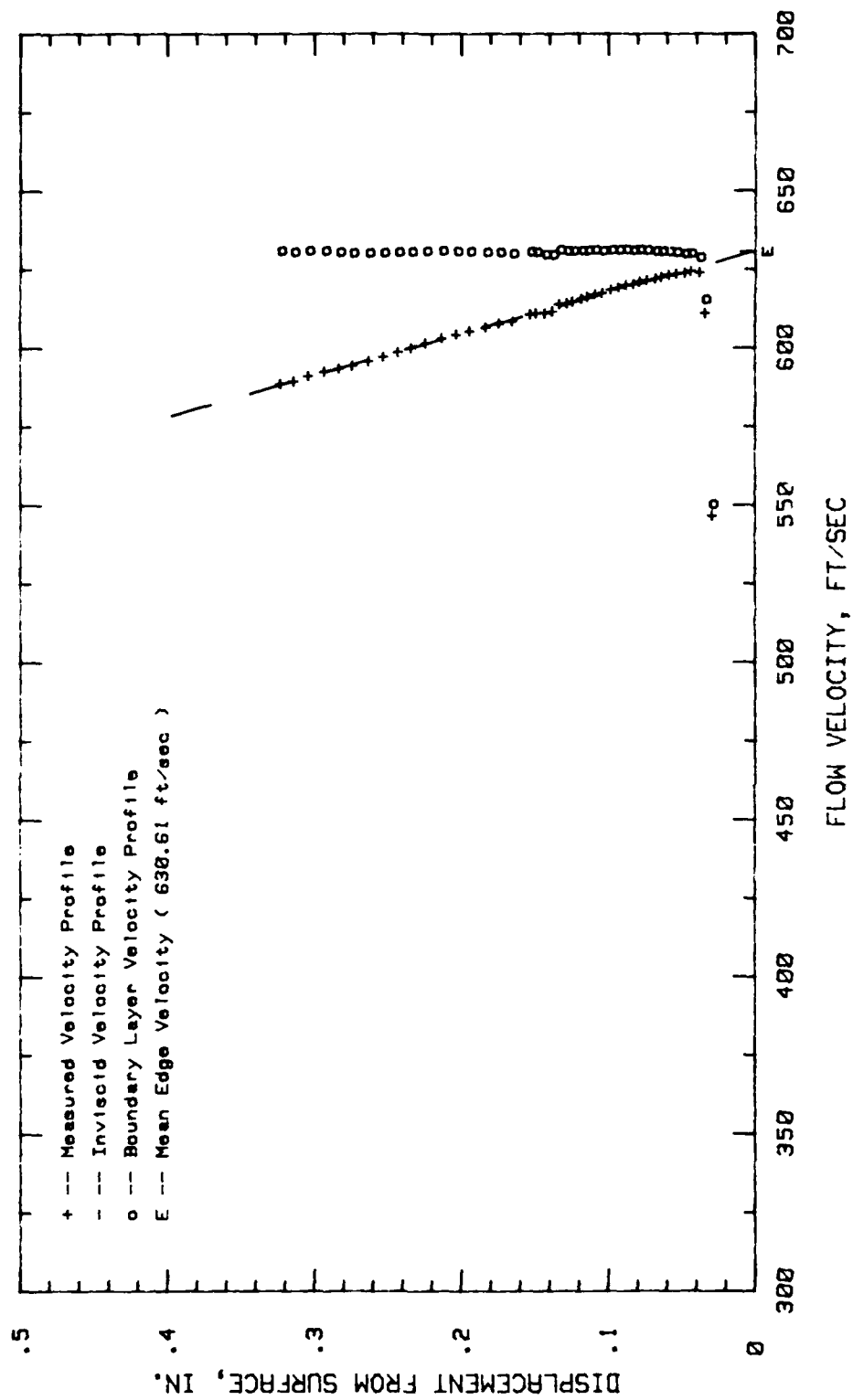


Fig.55. Boundary Layer Velocity Profiles, Conf.#1 at 9.37% Chord LOW TURB.

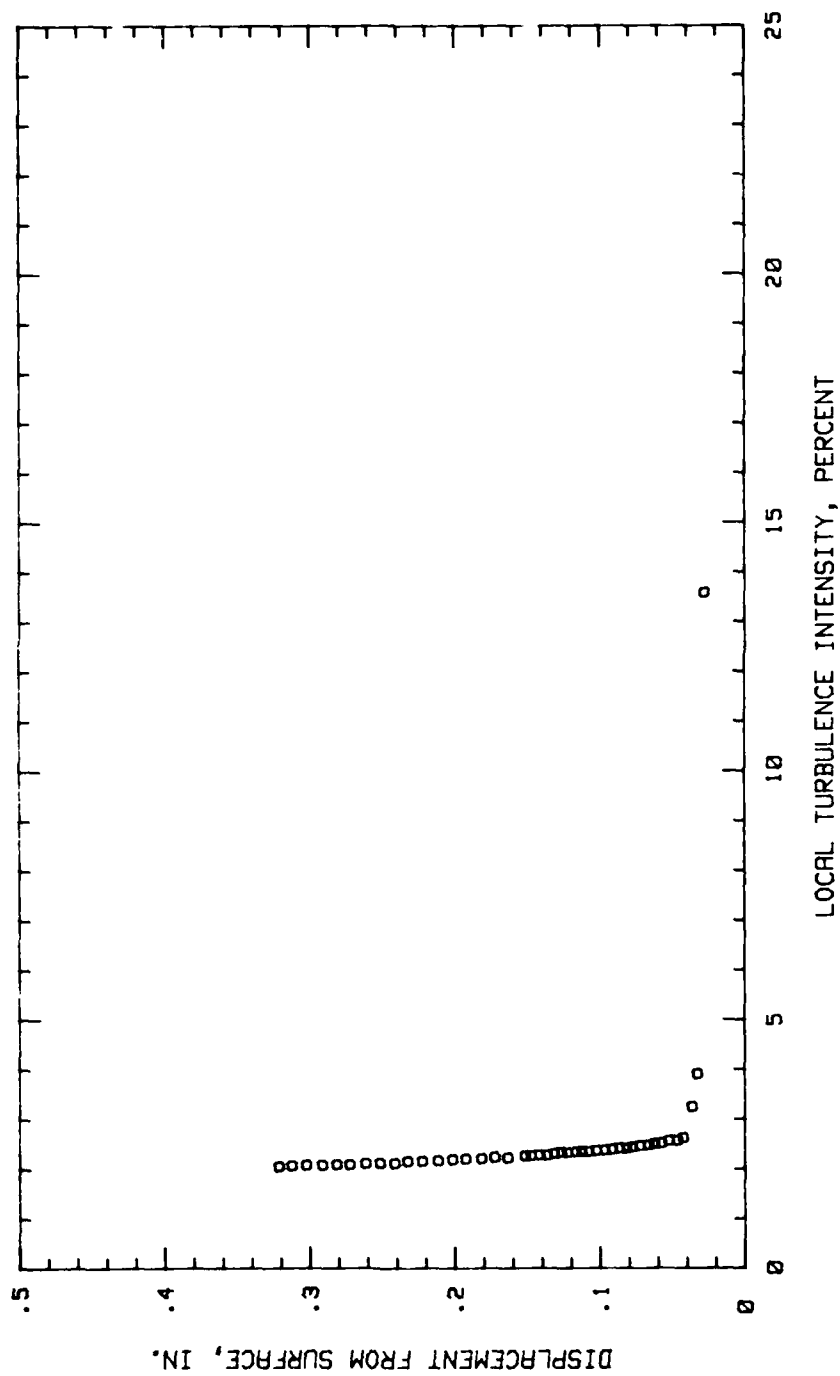


Fig.56. Boundary Layer Turb. Intensity Profile, Conf.#1 at 9.37% Chord LOW TURB.

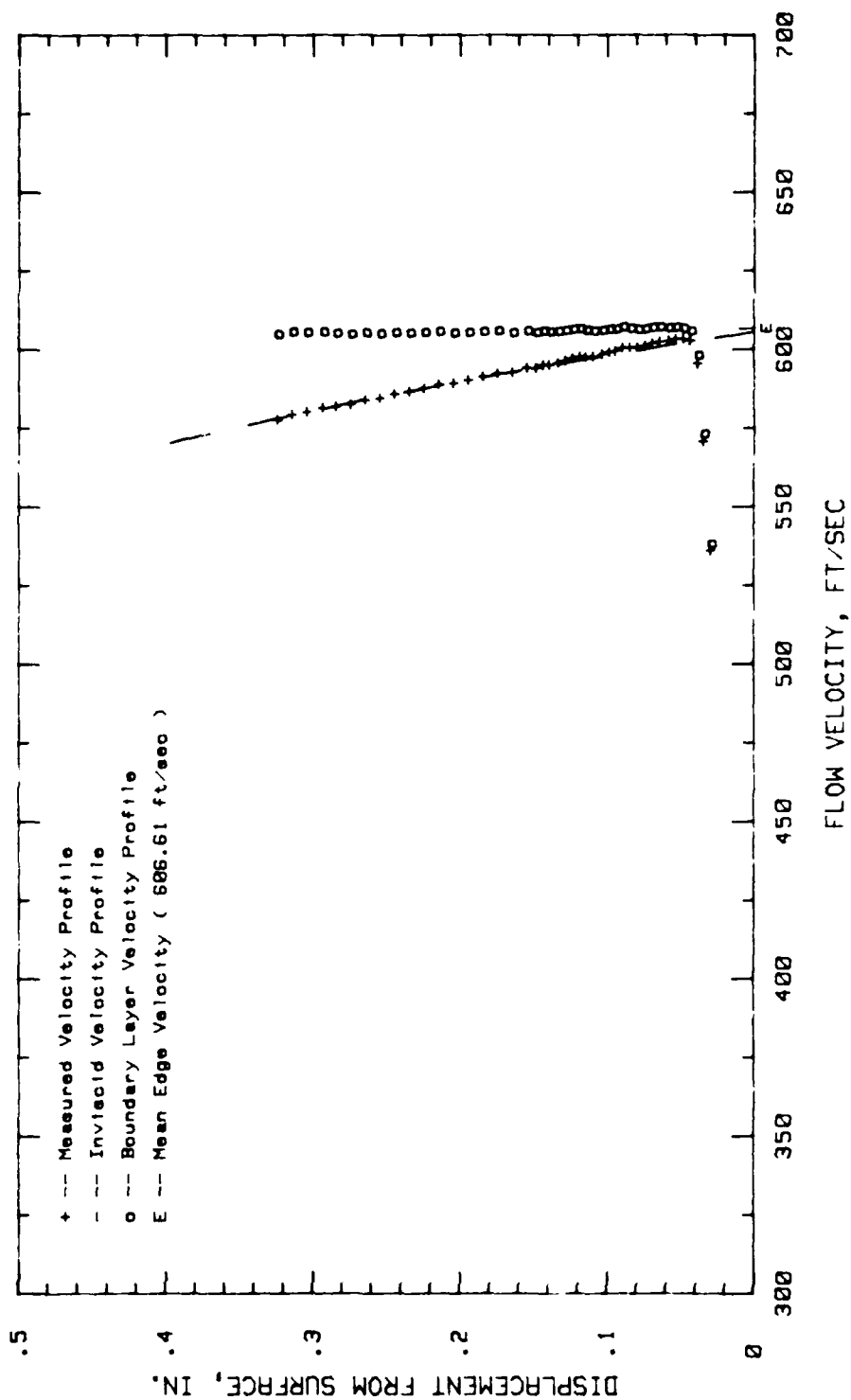


Fig.57. Boundary Layer Velocity Profiles, Conf.#1 at 25% Chord LOW TURB.

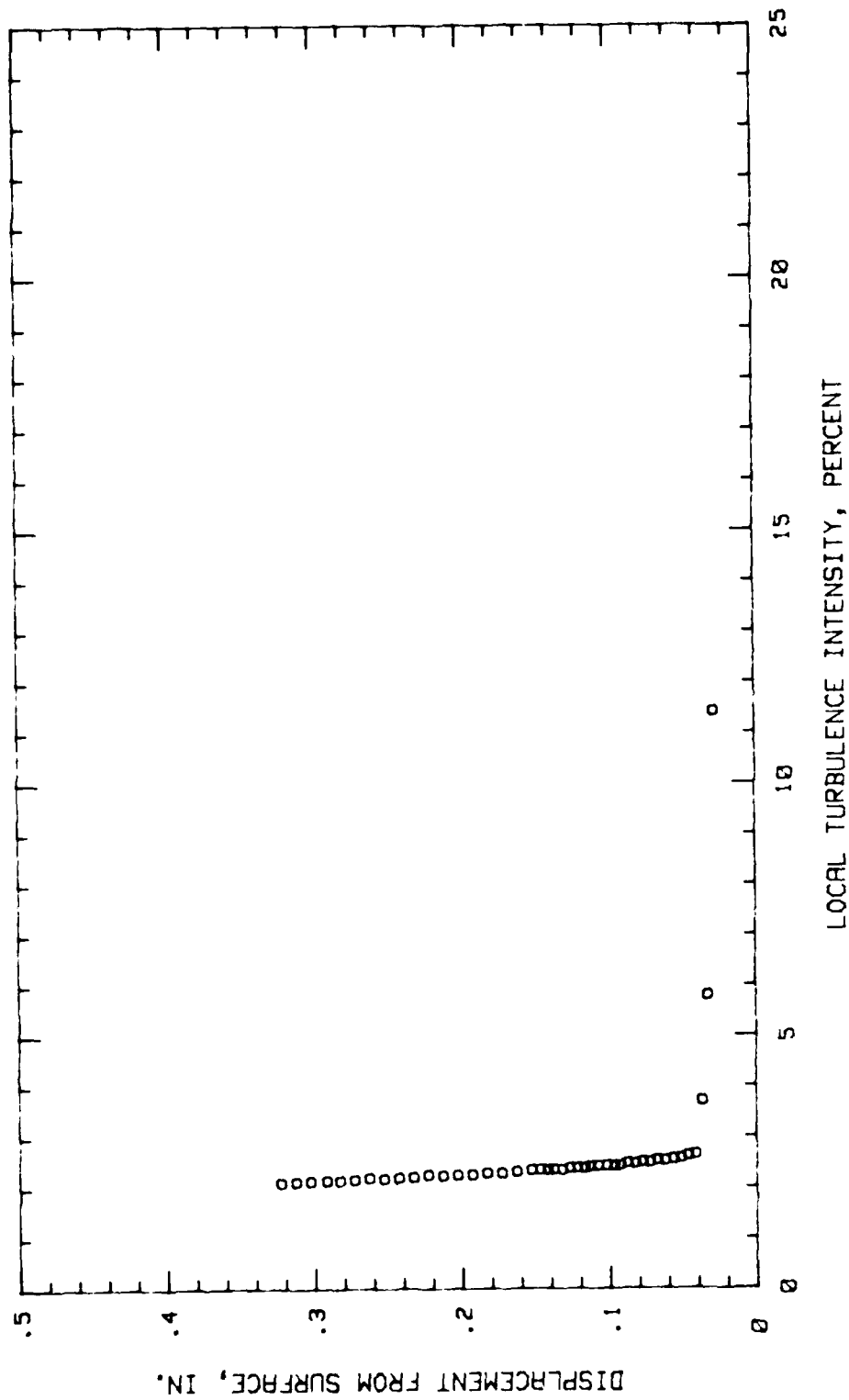


Fig.58. Boundary Layer Turb. Intensity Profile, Conf.#1 at 25% Chord LOW TURB.

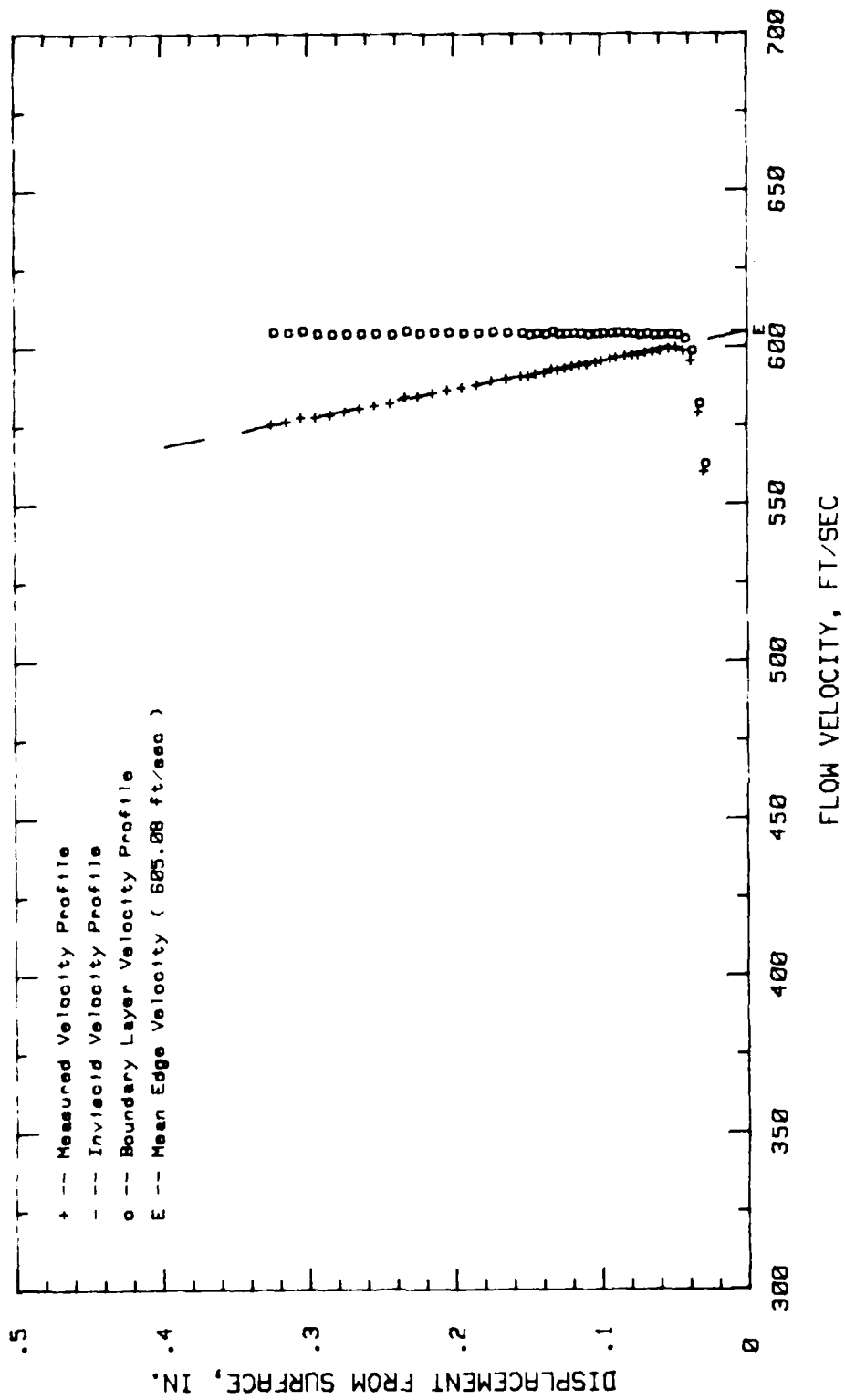


Fig.59. Boundary Layer Velocity Profiles, Conf.#1 at 29.68% Chord LOW TURB.

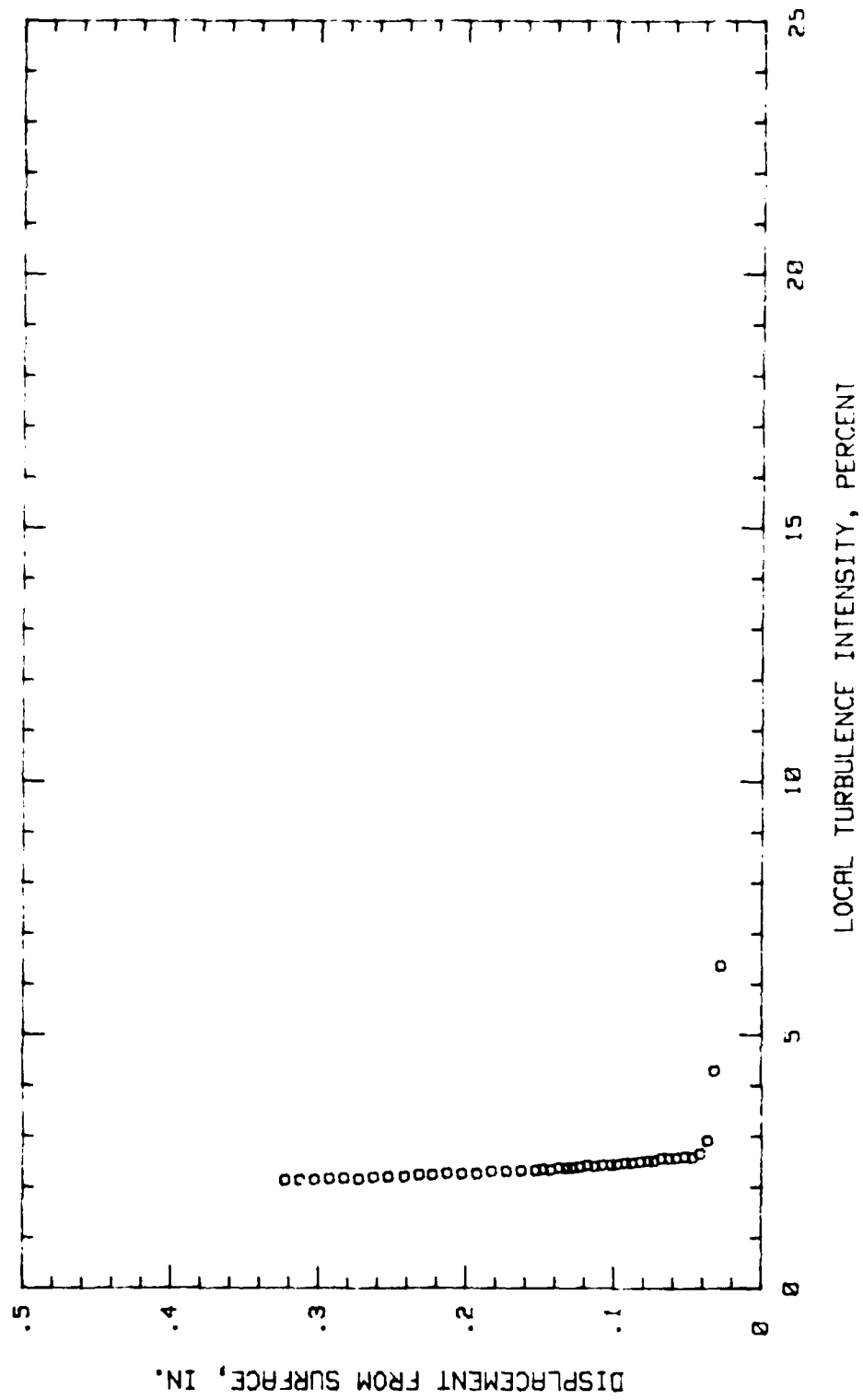


Fig.60. Boundary Layer Turb. Intensity Profile, Conf.#1 at 29.68% Chord LOW TURB.

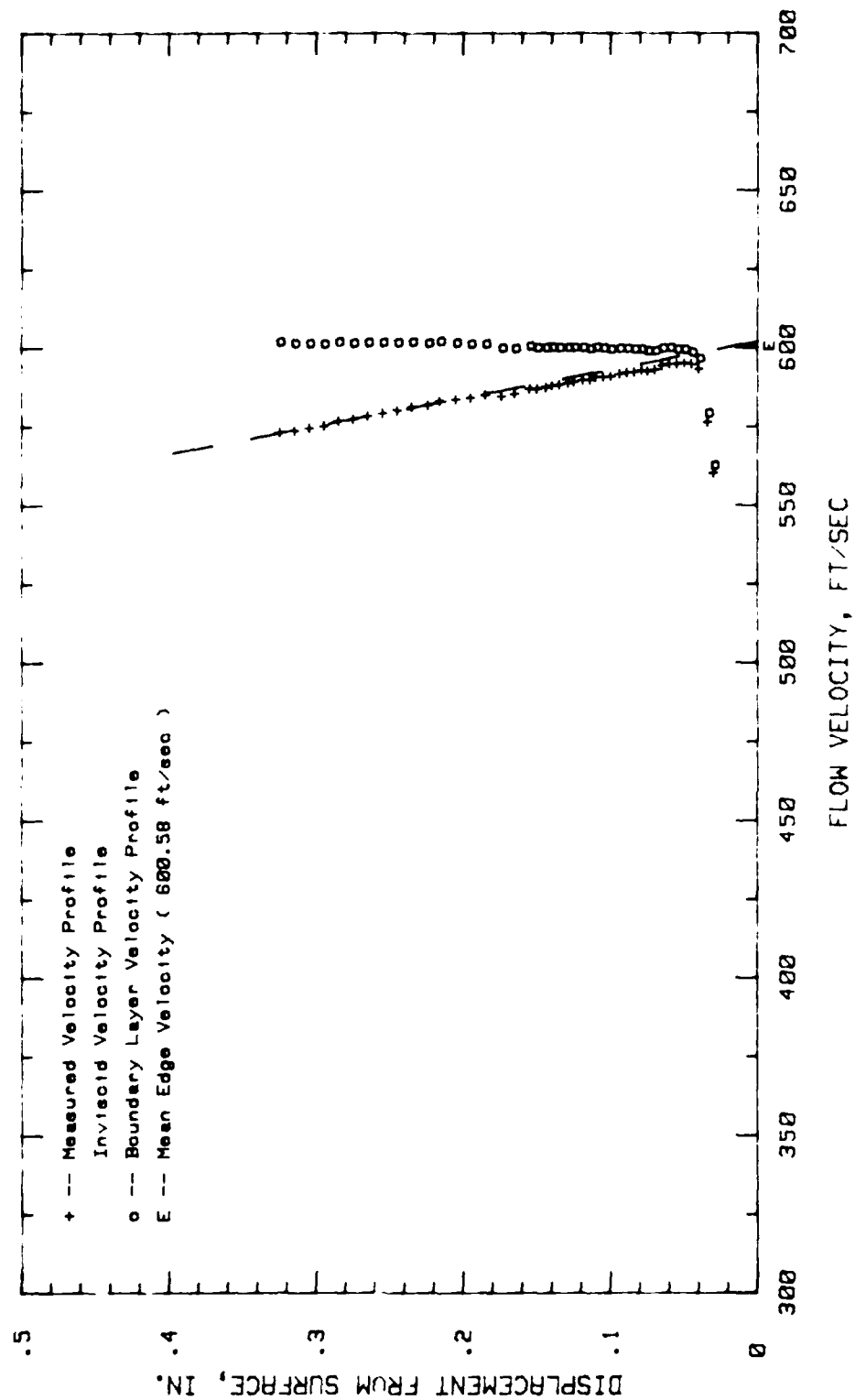


Fig.61. Boundary Layer Velocity Profiles, Conf.#1 at 34.37% Chord LOW TURB.

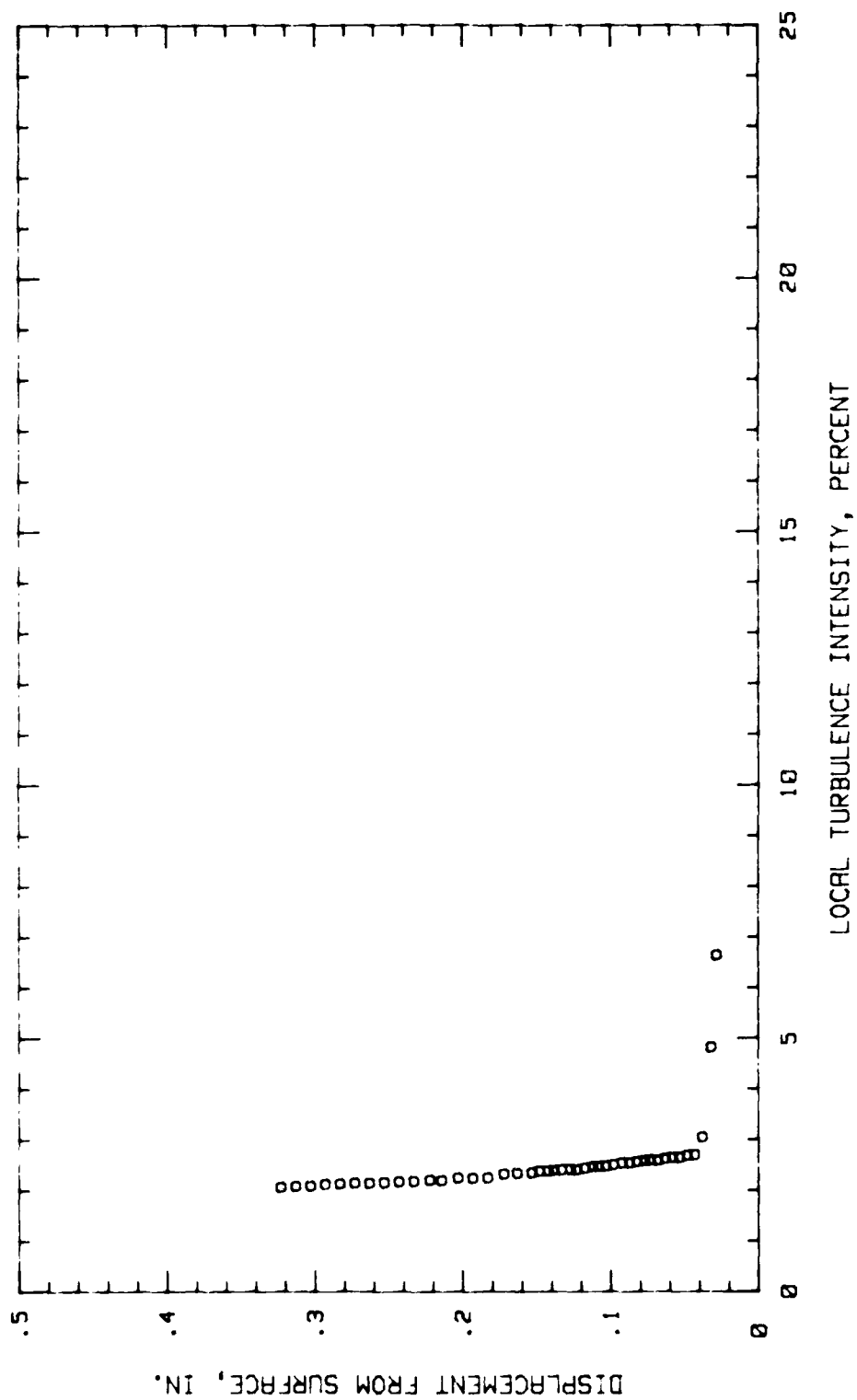


Fig.62. Boundary Layer Turb. Intensity Profile, Conf.#1 at 34.37% Chord LOW TURB.

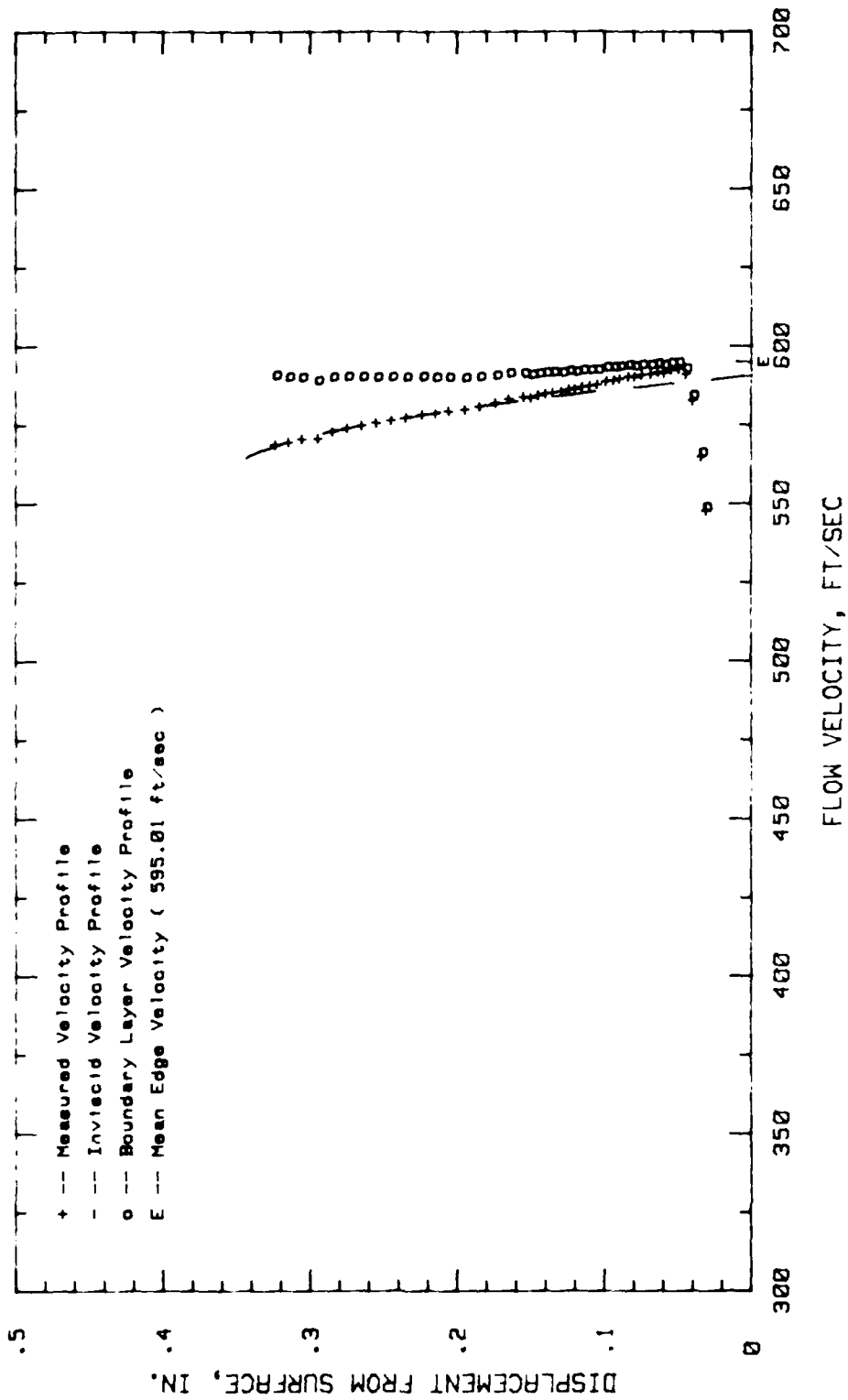


Fig.63. Boundary Layer Velocity Profiles, Conf.#1 at 40.62% Chord LOW TURB.

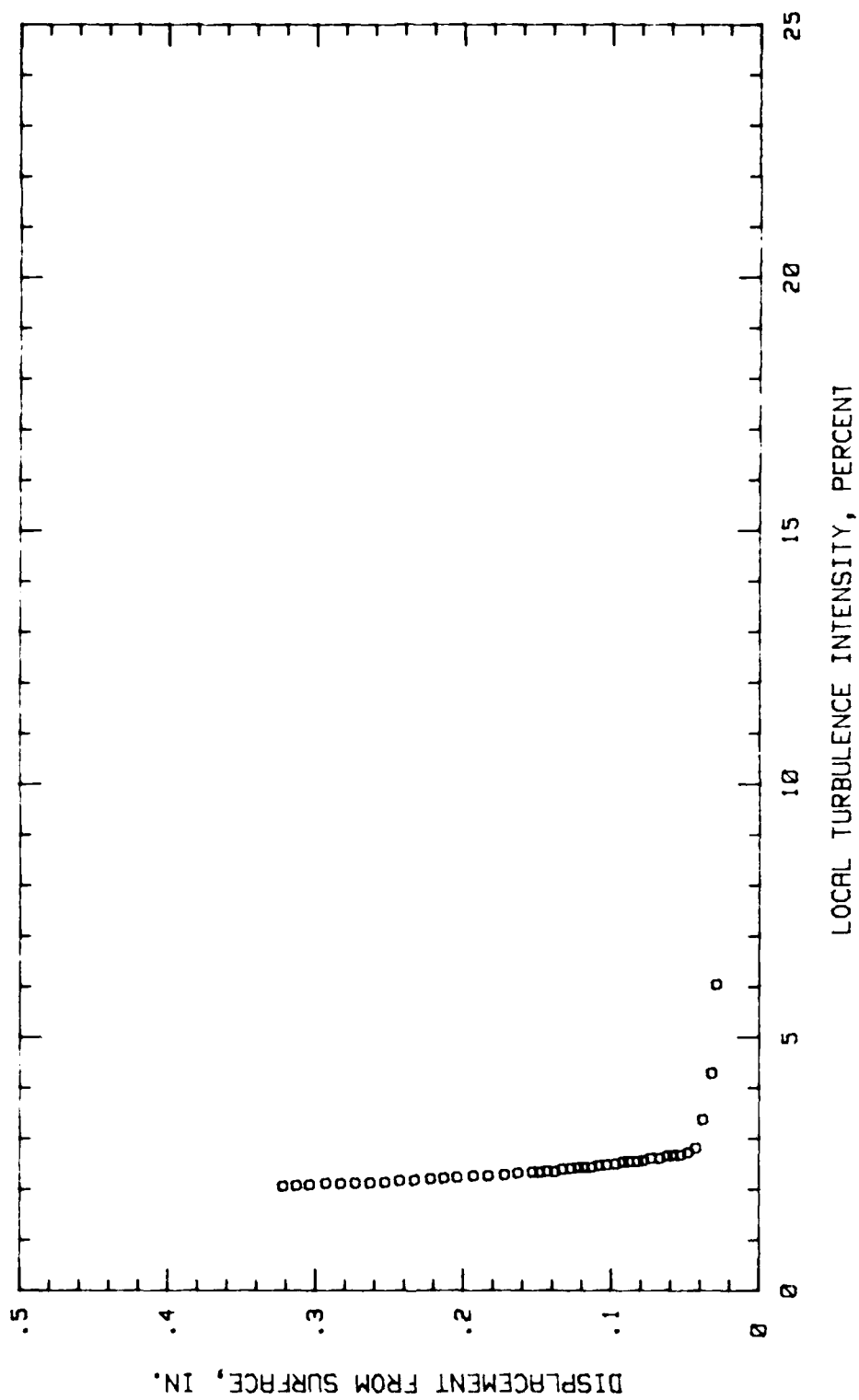


Fig.64. Boundary Layer Turb. Intensity Profile, Conf.#1 at 40.62% Chord LOW TURB.

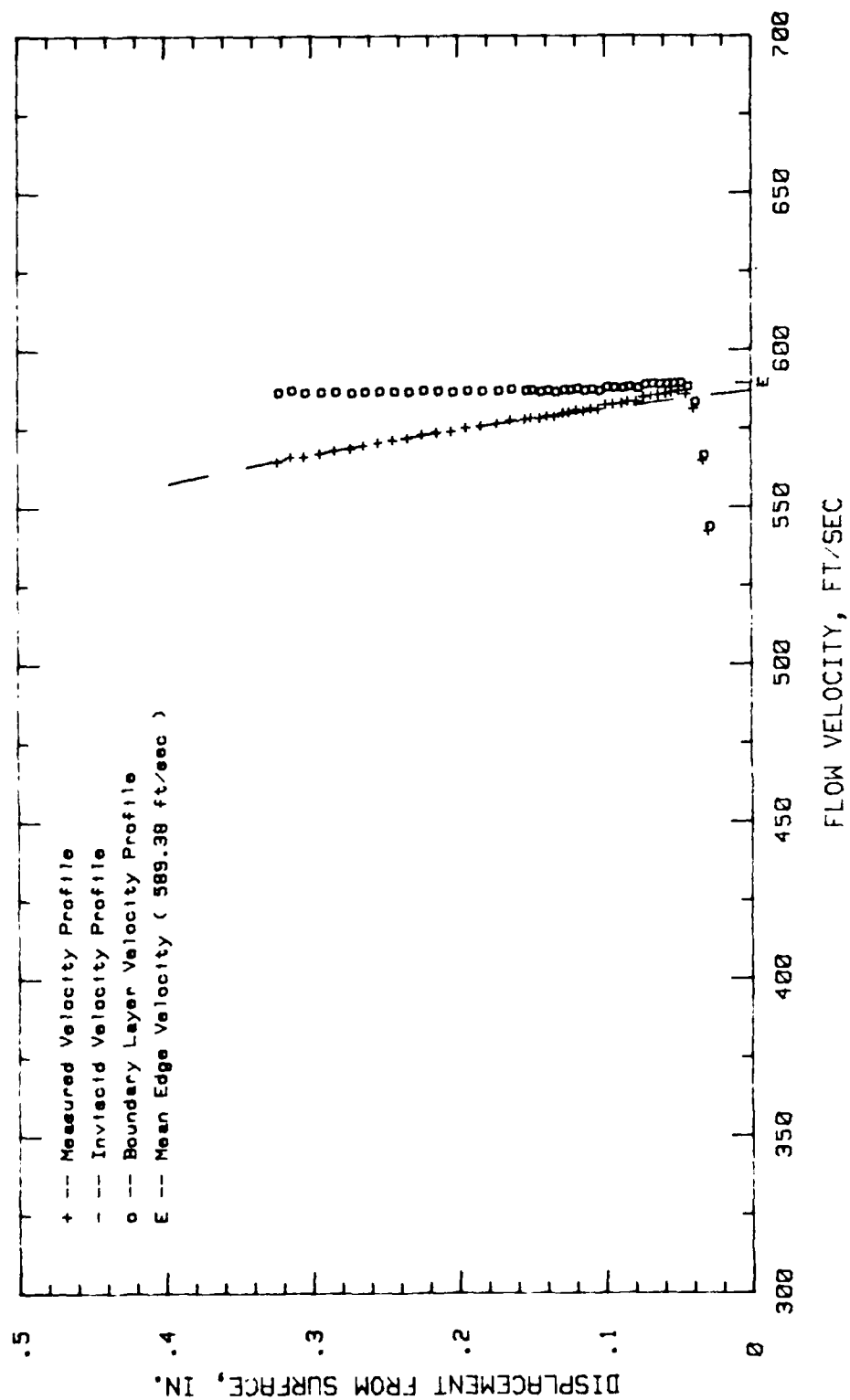


Fig.65. Boundary Layer Velocity Profiles, Conf.#1 at 45.31% Chord LOW TURB.

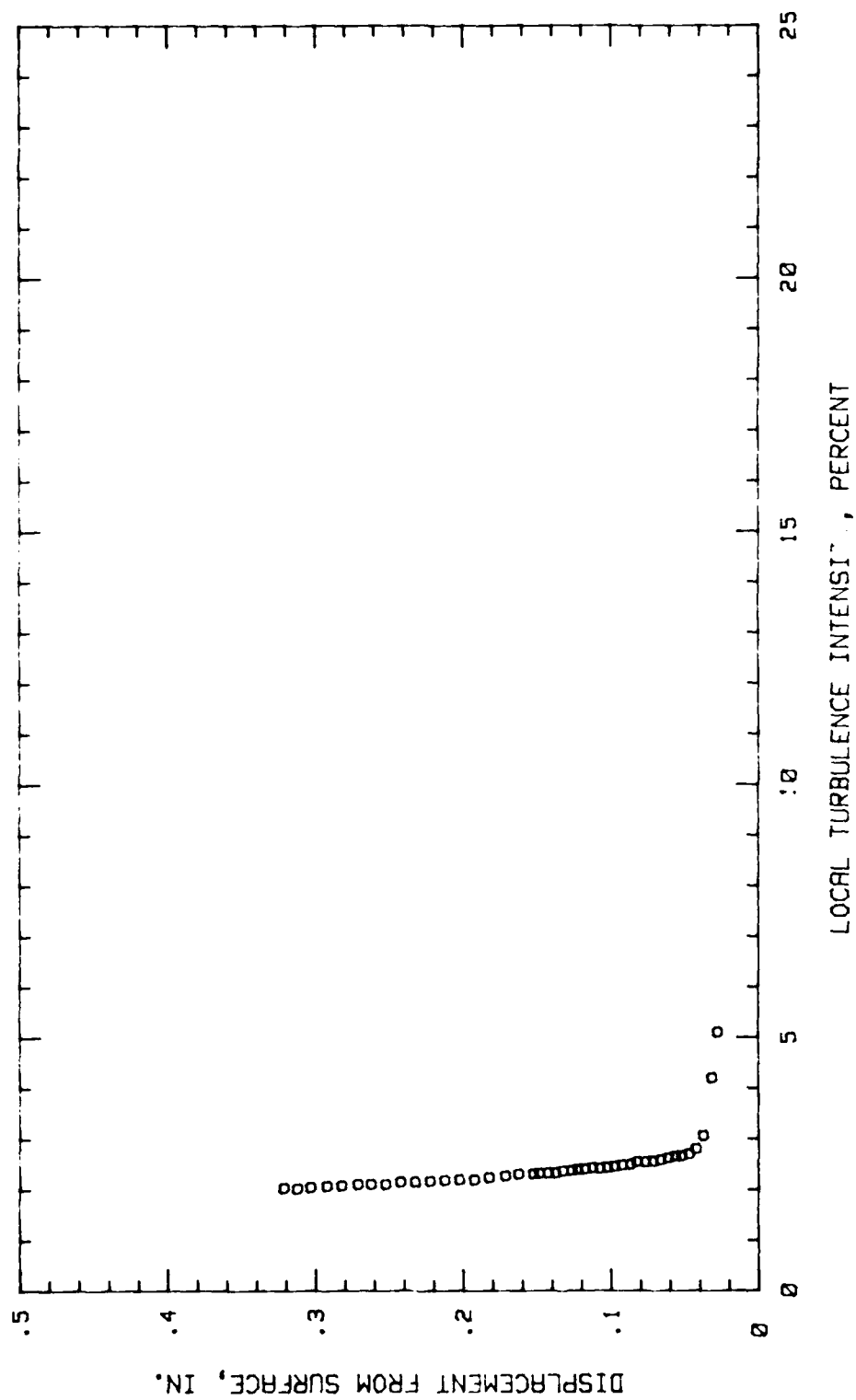


Fig.66. Boundary Layer Turb. Intensity Profile, Conf.#1 at 45.31% Chord LOW TURB.

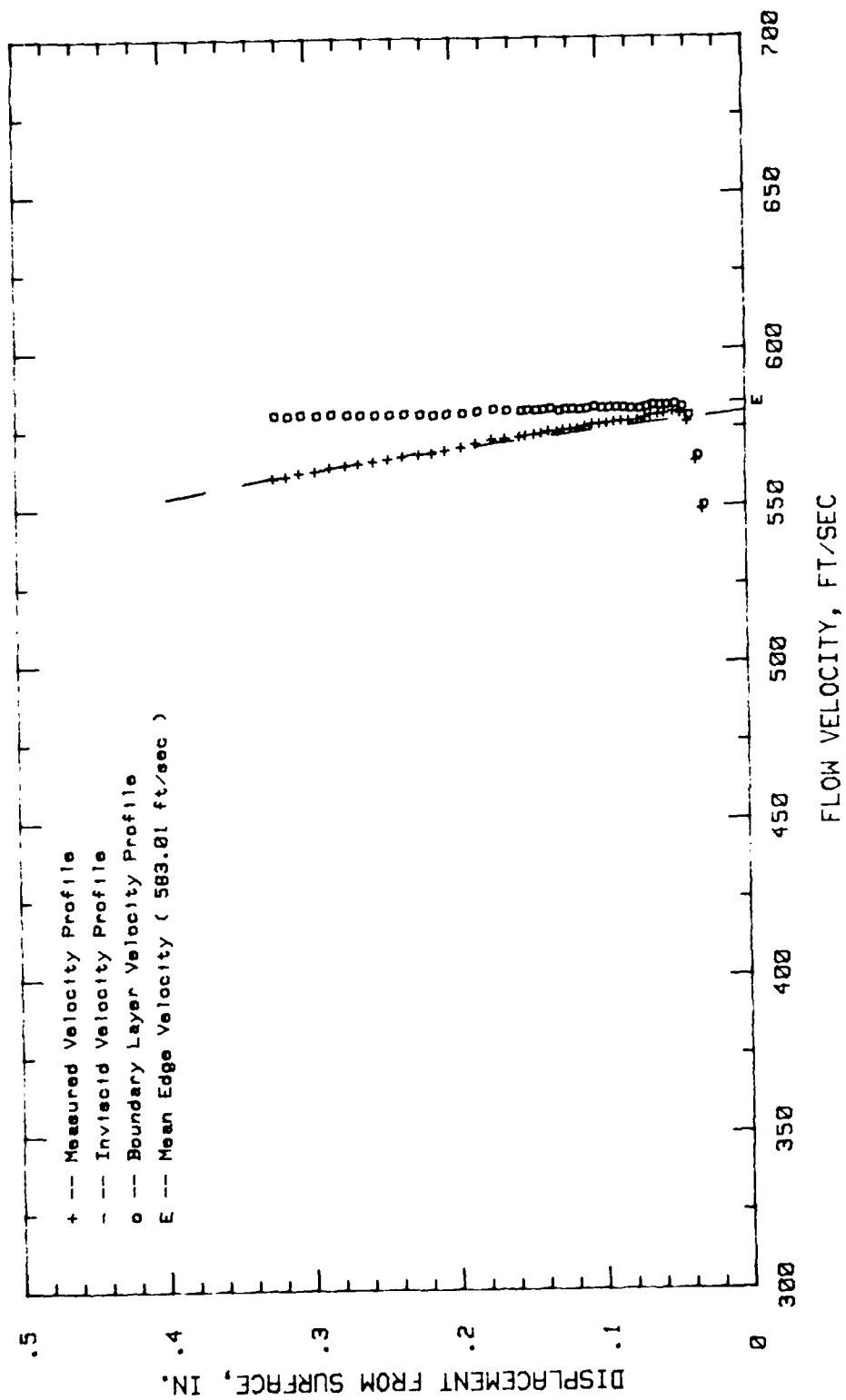


Fig.67. Boundary Layer Velocity Profiles, Conf.#1 at 50% Chord LOW TURB.

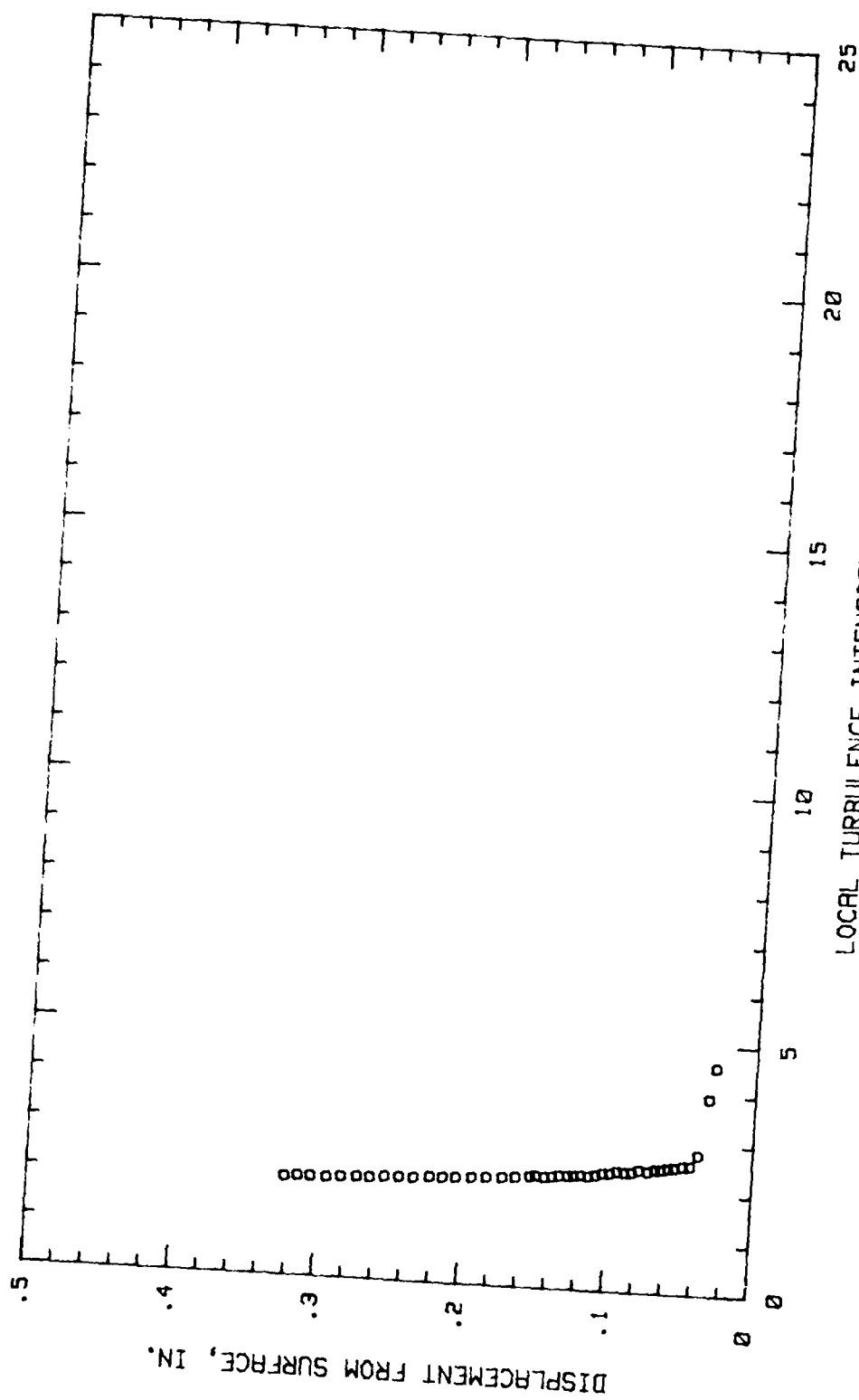


Fig. 68. Boundary Layer Turb. Intensity Profile, Conf. #1 at 50% Chord LOW TURB.

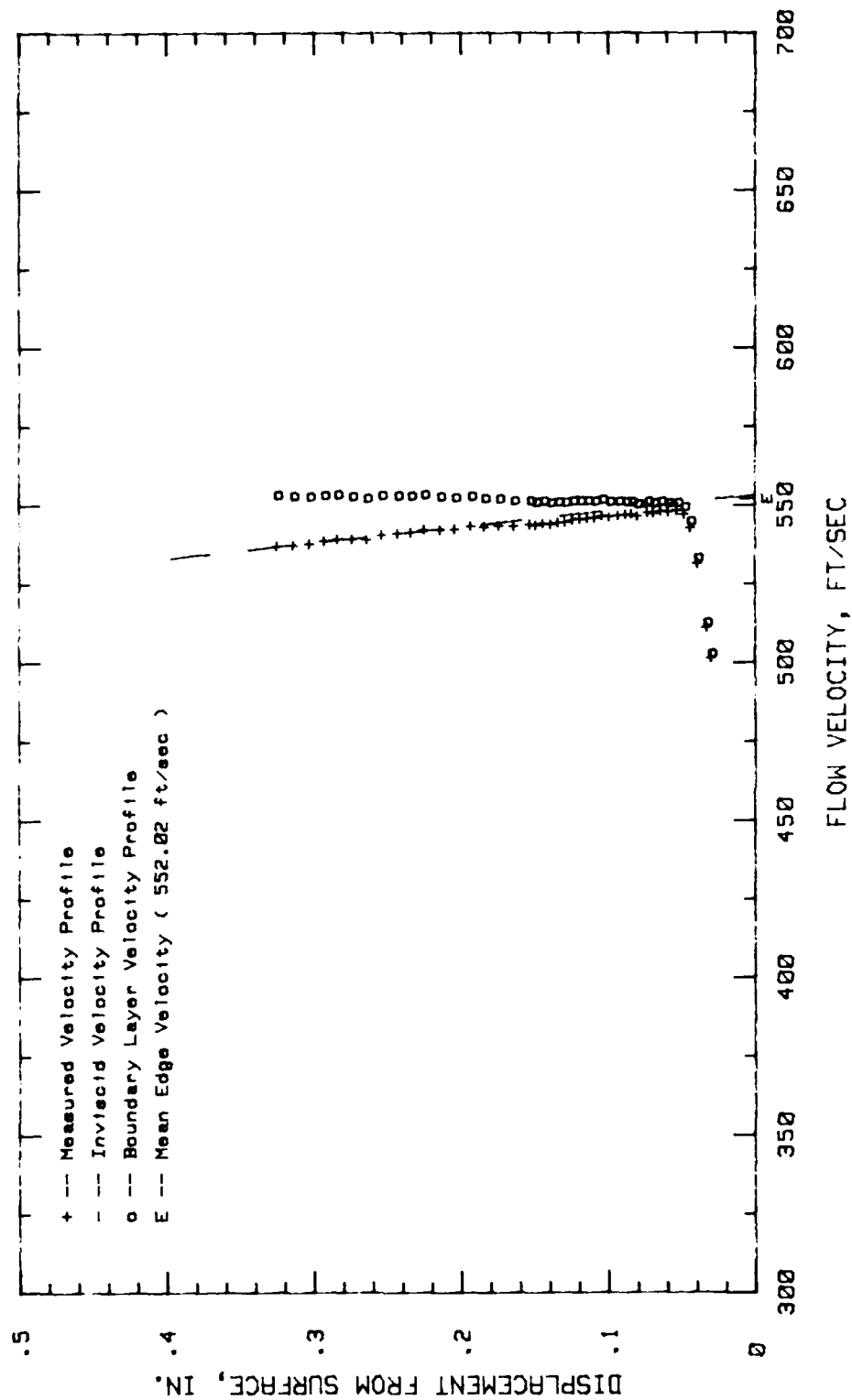


Fig.69. Boundary Layer Velocity Profiles, Conf.#1 at 65.62% Chord LOW TURB.

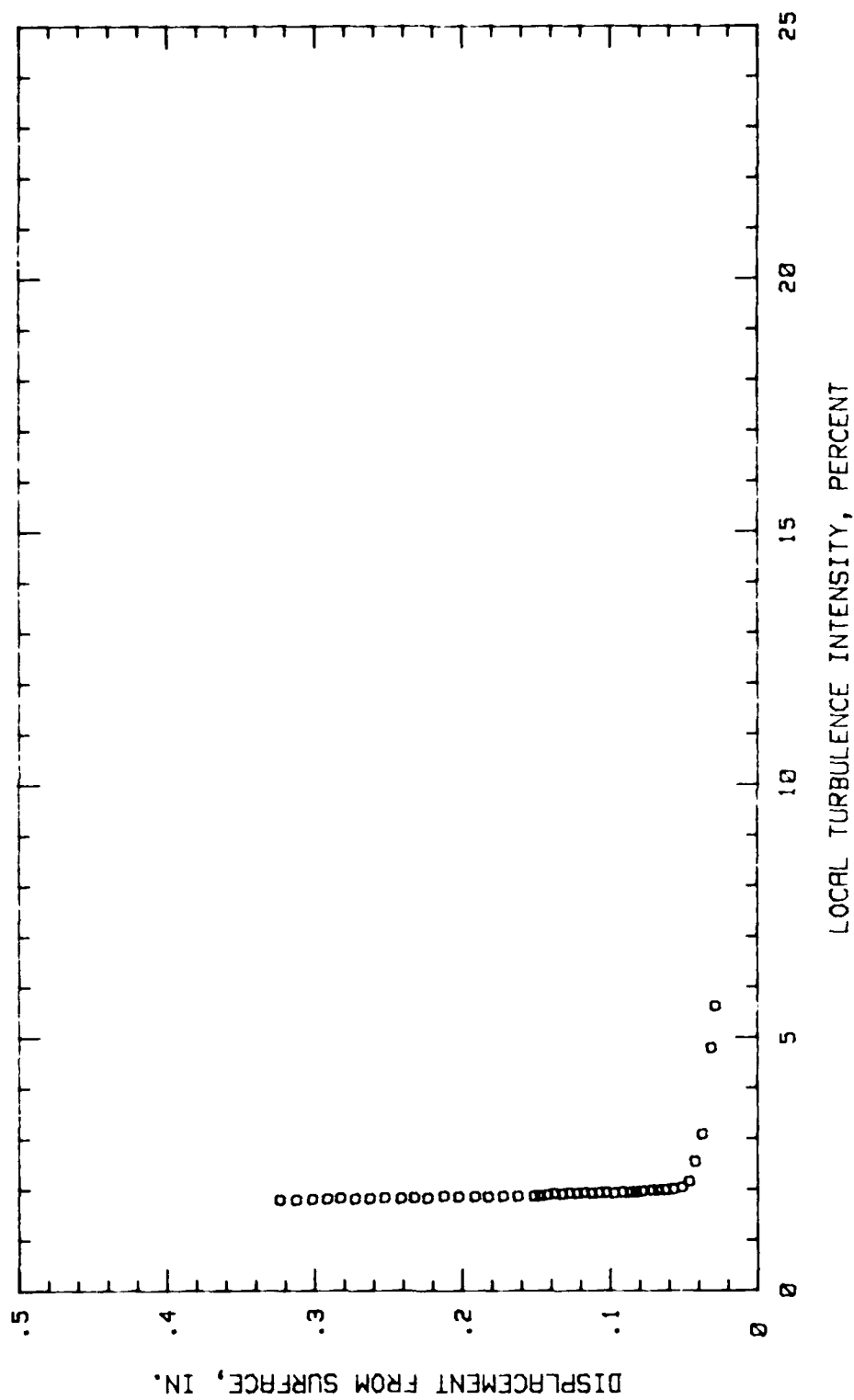


Fig.70. Boundary Layer Turb. Intensity Profile, Conf.#1 at 65.62% Chord LOW TURB.

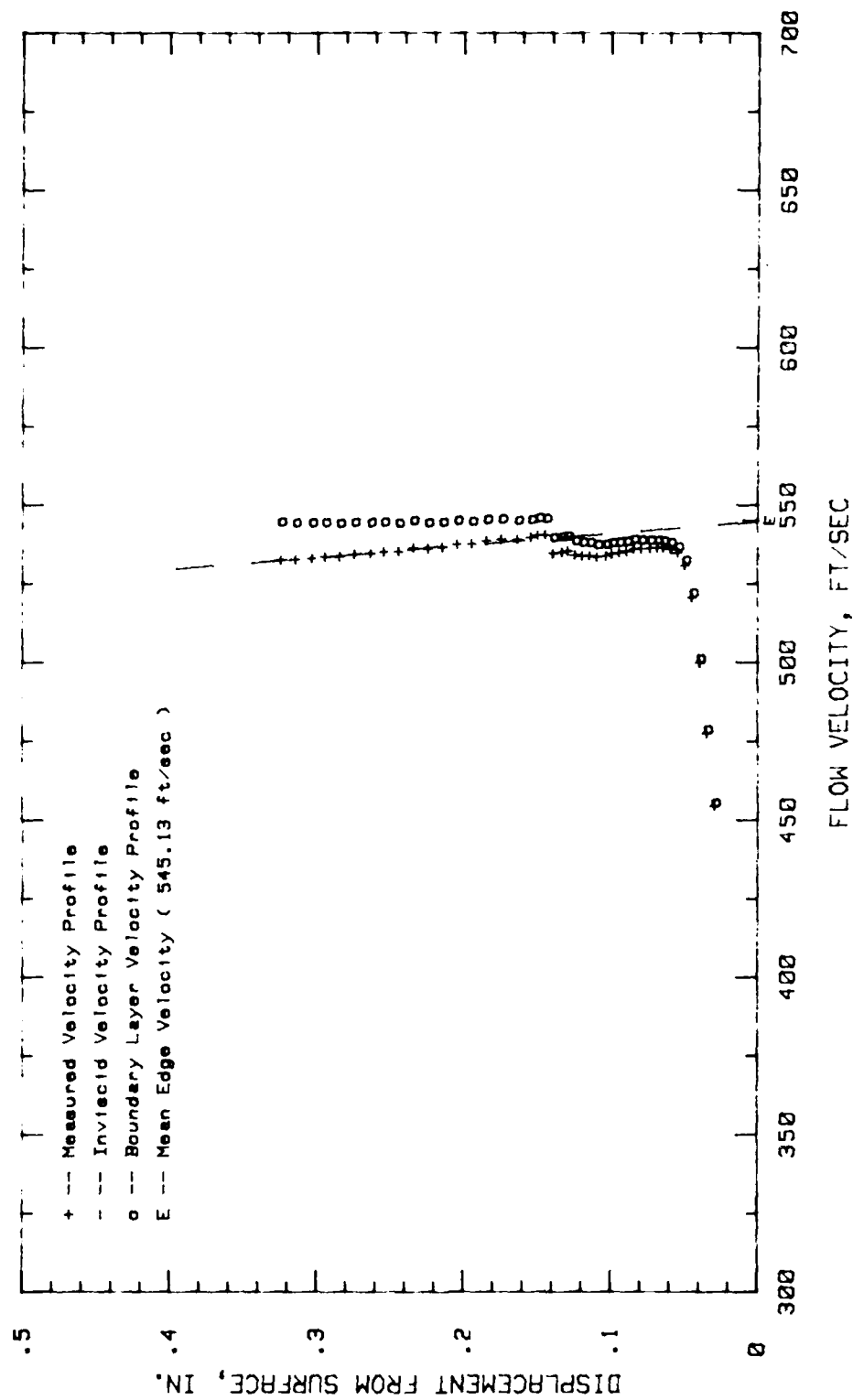


Fig.71. Boundary Layer Velocity Profiles, Conf.#1 at 70.31% Chord LOW TURB.

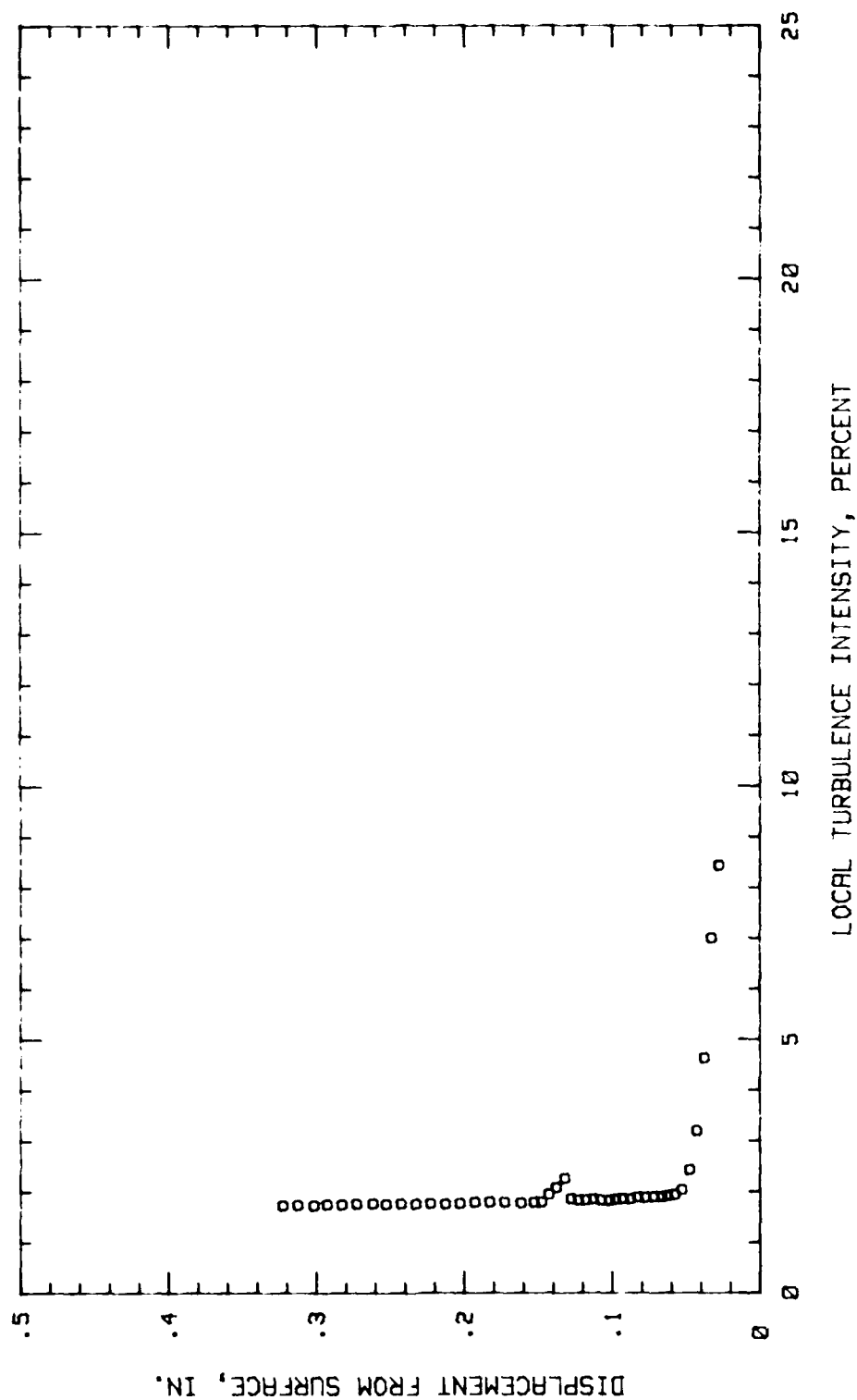


Fig.72. Boundary Layer Turb. Intensity Profile, Conf.#1 at 70.31% Chord LOW TURB.

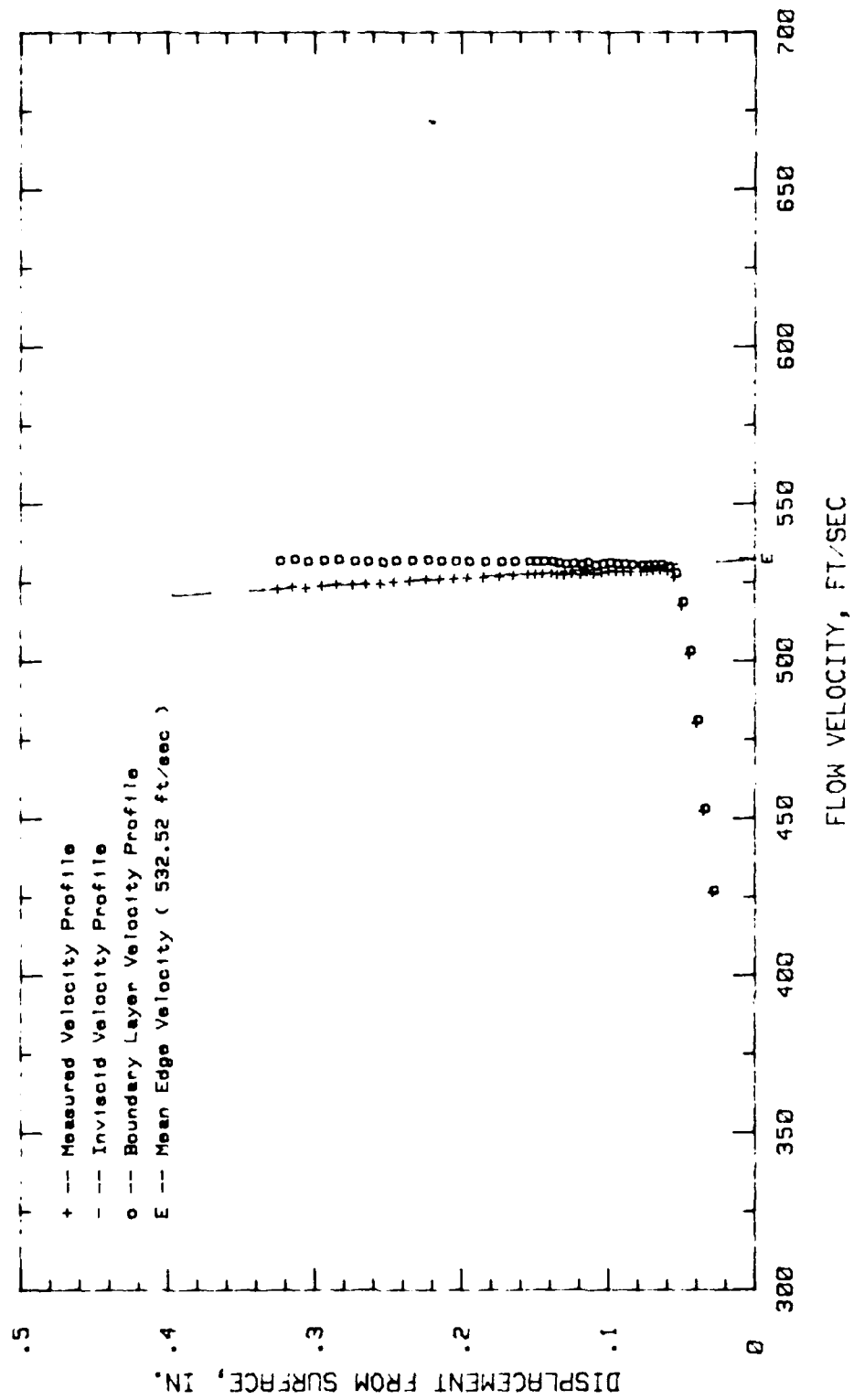


Fig.73. Boundary Layer Velocity Profiles, Conf.#1 at 75% Chord LOW TURB.

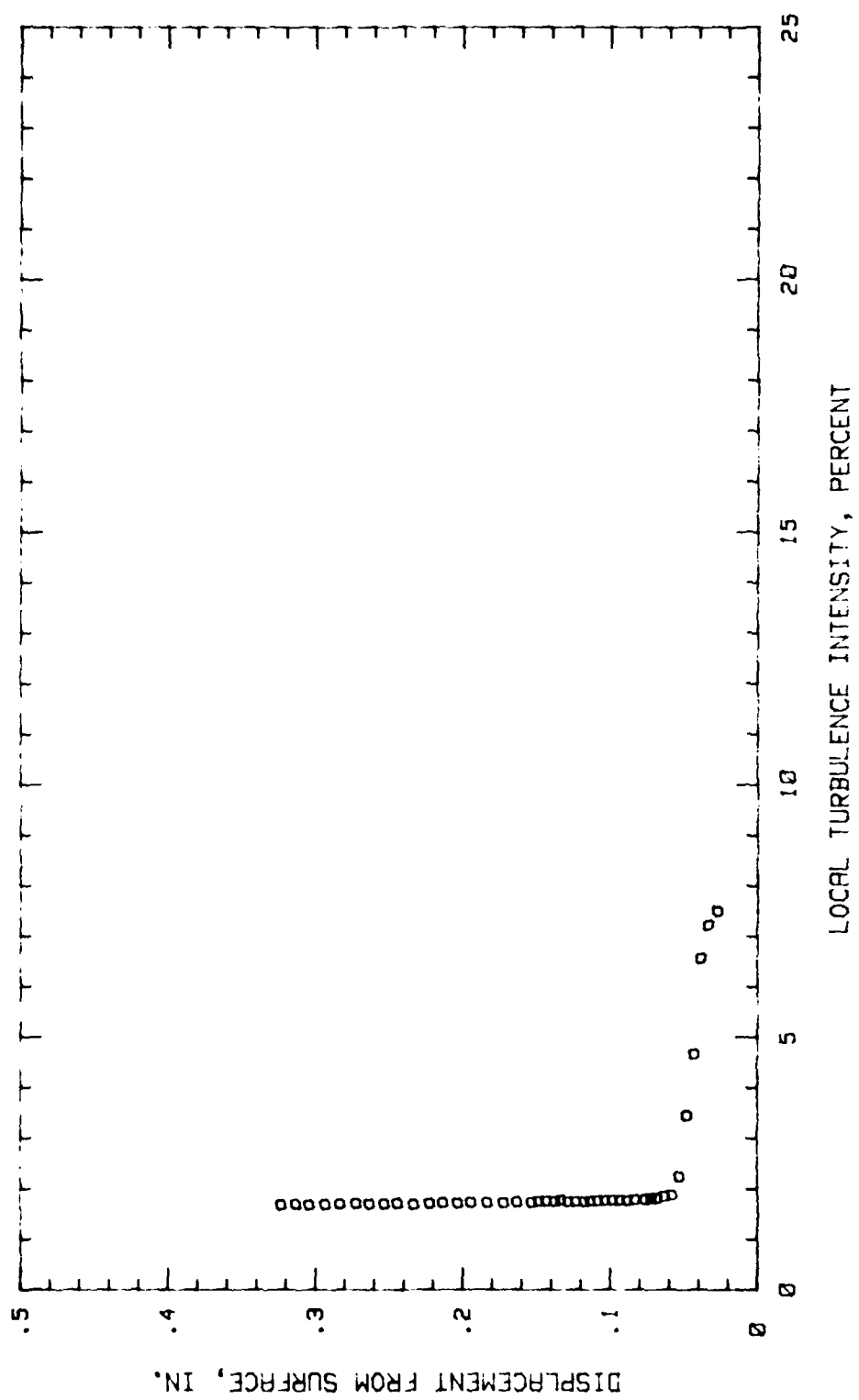


Fig.74. Boundary Layer Turb. Intensity Profile, Conf. #1 at 75% Chord LOW TURB.

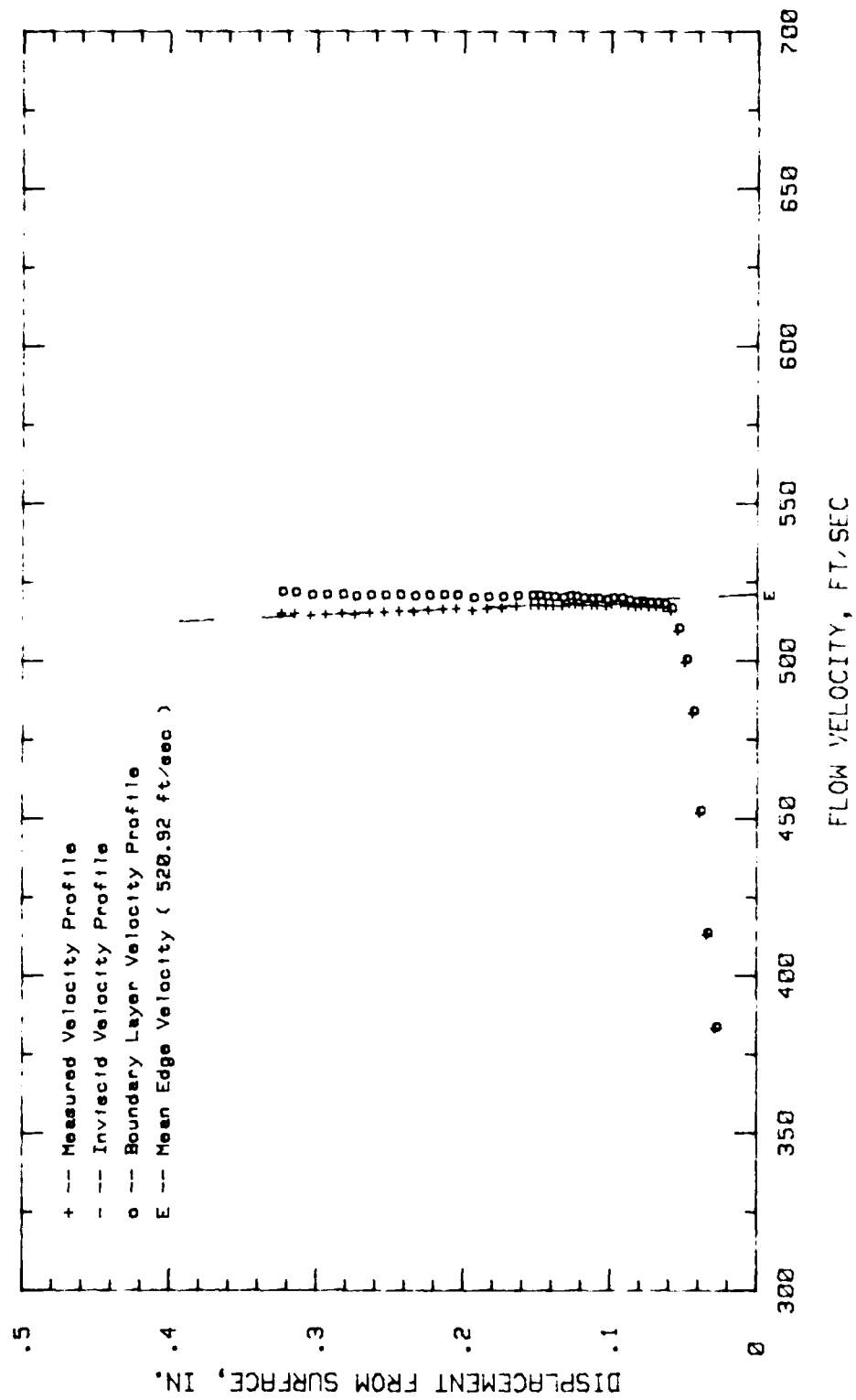


Fig.75. Boundary Layer Velocity Profiles, Conf.#1 at 79.68% Chord LOW TURB.

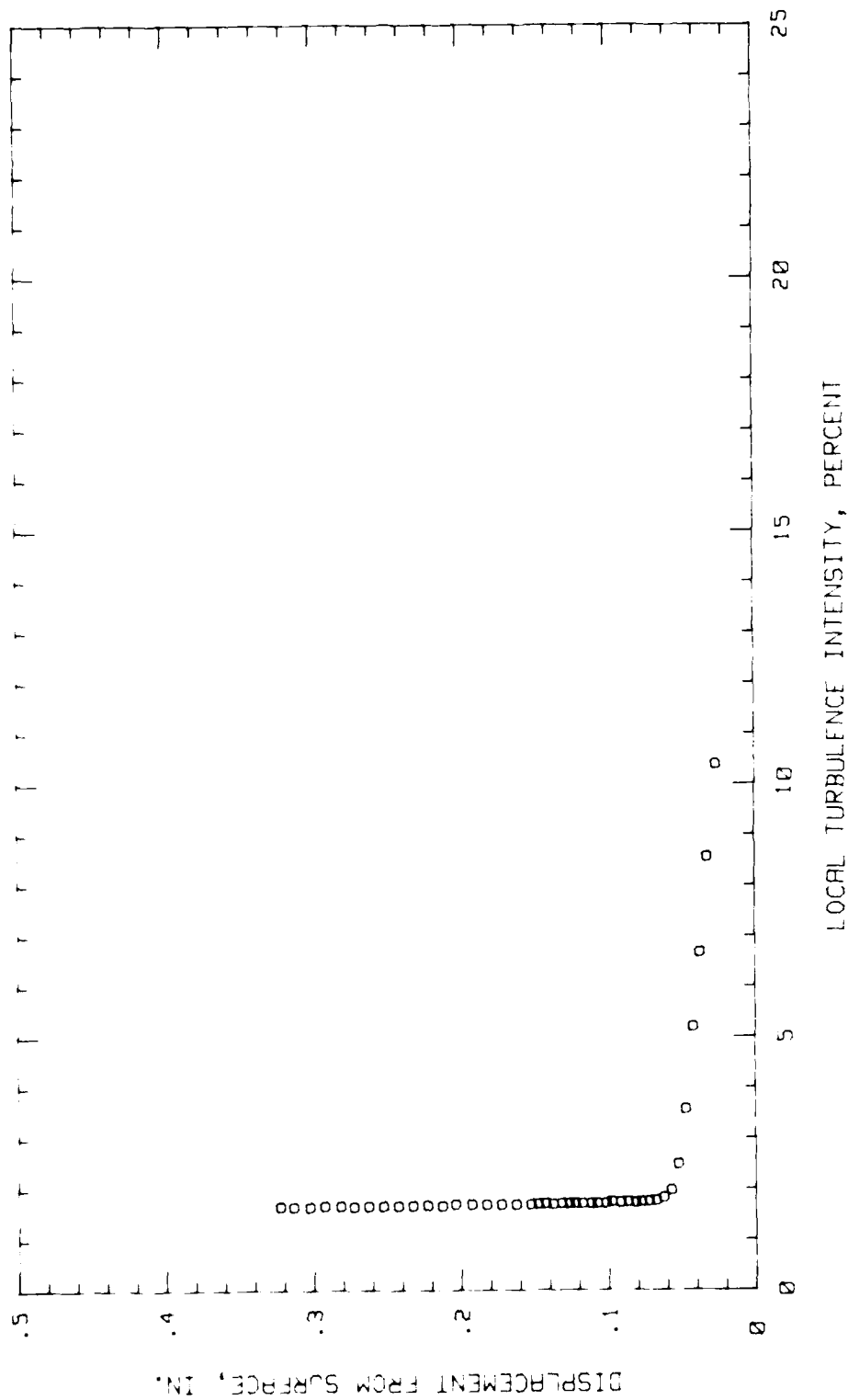


Fig.76. Boundary Layer Turb. Intensity Profile, Conf. #1 at 79.68% Chord LOW TURB.

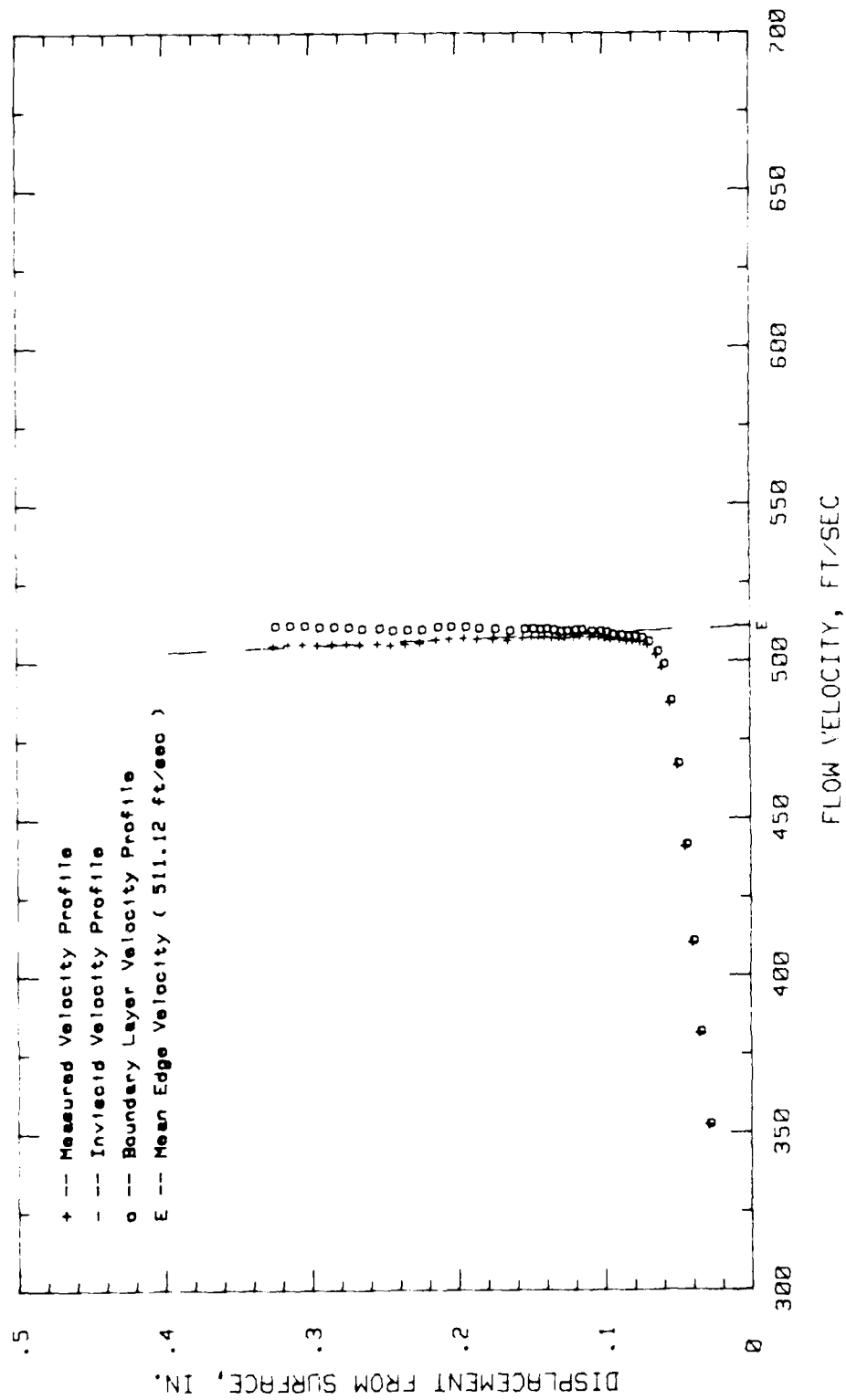


Fig.77. Boundary Layer Velocity Profiles, Conf.#1 at 84.37% Chord LOW TURB.

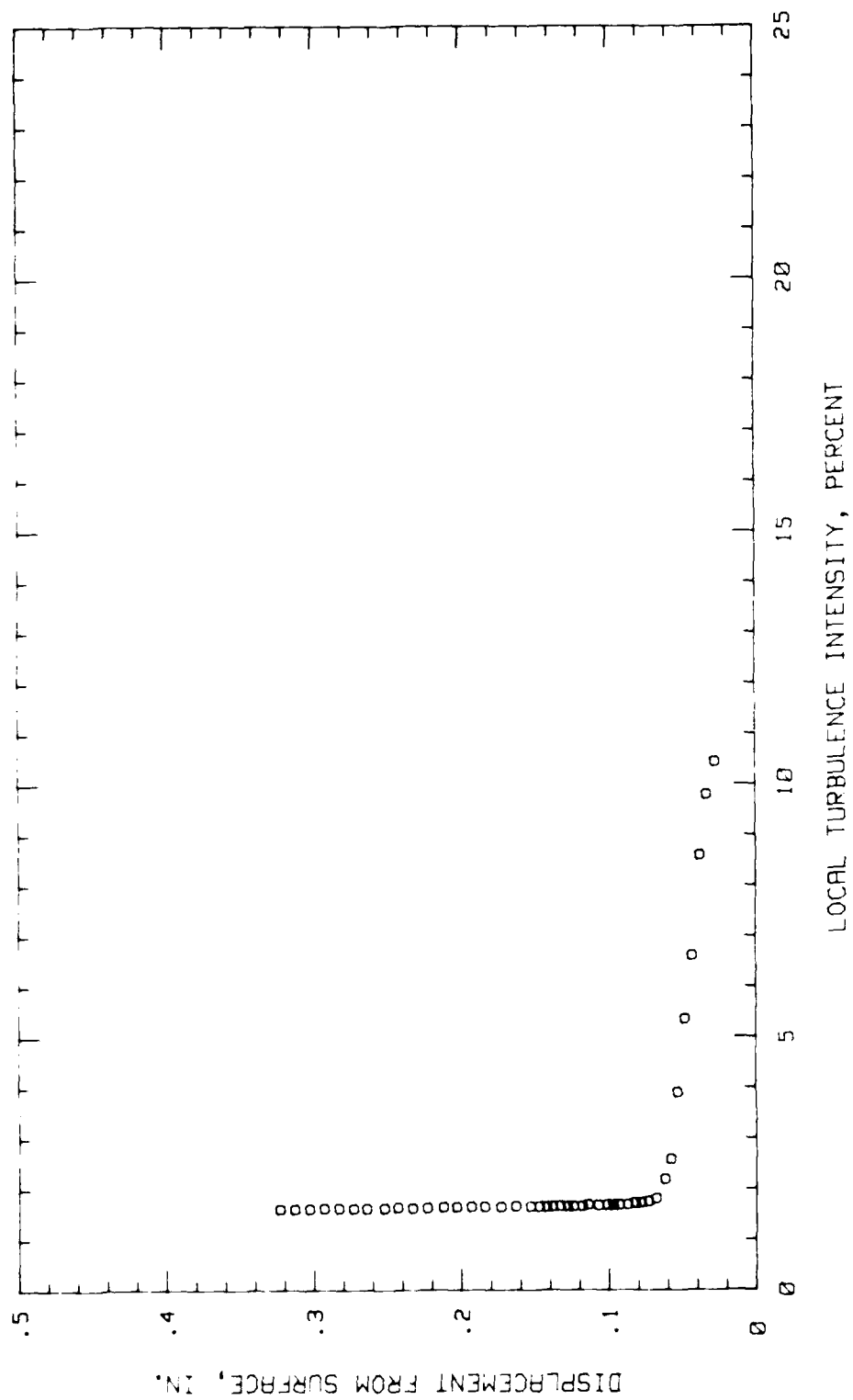


Fig.78. Boundary Layer Turb. Intensity Profile, Conf.#1 at 84.37% Chord LOW TURB.

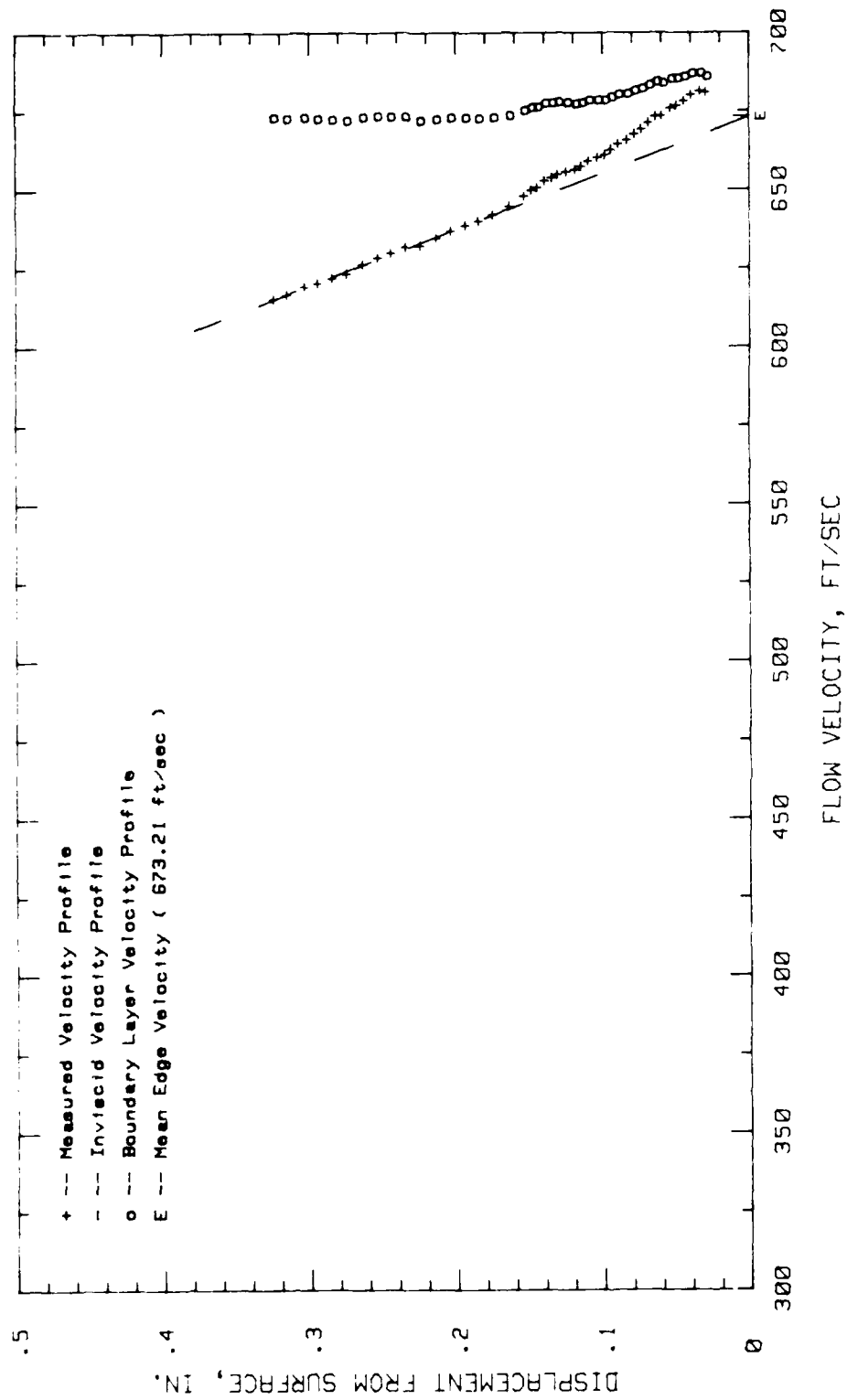


Fig.79. Boundary Layer Velocity Profiles, Conf.#1 at 4.68% Chord HIGH TURB.

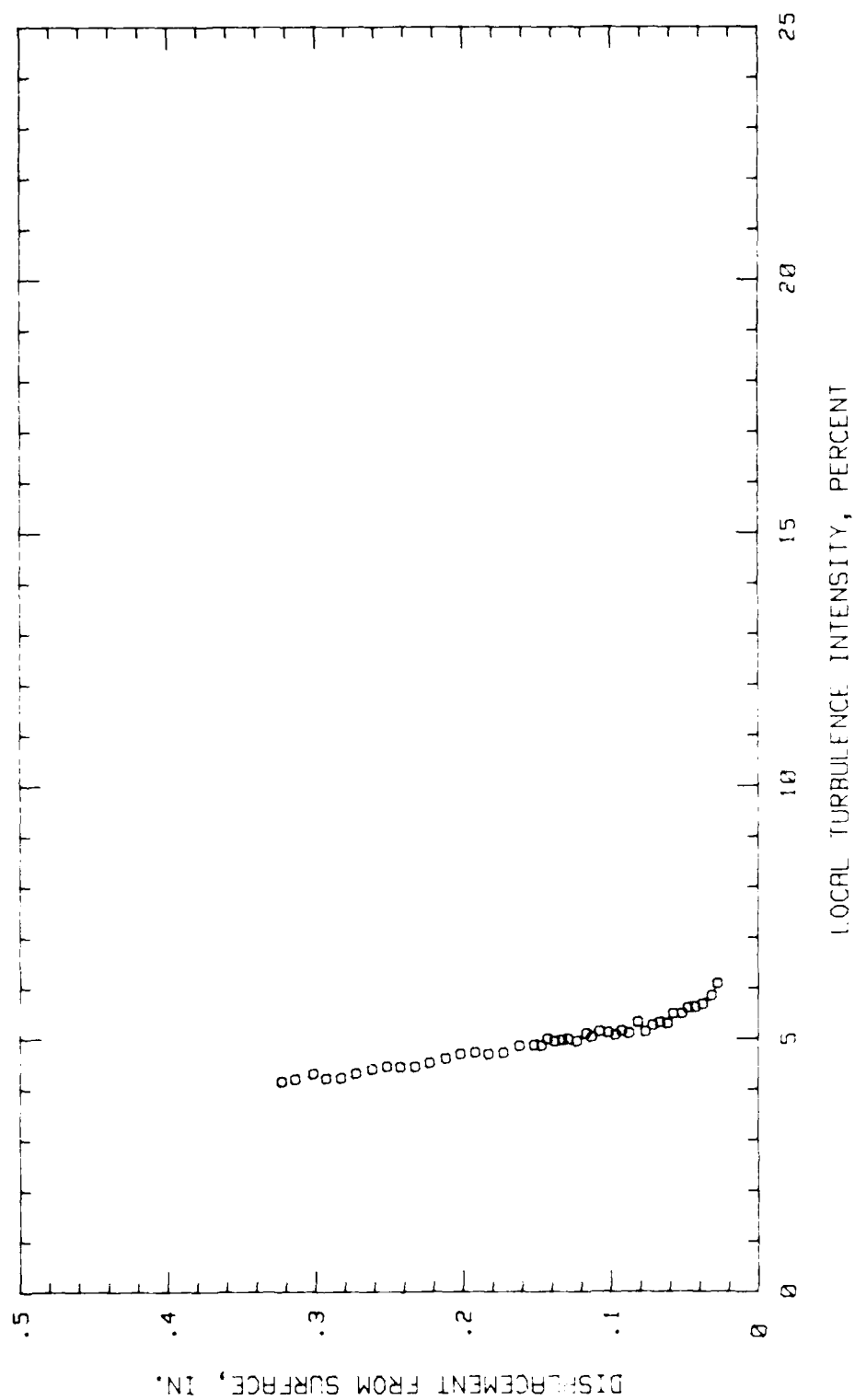


Fig. 80. Boundary Layer Turb. Intensity Profile, Conf. #1 at 4.68% Chord HIGH TURB.

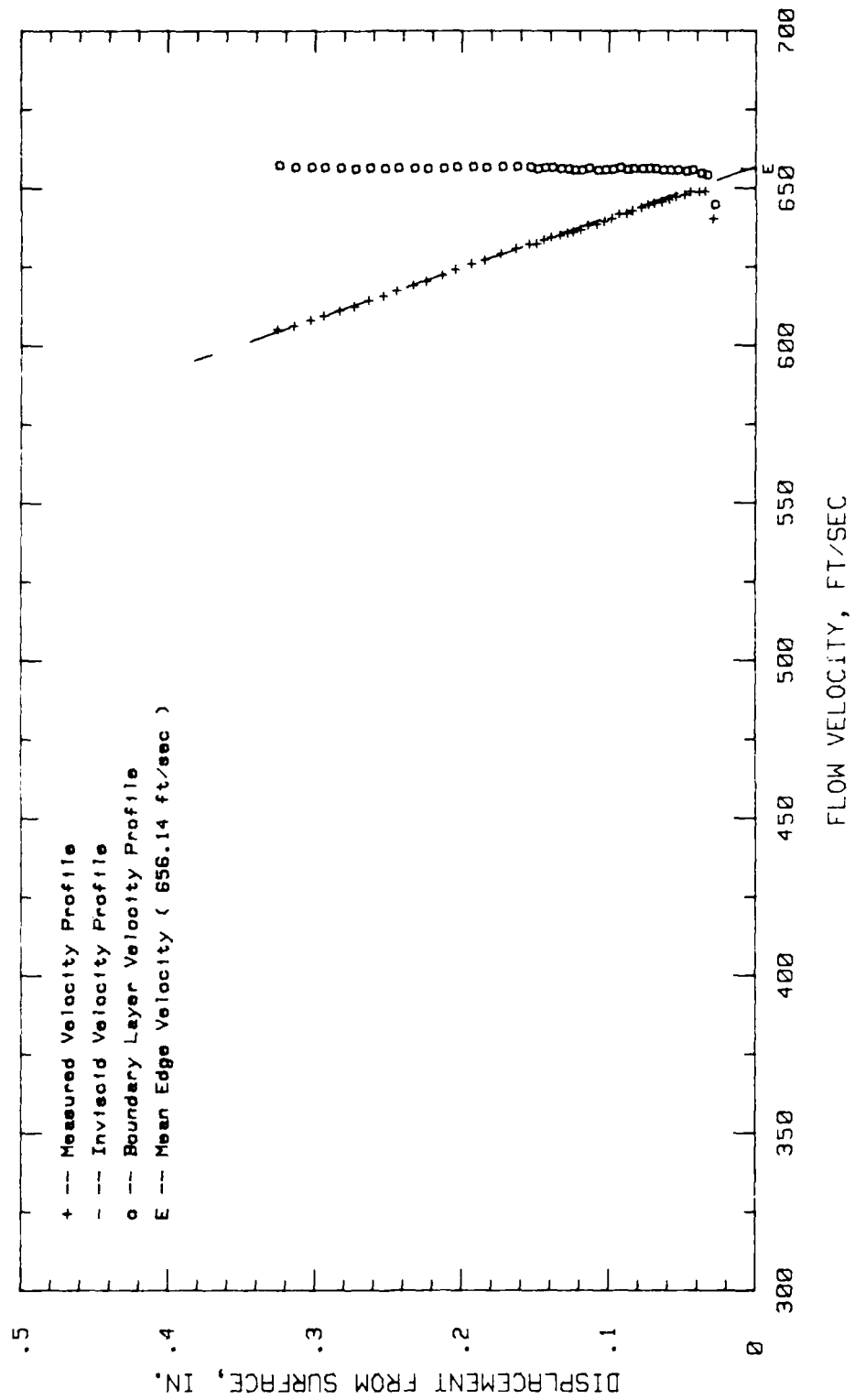


Fig.81. Boundary Layer Velocity Profiles, Conf.#1 at 9.37% Chord HIGH TURB.

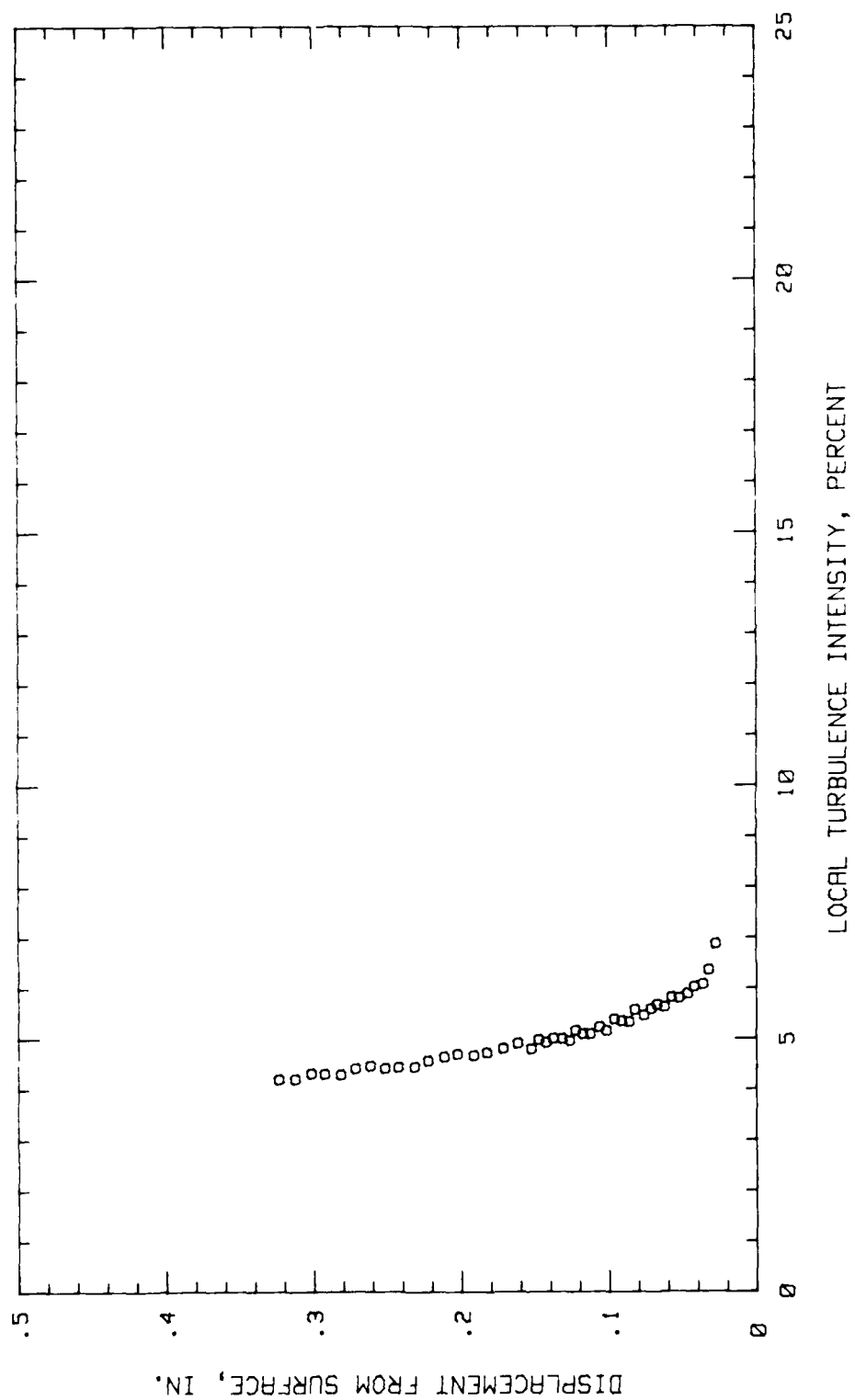


Fig.82. Boundary Layer Turb. Intensity Profile, Conf.#1 at 9.37% Chord HIGH TURB.

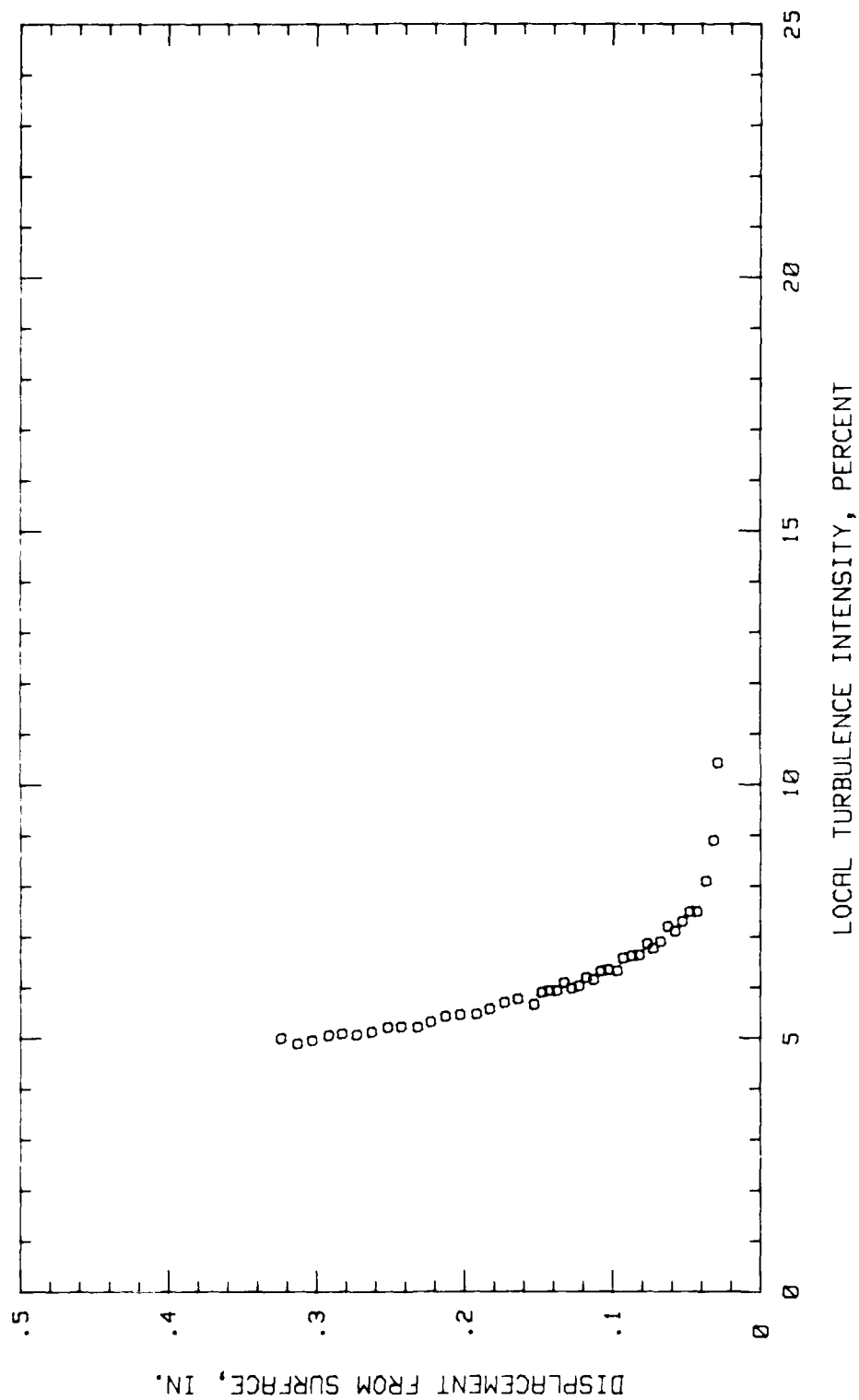


Fig.84. Boundary Layer Turb. Intensity Profile, Conf.#1 at 25% Chord HIGH TURB.

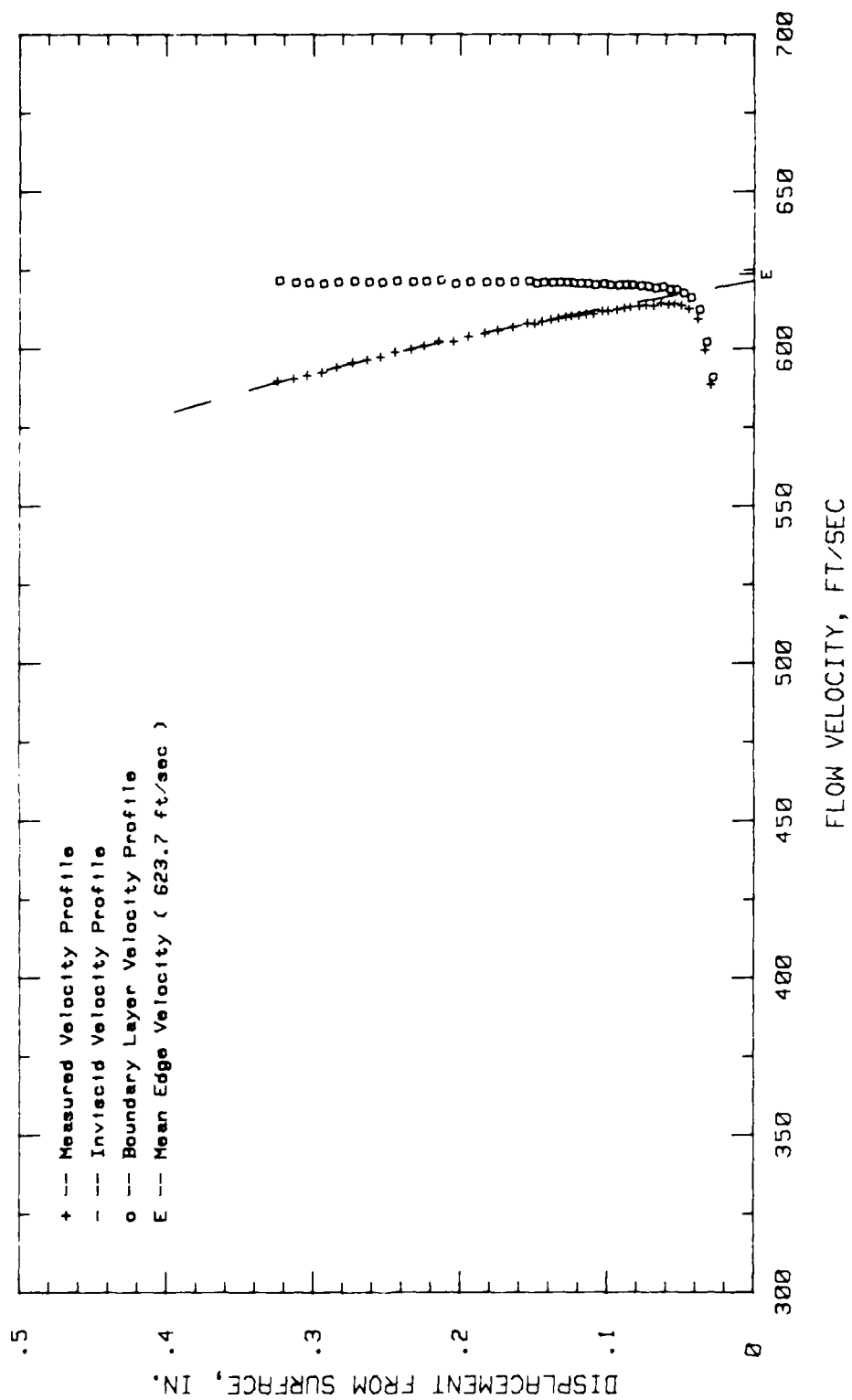


Fig.85. Boundary Layer Velocity Profiles, Conf.#1 at 29.68% Chord HIGH TURB.

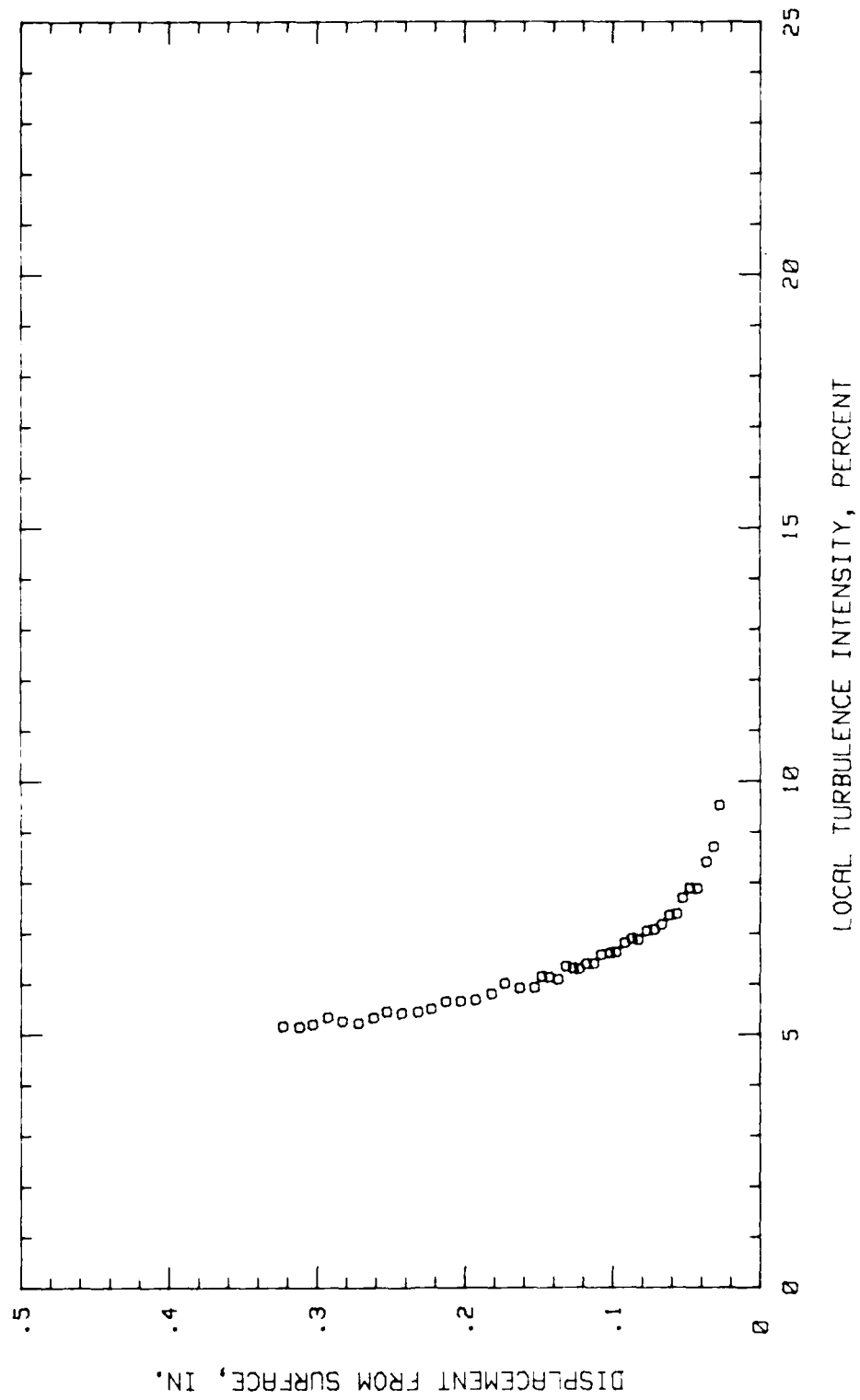


Fig.86. Boundary Layer Turb. Intensity Profile, Conf.#1 at 29.68% Chord HIGH TURB

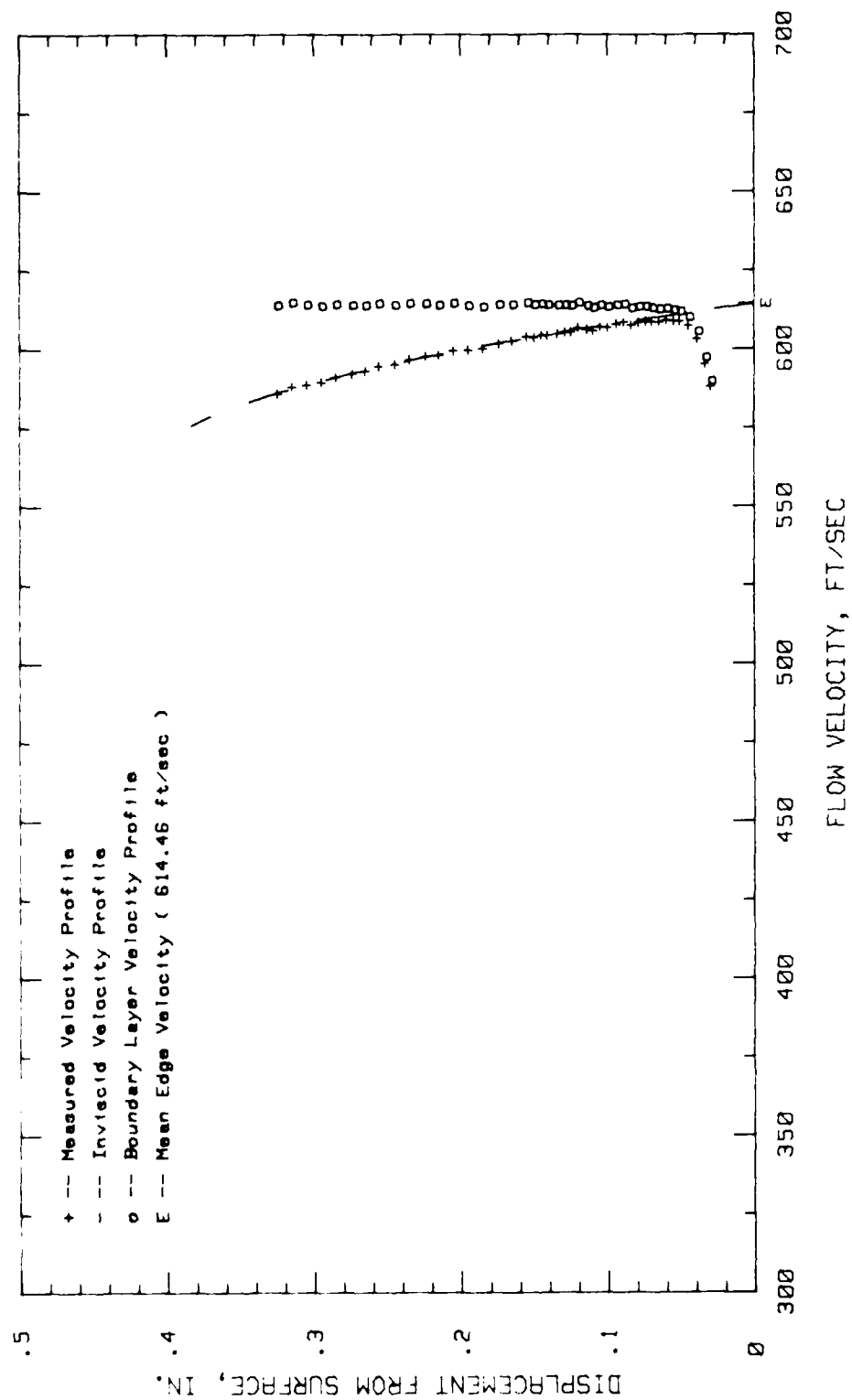


Fig.87. Boundary Layer Velocity Profiles, Conf.#1 at 34.37% Chord HIGH TURB.

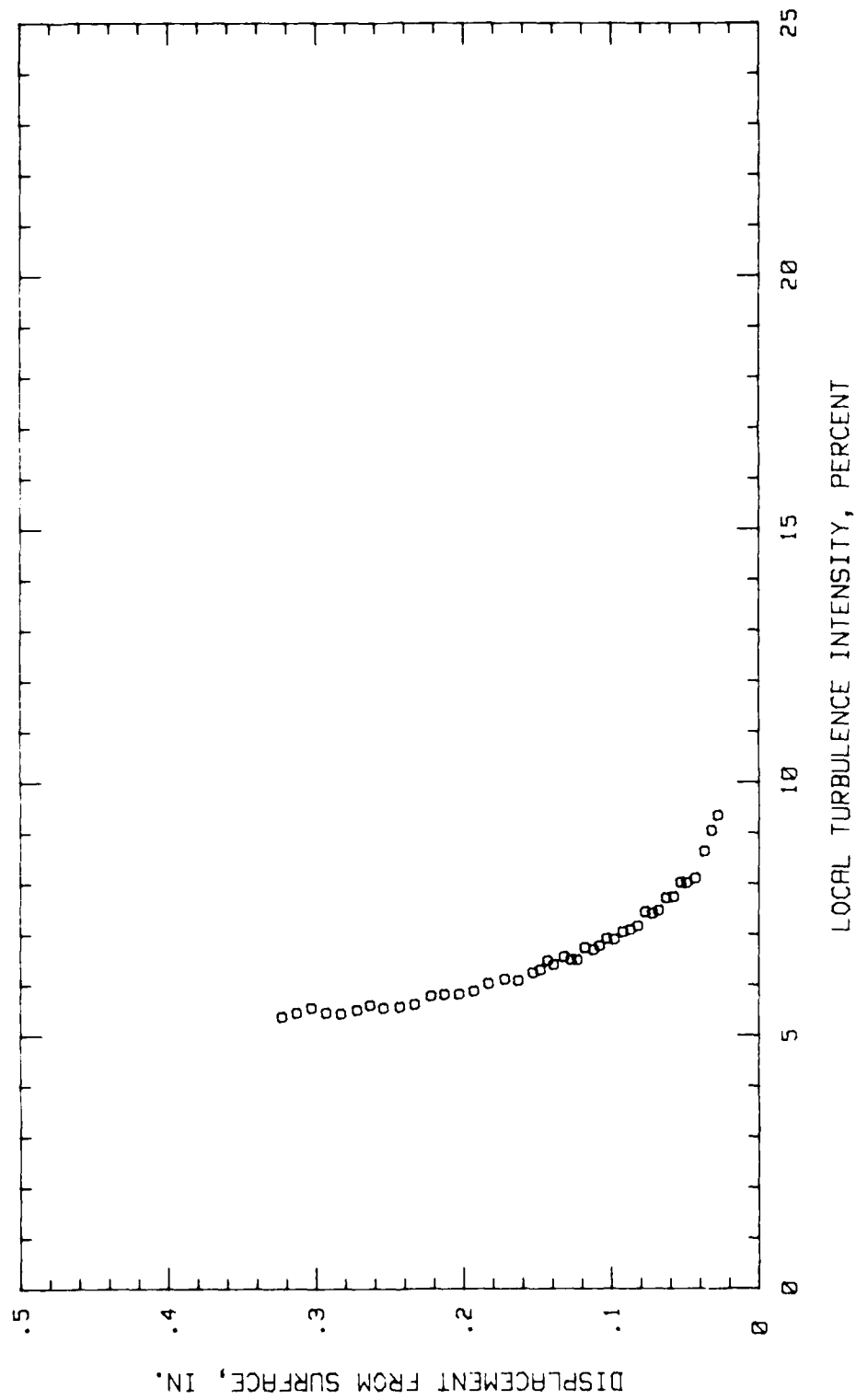


Fig.88. Boundary Layer Turb. Intensity Profile, Conf.#1 at 34.37% Chord HIGH TURB

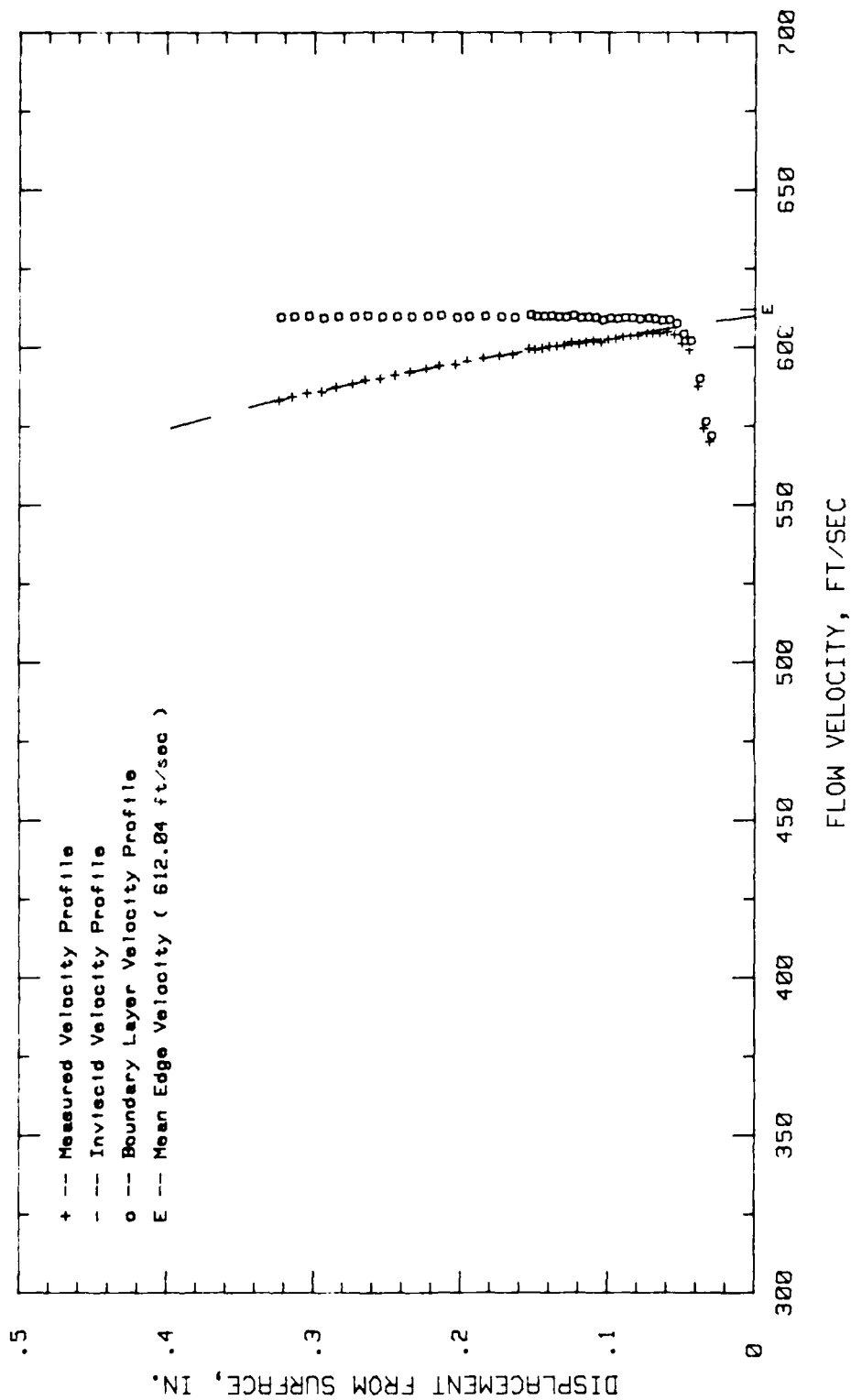


Fig.89. Boundary Layer Velocity Profiles, Conf.#1 at 40.62% Chord HIGH TURB.

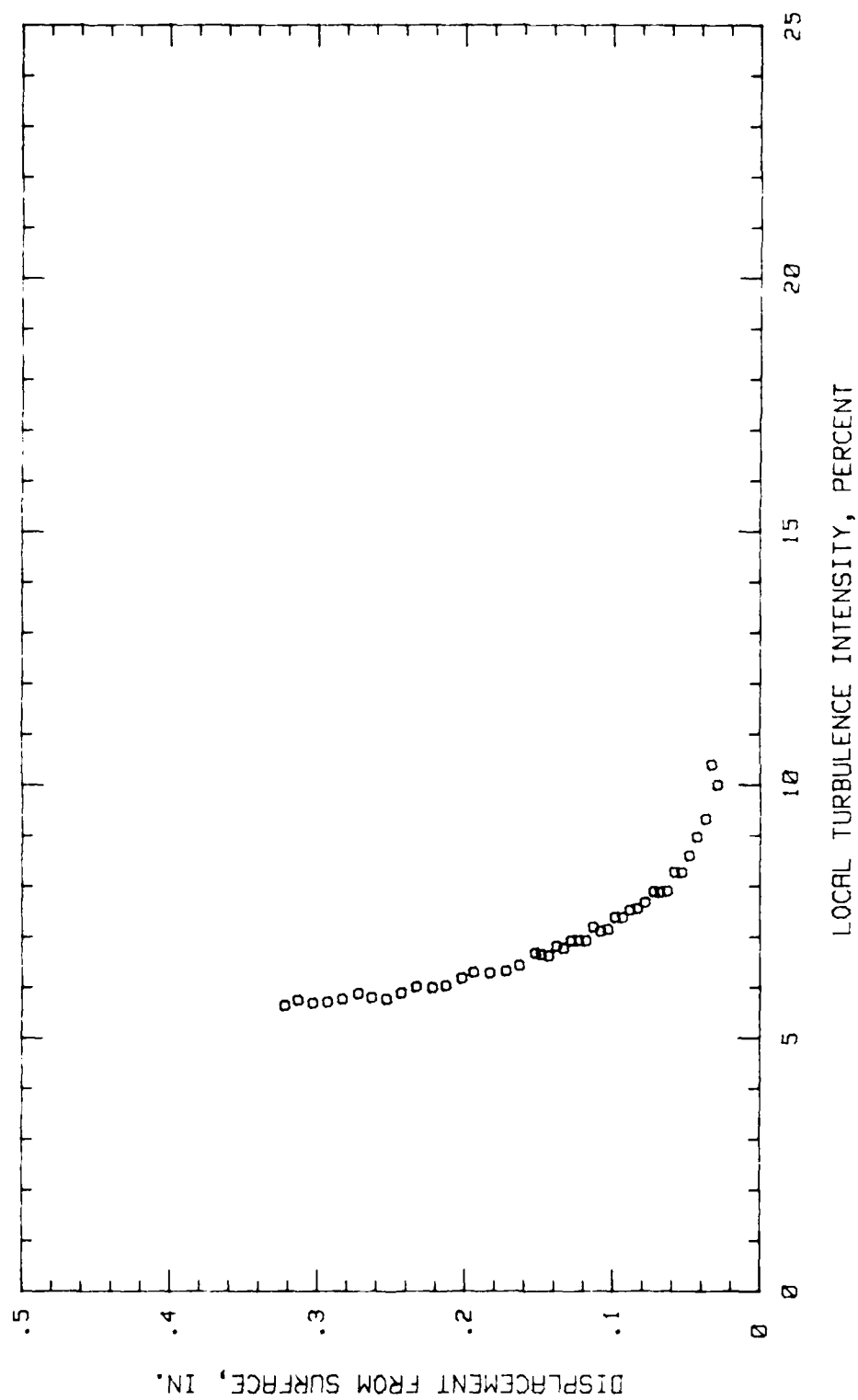


Fig.90. Boundary Layer Turb. Intensity Profile, Conf.#1 at 40.62% Chord HIGH TURB

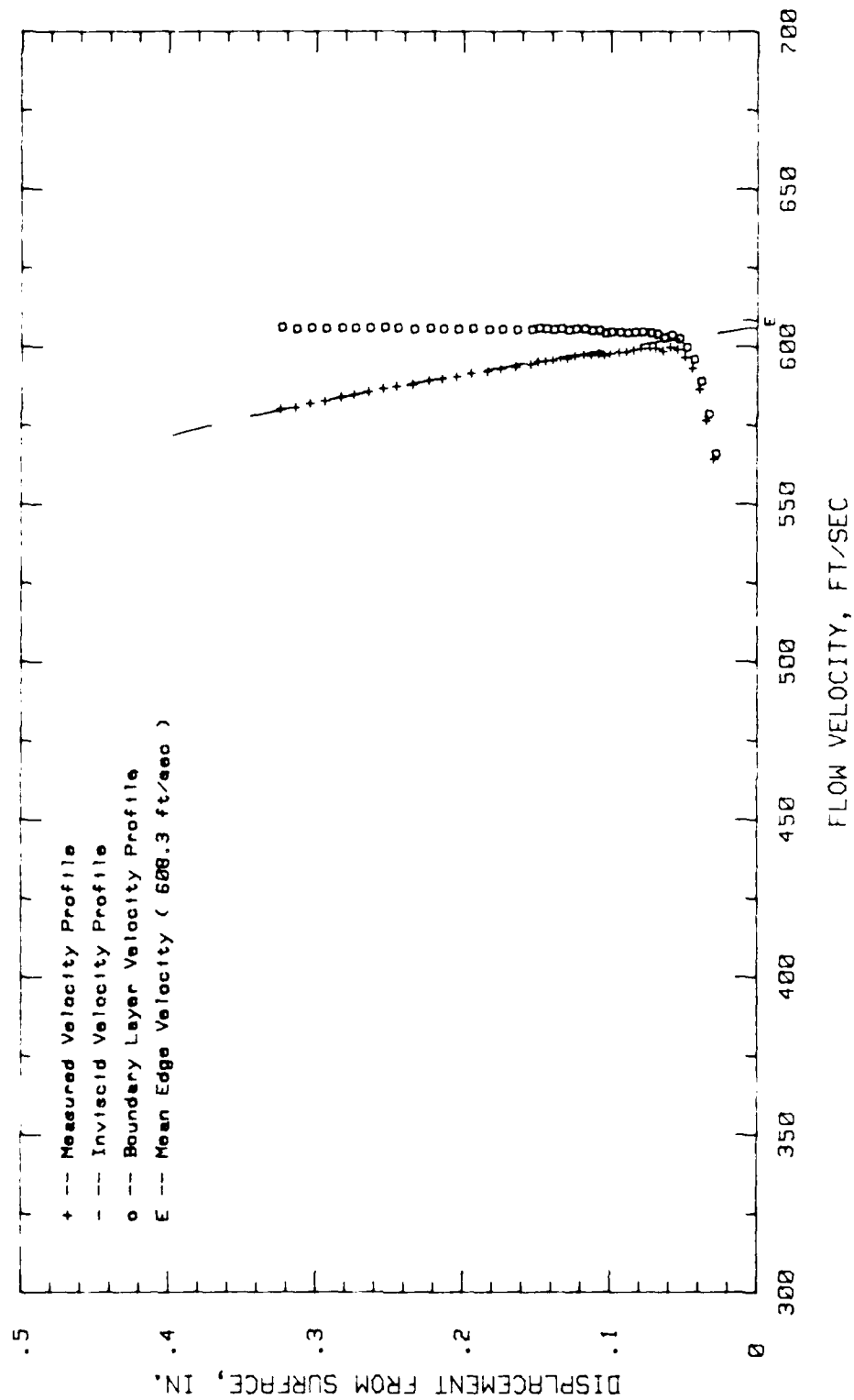


Fig.91. Boundary Layer Velocity Profiles, Conf.#1 at 45.31% Chord HIGH TURB.

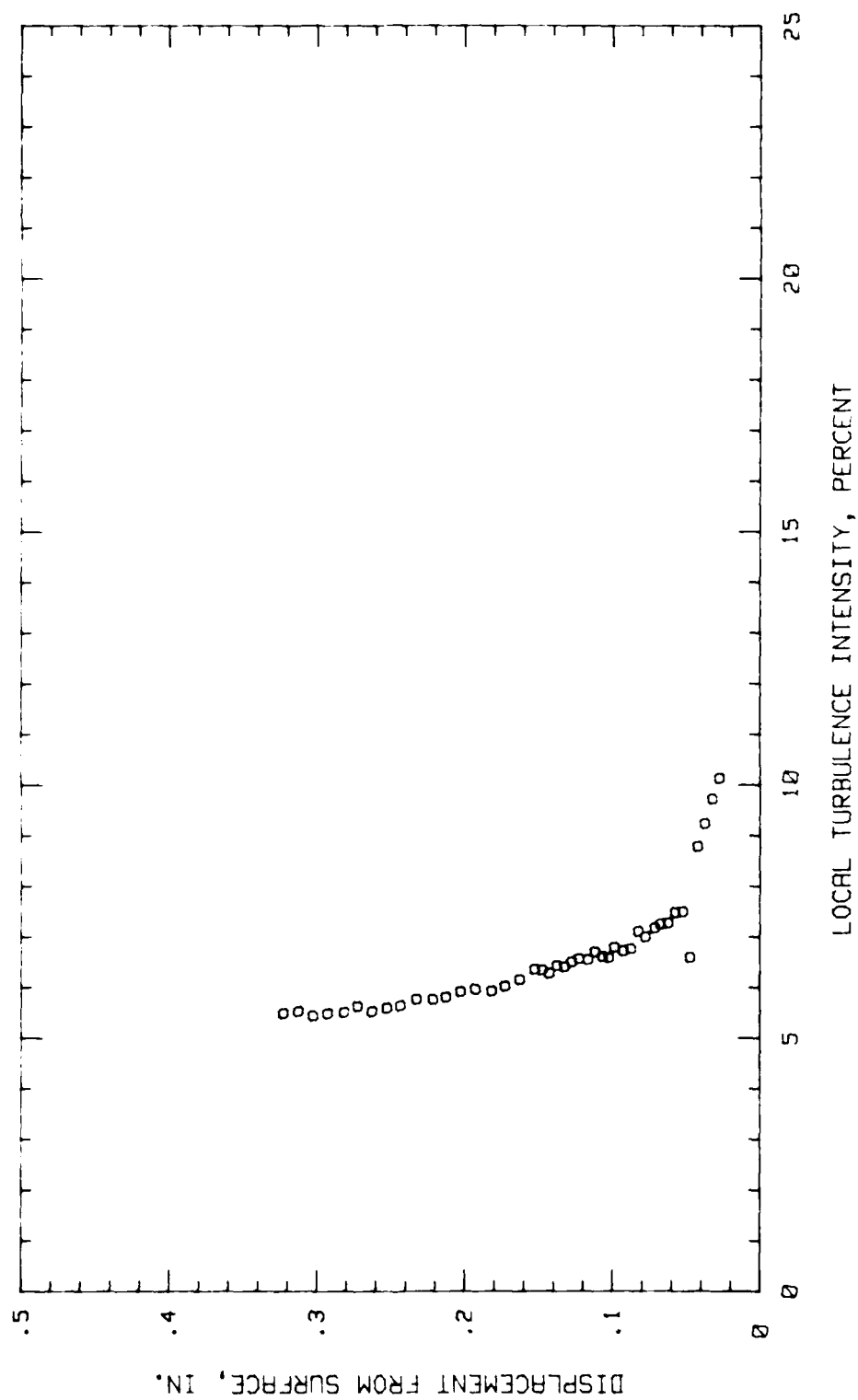


Fig.92. Boundary Layer Turb. Intensity Profile, Conf.#1 at 45.31% Chord HIGH TURB

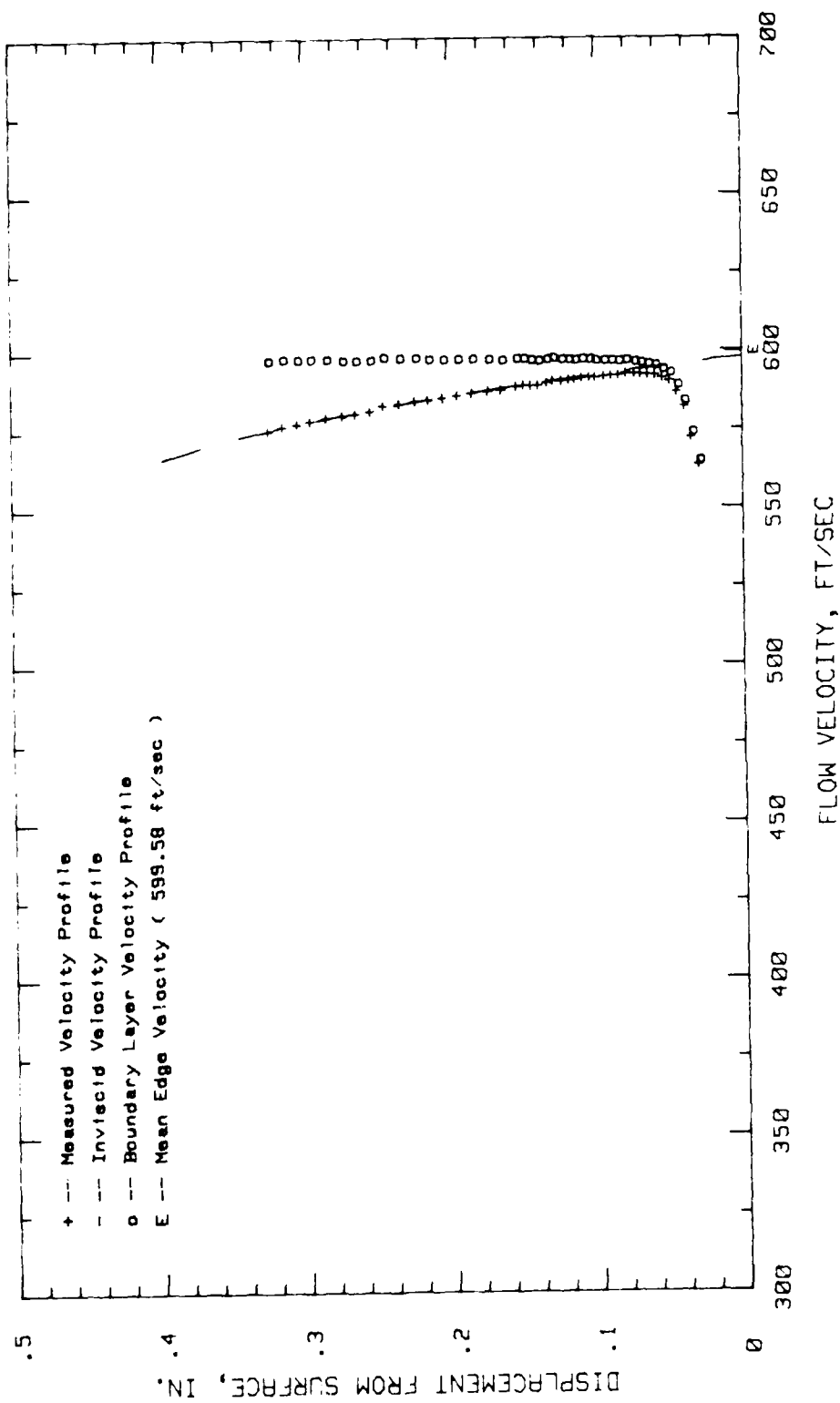


Fig.93. Boundary Layer Velocity Profiles, Conf.#1 at 50% Chord HIGH TURB.

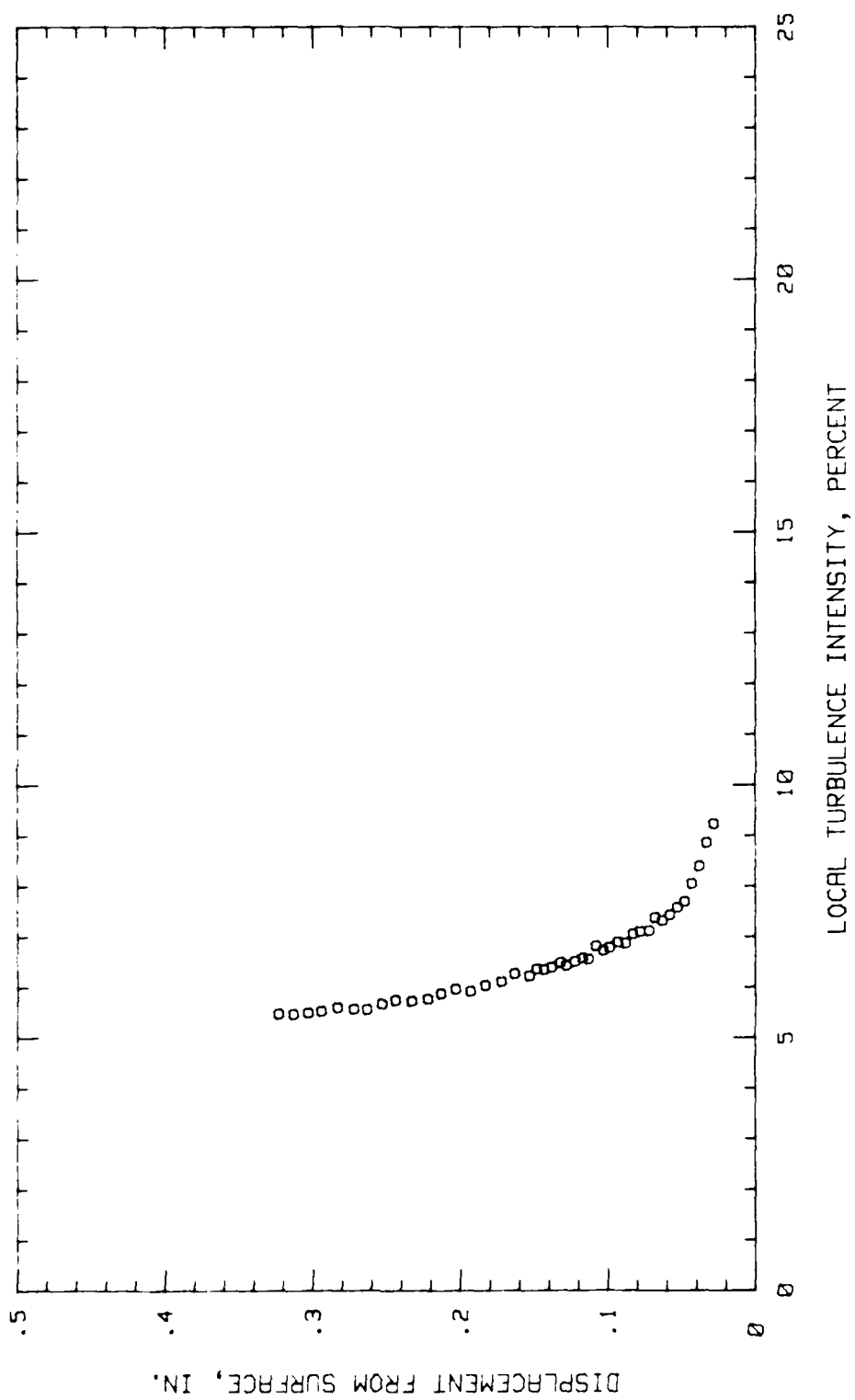


Fig. 94. Boundary Layer Turb. Intensity Profile, Conf. #1 at 50% Chord HIGH TURB.

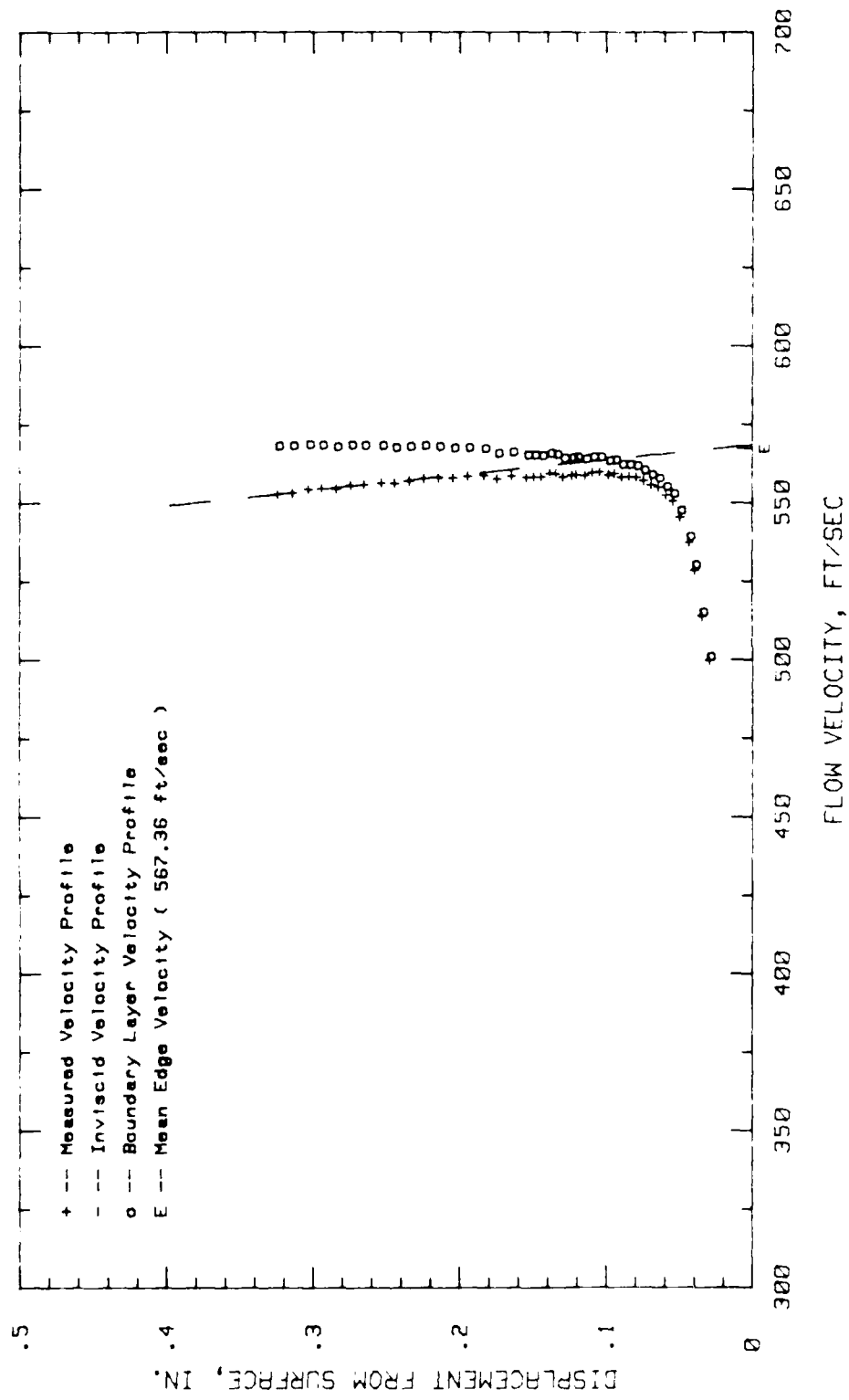


Fig.95. Boundary Layer Velocity Profiles, Conf.#1 at 65.62% Chord HIGH TURB.

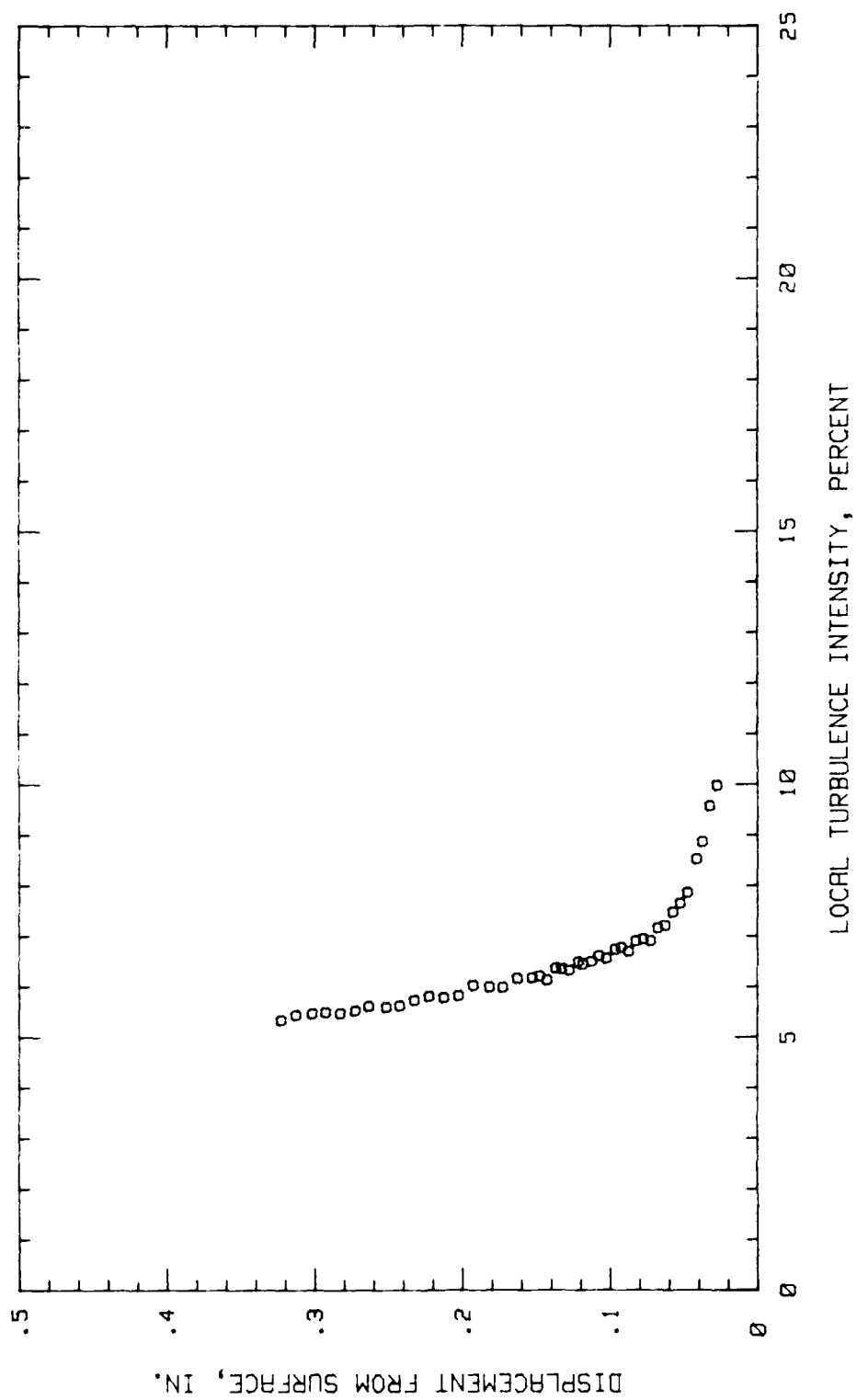


Fig.96. Boundary Layer Turb. Intensity Profile, Conf.#1 at 65.62% Chord HIGH TURB

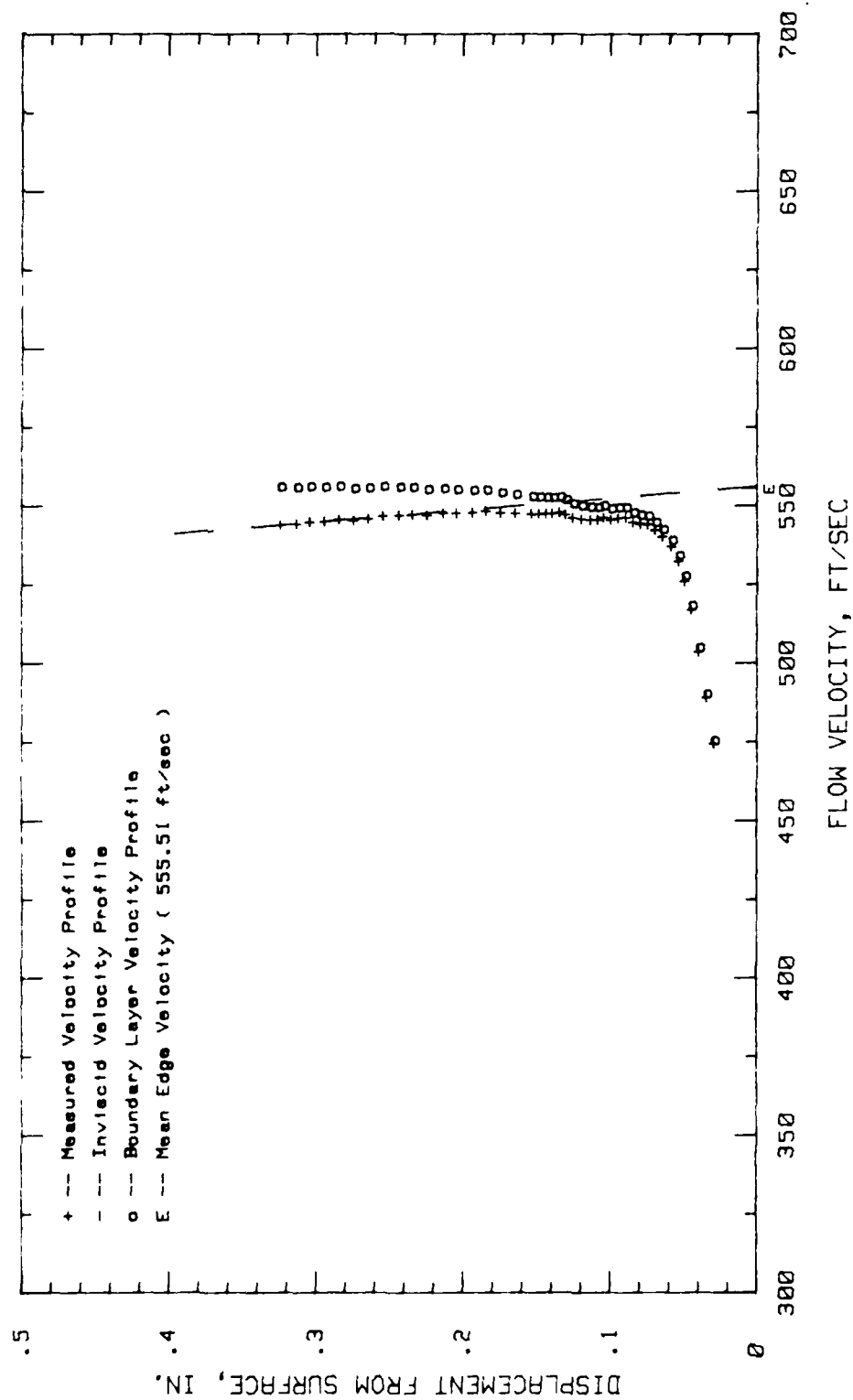


Fig.97. Boundary Layer Velocity Profiles, Conf.#1 at 70.31% Chord HIGH TURB.

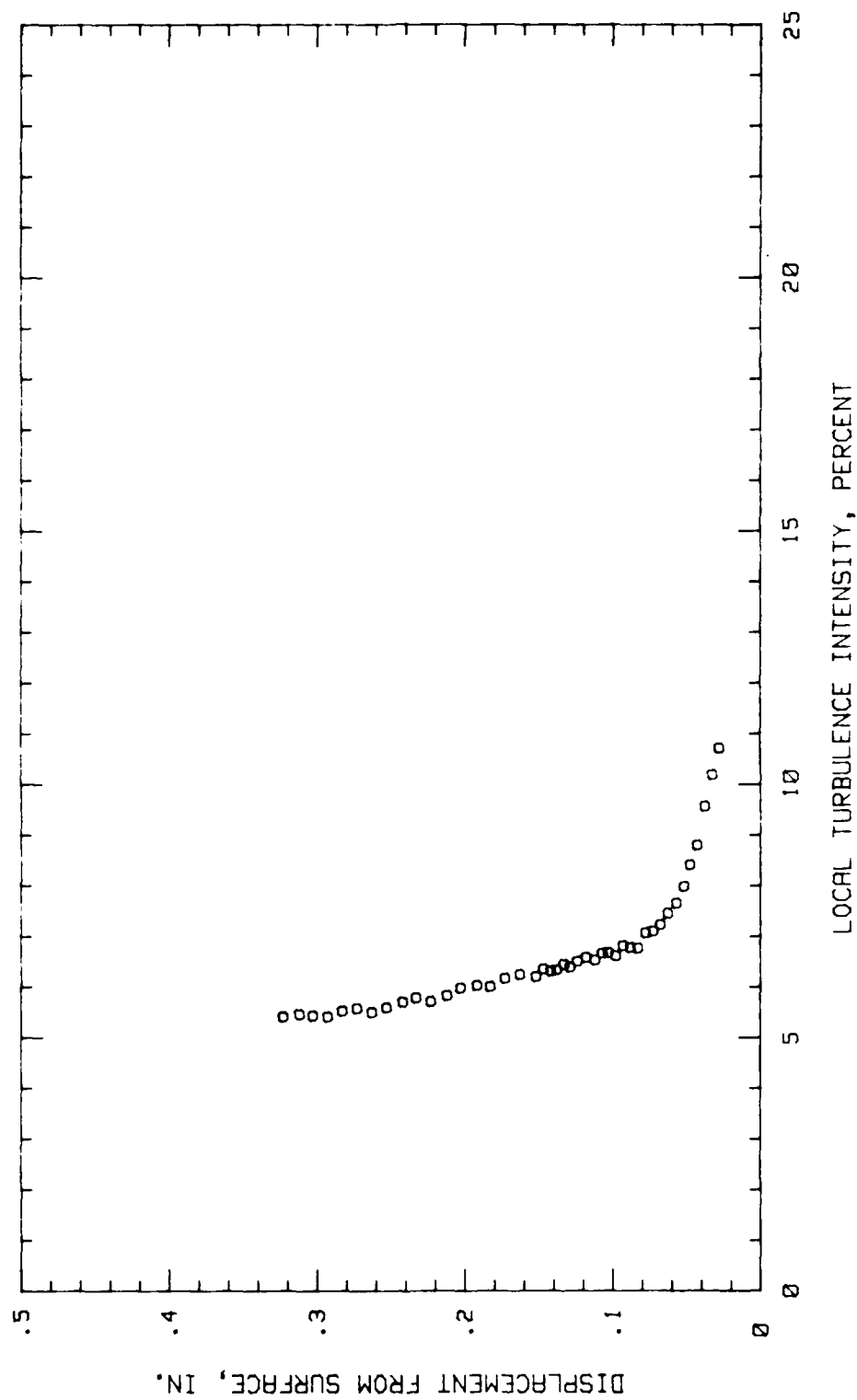


Fig.98. Boundary Layer Turb. Intensity Profile, Conf.#1 at 70.31% Chord HIGH TURB

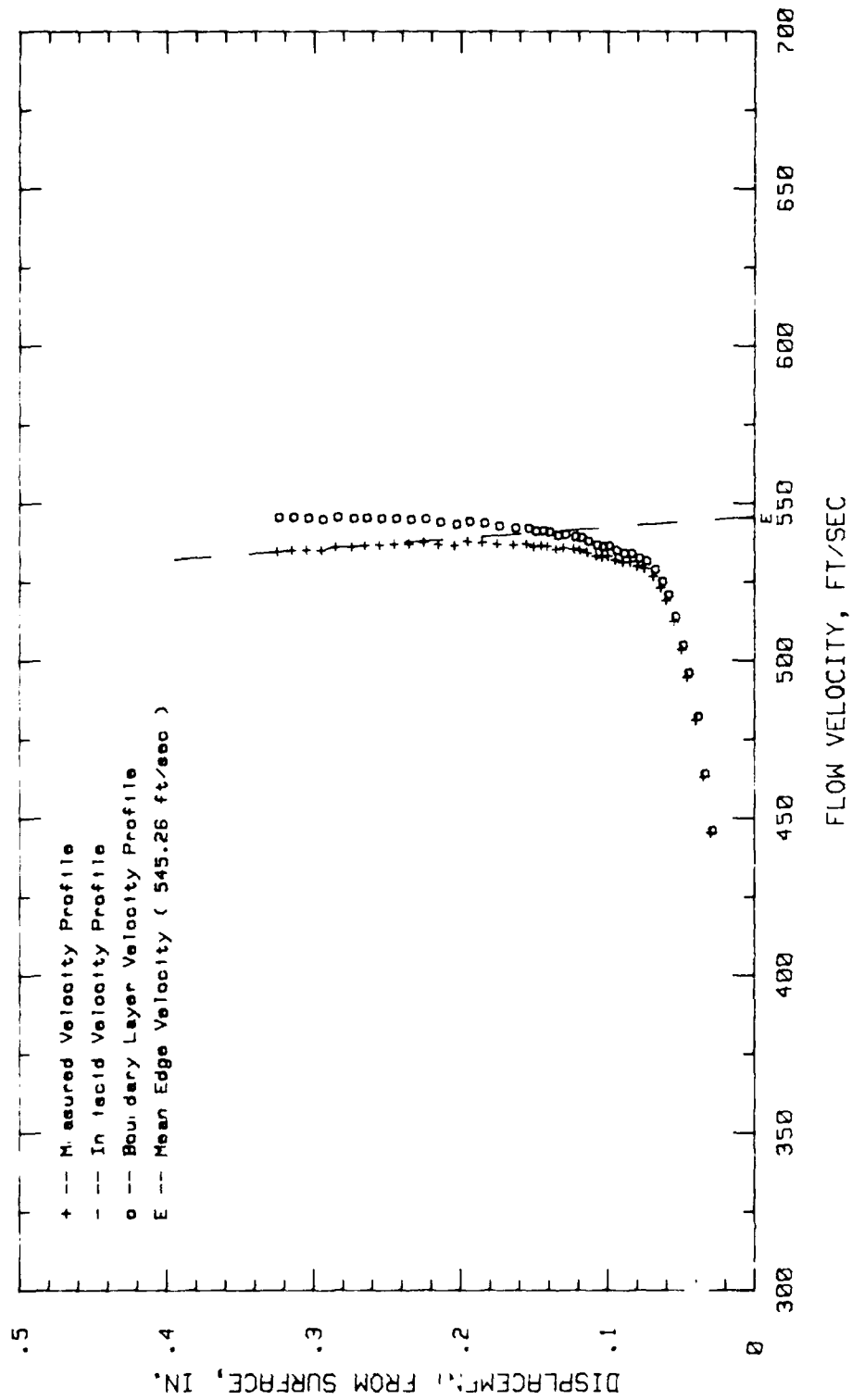


Fig.99. Boundary Layer Velocity Profiles, Conf.#1 at 75% Chord HIGH TURB.

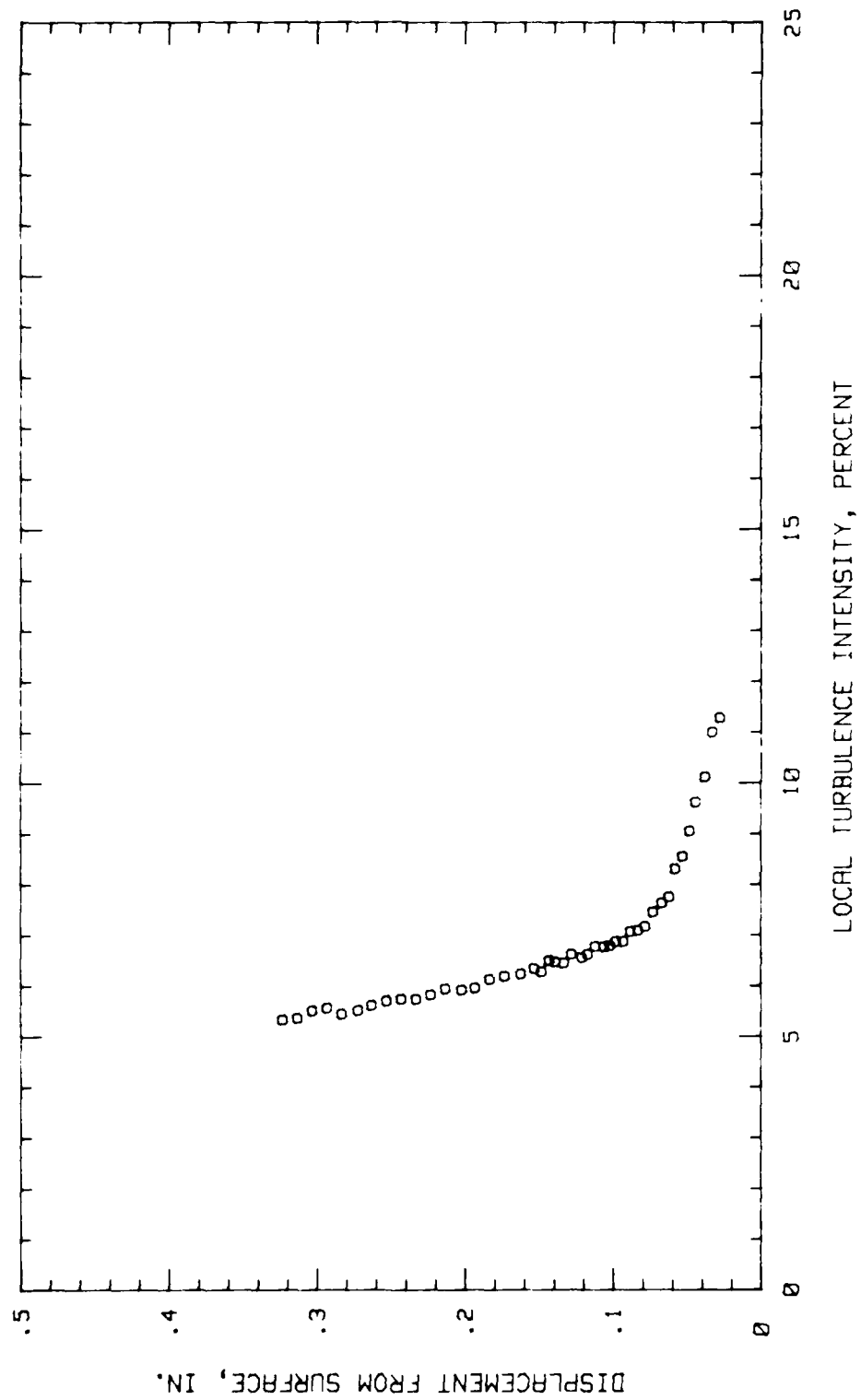


Fig.100.Boundary Layer Turb. Intensity Profile, Conf.#1 at 75% Chord HIGH TURB.

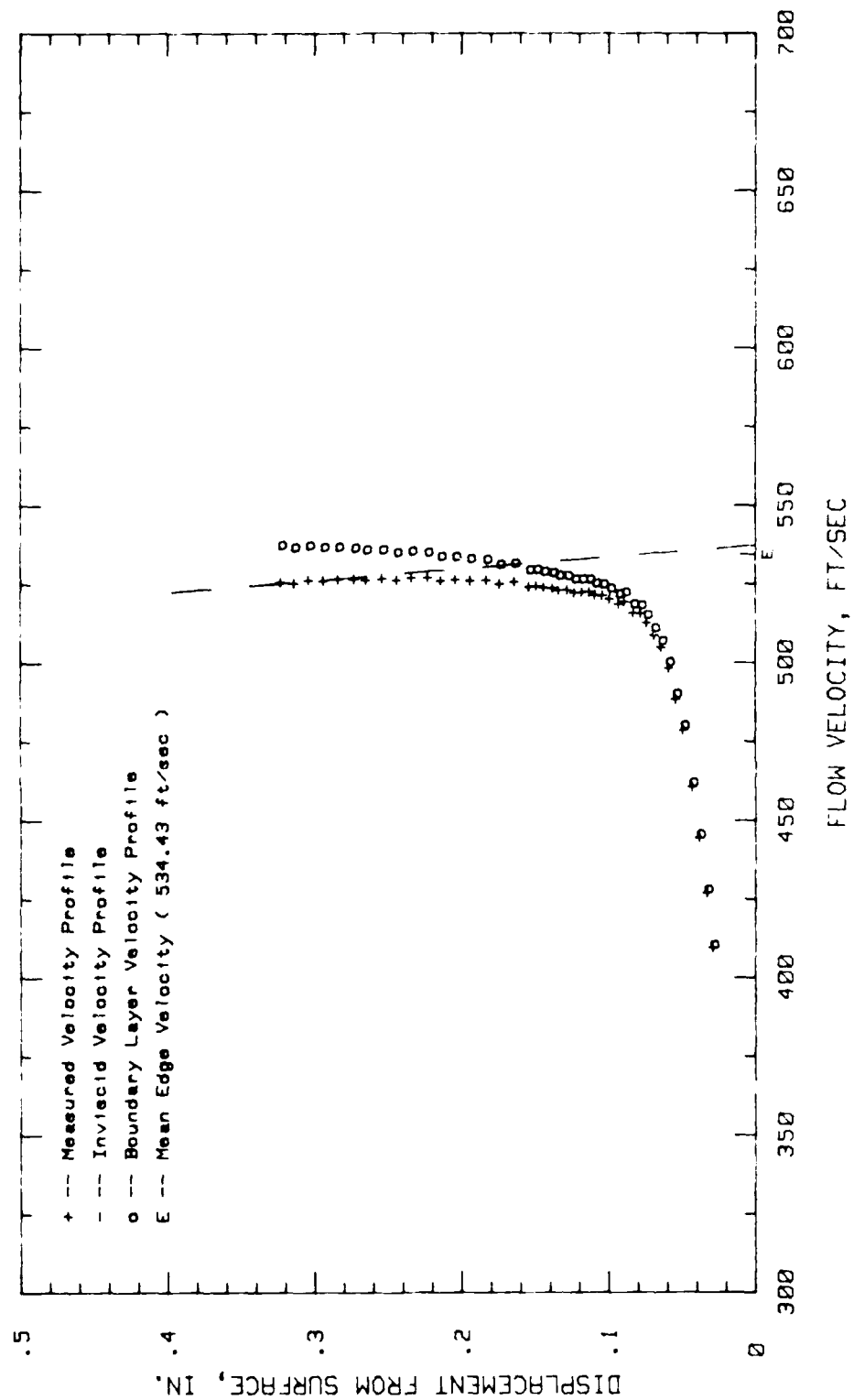


Fig.101. Boundary Layer Velocity Profiles, Conf.#1 at 79.68% Chord HIGH TURB.

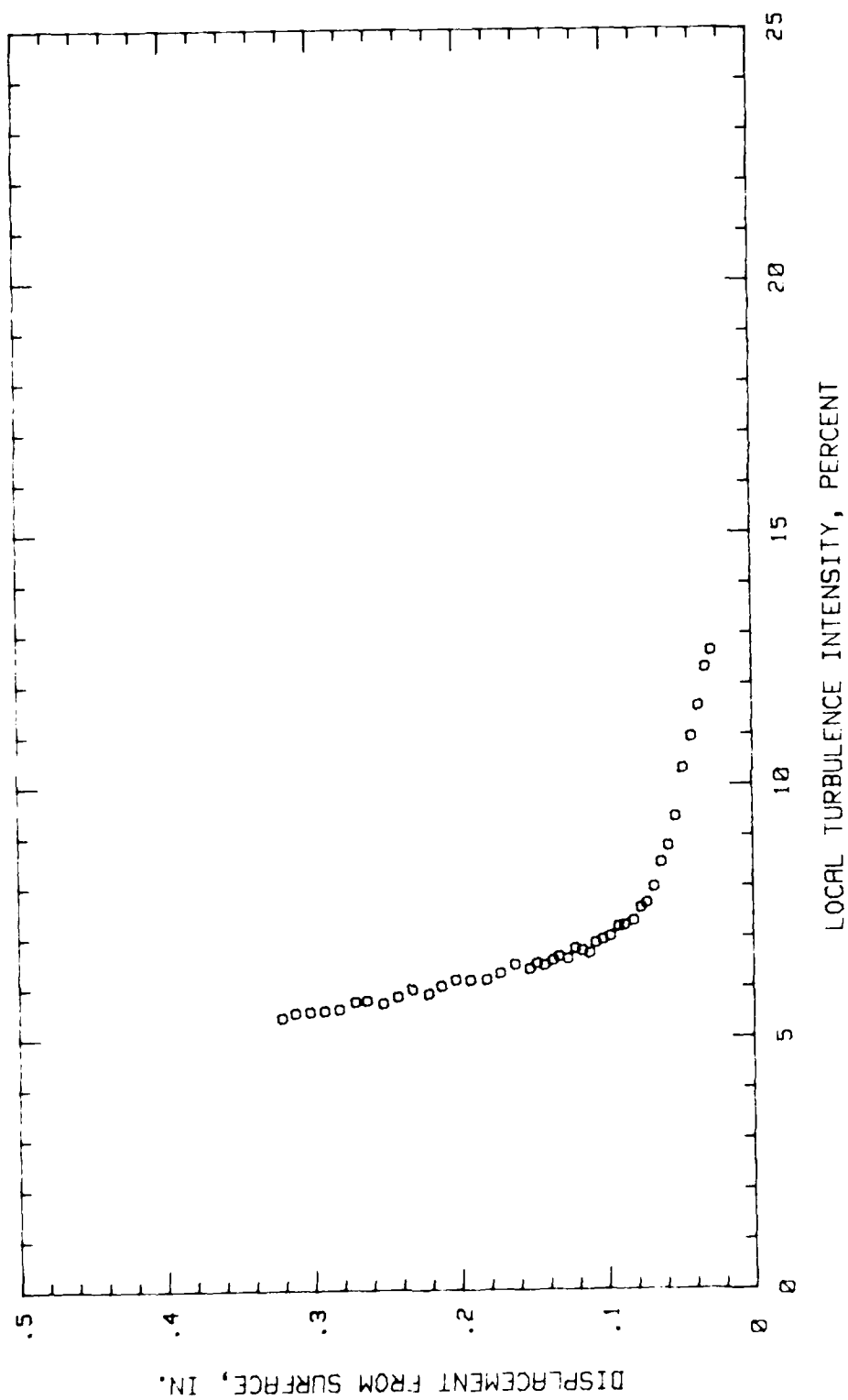


Fig.102.Boundary Layer Turb. Intensity Profile, Conf.#1 at 79.68% Chord HIGH TUR

APPENDIX C

Boundary Layer Velocity & Turbulence Intensity Profiles

Configuration #2, Low and High Freestream Turbulence

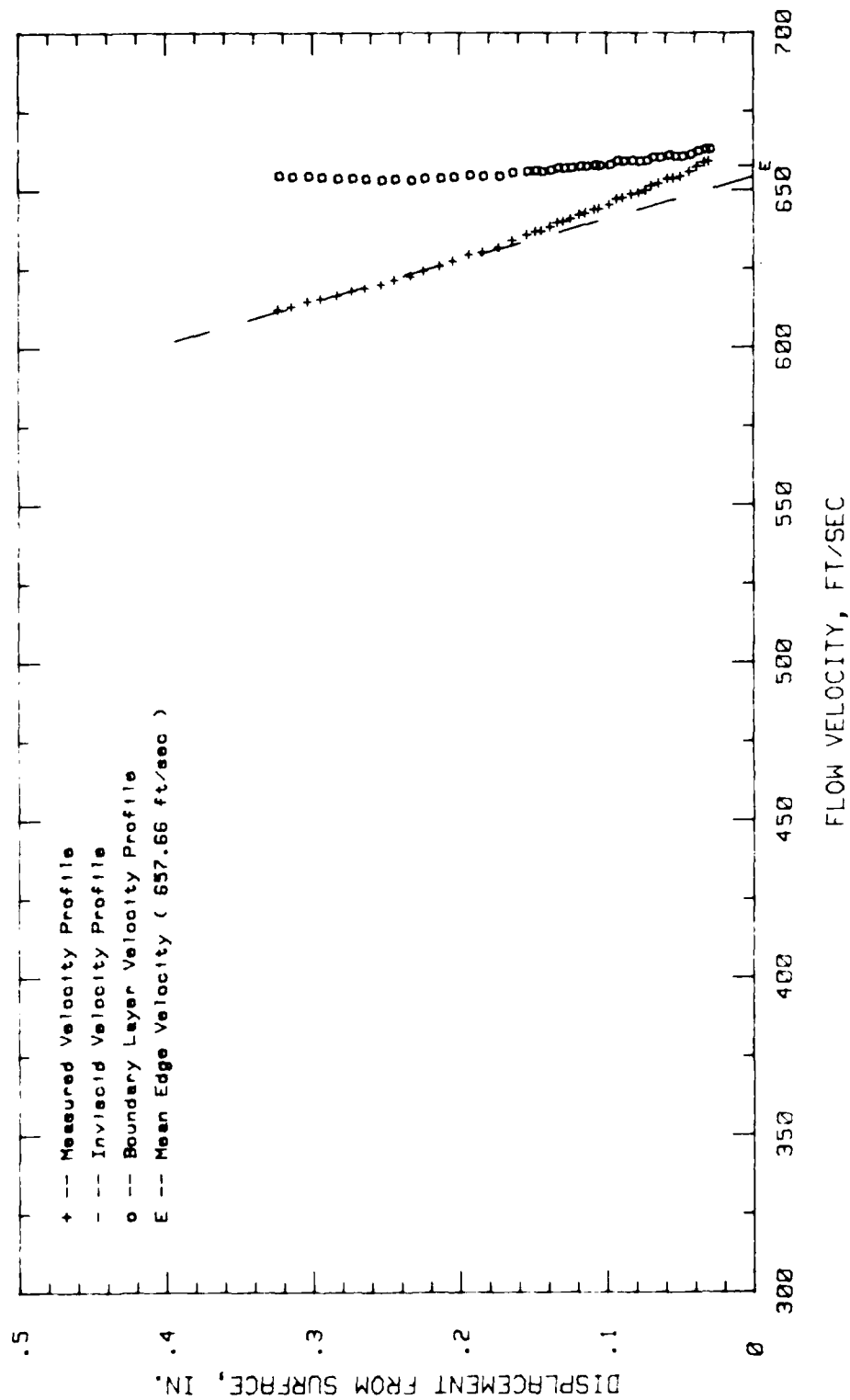


Fig. 103. Boundary Layer Velocity Profiles, Conf. #2 at 4.68% Chord LOW TURB.

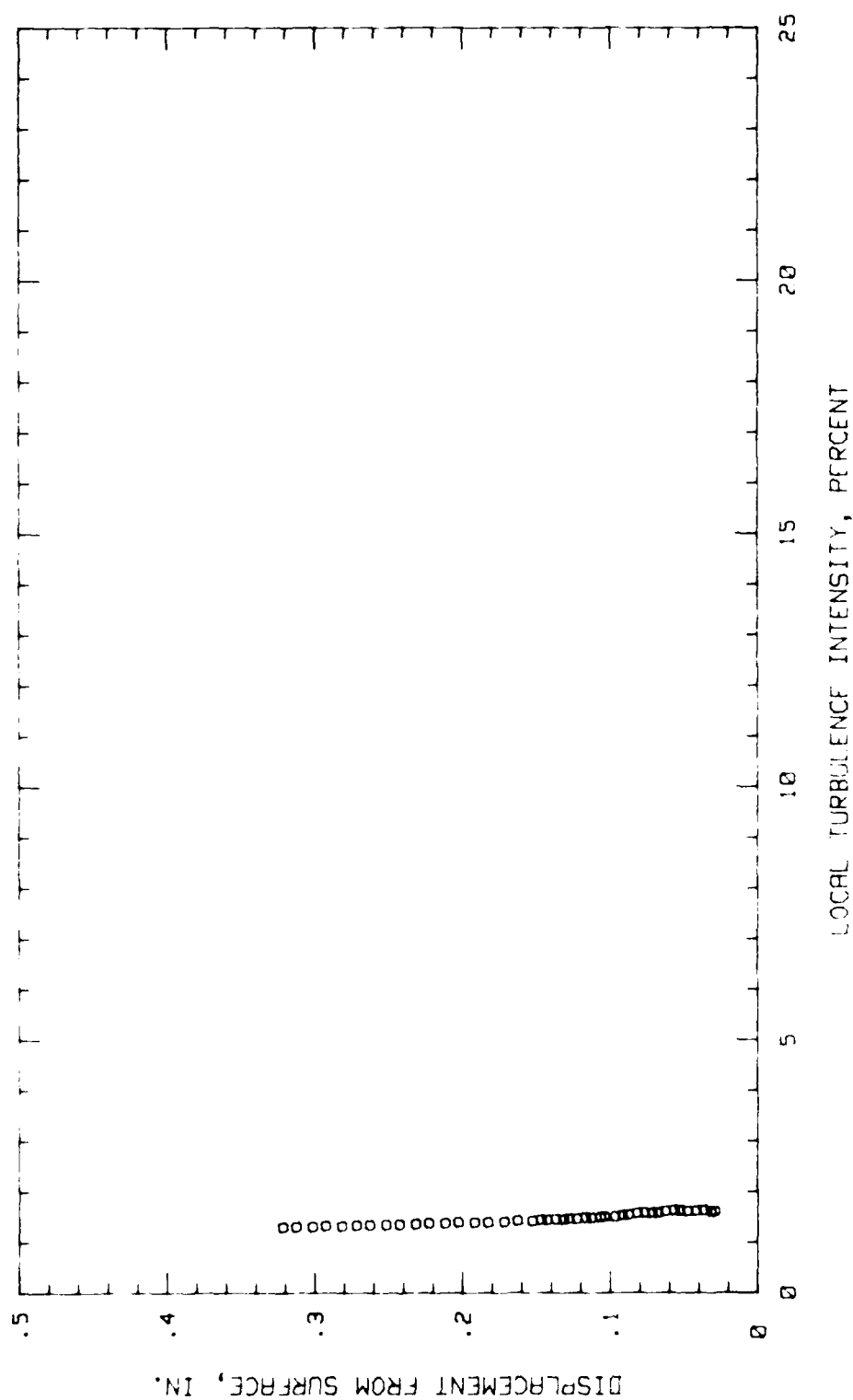


Fig. 104. Boundary Layer Turb. Intensity Profile, Conf. #2 at 4.68% Chord LOW TURB.

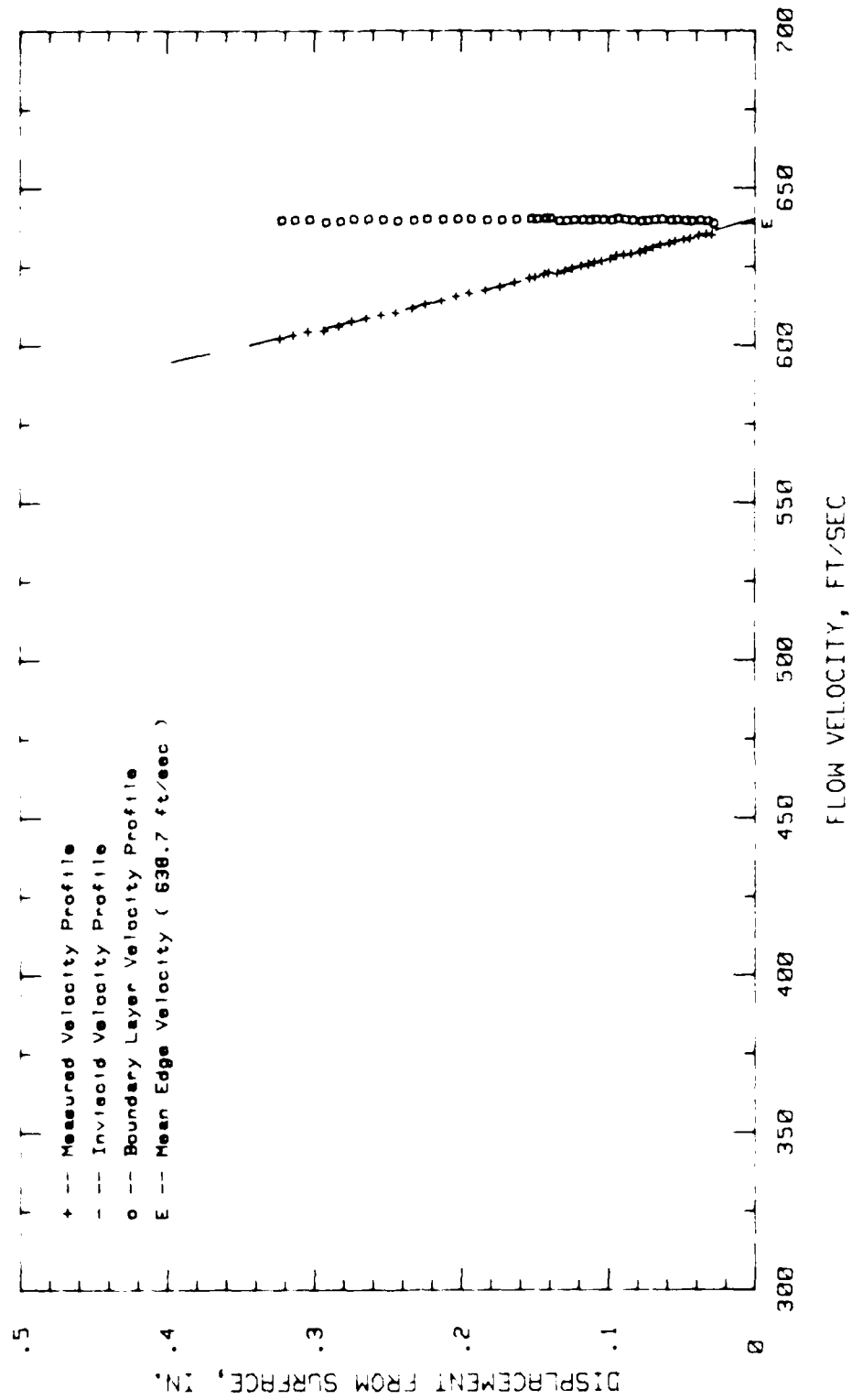


Fig.105. Boundary Layer Velocity Profiles, Conf.#2 at 9.37% Chord LOW TURB.

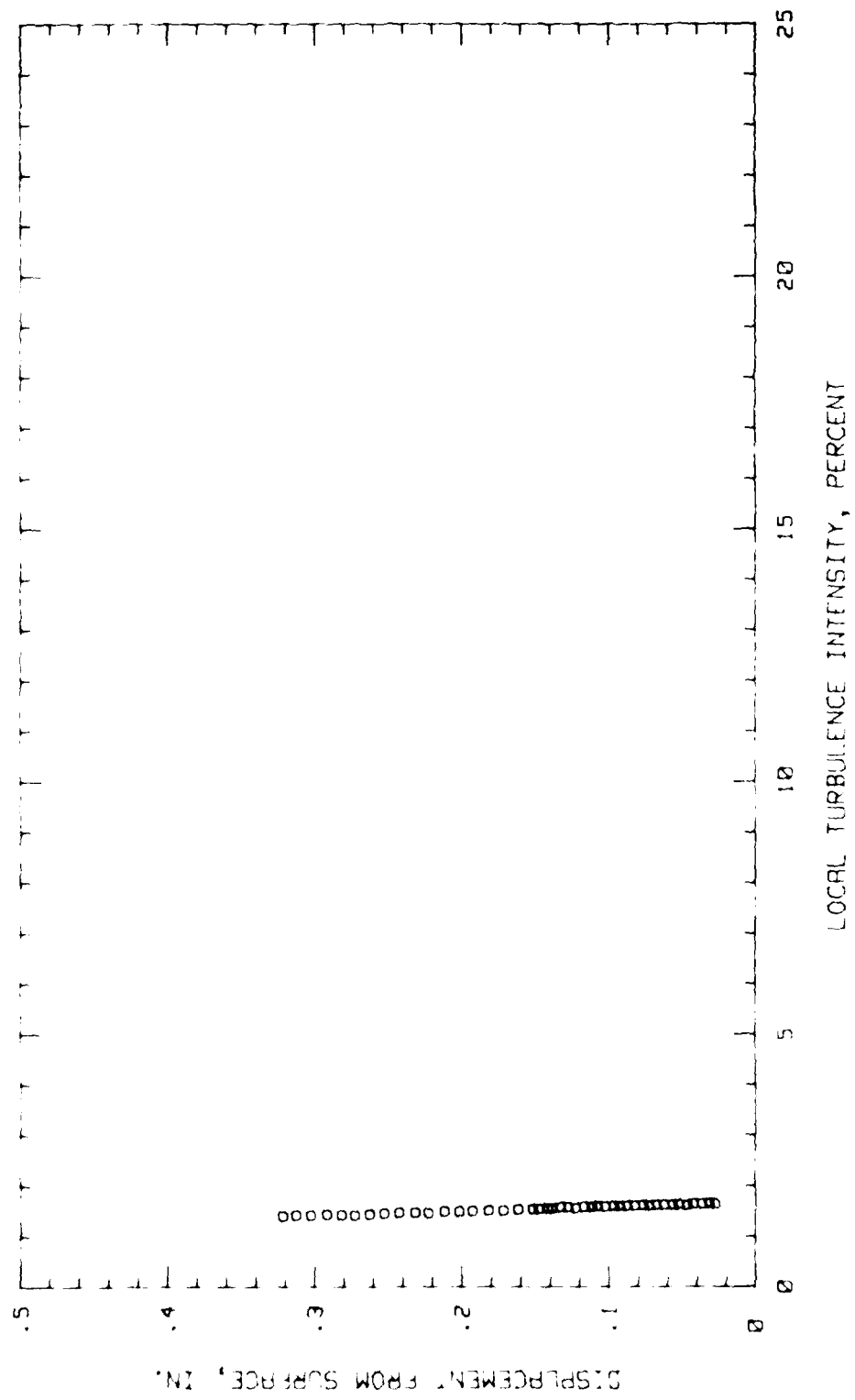


Fig.106.Boundary Layer Turb. Intensity Profile, Conf.#2 at 9.37% Chord LOW TURB.

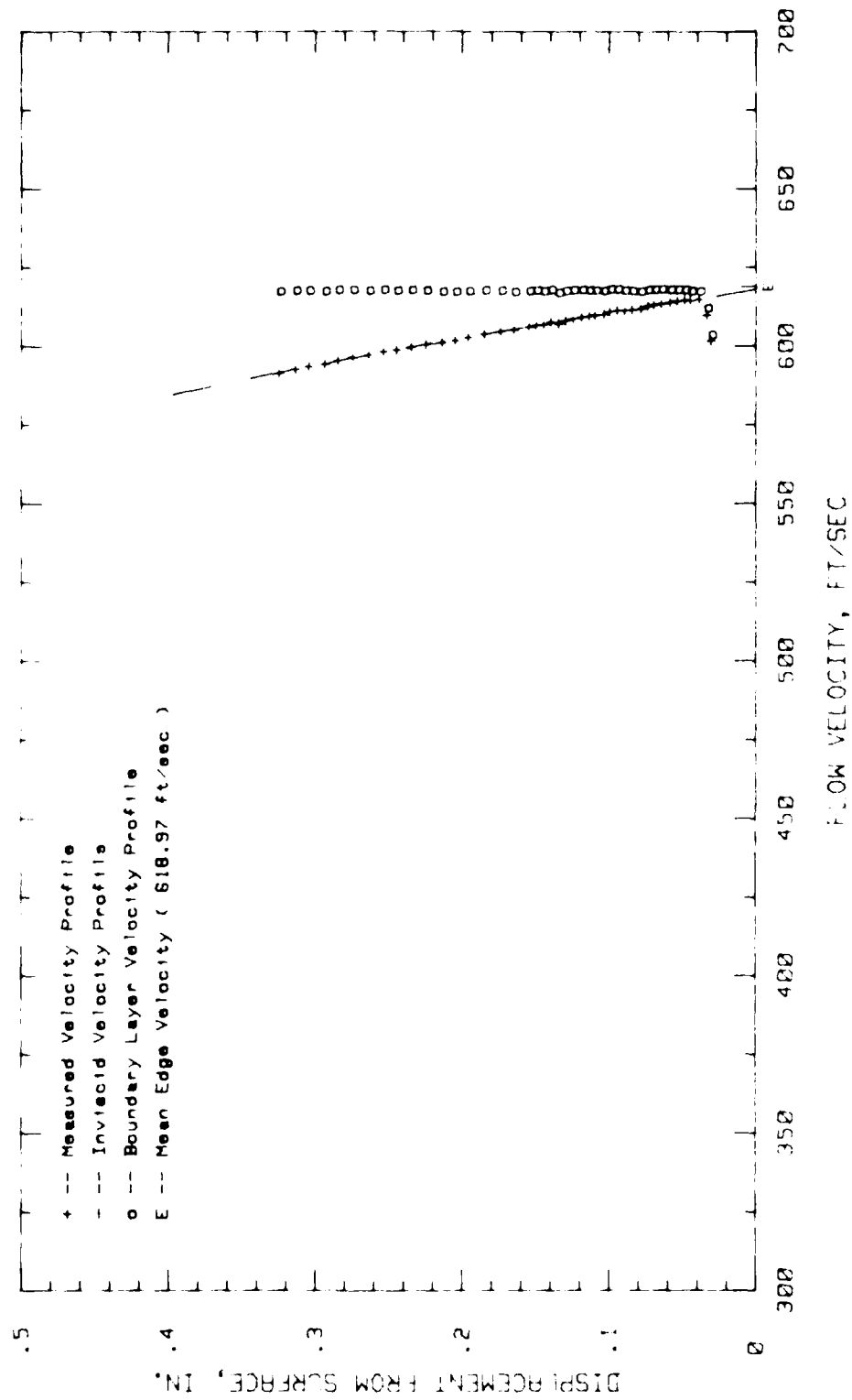


Fig.107. Boundary Layer Velocity Profiles, Conf.#2 at 25% Chord LOW TURB.

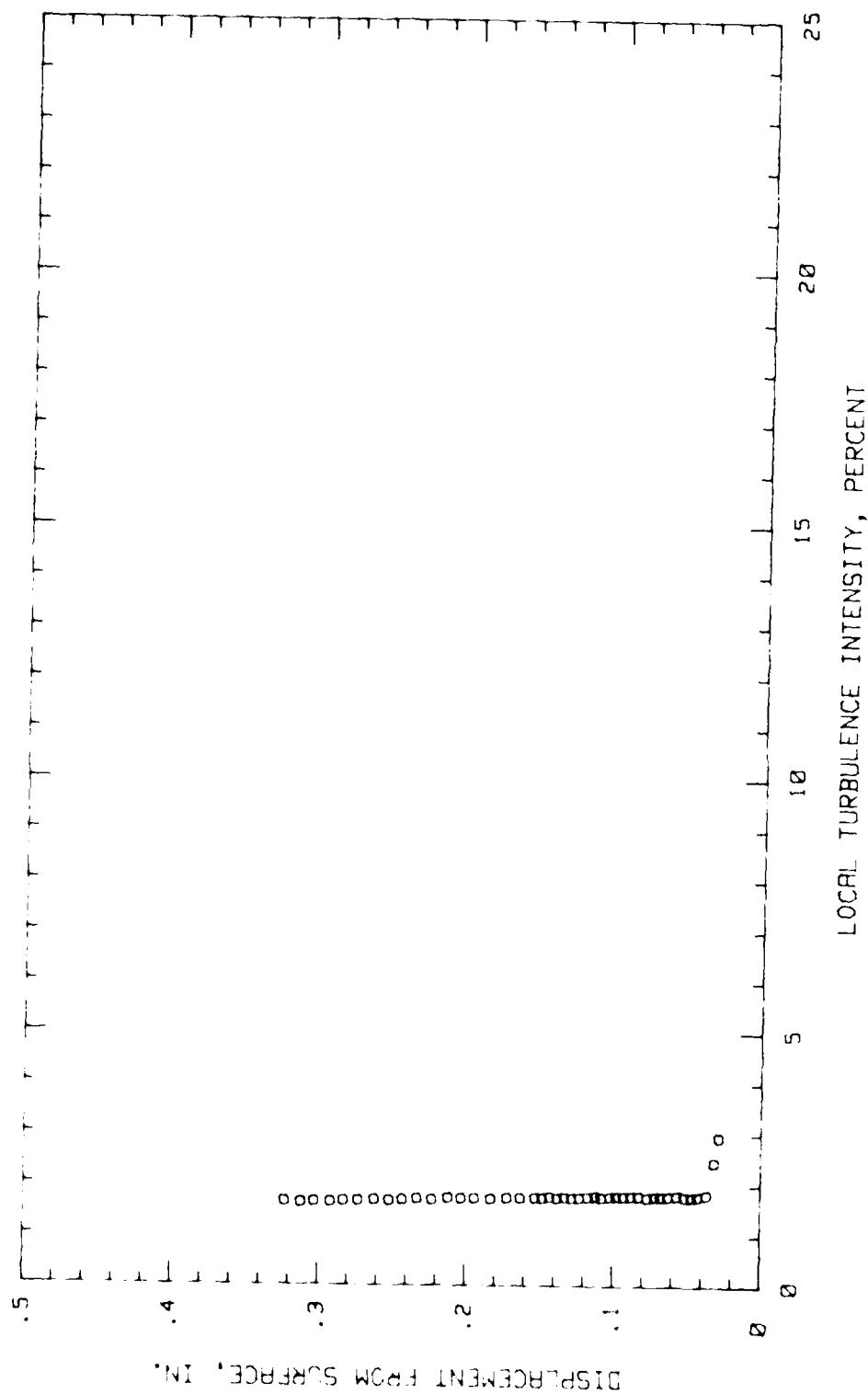


Fig.108.Boundary Layer Turb. Intensity Profile, Conf.#2 at 25% Chord LOW TURB.

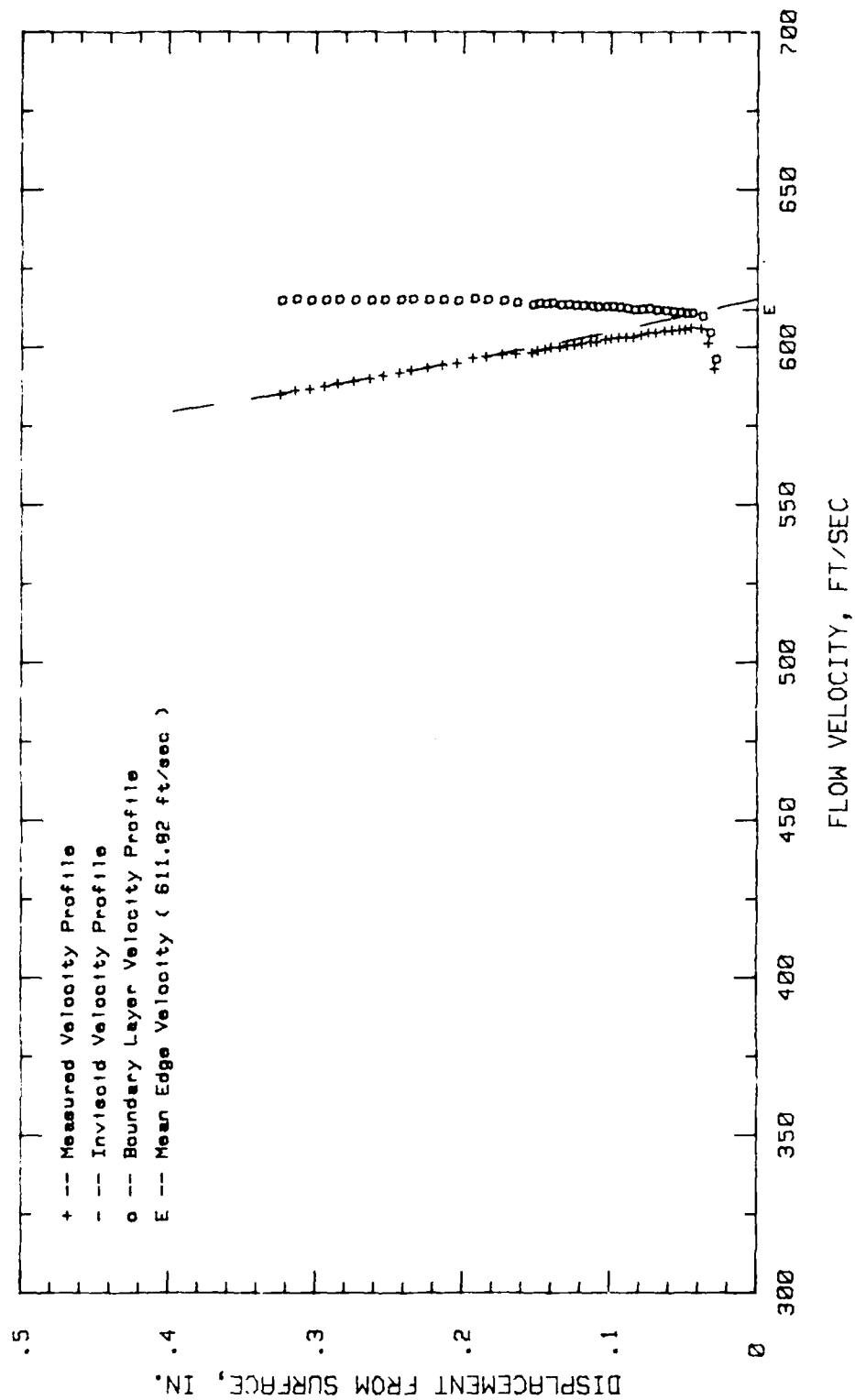


Fig.109. Boundary Layer Velocity Profiles, Conf.#2 at 29.68% Chord LOW TURB.

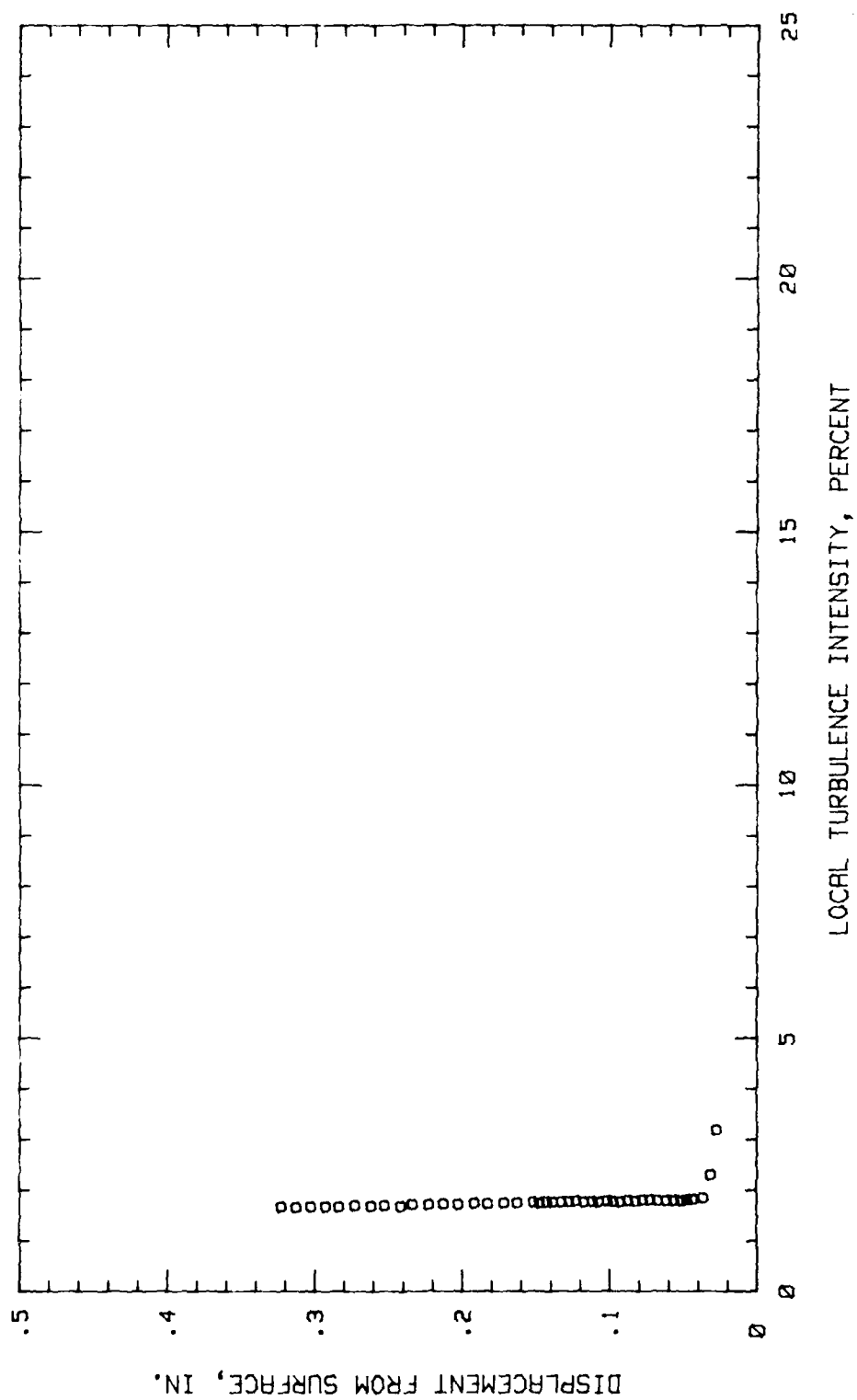


Fig. 110. Boundary Layer Turb. Intensity Profile, Conf. #2 at 29.68% Chord LOW TURB

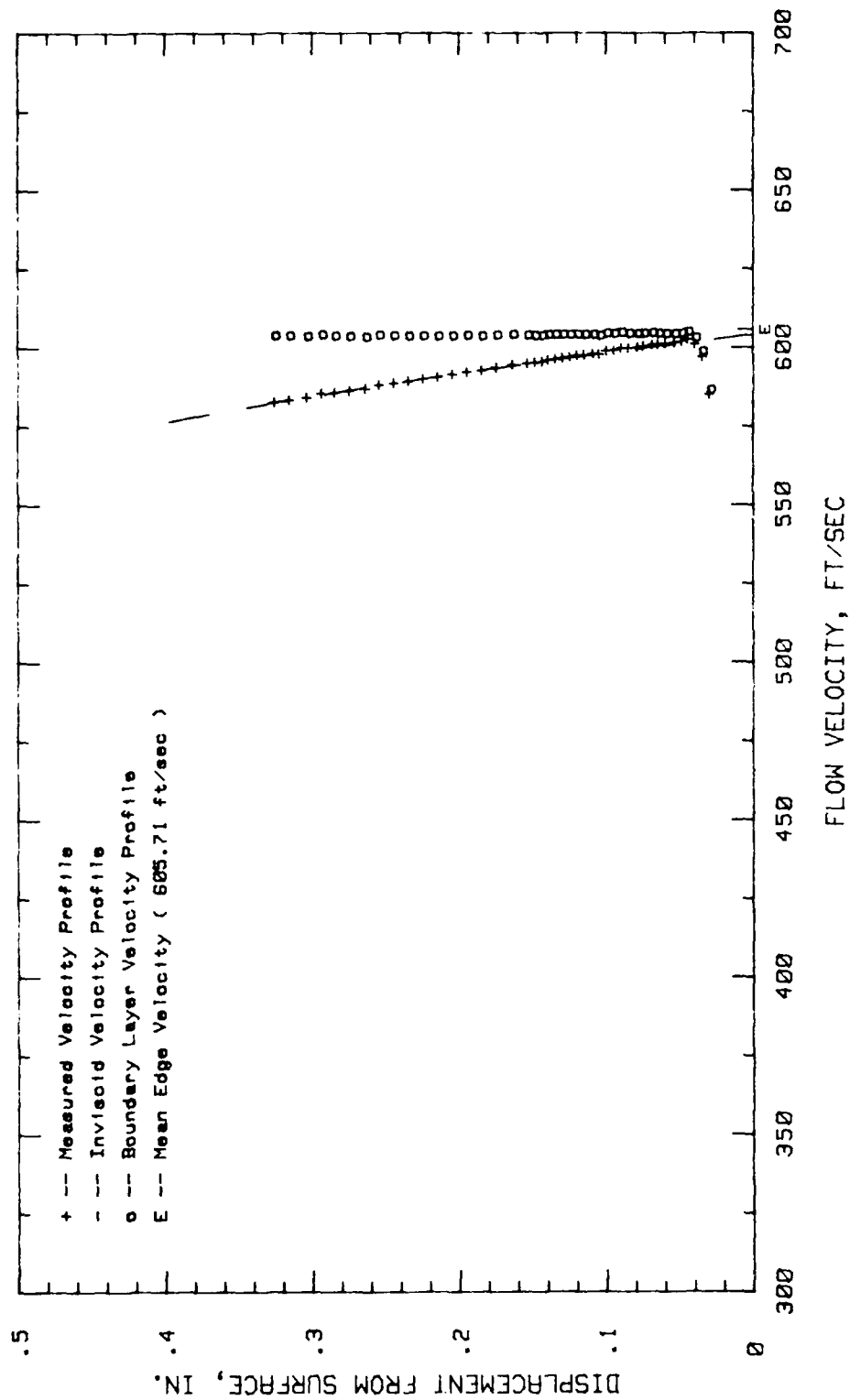


Fig.111.Boundary Layer Velocity Profiles, Conf.#2 at 34.37% Chord LOW TURB.

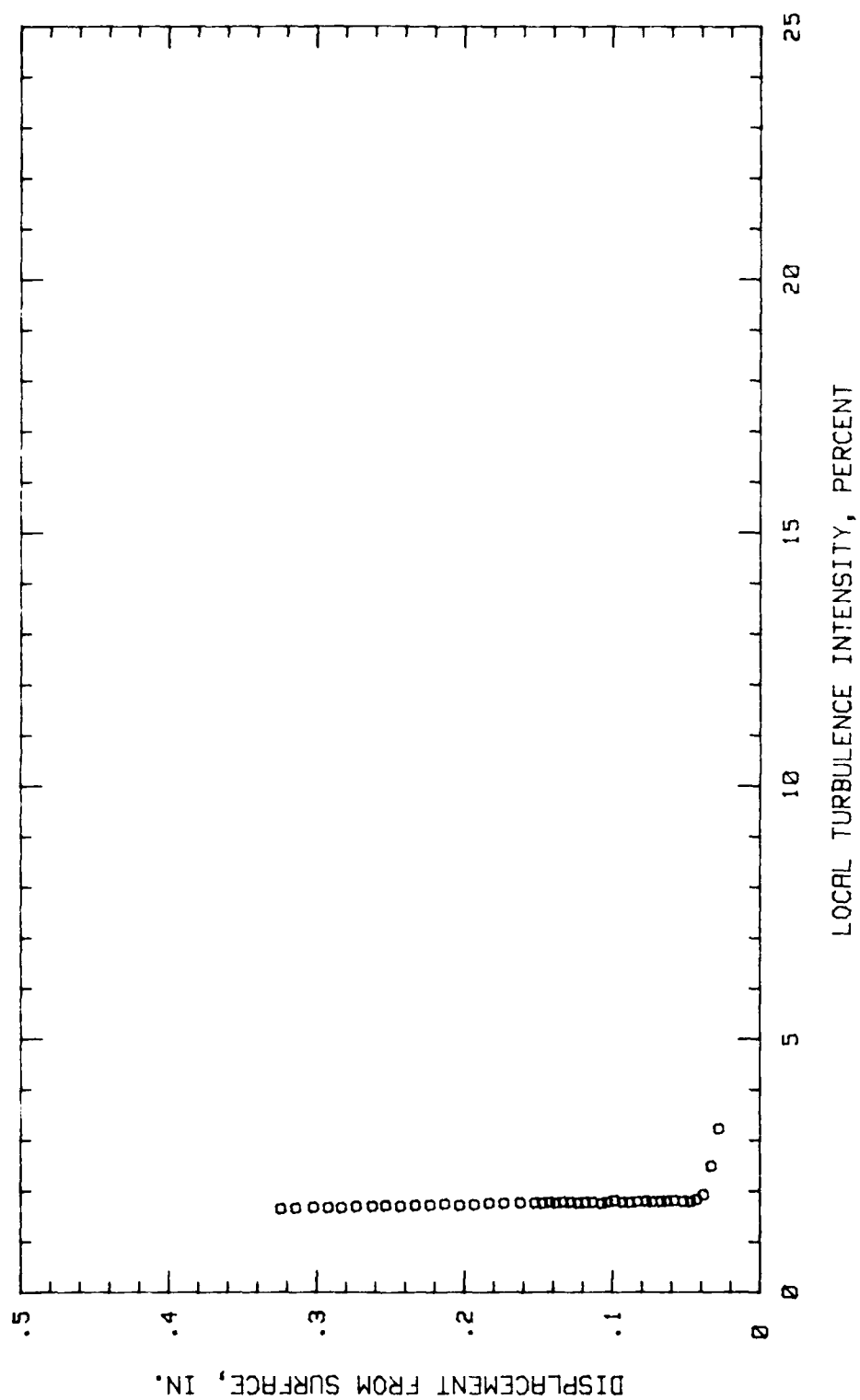


Fig.112. Boundary Layer Turb. Intensity Profile, Conf.#2 at 34.37% Chord LOW TURB

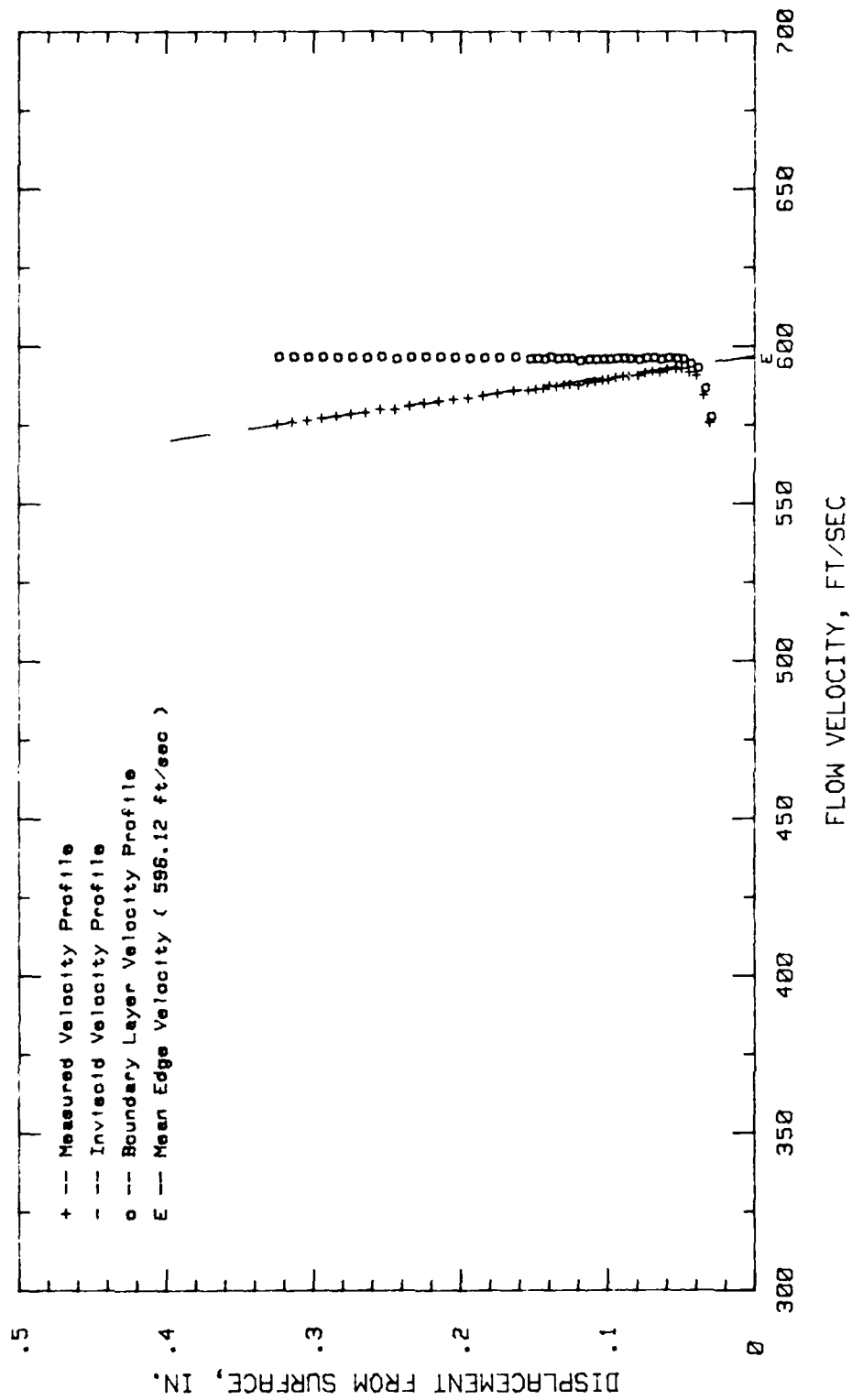


Fig.113.Boundary Layer Velocity Profiles, Conf.#2 at 40.62% Chord LOW TURB.

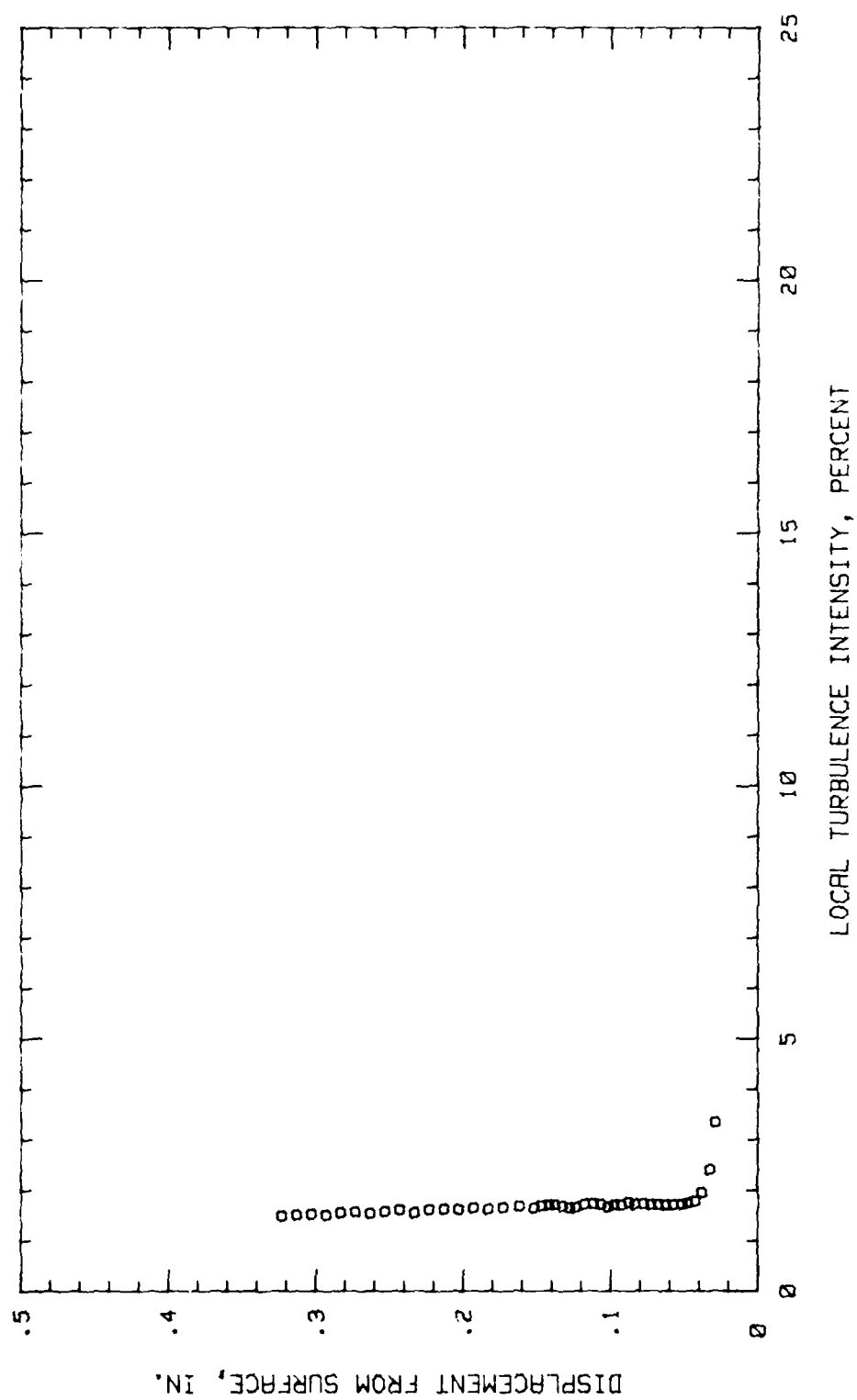


Fig.114. Boundary Layer Turb. Intensity Profile, Conf.#2 at 40.62% Chord LOW TURB

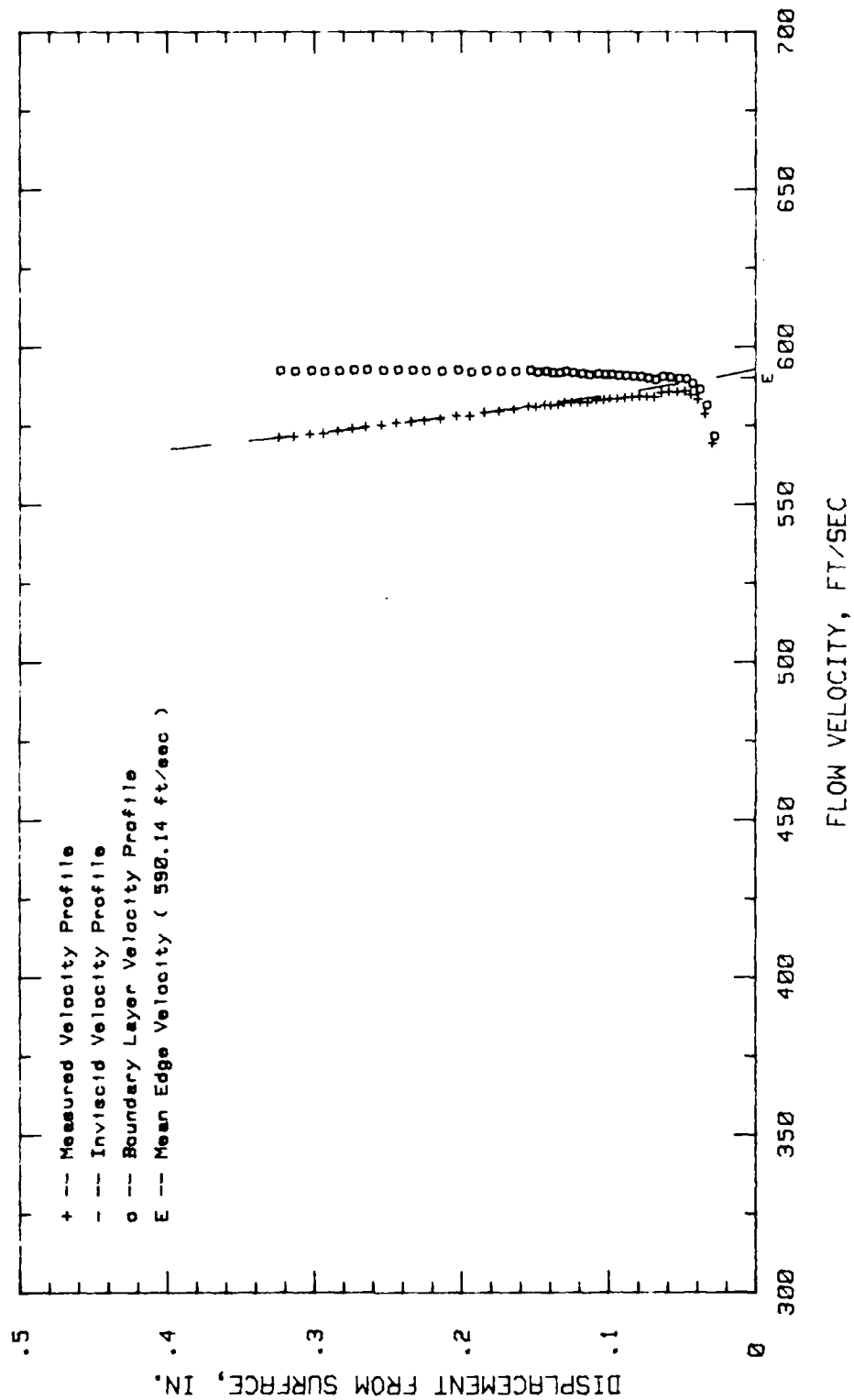


Fig.115. Boundary Layer Velocity Profiles, Conf.#1 at 45.31% Chord LOW TURB.

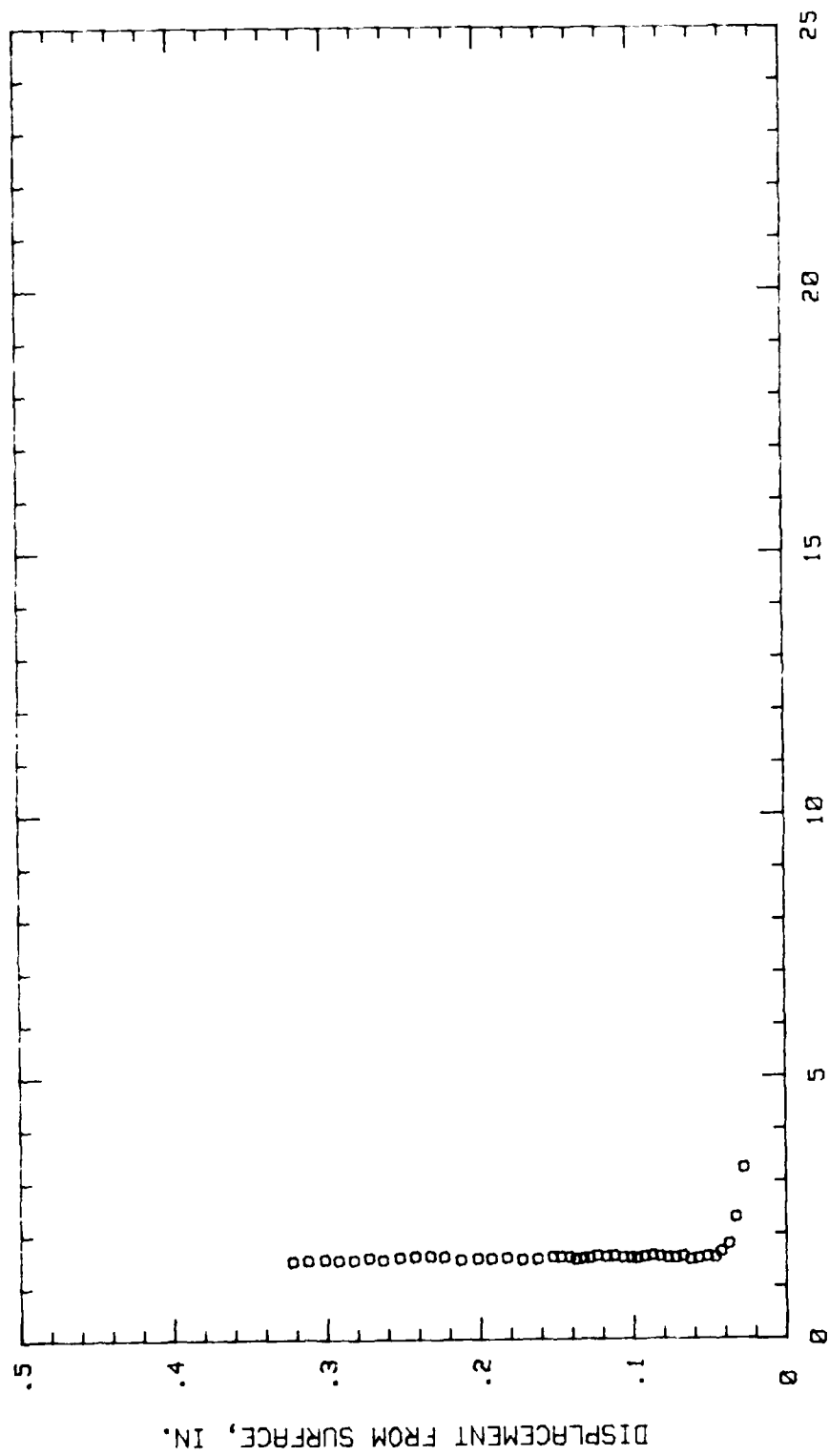


Fig.116. Boundary Layer Turb. Intensity Profile, Conf.#2 at 45.31% Chord LOW TURB

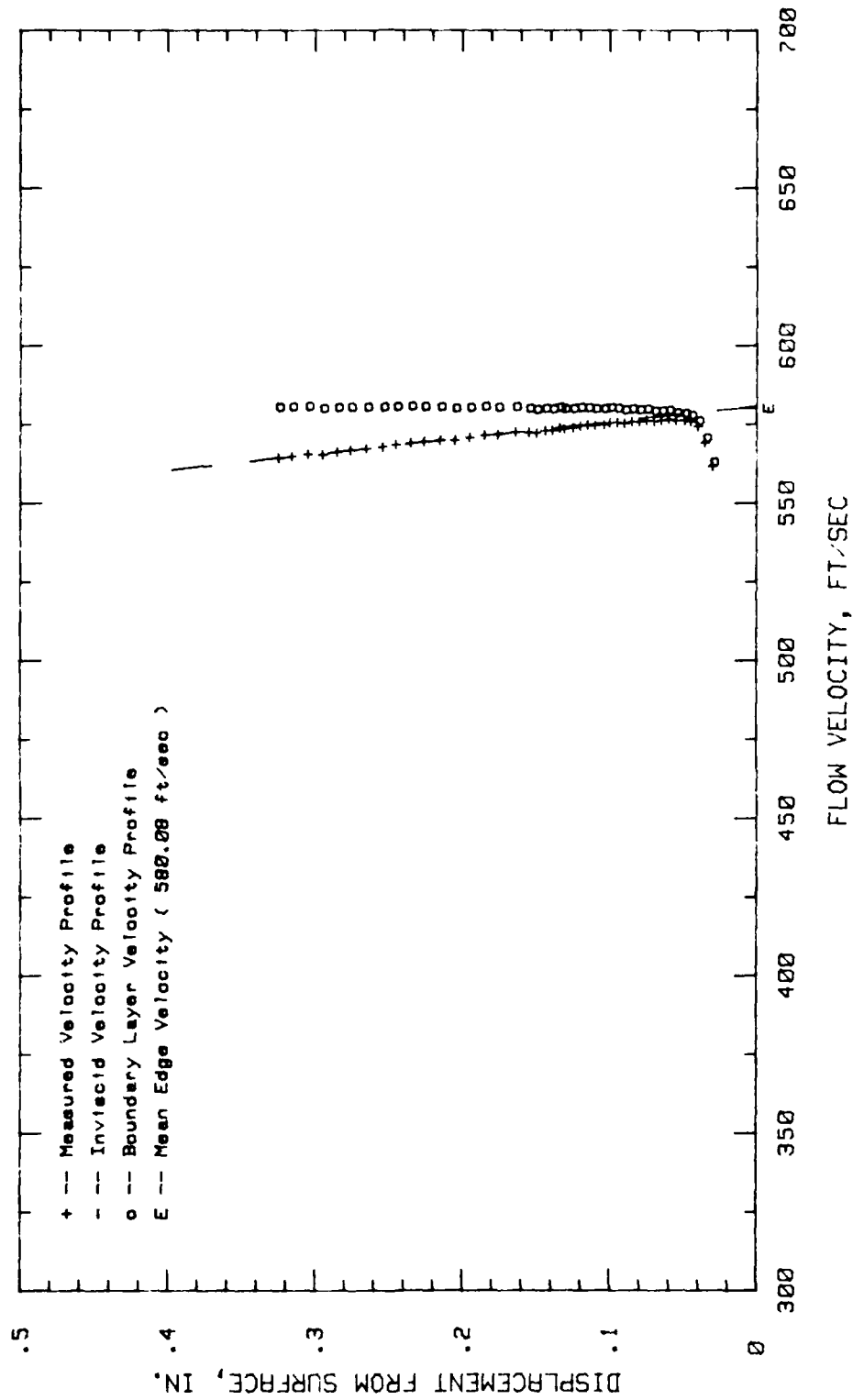


Fig.117.Boundary Layer Velocity Profiles, Conf.#2 at 50% Chord LOW TURB.

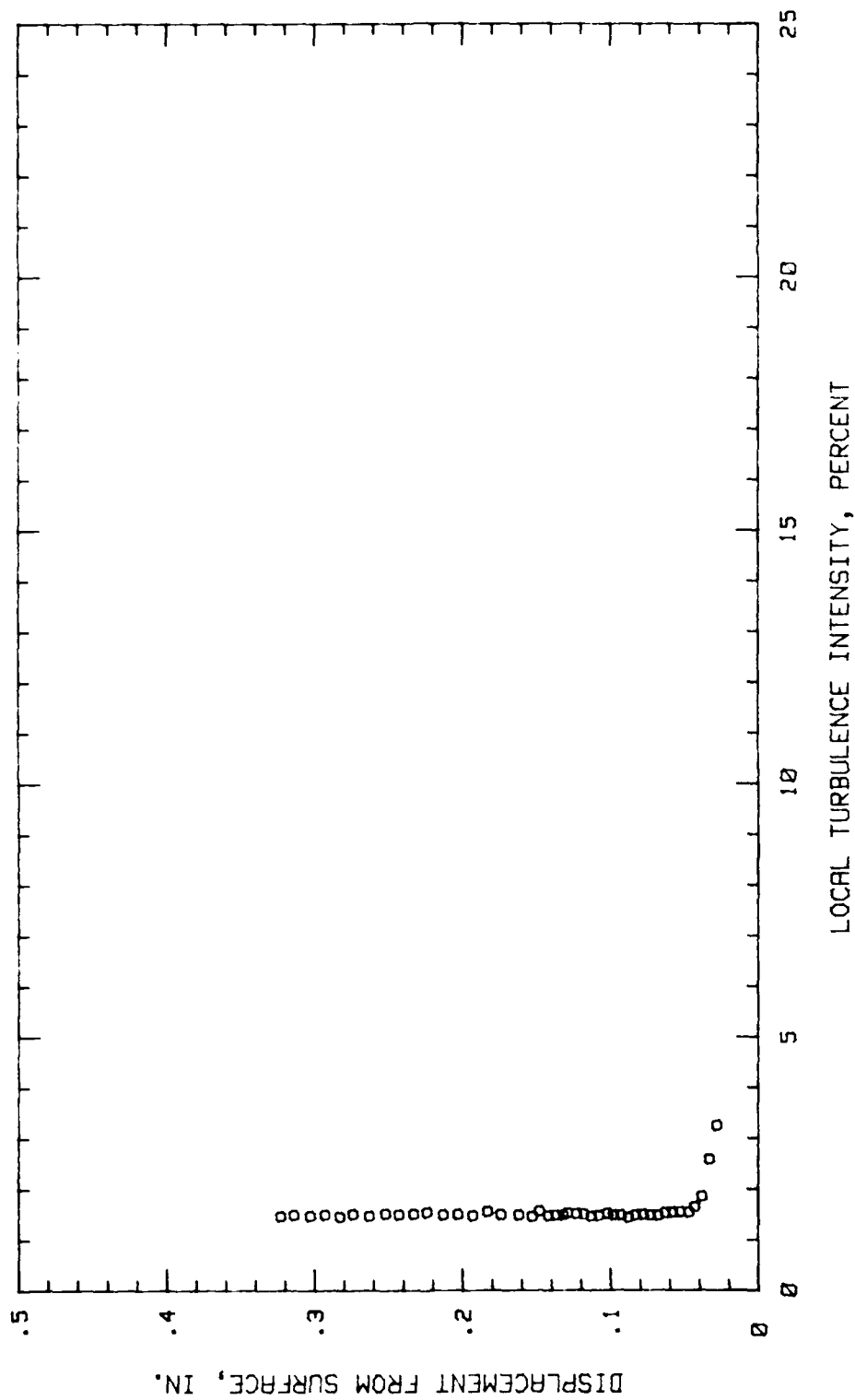


Fig.118.Boundary Layer Turb. Intensity Profile, Conf.#2 at 50% Chord LOW TURB.

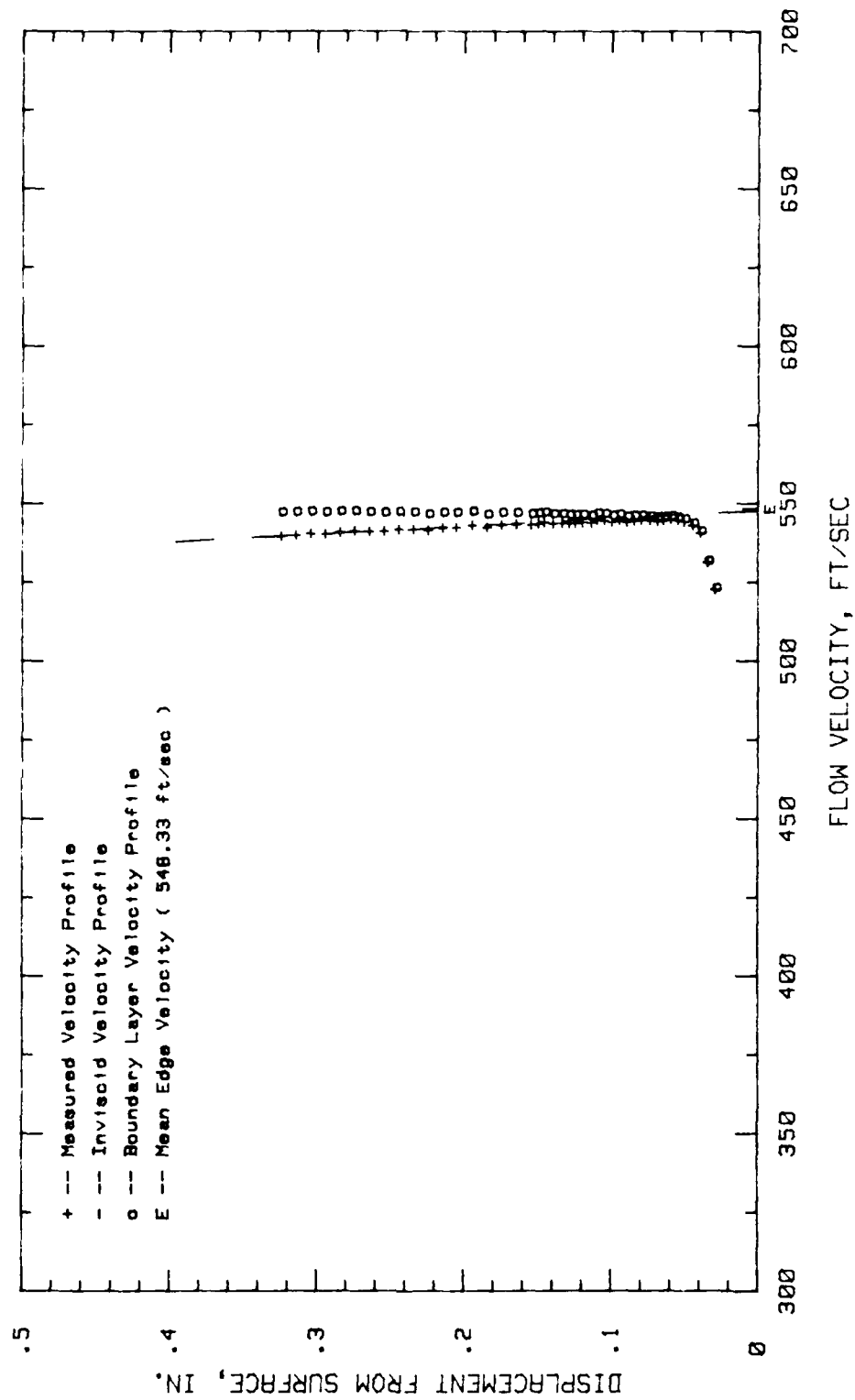


Fig.119. Boundary Layer Velocity Profiles, Conf.#2 at 65.62% Chord LOW TURB.

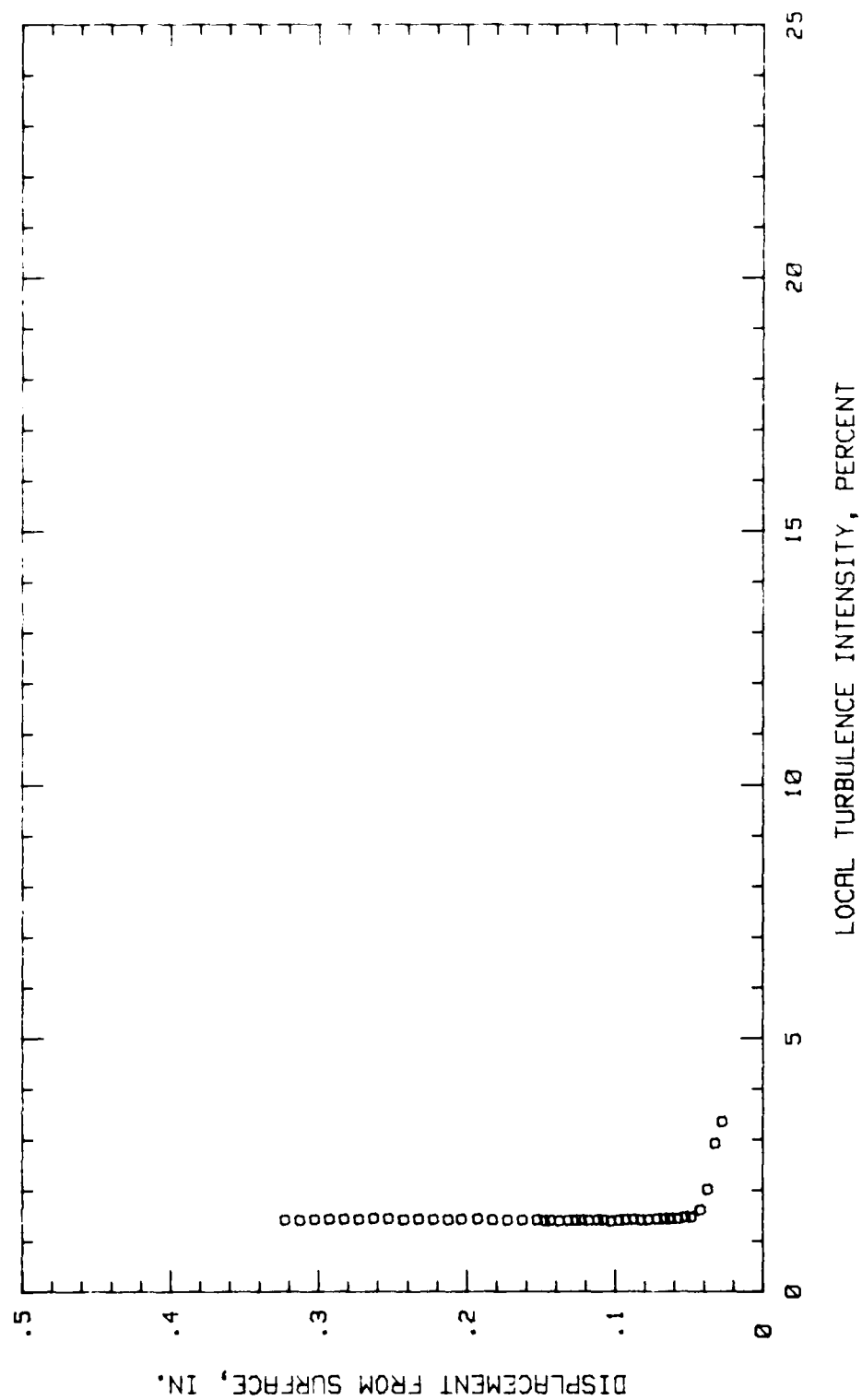


Fig.120. Boundary Layer Turb. Intensity Profile, Conf.#2 at 65.62% Chord LOW TURB

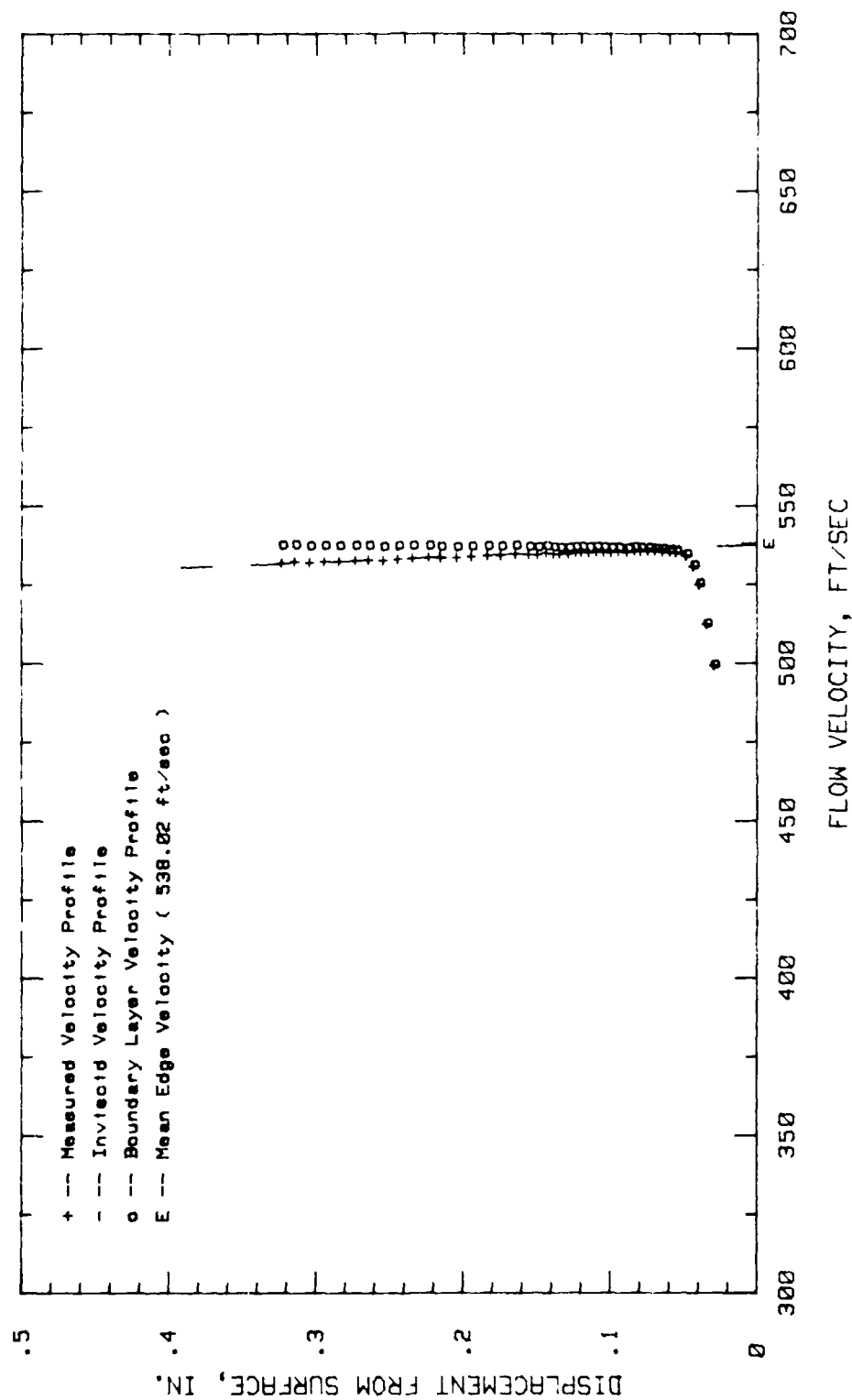
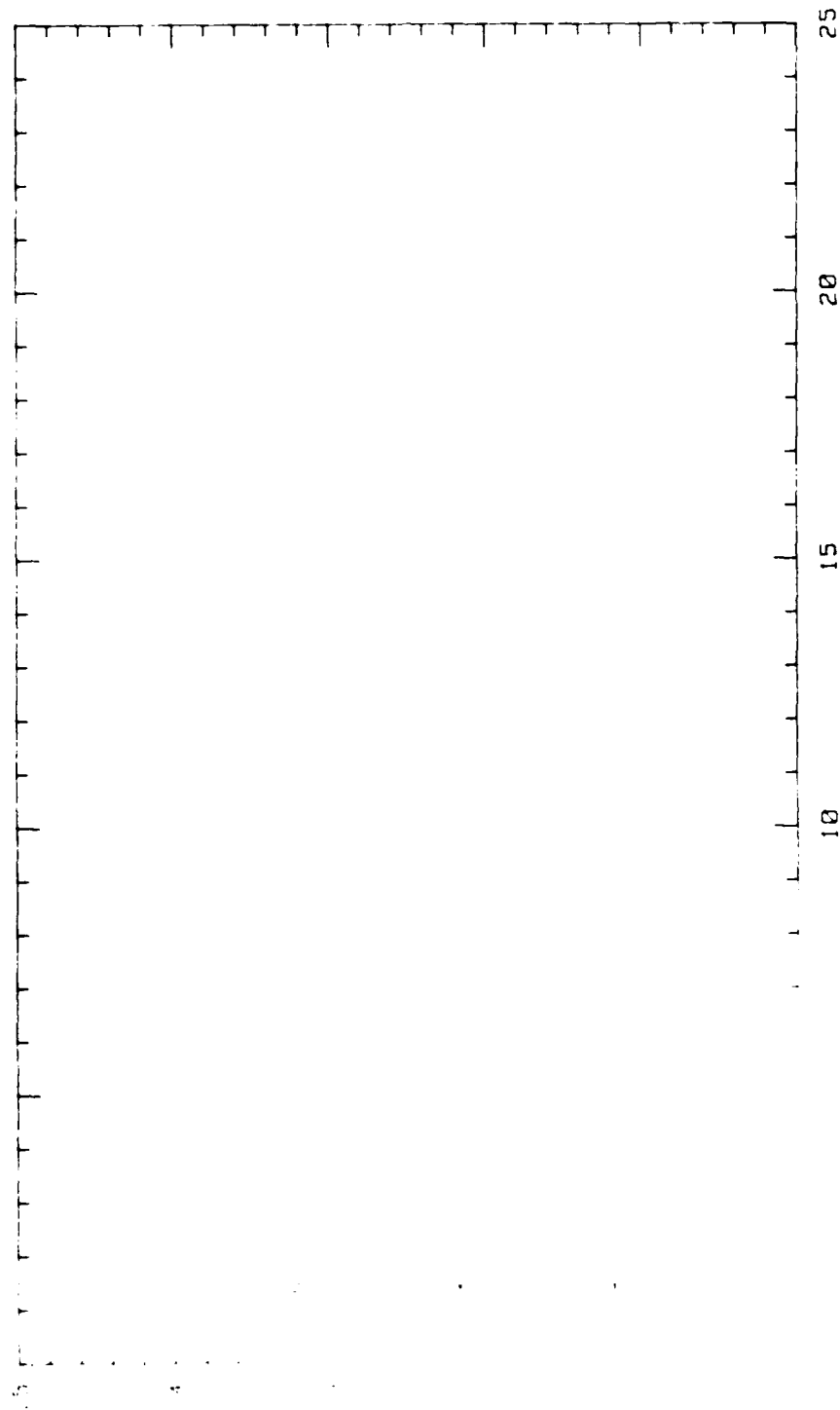


Fig.121. Boundary Layer Velocity Profiles, Conf.#2 at 78.31% Chord LOW TURB.



TURBULENCE INTENSITY, PERCENT

Intensity Profile, Conf.#2 at 70.31% Chord LOW TURB

VD-R190 615

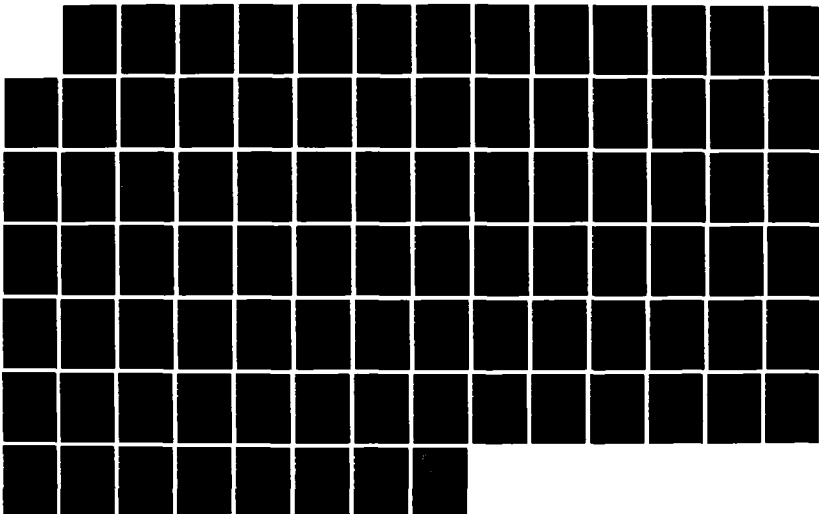
EFFECT OF FREESTREAM TURBULENCE ON A TWO DIMENSIONAL
CASCADE WITH DIFFERE. (U) AIR FORCE INST OF TECH
WRIGHT-PATTERSON AFB OH SCHOOL OF ENGI.. 5 ABSTAR
MAR 88 AFIT/BAE/RA/88H-1

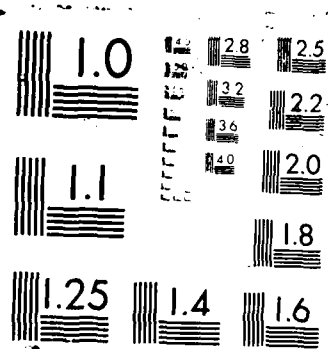
3/3

UNCLASSIFIED

F/8 28/4

ML





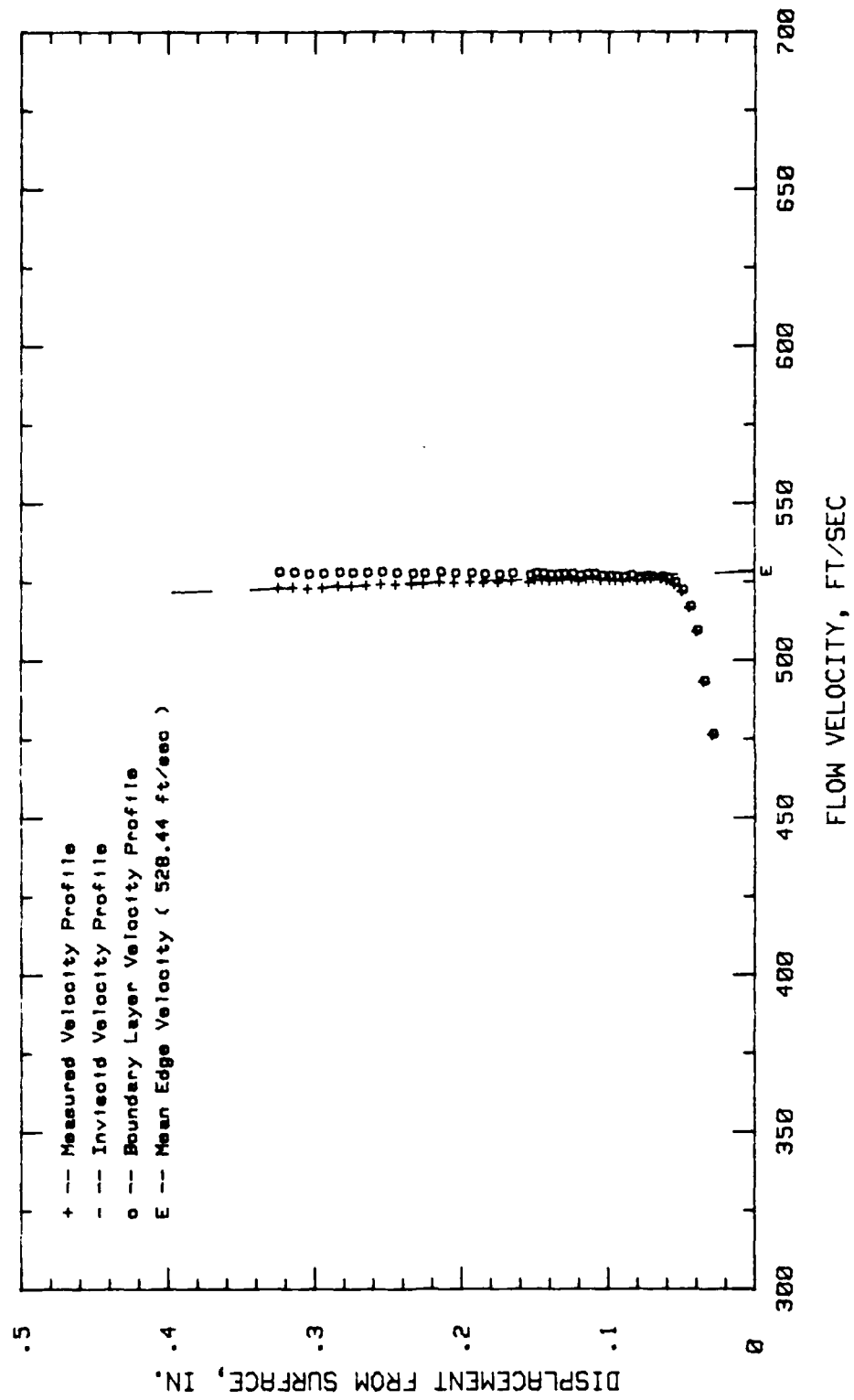


Fig.123.Boundary Layer Velocity Profiles, Conf.#2 at 75% Chord LOW TURB.

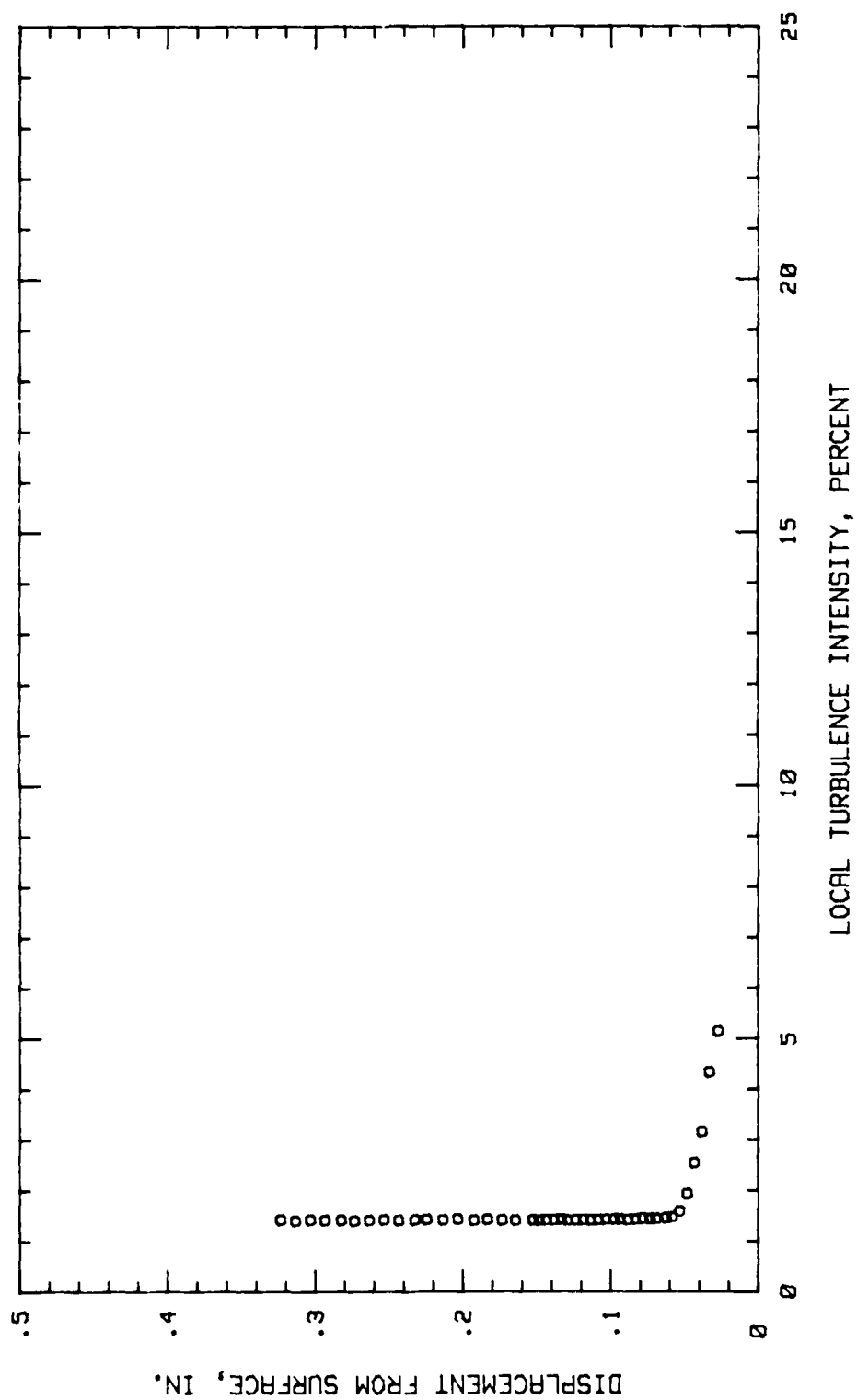


Fig.124.Boundary Layer Turb. Intensity Profile, Conf.#2 at 75% Chord LOW TURB.

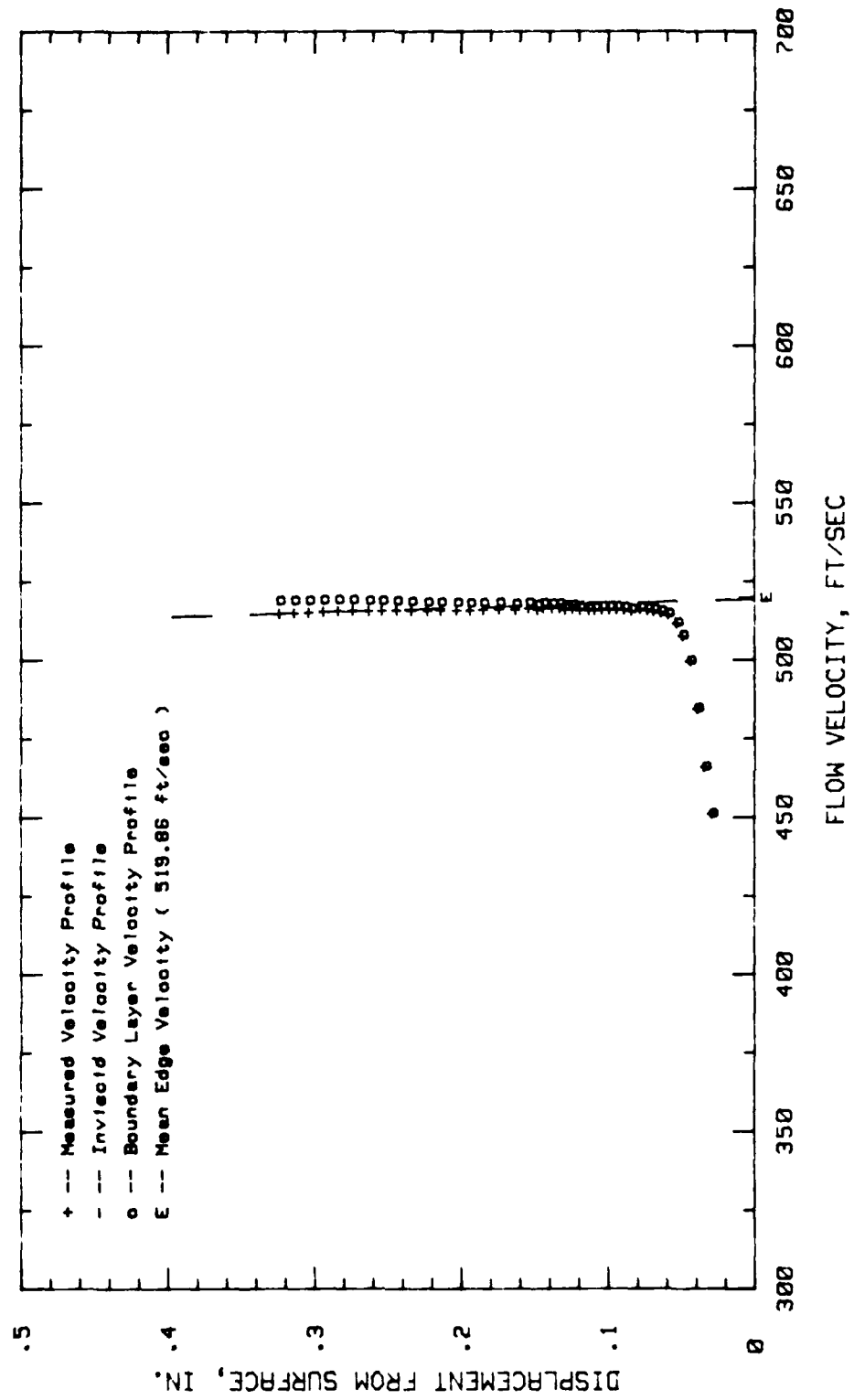


Fig.125.Boundary Layer Velocity Profiles, Conf.#2 at 79.68% Chord LOW TURB.

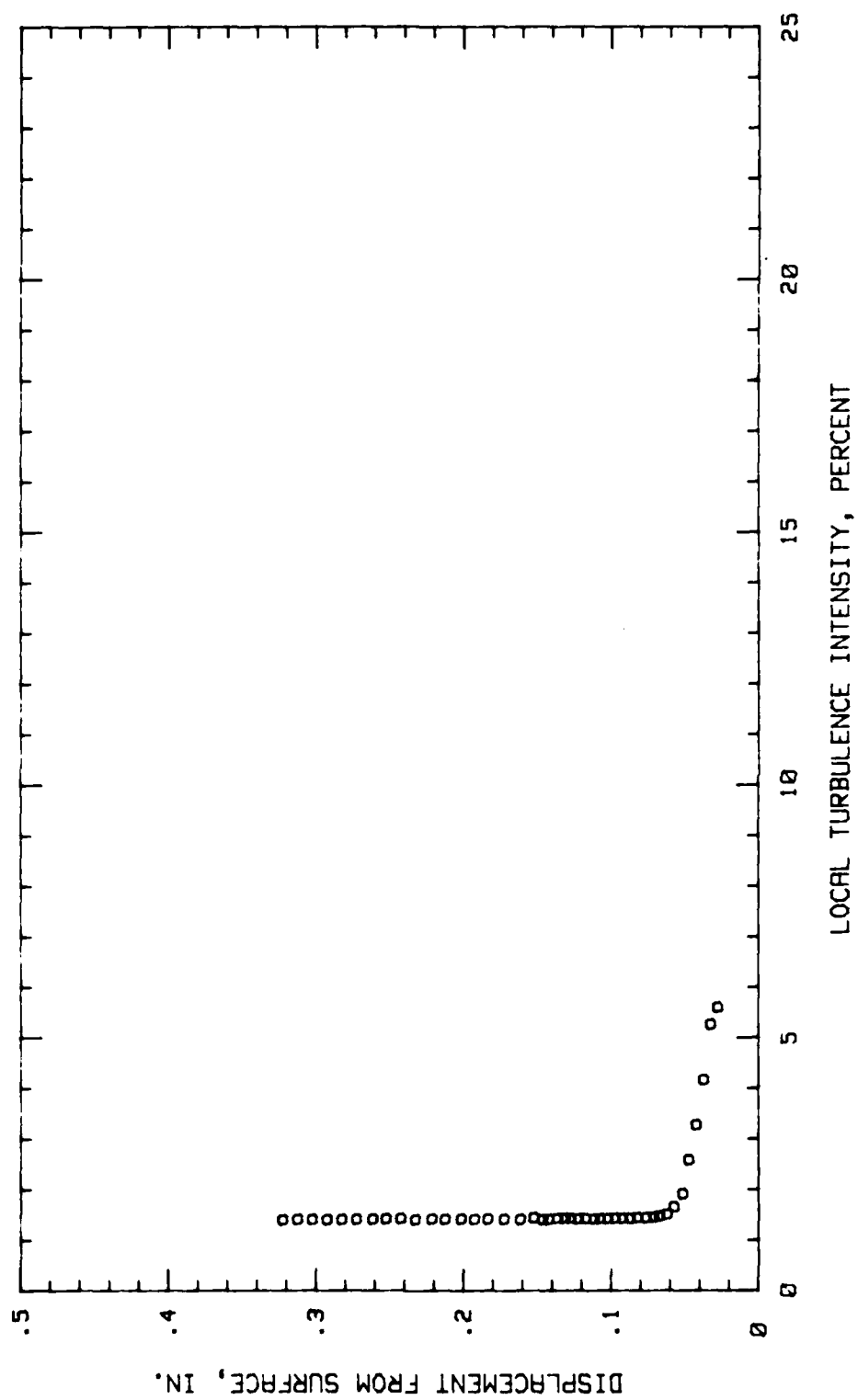


Fig. 126. Boundary Layer Turb. Intensity Profile, Conf. #2 at 79.68% Chord LOW TURB

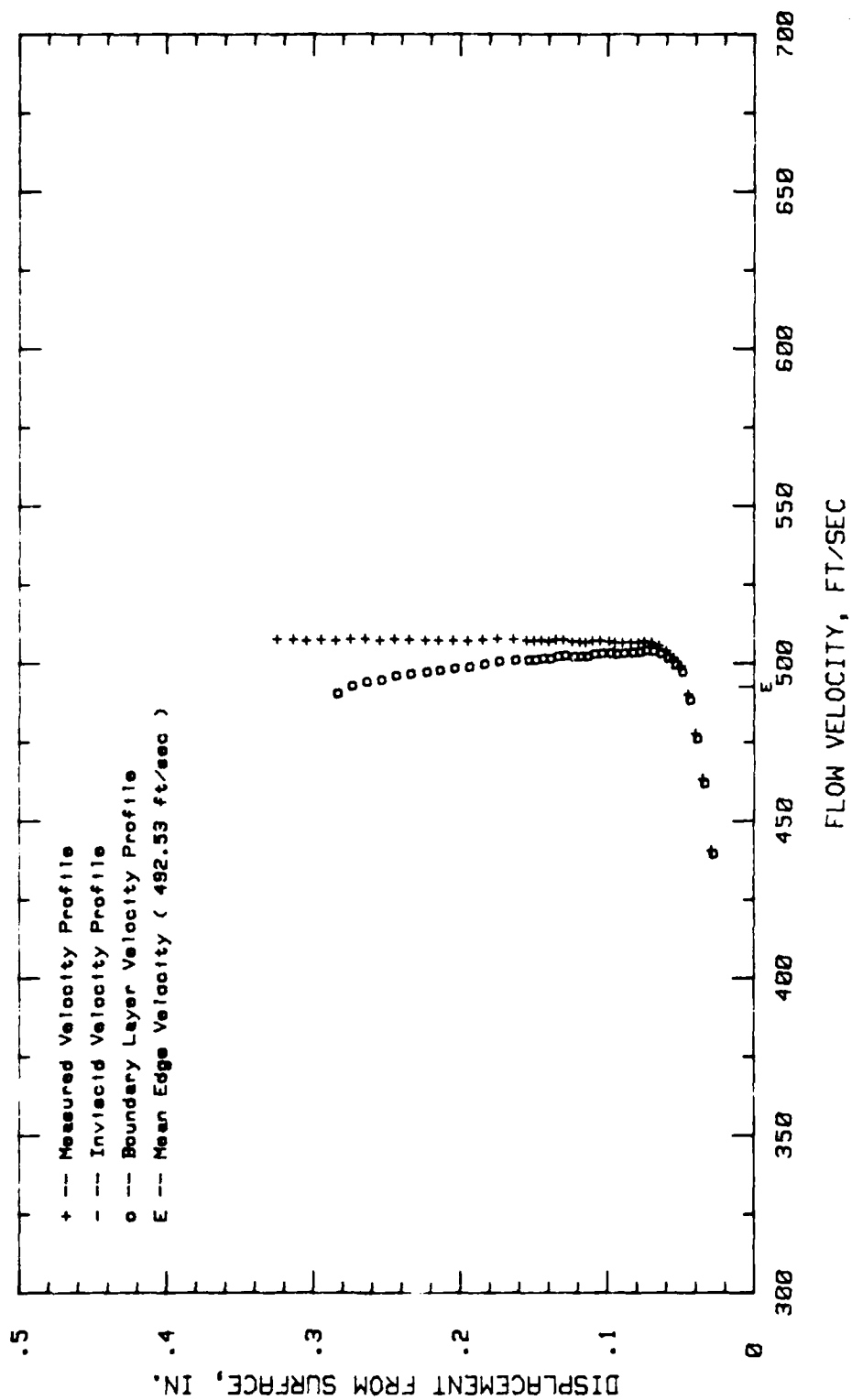


Fig. 127. Boundary Layer Velocity Profiles, Conf. #2 at 84.37% Chord LOW TURB.

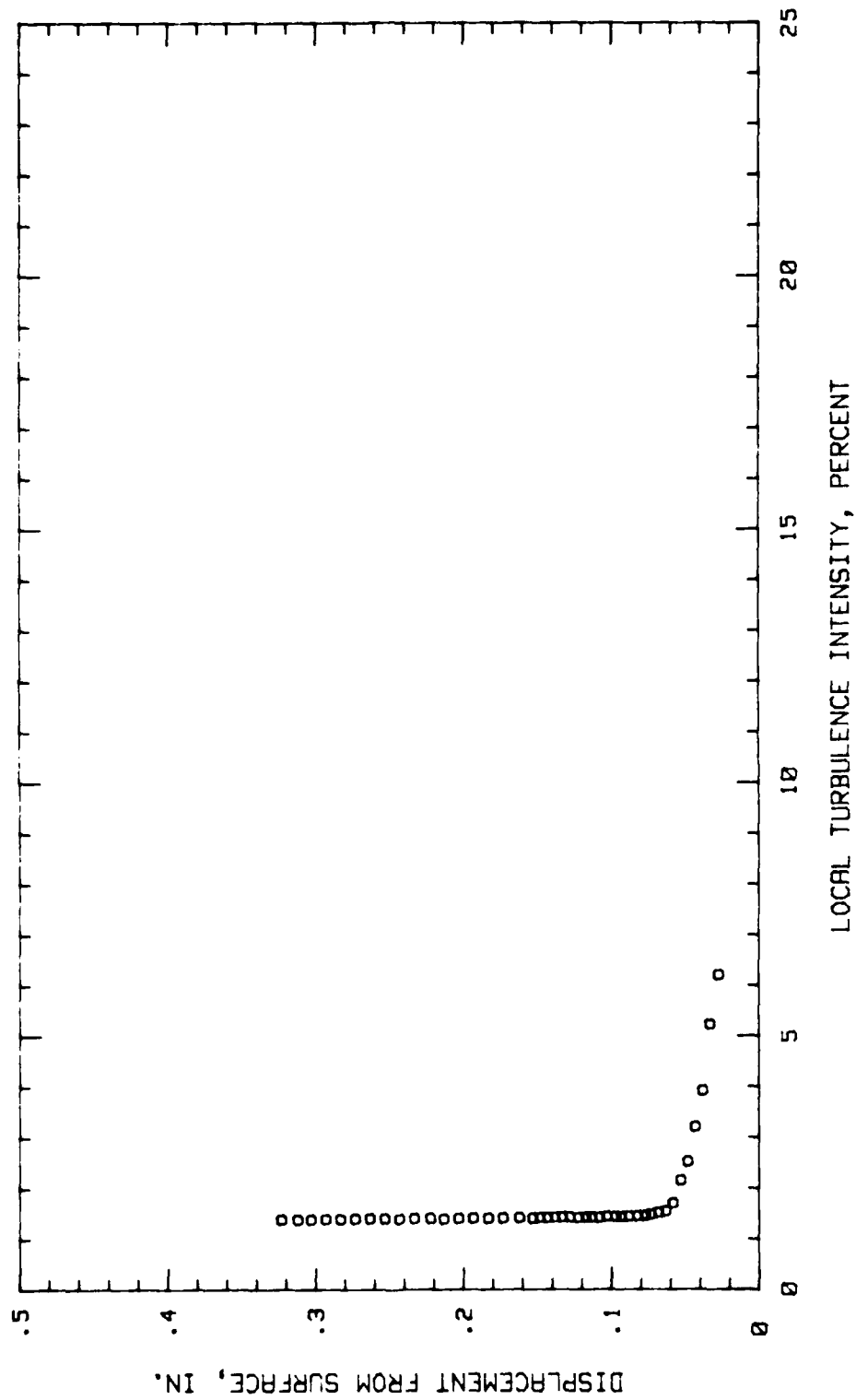


Fig.128.Boundary Layer Turb. Intensity Profile, Conf.#2 at 84.37% Chord LOW TURB

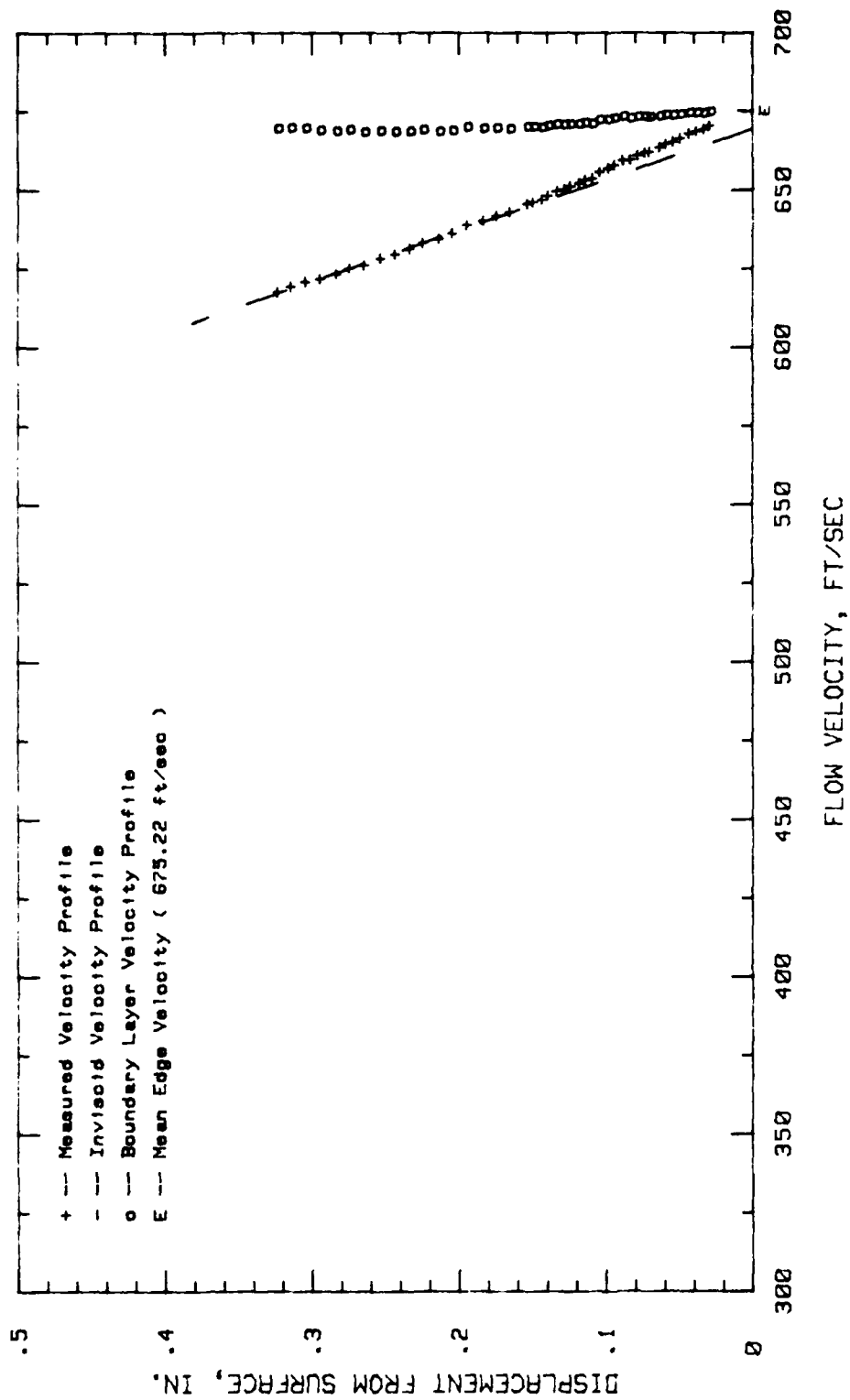


Fig.129. Boundary Layer Velocity Profiles, Conf.#2 at 4.68% Chord HIGH TURB.

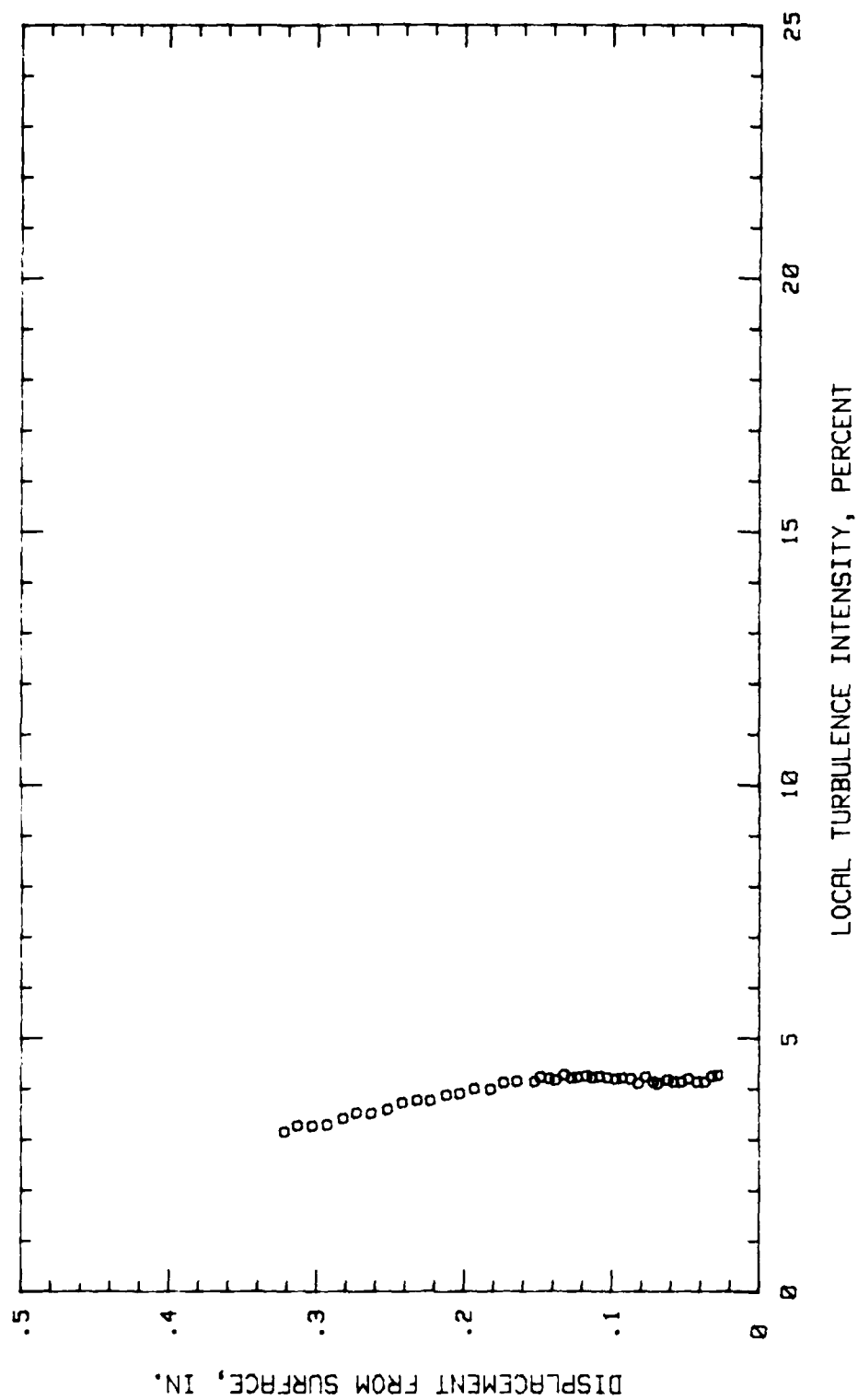


Fig. 130. Boundary Layer Turb. Intensity Profile, Conf. #2 at 4.68% Chord HIGH TURB

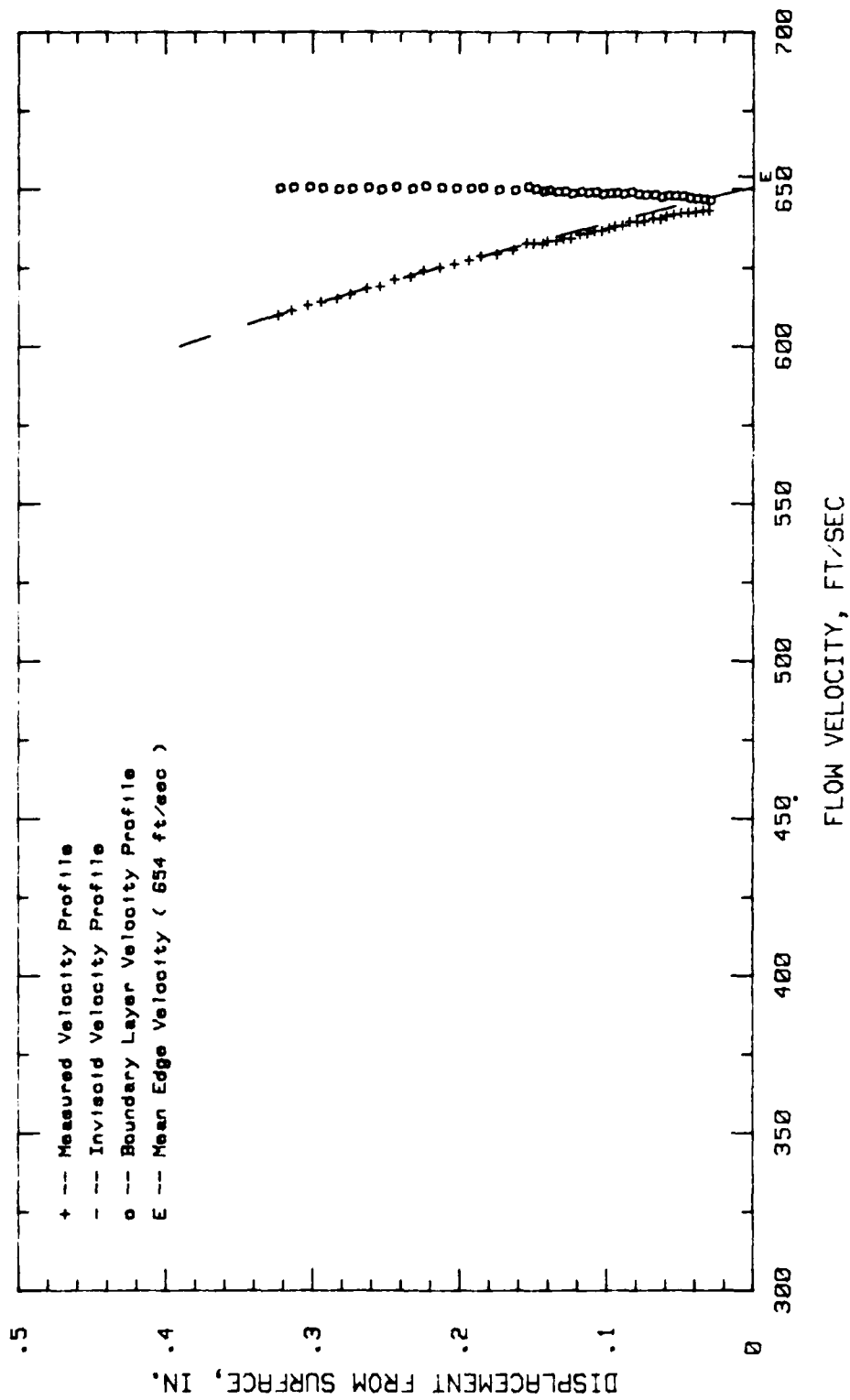


Fig.131. Boundary Layer Velocity Profiles, Conf.#2 at 9.37% Chord HIGH TURB.

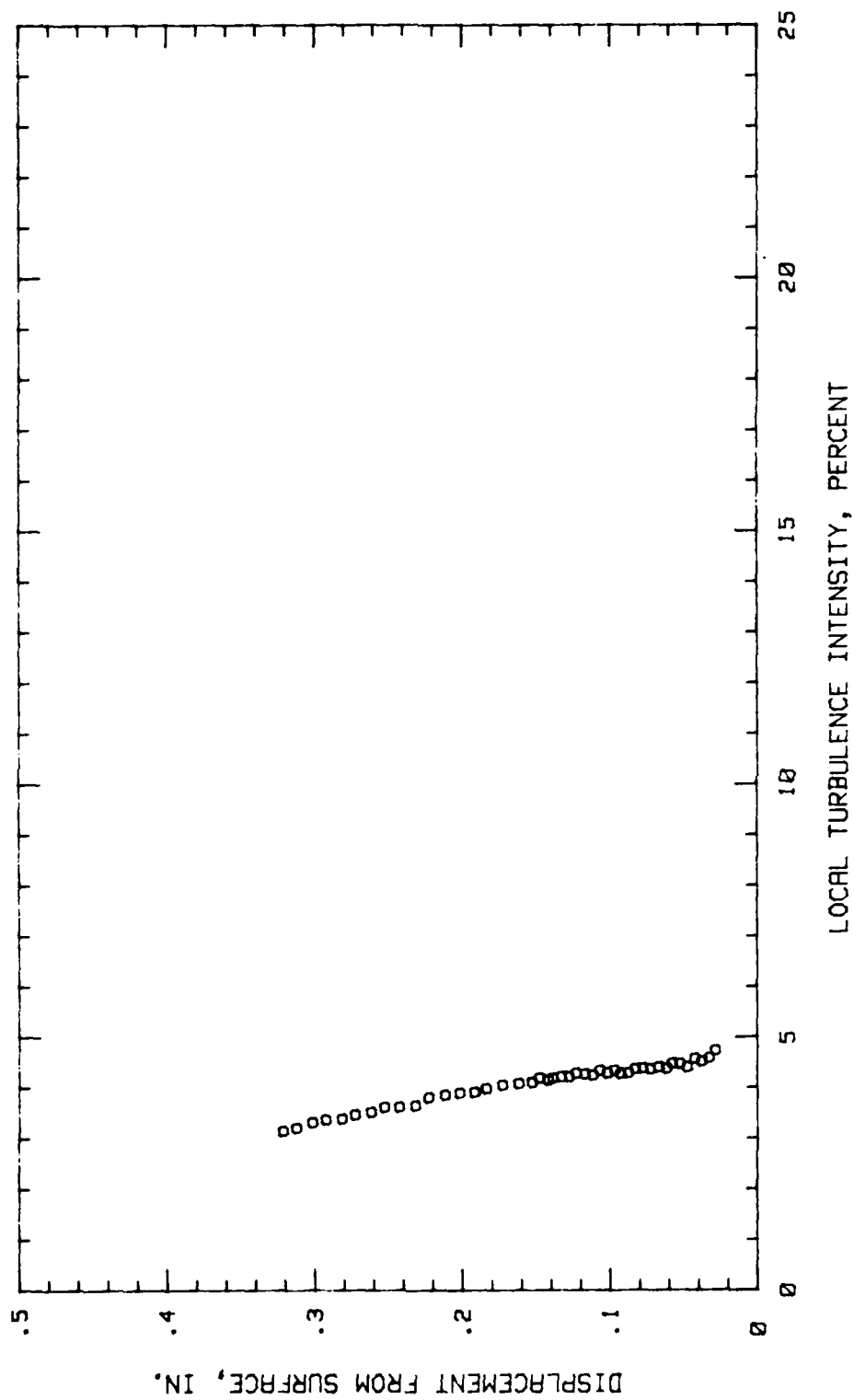


Fig. 132. Boundary Layer Turb. Intensity Profile, Conf. #2 at 9.37% Chord HIGH TURB

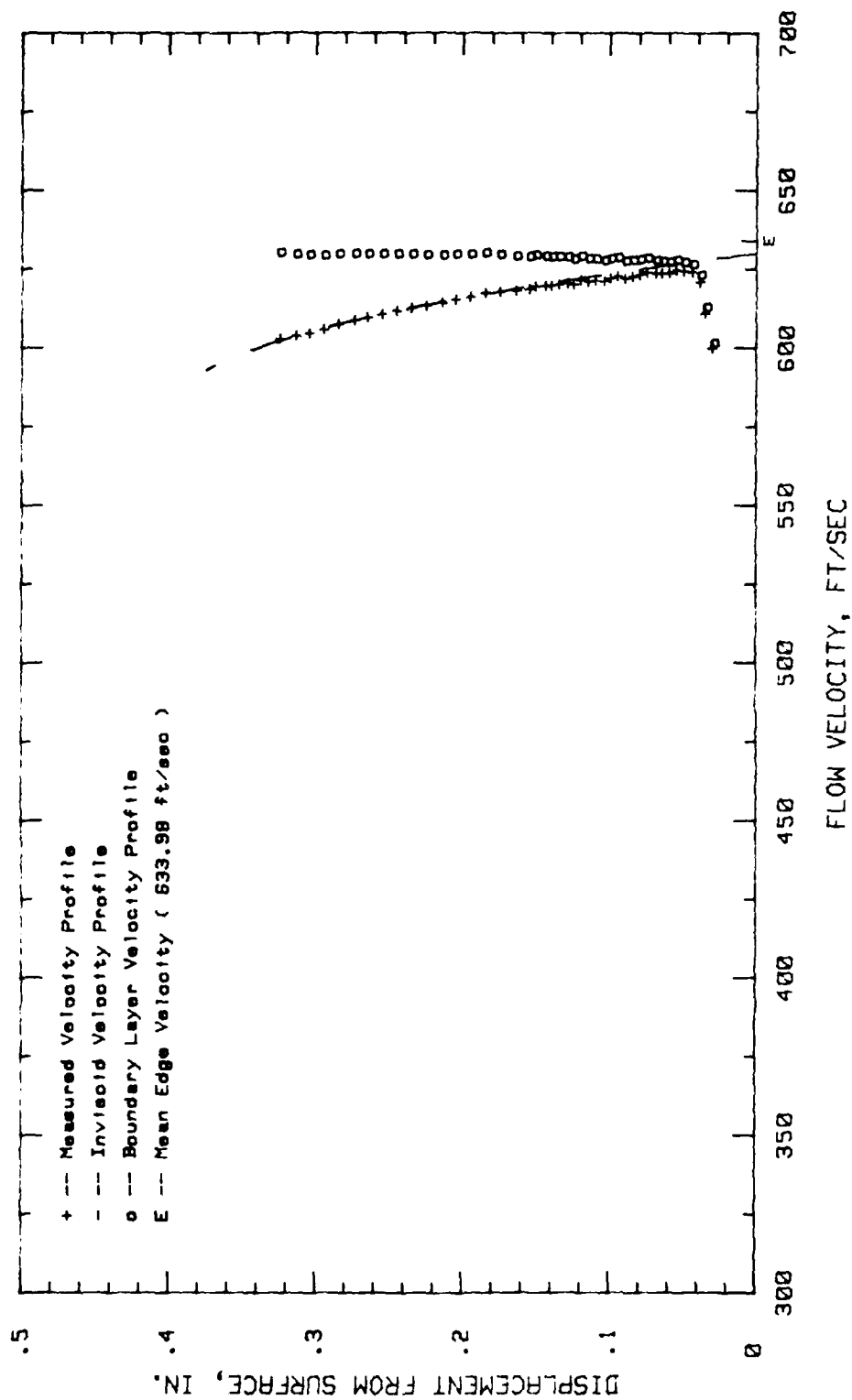


Fig.133.Boundary Layer Velocity Profiles, Conf.#2 at 25% Chord HIGH TURB.

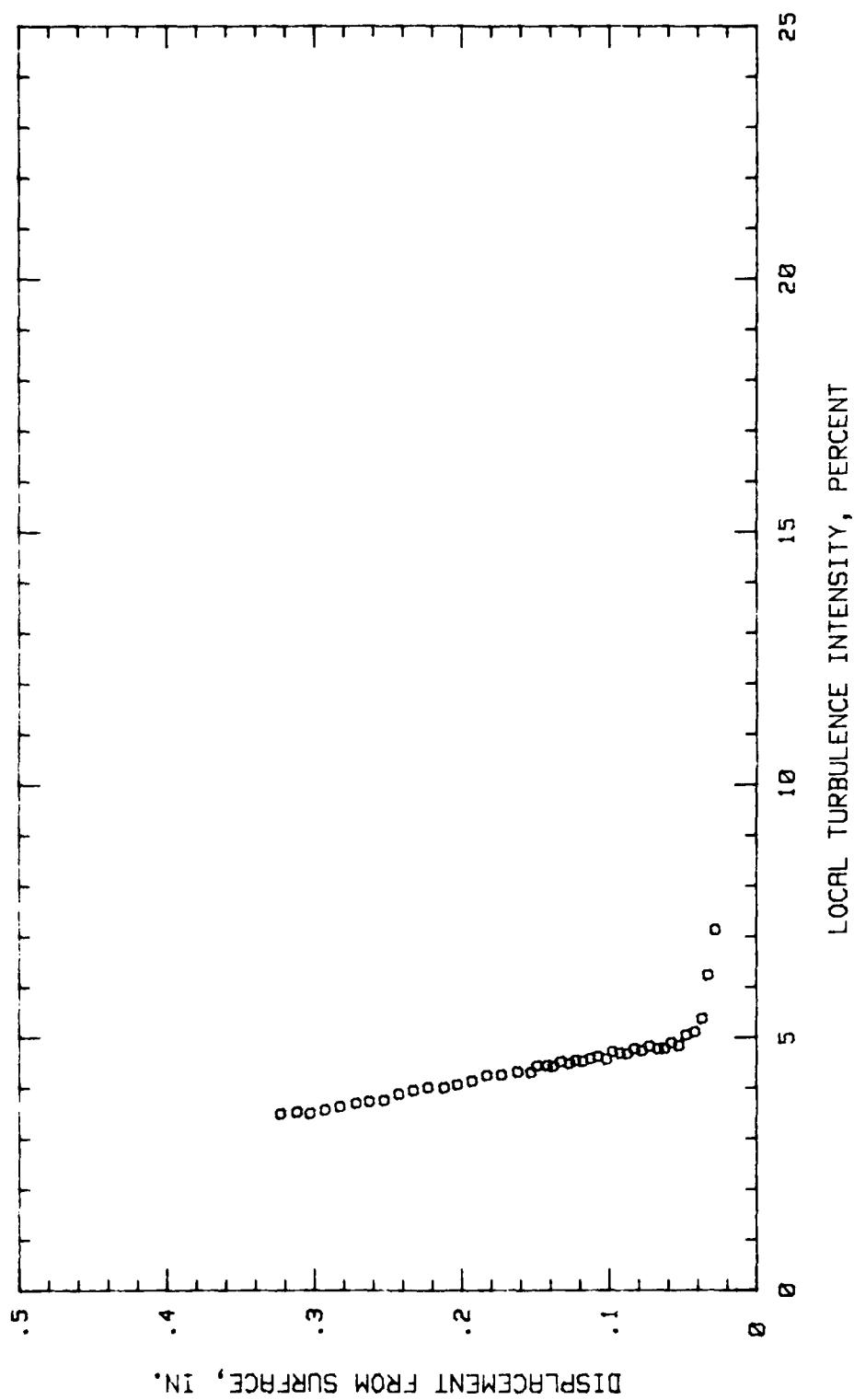


Fig.134. Boundary Layer Turb. Intensity Profile, Conf.#2 at 25% Chord HIGH TURB.

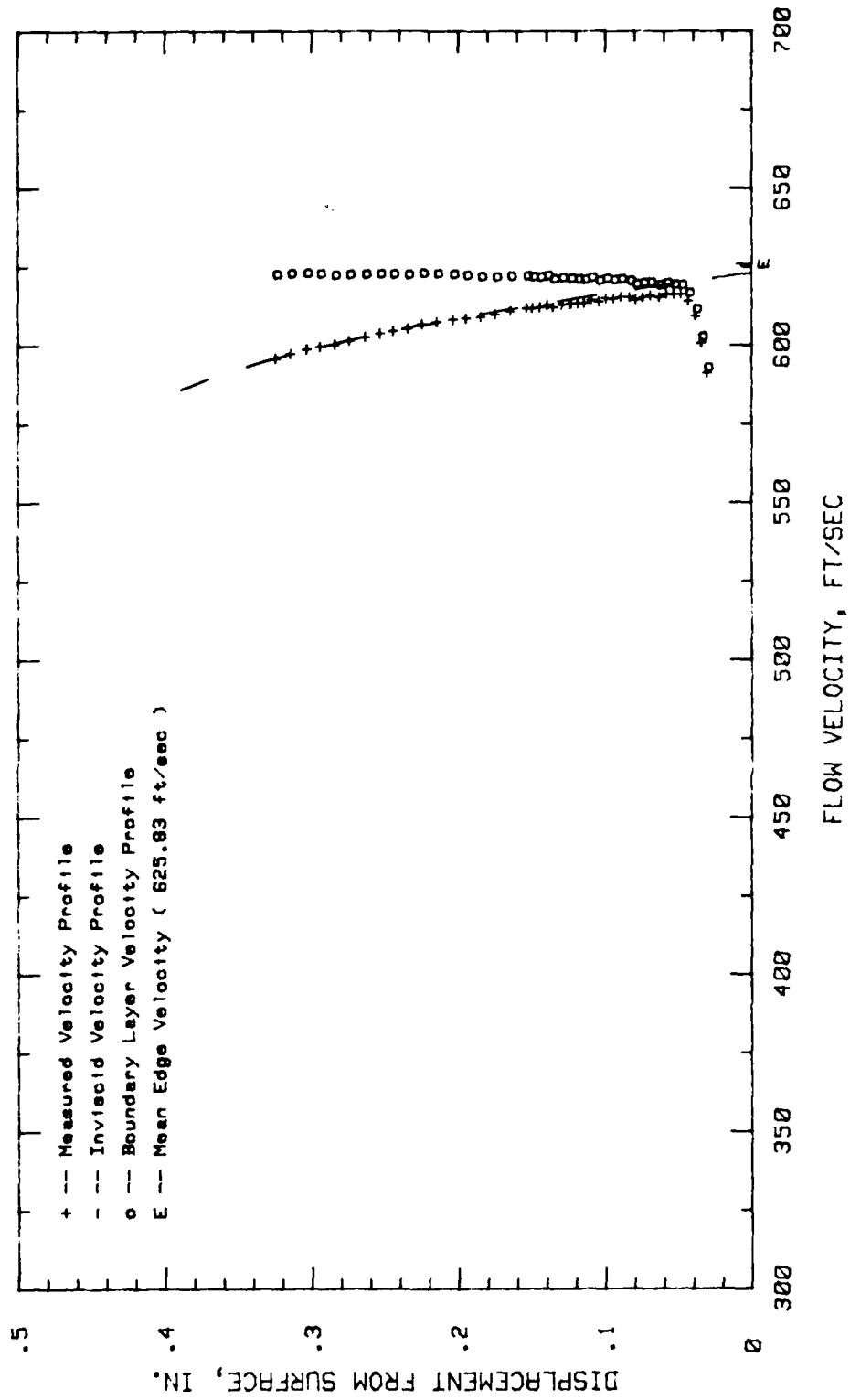


Fig.135. Boundary Layer Velocity Profiles, Conf.#2 at 29.68% Chord HIGH TURB.

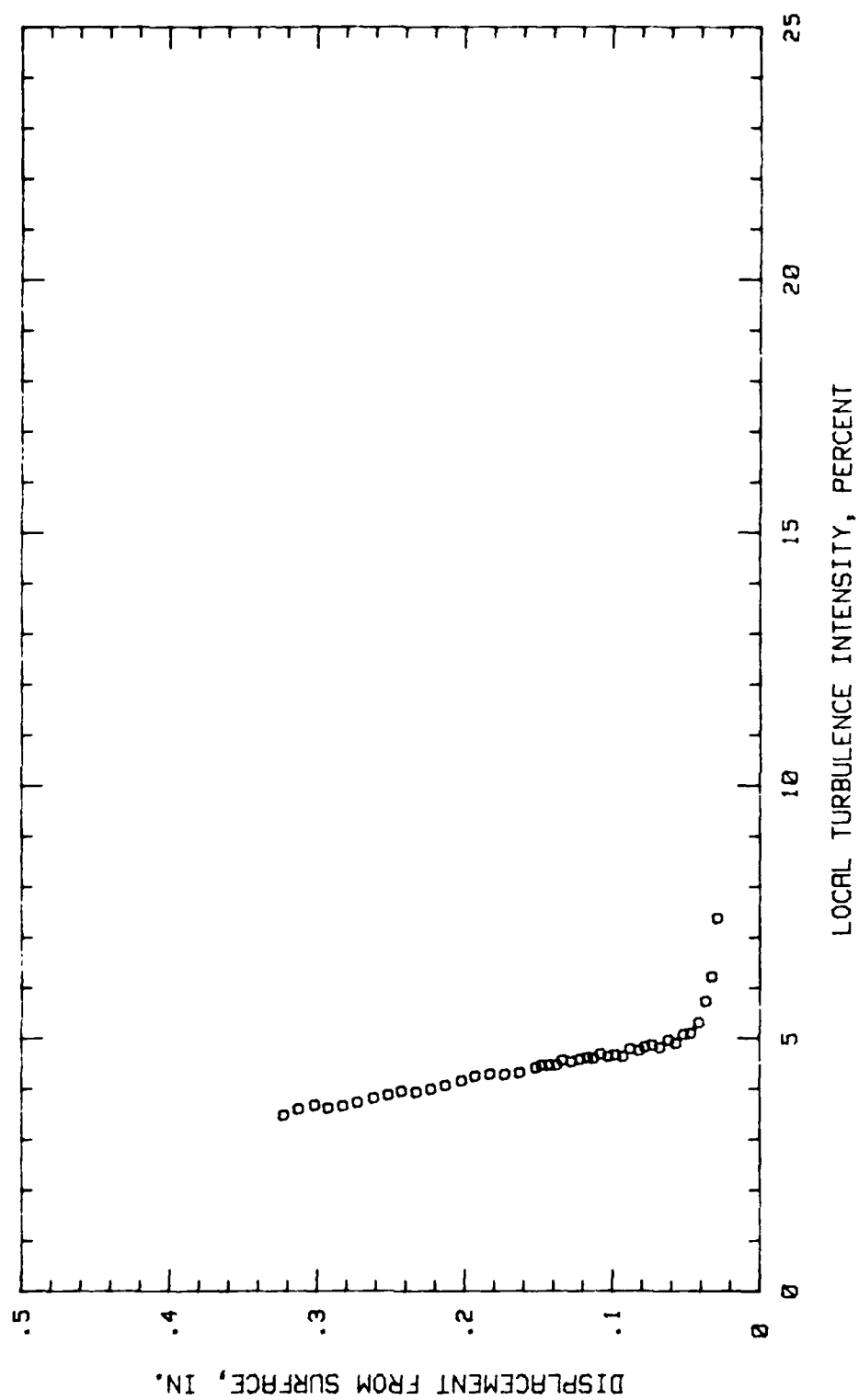


Fig. 136. Boundary Layer Turb. Intensity Profile, Conf. #2 at 29.68% Chord HIGH TUR

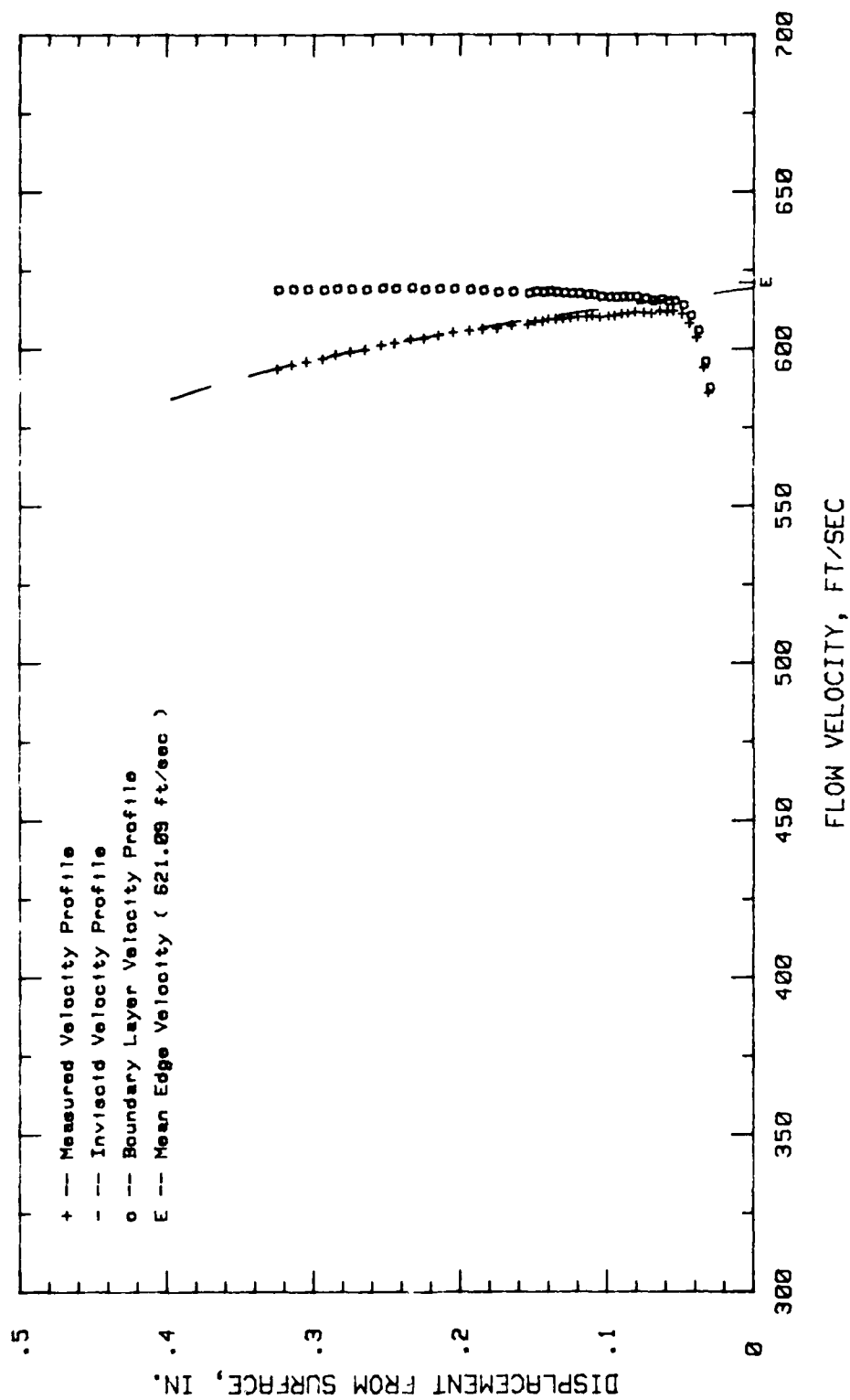


Fig.137. Boundary Layer Velocity Profiles, Conf. #2 at 34.37% Chord HIGH TURB.

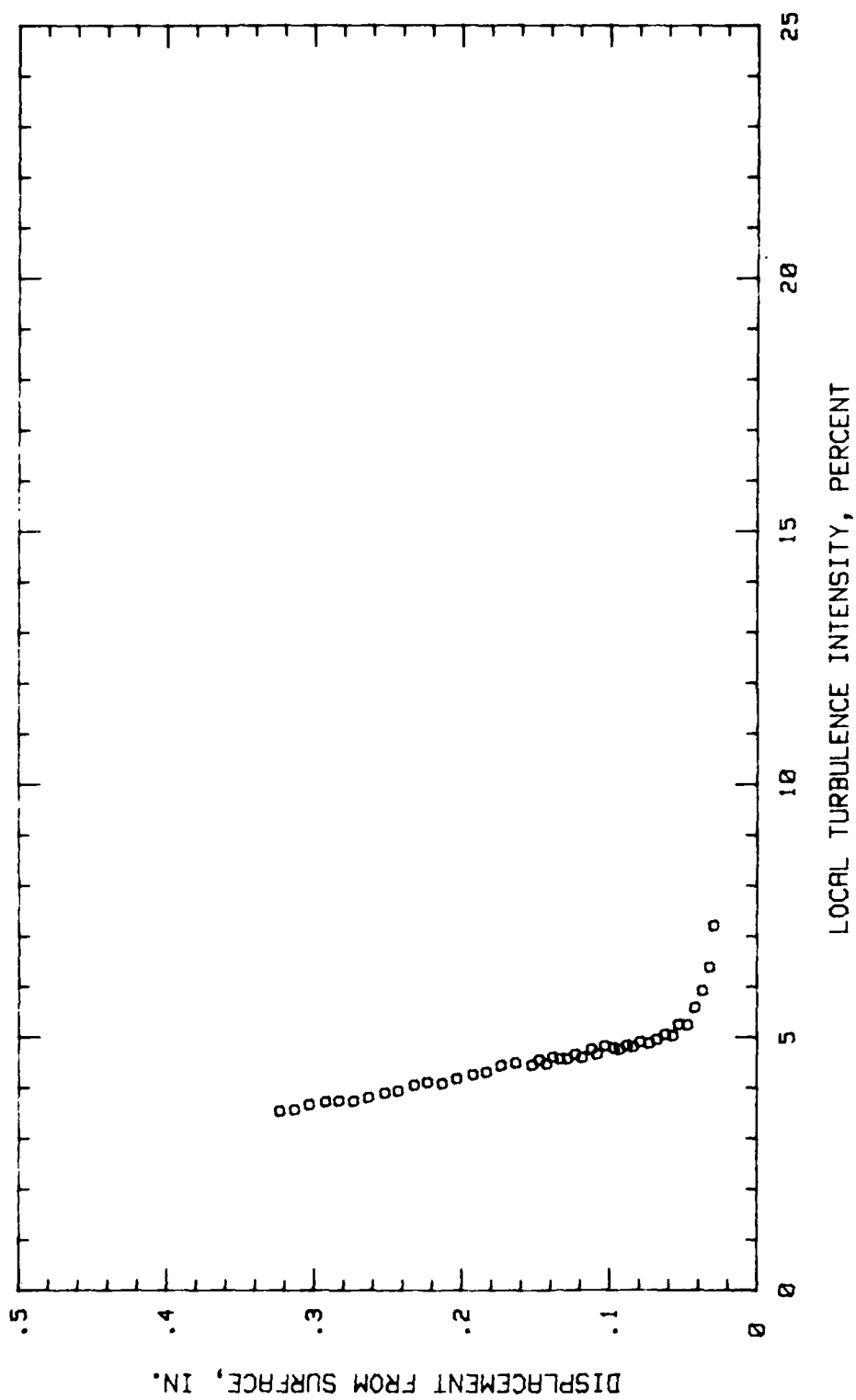


Fig. 138. Boundary Layer Turb. Intensity Profile, Conf. #2 at 34.37% Chord HIGH TUR

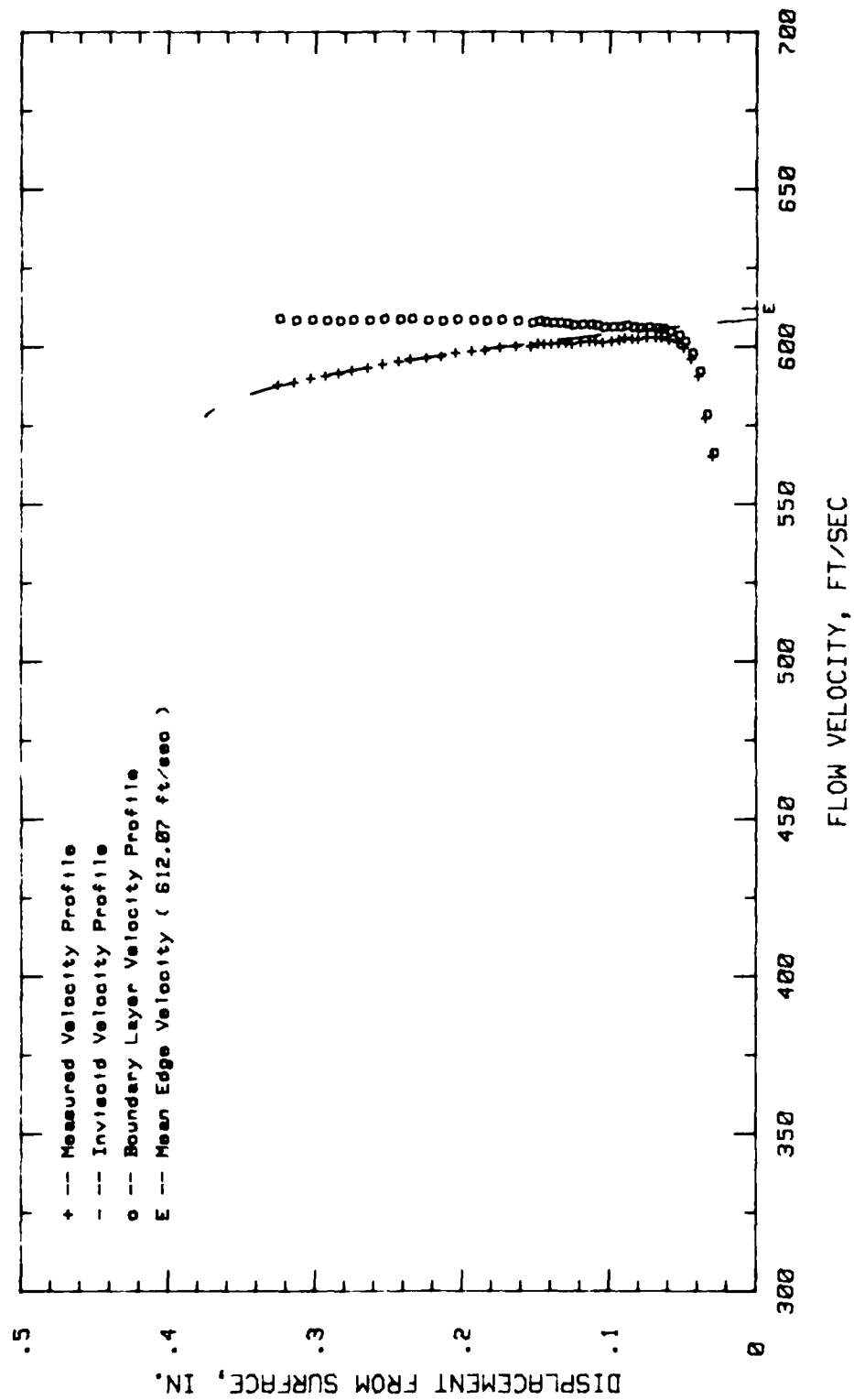


Fig.139. Boundary Layer Velocity Profiles, Conf.#2 at 40.62% Chord HIGH TURB.

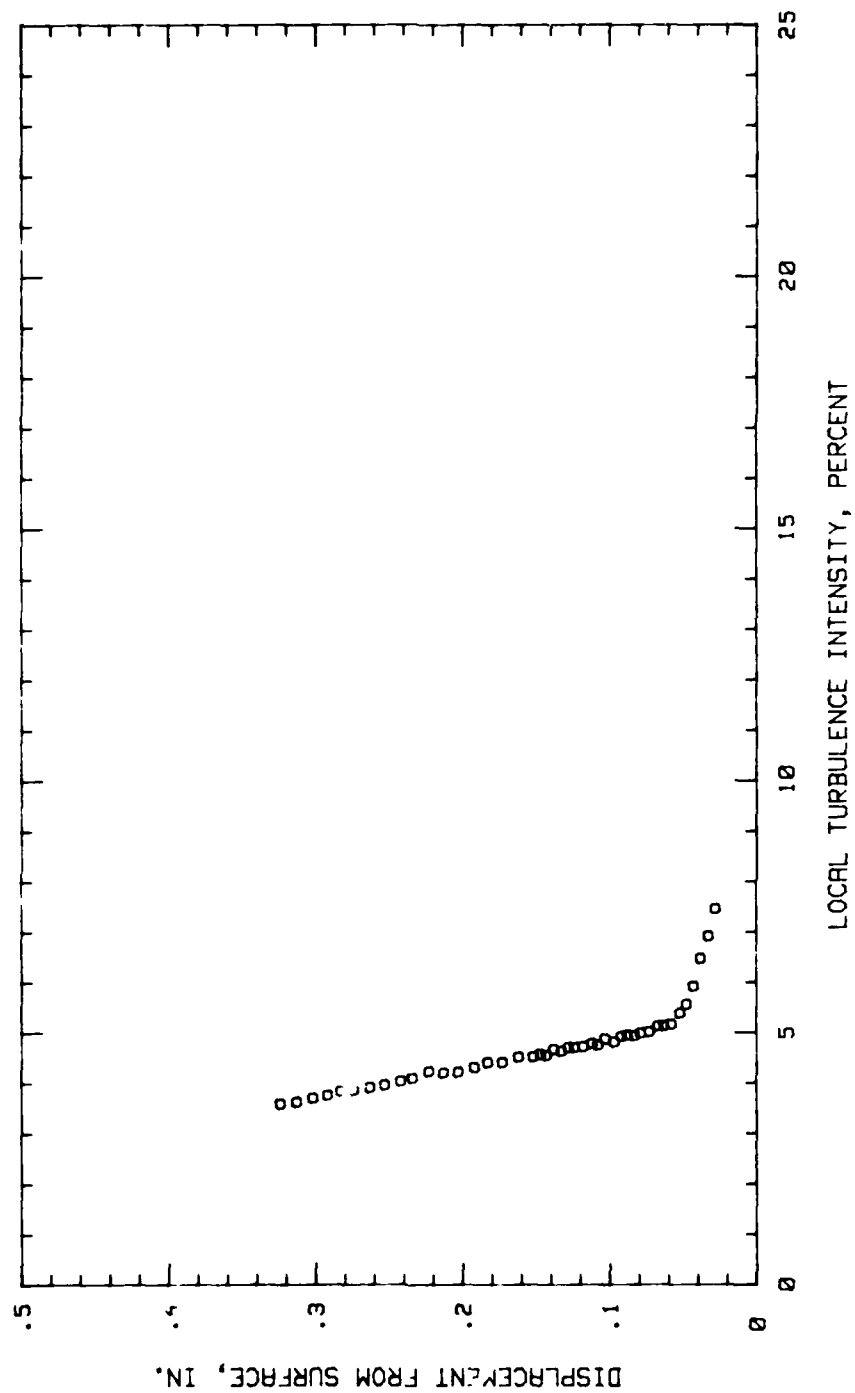


Fig.140. Boundary Layer Turb. Intensity Profile, Conf.#2 at 40.62% Chord HIGH TUR

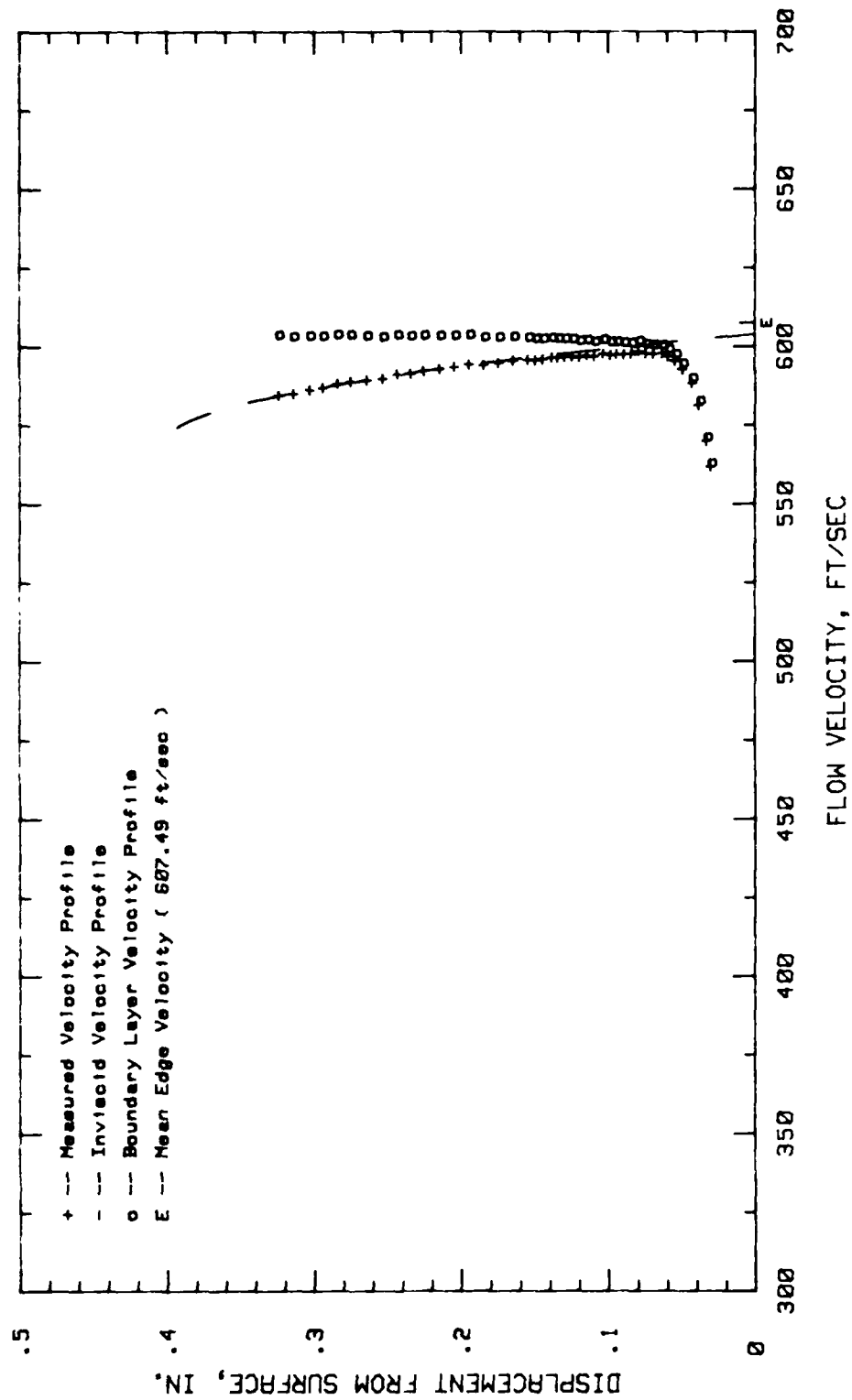


Fig.141. Boundary Layer Velocity Profiles, Conf.#2 at 45.31% Chord HIGH TURB.

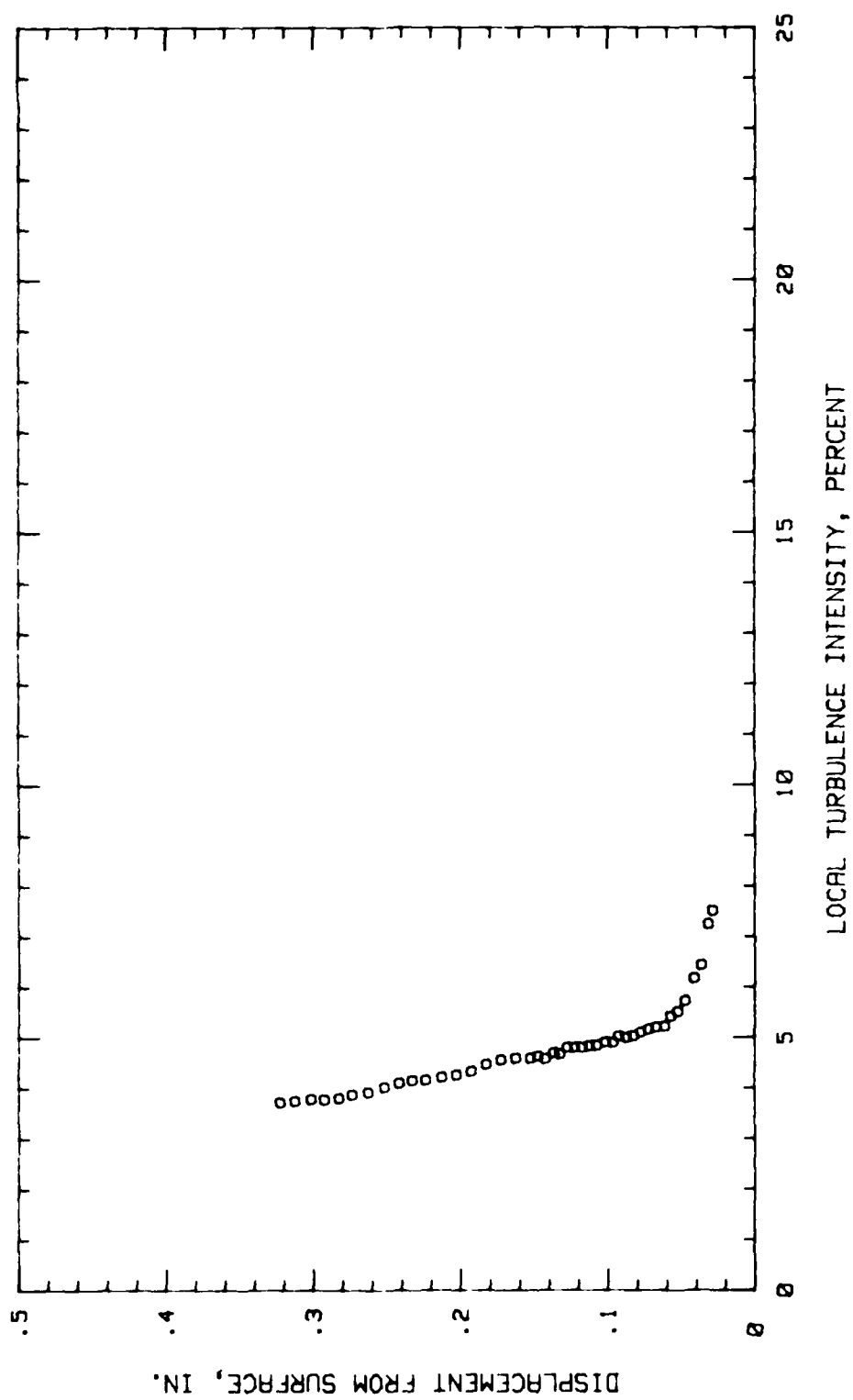


Fig. 142. Boundary Layer Turb. Intensity Profile, Conf. #2 at 45.31% Chord HIGH TURB

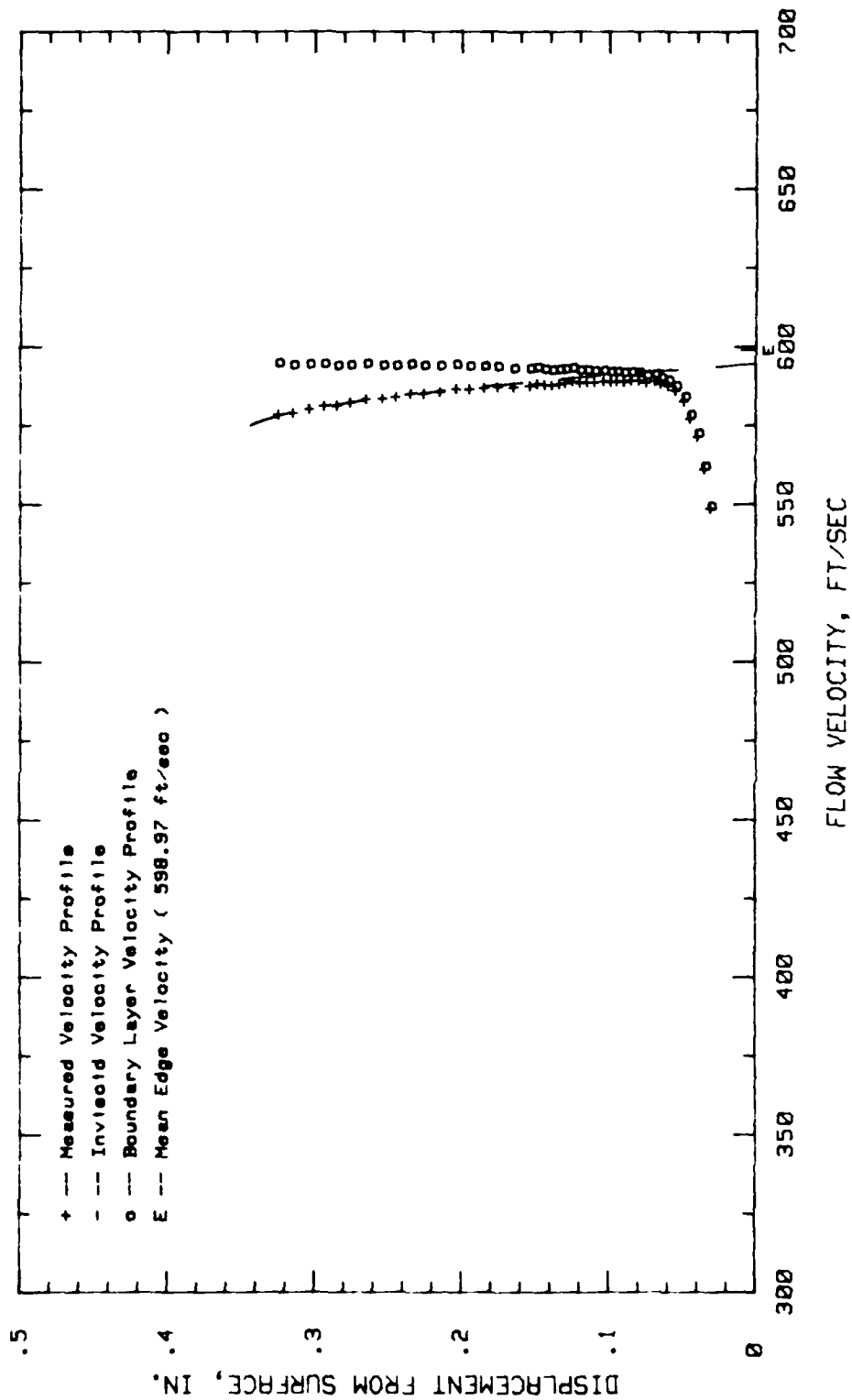


Fig.143.Boundary Layer Velocity Profiles, Conf.#2 at 50% Chord HIGH TURB.

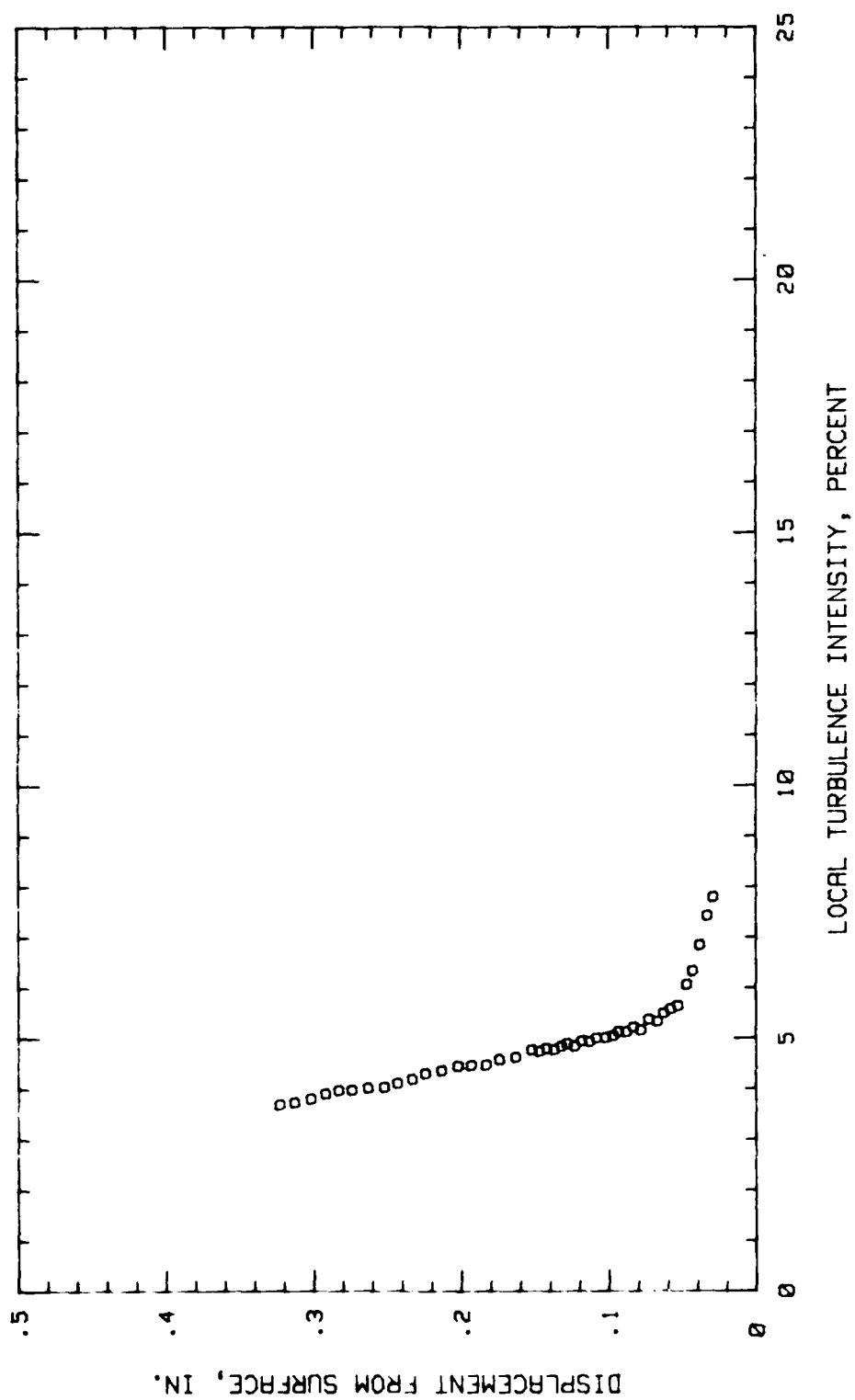


Fig.144.Boundary Layer Turb.Intensity Profile, Conf.#2 at 50% Chord HIGH TURB.

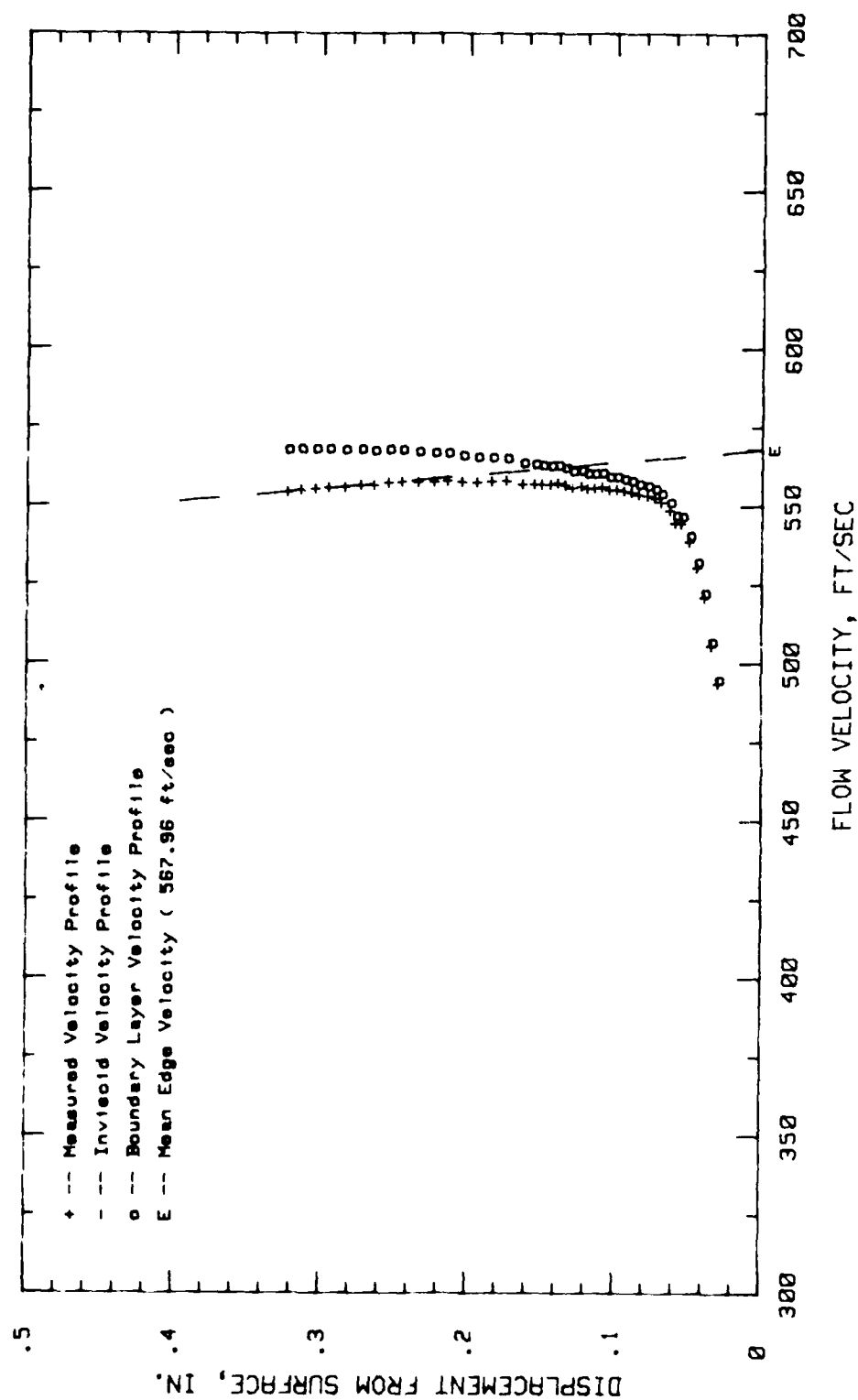


Fig.145. Boundary Layer Velocity Profiles, Conf.#2 at 65.62% Chord HIGH TURB.

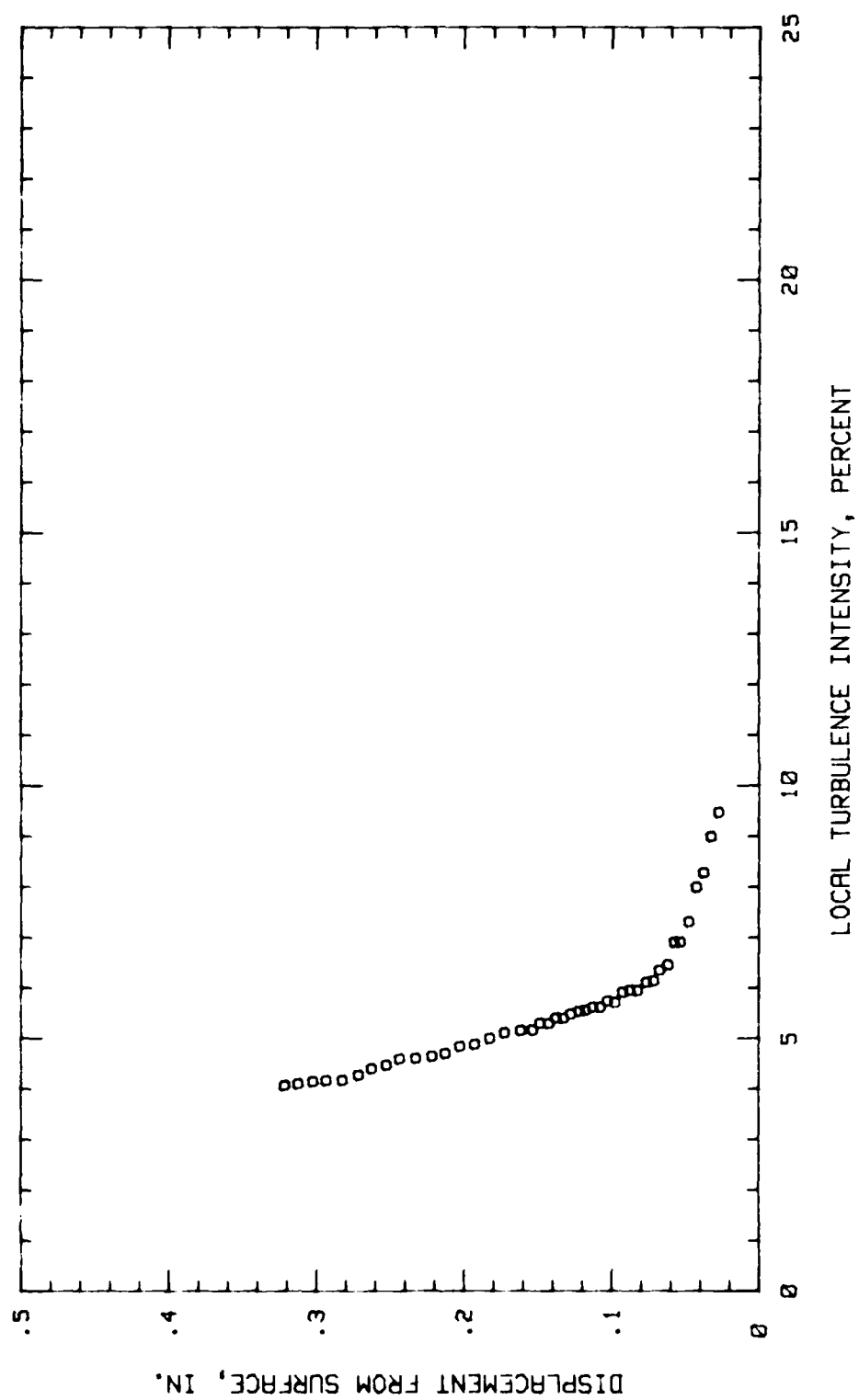


Fig. 146. Boundary Layer Turb. Intensity Profile, Conf. #2 at 65.62% Chord HIGH TURB

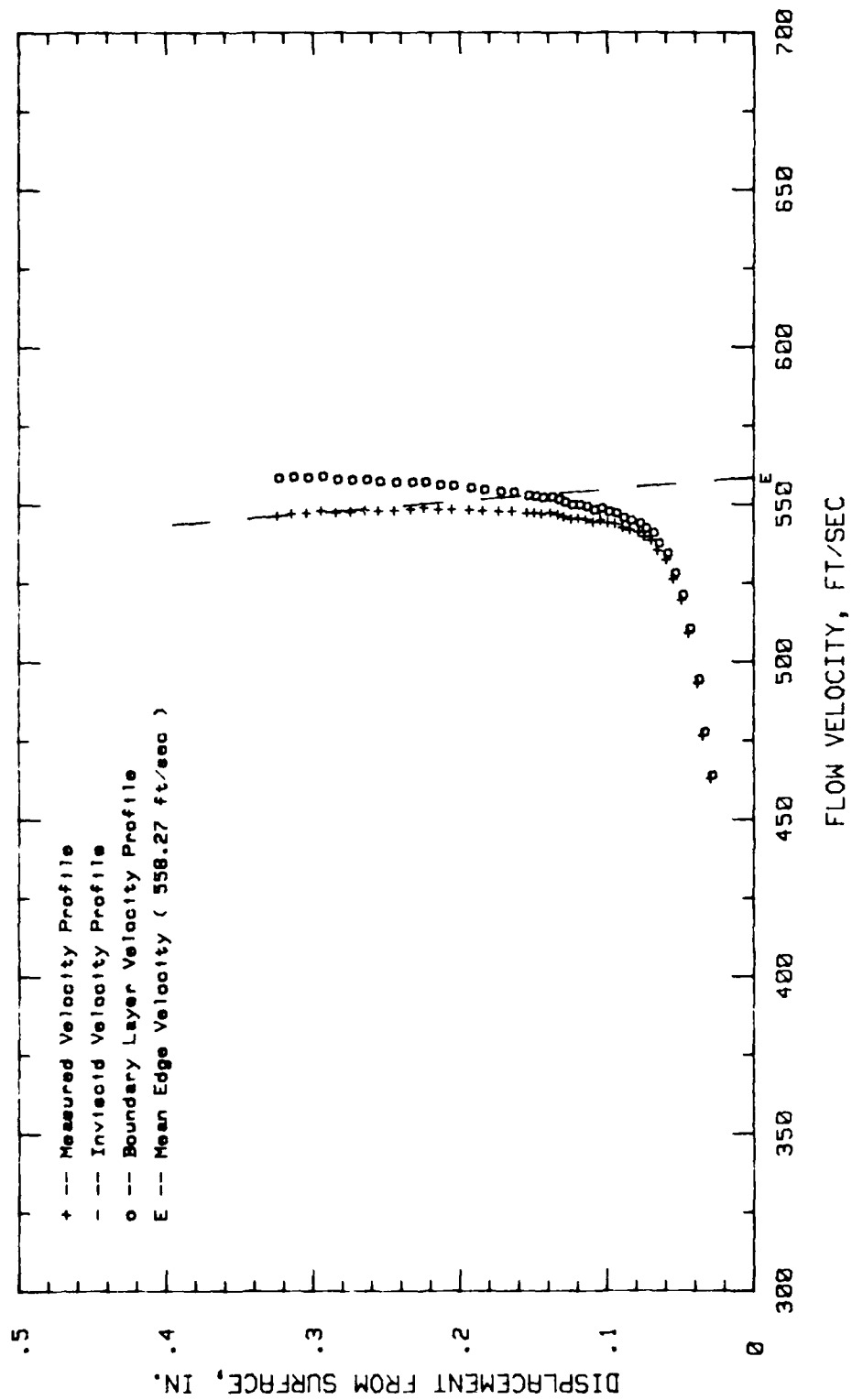


Fig.147. Boundary Layer Velocity Profiles, Conf.#2 at 70.31% Chord HIGH TURB.

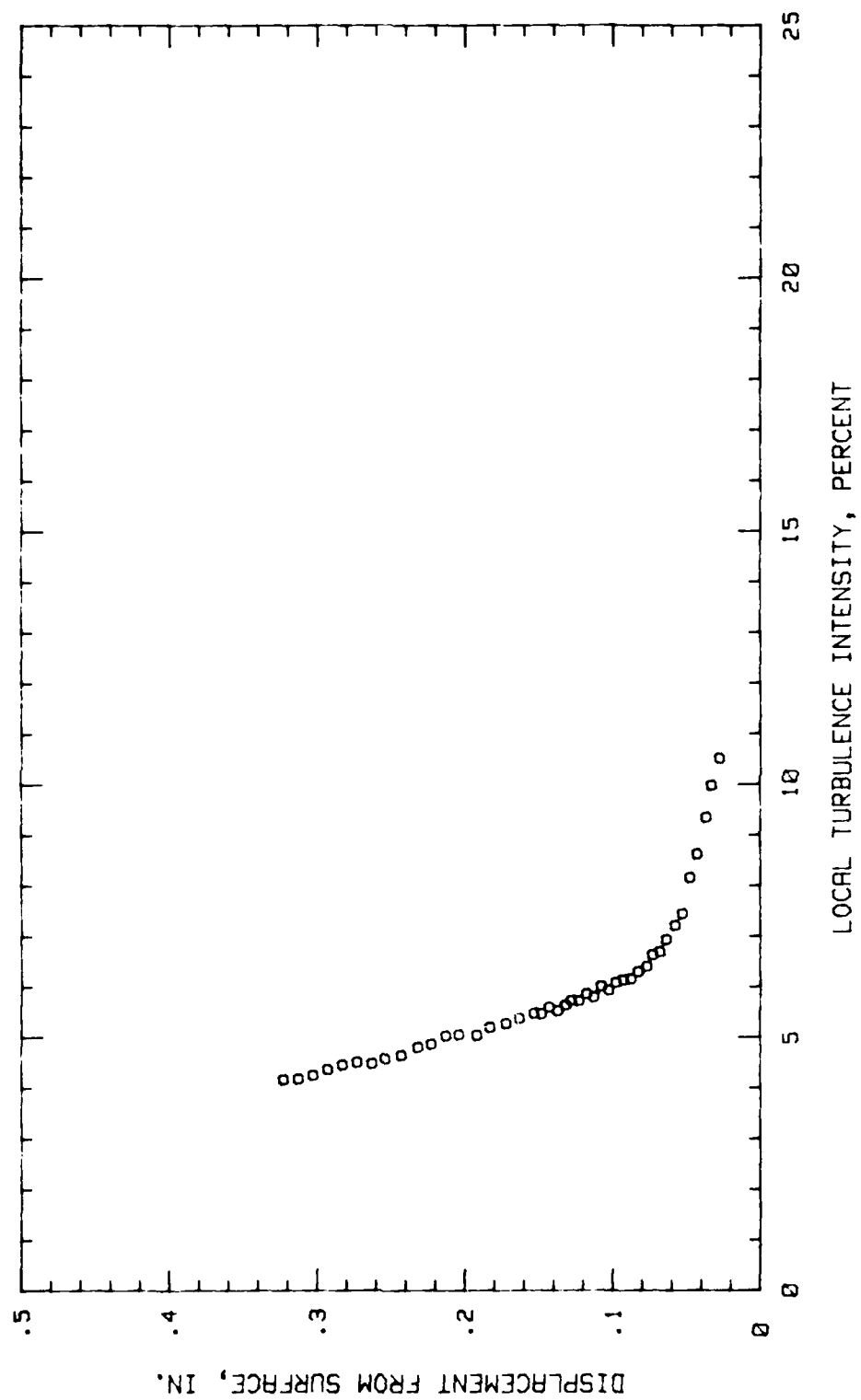


Fig.148.Boundary Layer Turb.Intensity Profile, Conf.#2 at 70.31% Chord HIGH TURB

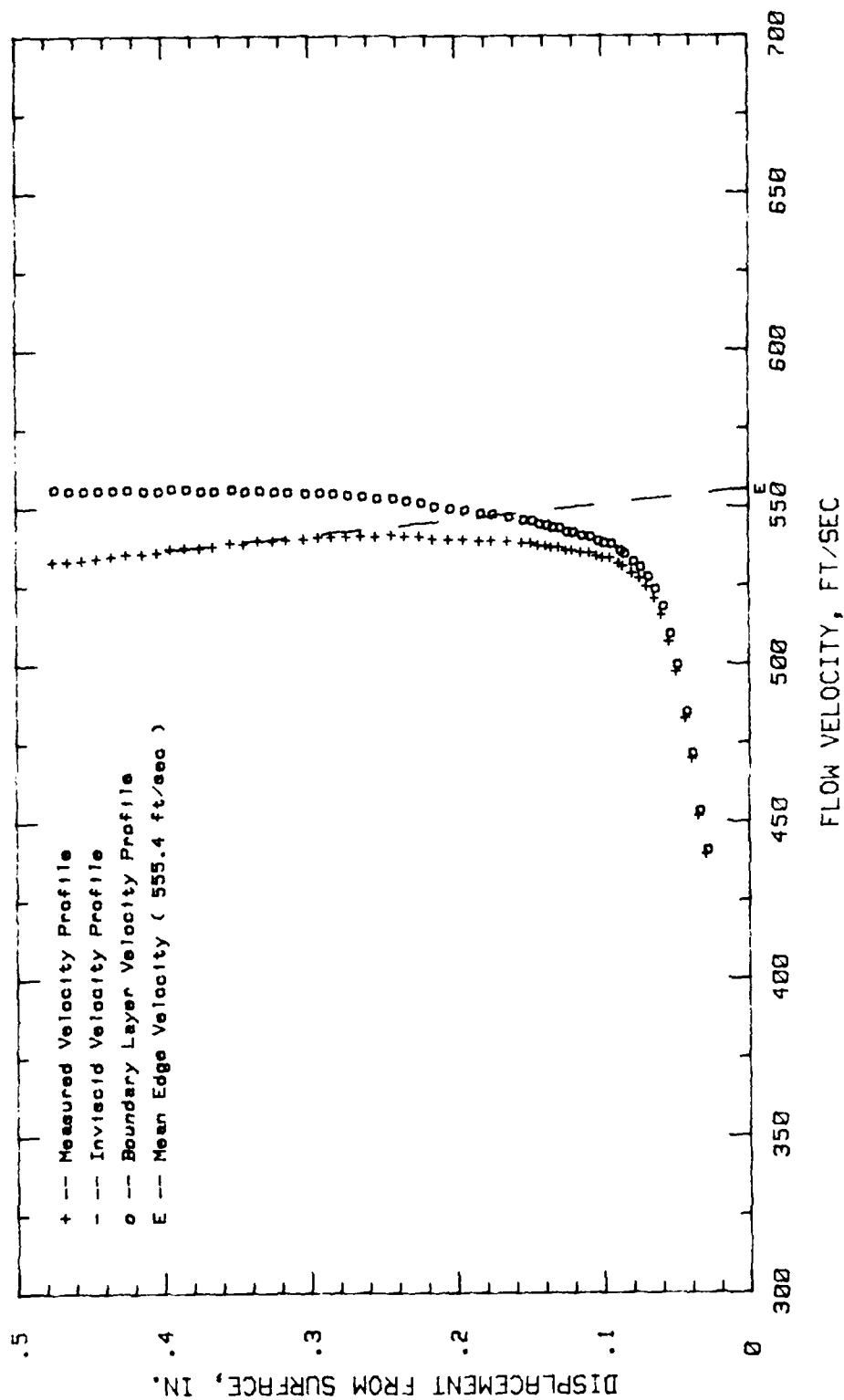


Fig. 149. Boundary Layer Velocity Profiles, Conf. #2 at 75% Chord HIGH TURB.

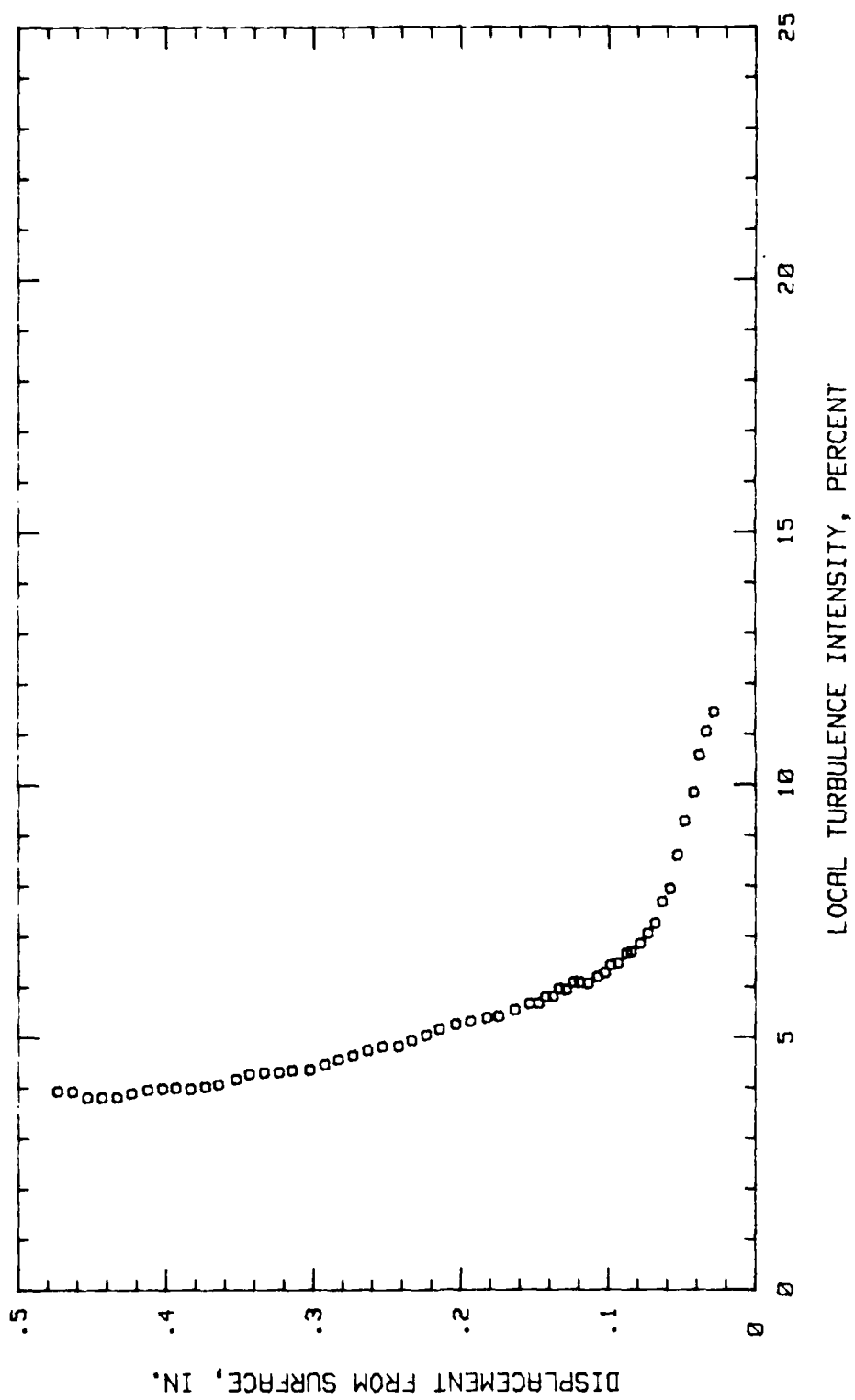


Fig. 150. Boundary Layer Turb. Intensity Profile, Conf. #2 at 75% Chord HIGH TURB.

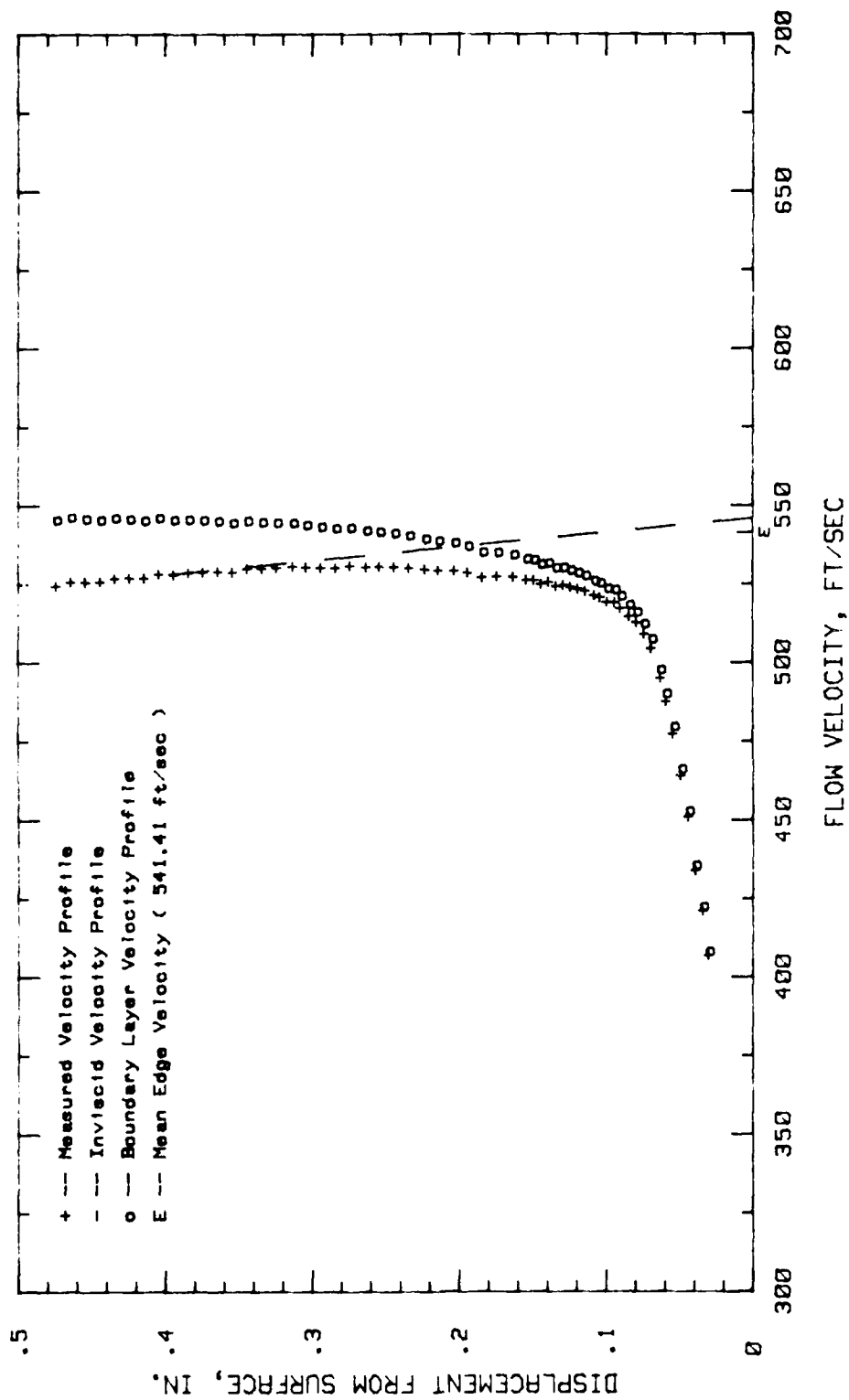


Fig.151. Boundary Layer Velocity Profiles, Conf.#2 at 79.68% Chord HIGH TURB.

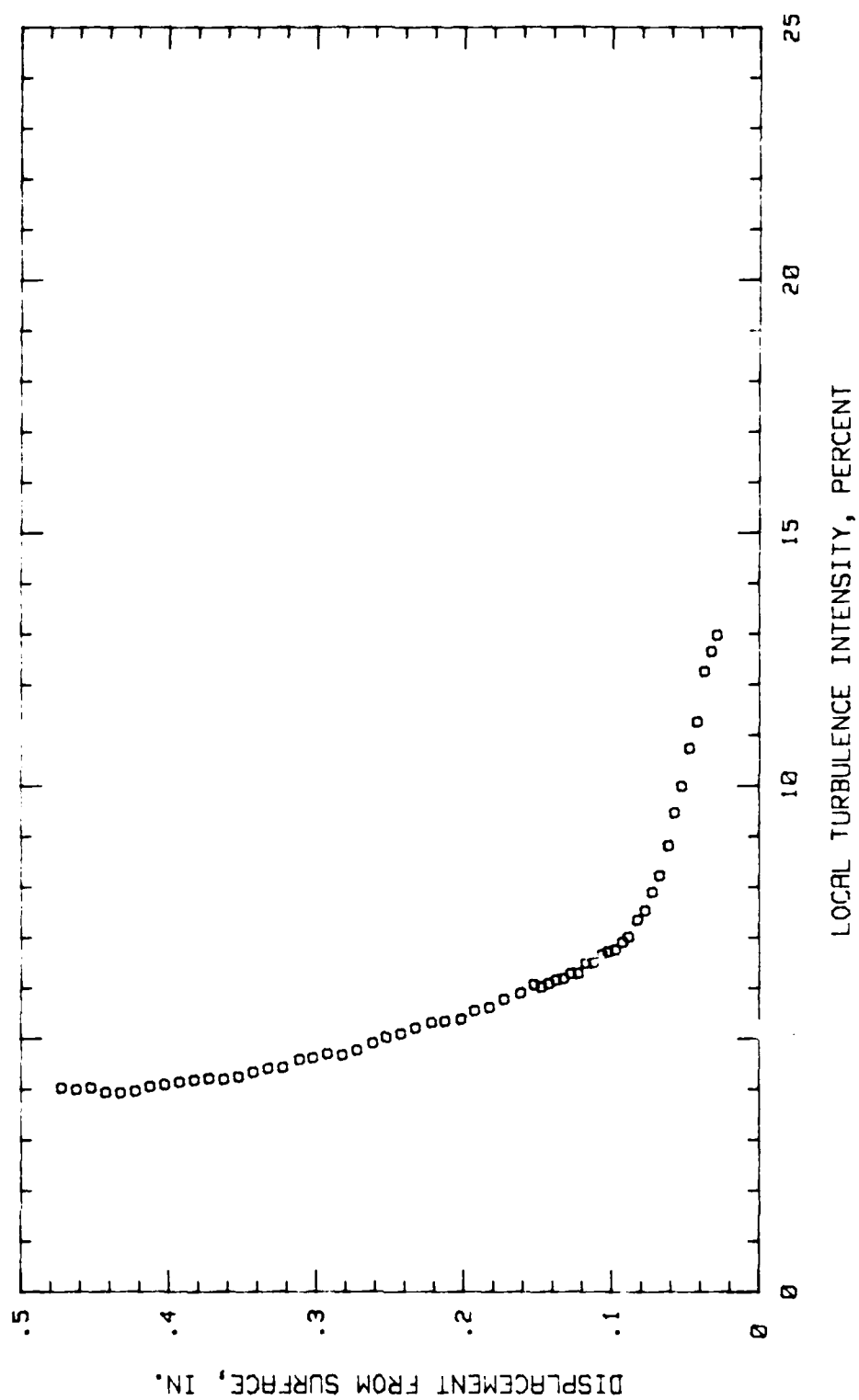


Fig. 152.B Boundary Layer Turb. Intensity Profile, Conf. #2 at 79.68% Chord HIGH TURB

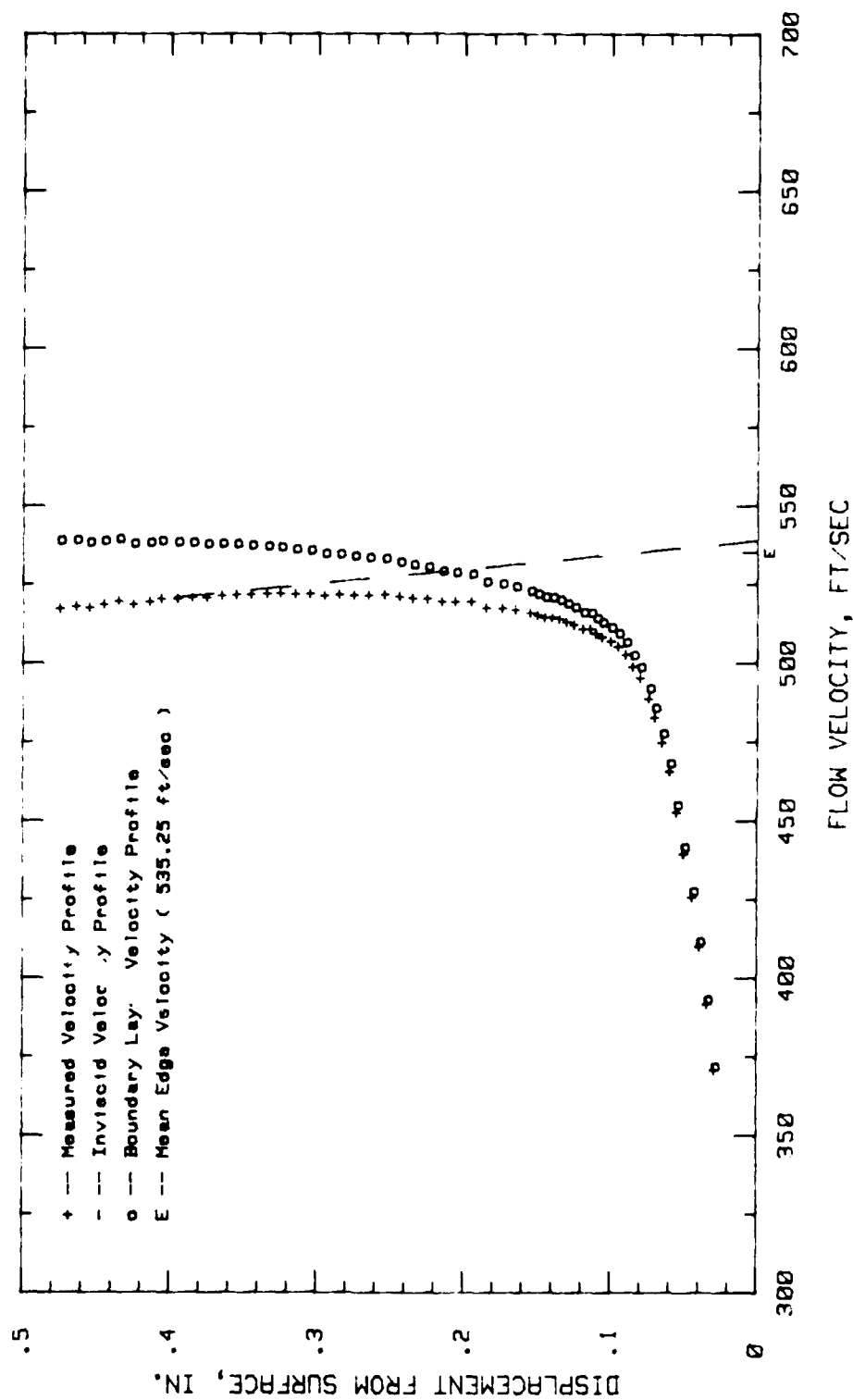


Fig.153. Boundary Layer Velocity Profiles, Conf.#2 at 84.37% Chord HIGH TURB.

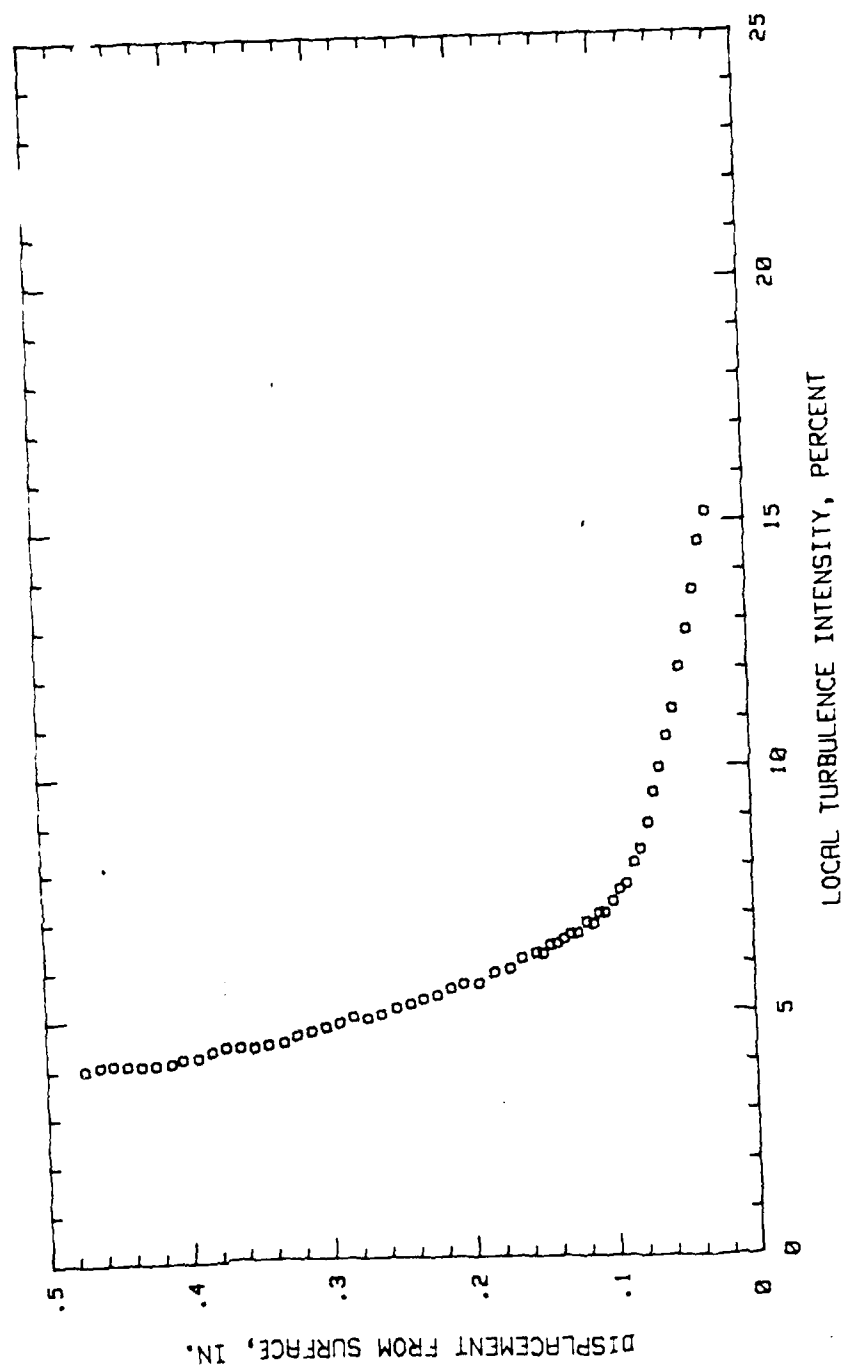


Fig. 154. Boundary Layer Turb. Intensity Profile, Conf. #2 at 84.37% Chord HIGH TURB

APPENDIX H

Boundary Layer Velocity & Turbulence Intensity Profiles

Configuration #3, Low and High Freestream Turbulence

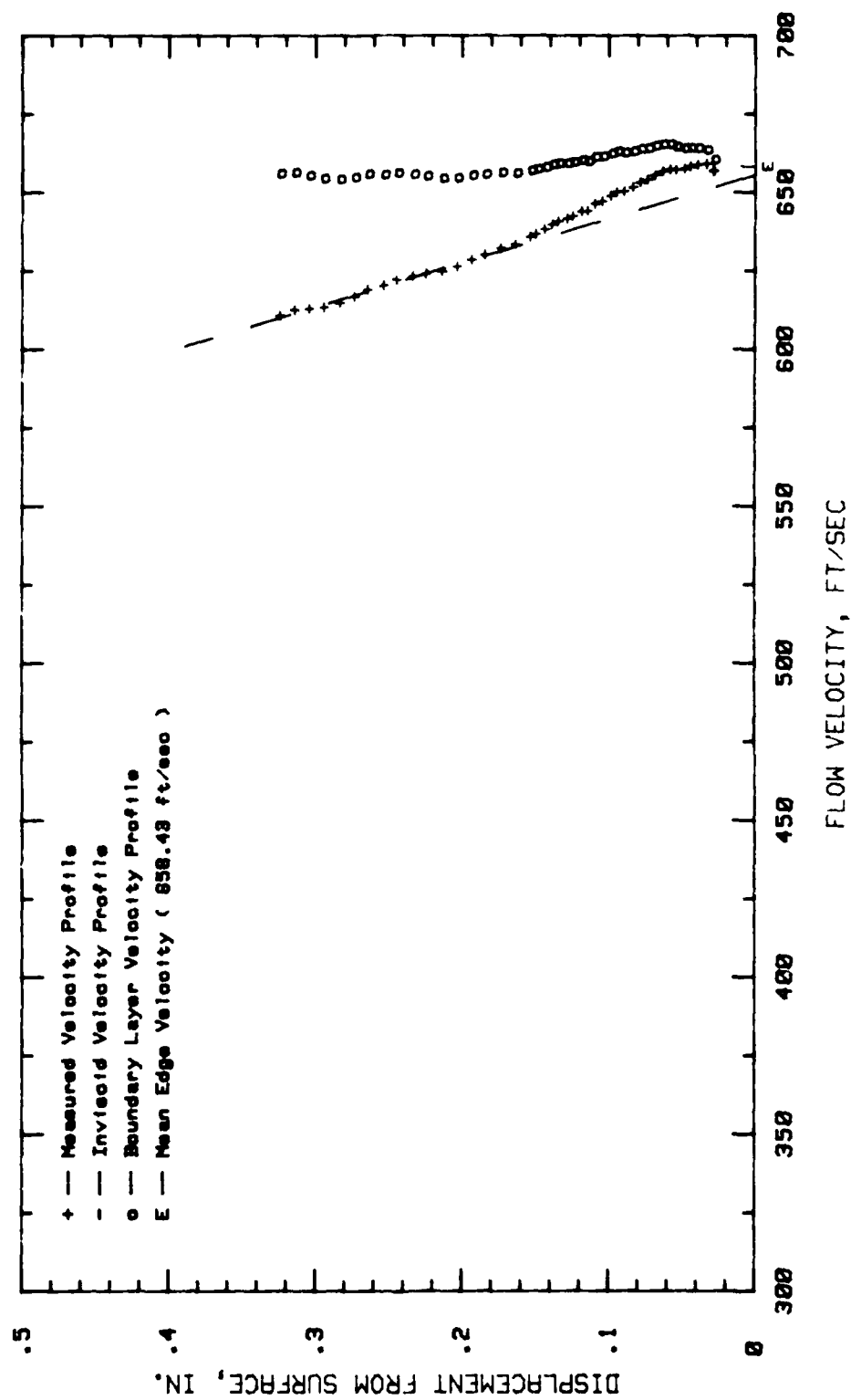


Fig.155.Boundary Layer Velocity Profiles, Conf.#3 at 4.68% Chord LOW TURB.

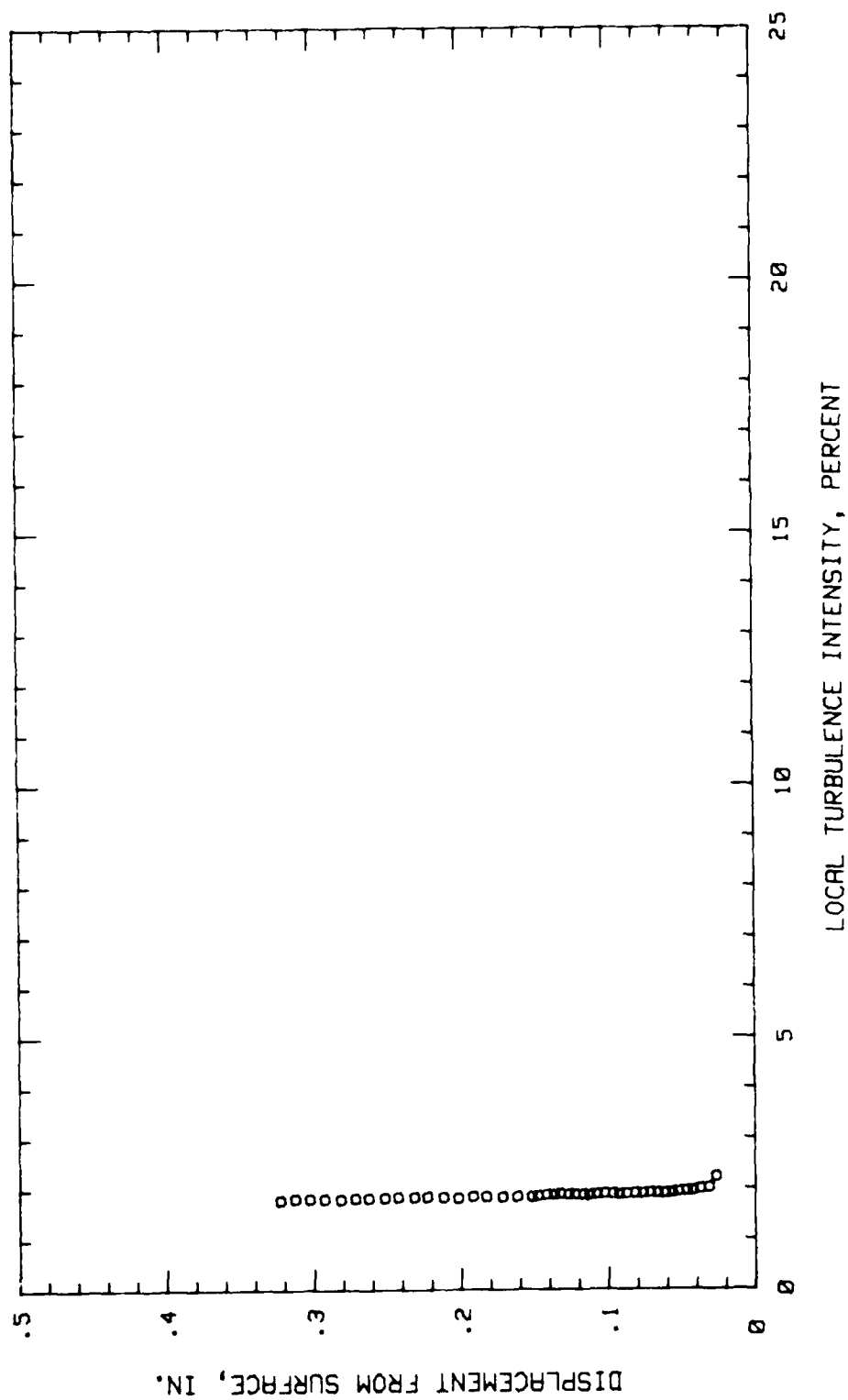


Fig. 156. Boundary Layer Turb. Intensity Profile, Conf. #3 at 4.68% Chord LOW TURB.

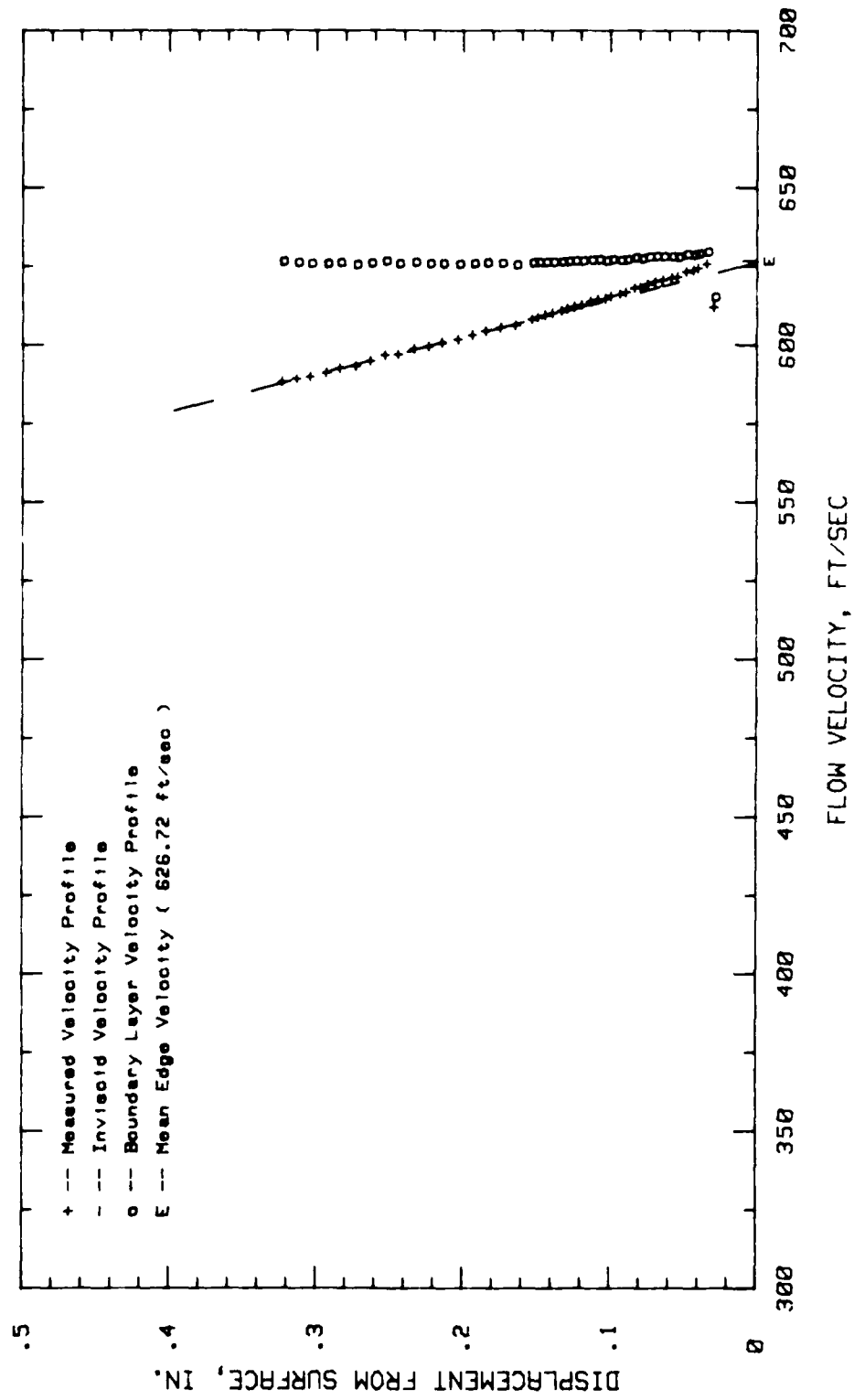


Fig.157. Boundary Layer Velocity Profiles, Conf.#3 at 9.37% Chord LOW TURB.

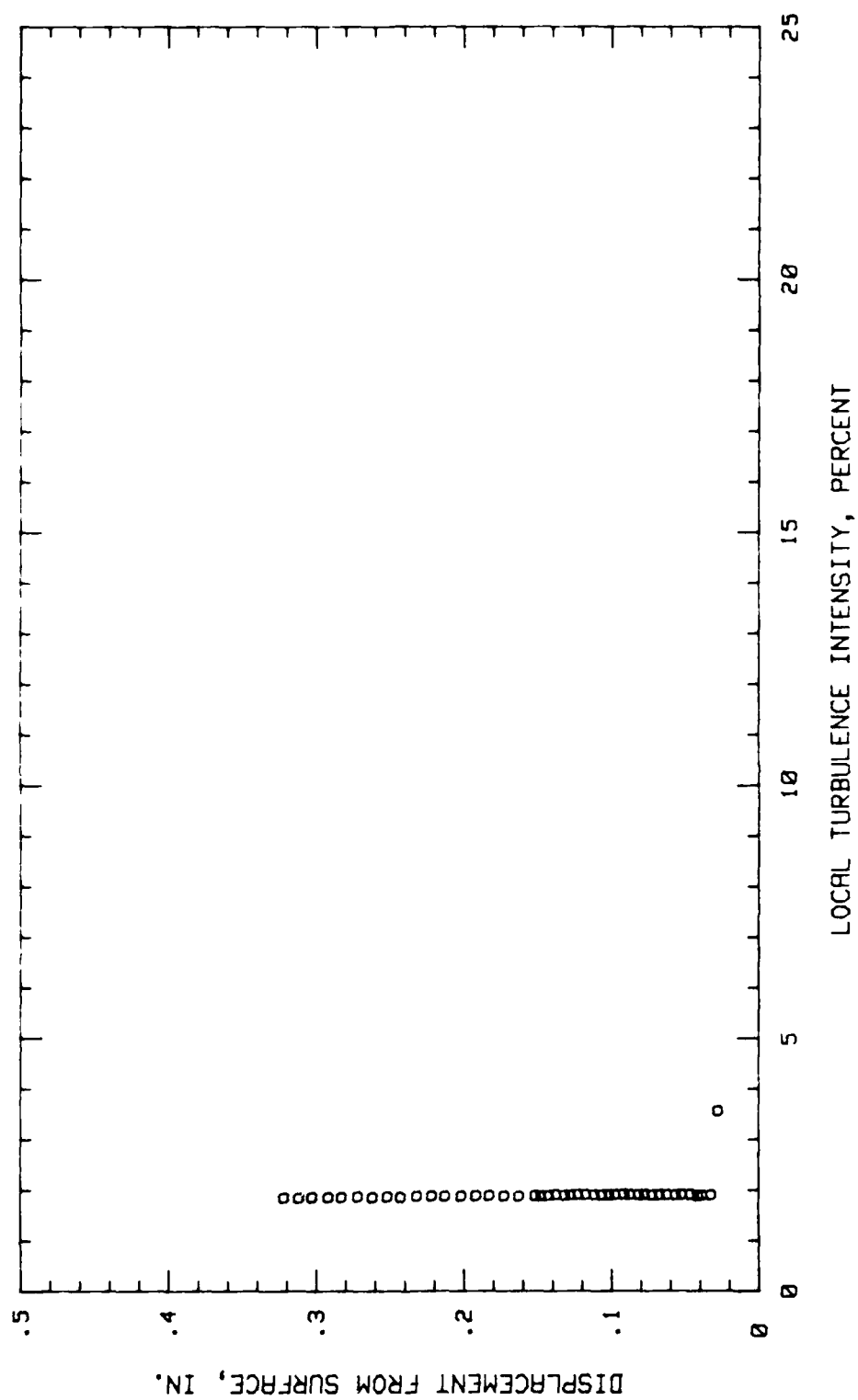


Fig.158.Boundary Layer Turb.Intensity Profile, Conf.#3 at 9.37% Chord LOW TURB.

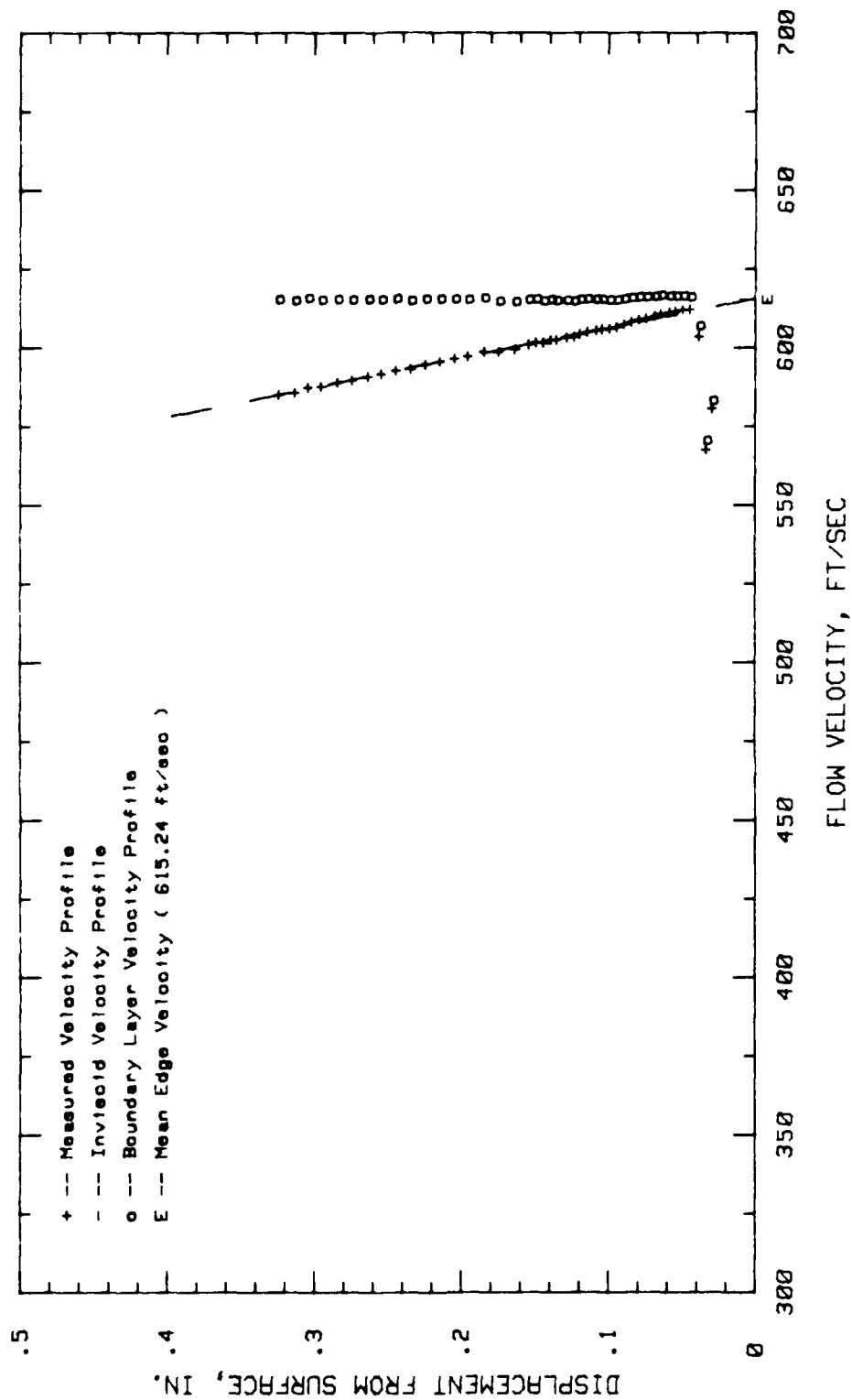


Fig. 159. Boundary Layer Velocity Profiles, Conf. #3 at 25% Chord LOW TURB.

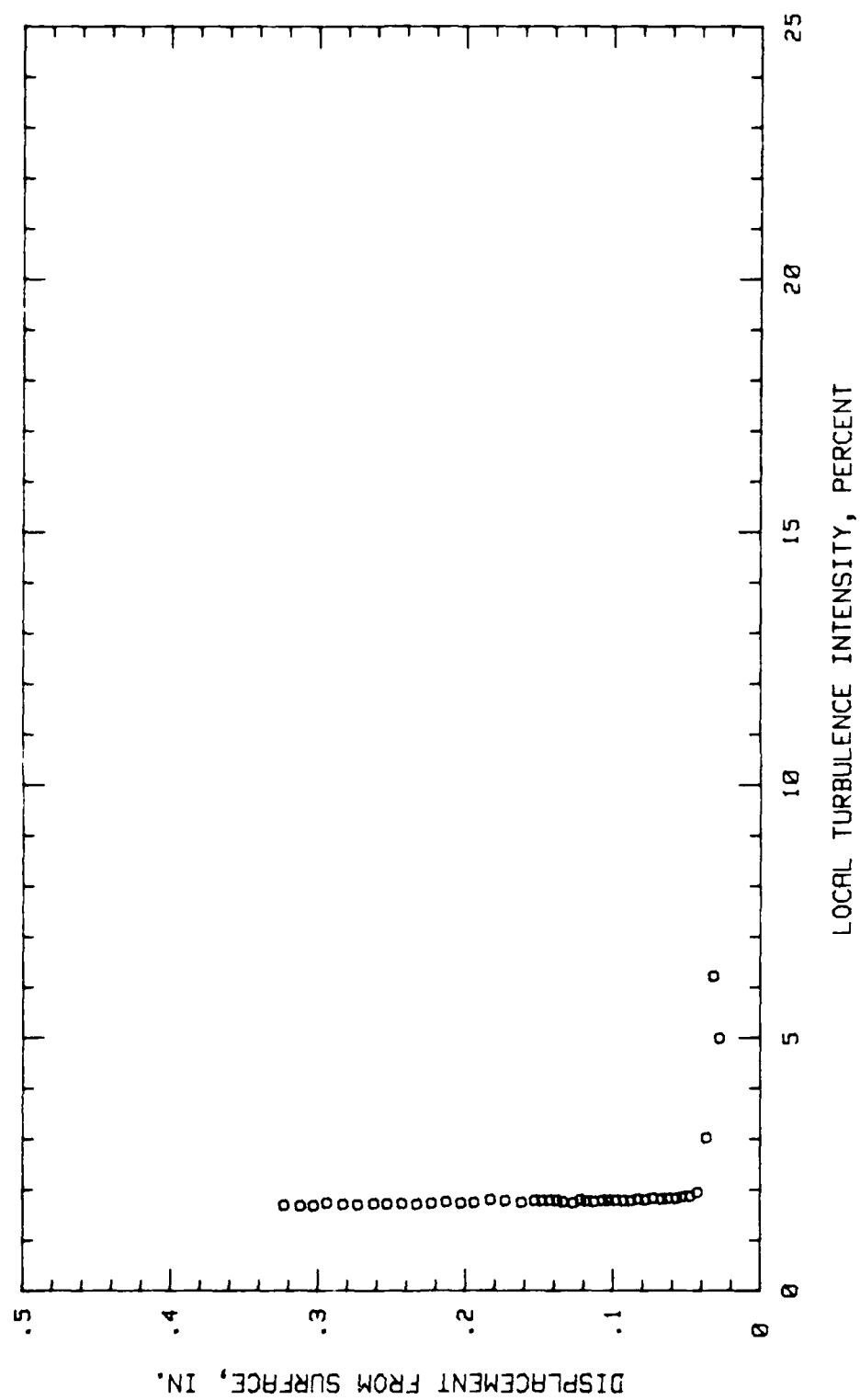


Fig. 160. Boundary Layer Turb. Intensity Profile, Conf. #3 at 25% Chord LOW TURB.

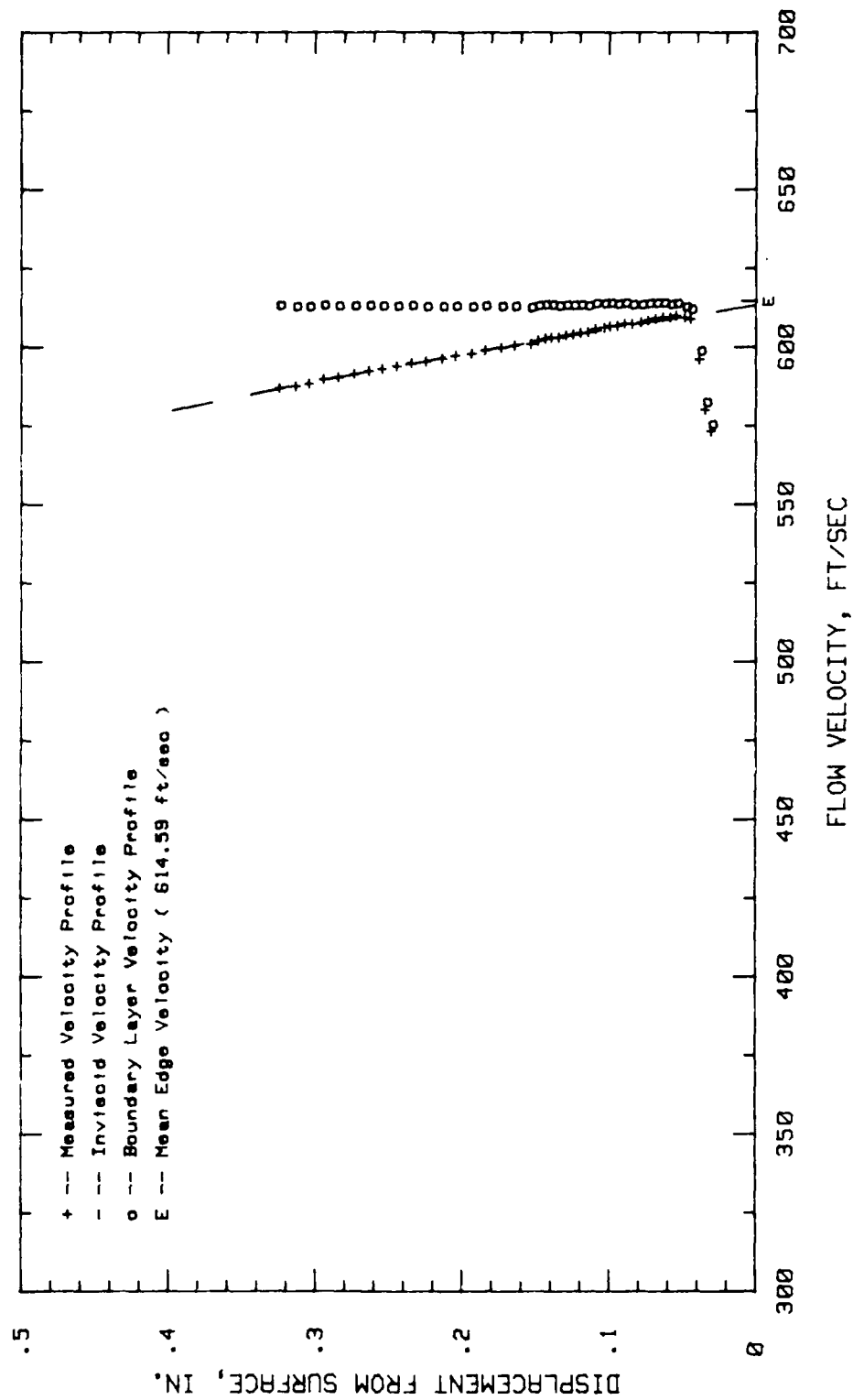


Fig.161. Boundary Layer Velocity Profiles, Conf.#3 at 29.68% Chord LOW TURB.

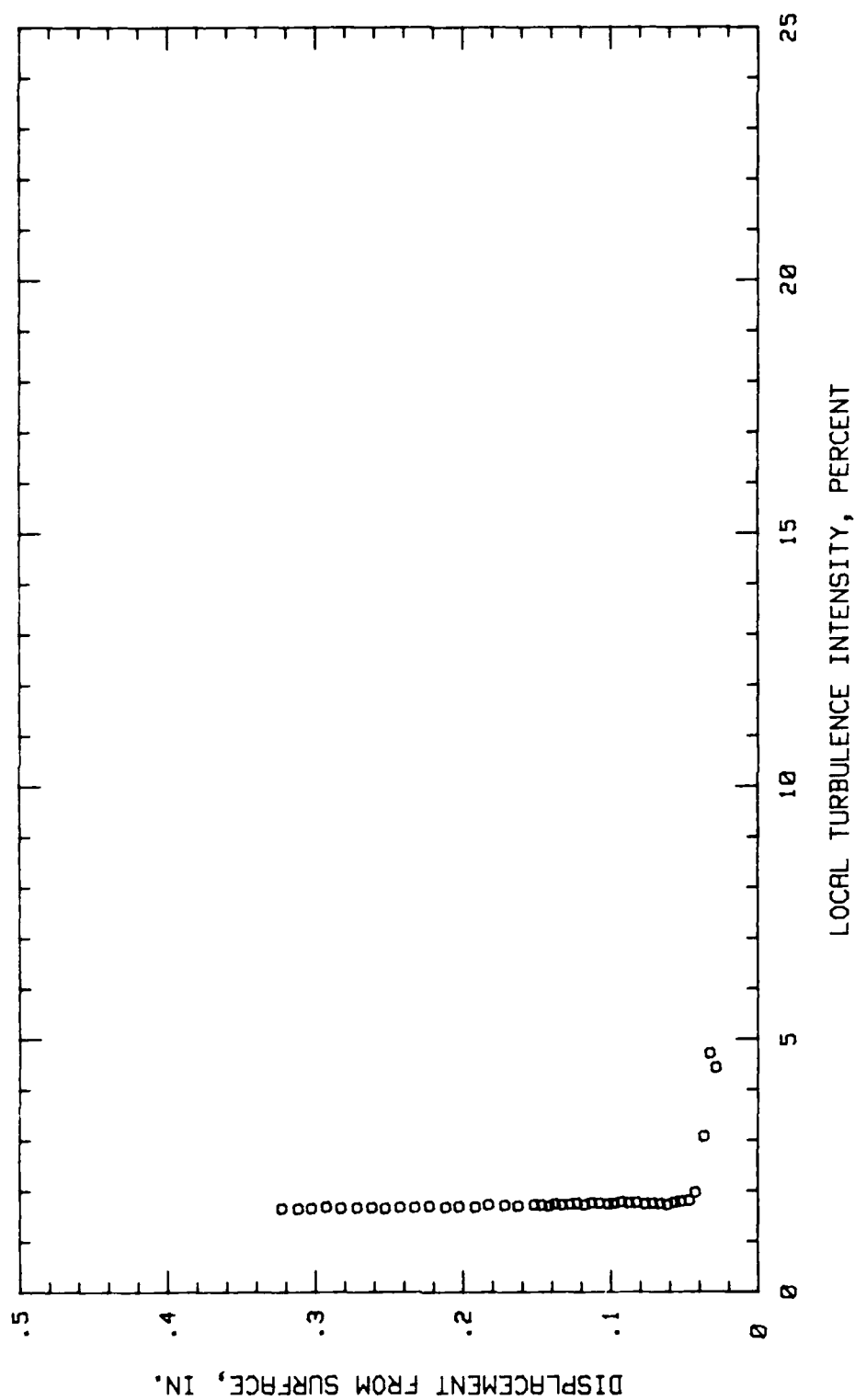


Fig.162.Boundary Layer Turb.Intensity Profile, Conf.#3 at 29.68% Chord LOW TURB.

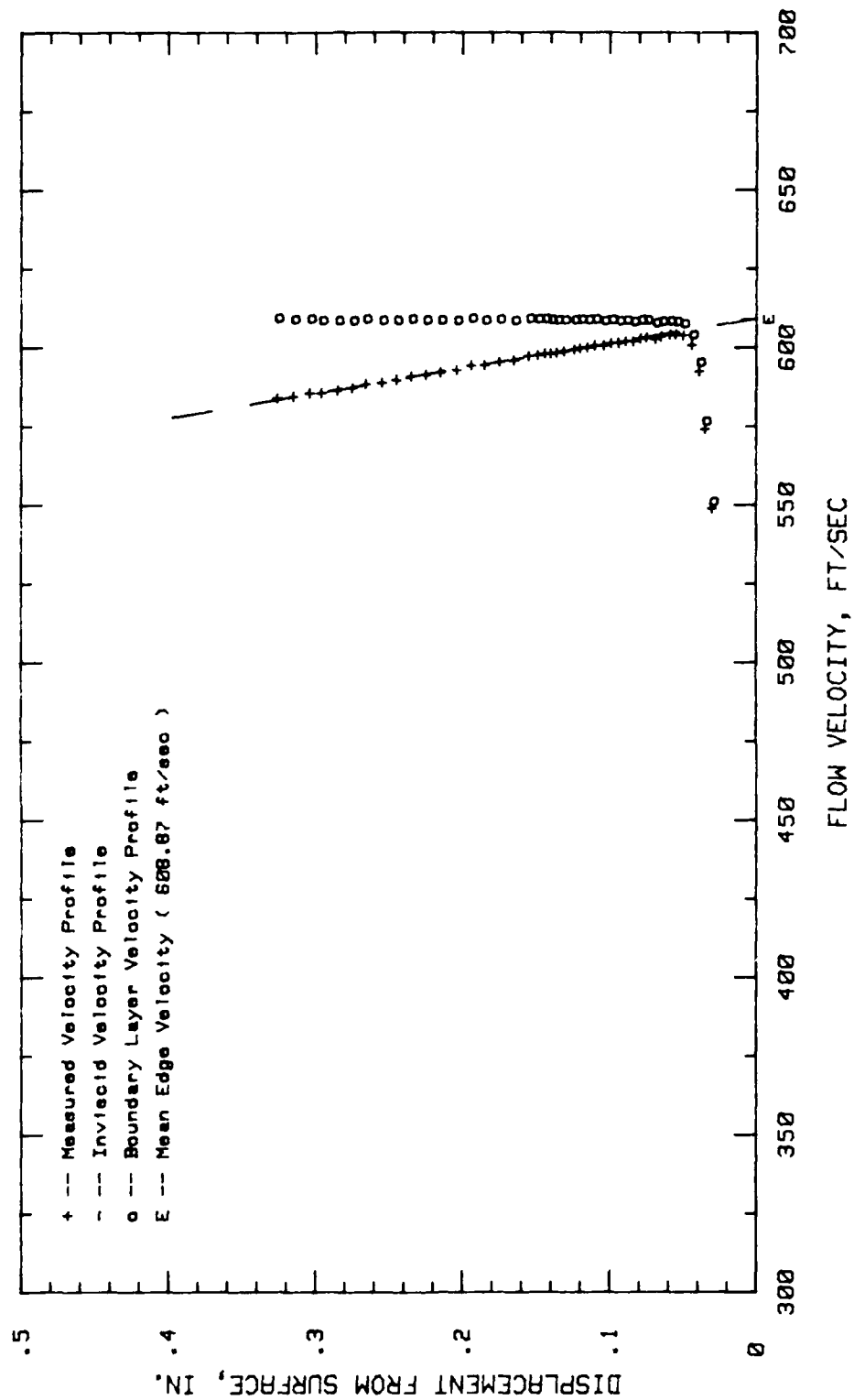


Fig.163. Boundary Layer Velocity Profiles, Conf.#3 at 34.37% Chord LOW TURB.

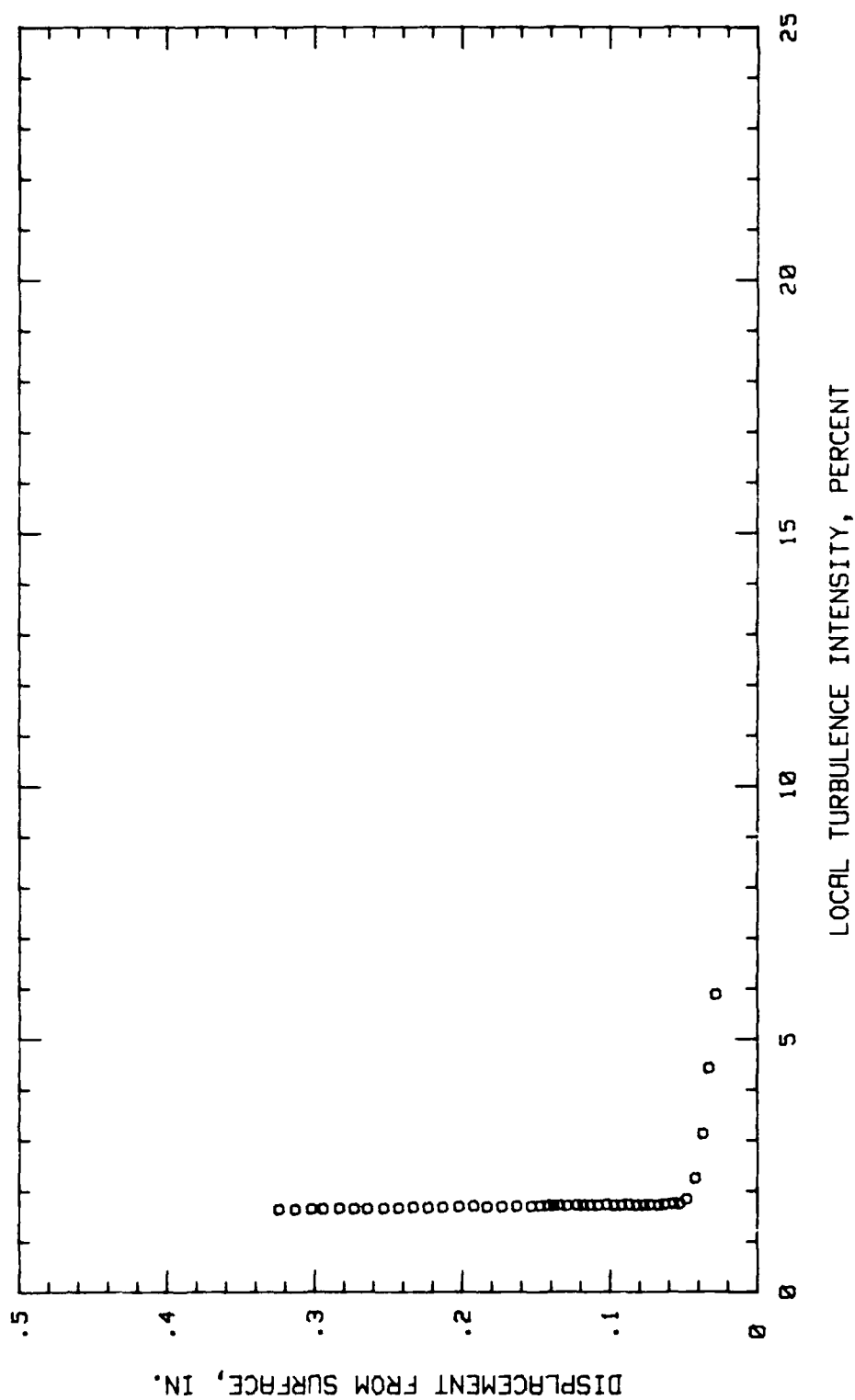


Fig. 164. Boundary Layer Turb. Intensity Profile, Conf. #3 at 34.37% Chord LOW TURB.

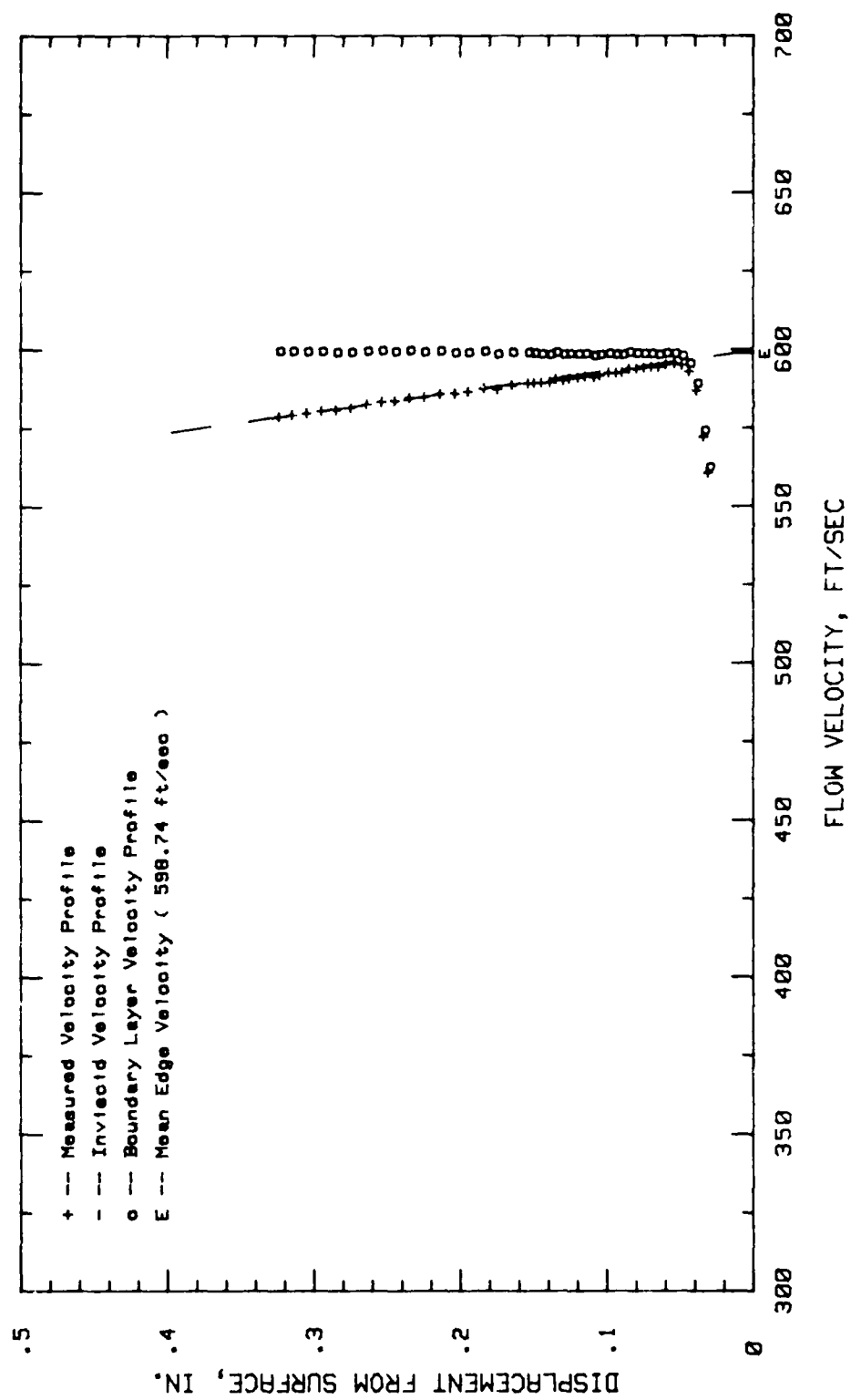


Fig.165. Boundary Layer Velocity Profiles, Conf.#3 at 40.62% Chord LOW TURB.

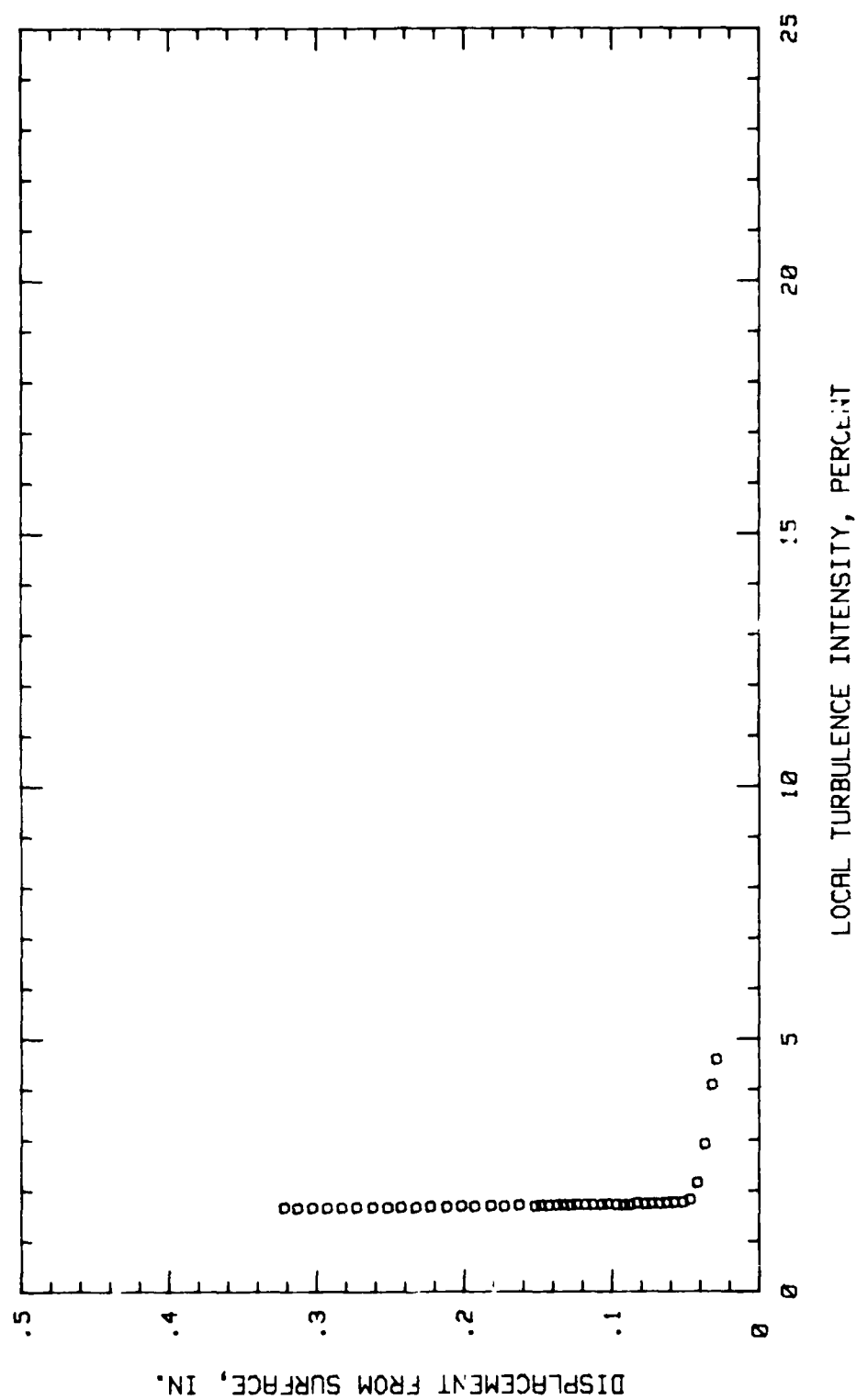


Fig. 166. Boundary Layer Turb. Intensity Profile, Conf. #3 at 40.62% Chord LOW TURB.

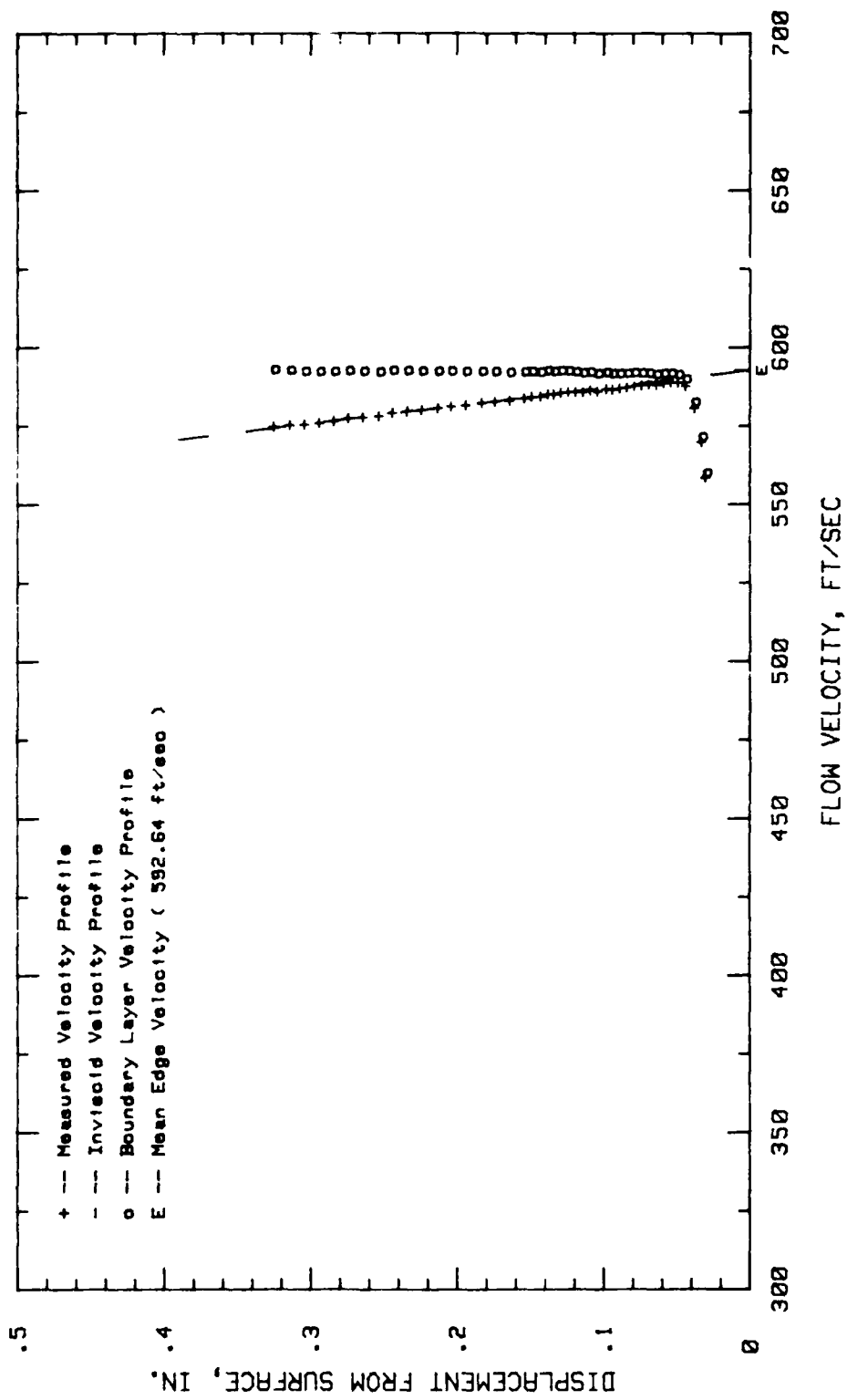


Fig.167. Boundary Layer Velocity Profiles, Conf.#3 at 45.31% Chord LOW TURB.

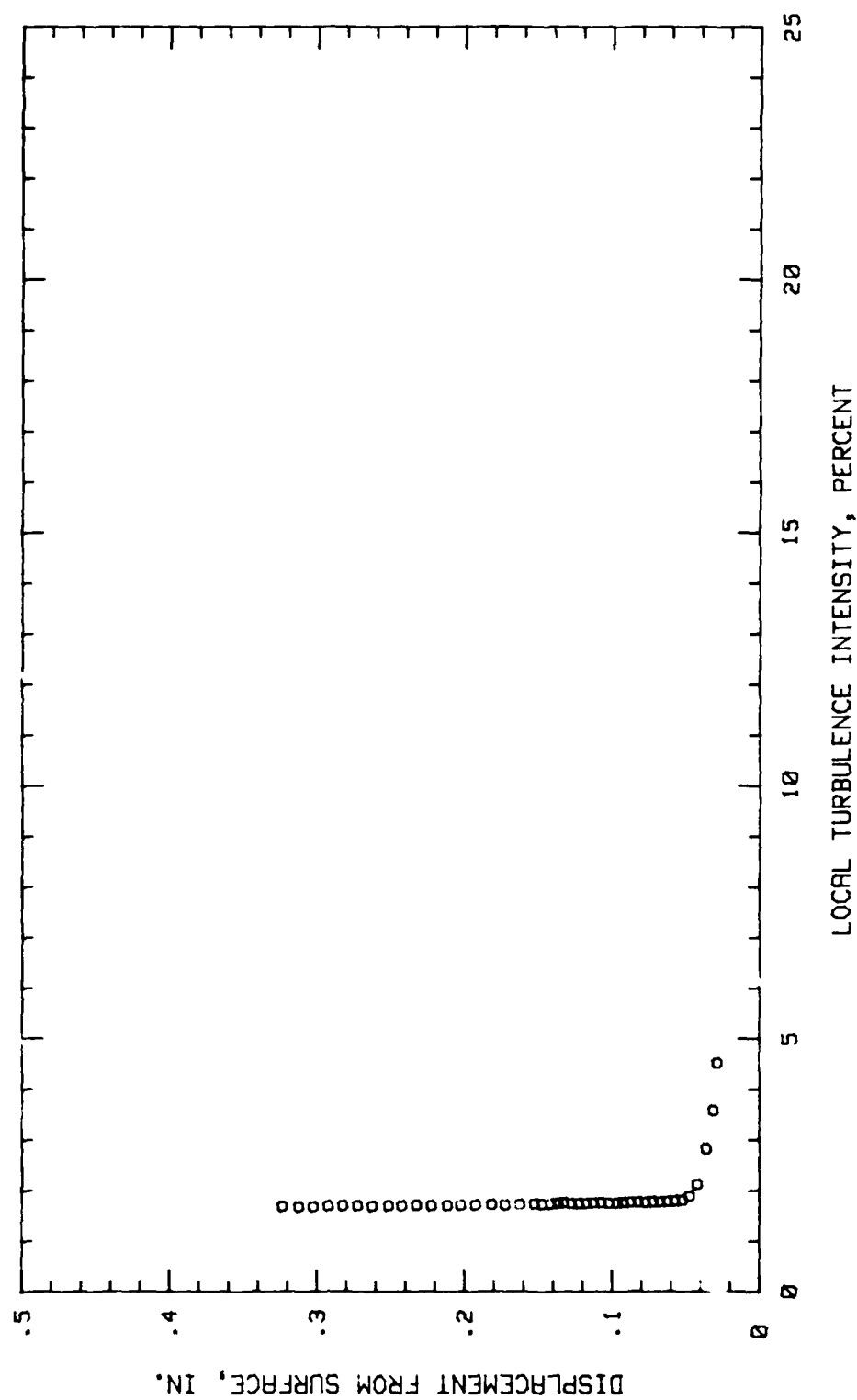


Fig. 168. Boundary Layer Turb. Intensity Profile, Conf. #3 at 45.31% Chord LOW TURB.

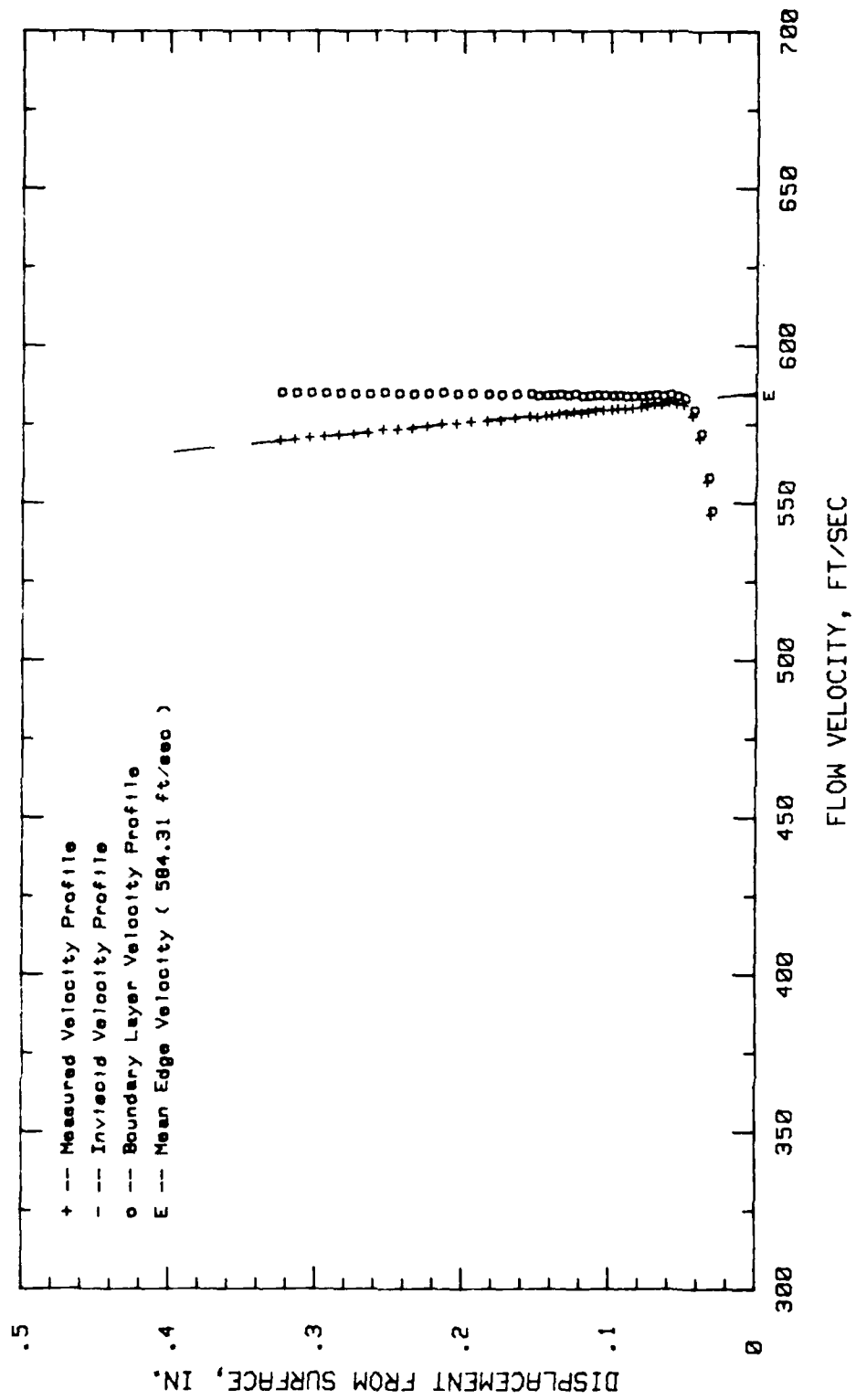


Fig.169.Boundary Layer Velocity Profiles, Conf.#3 at 50% Chord LOW TURB.

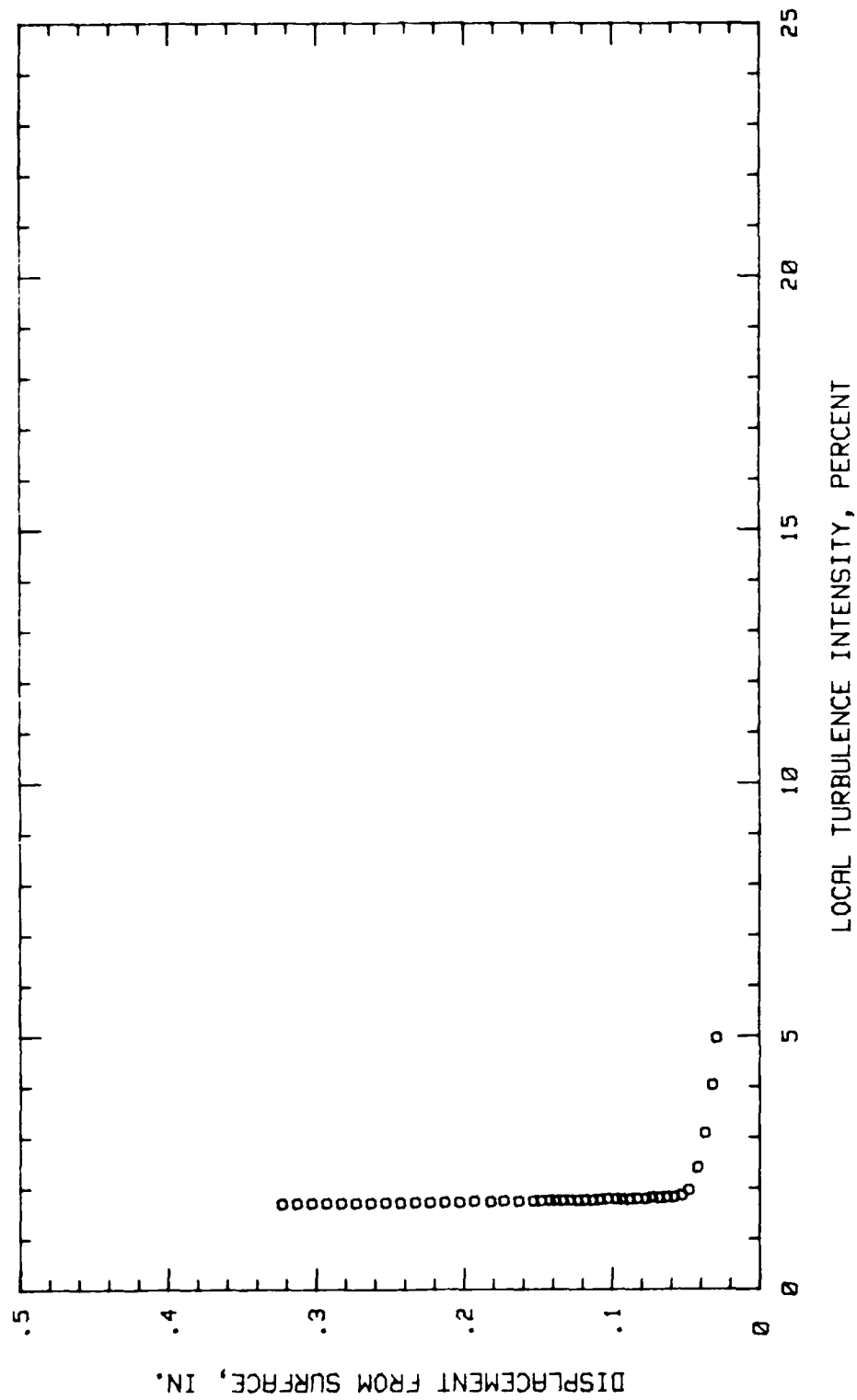


Fig.170. Boundary Layer Turb. Intensity Profile, Conf. #3 at 50% Chord LOW TURB.

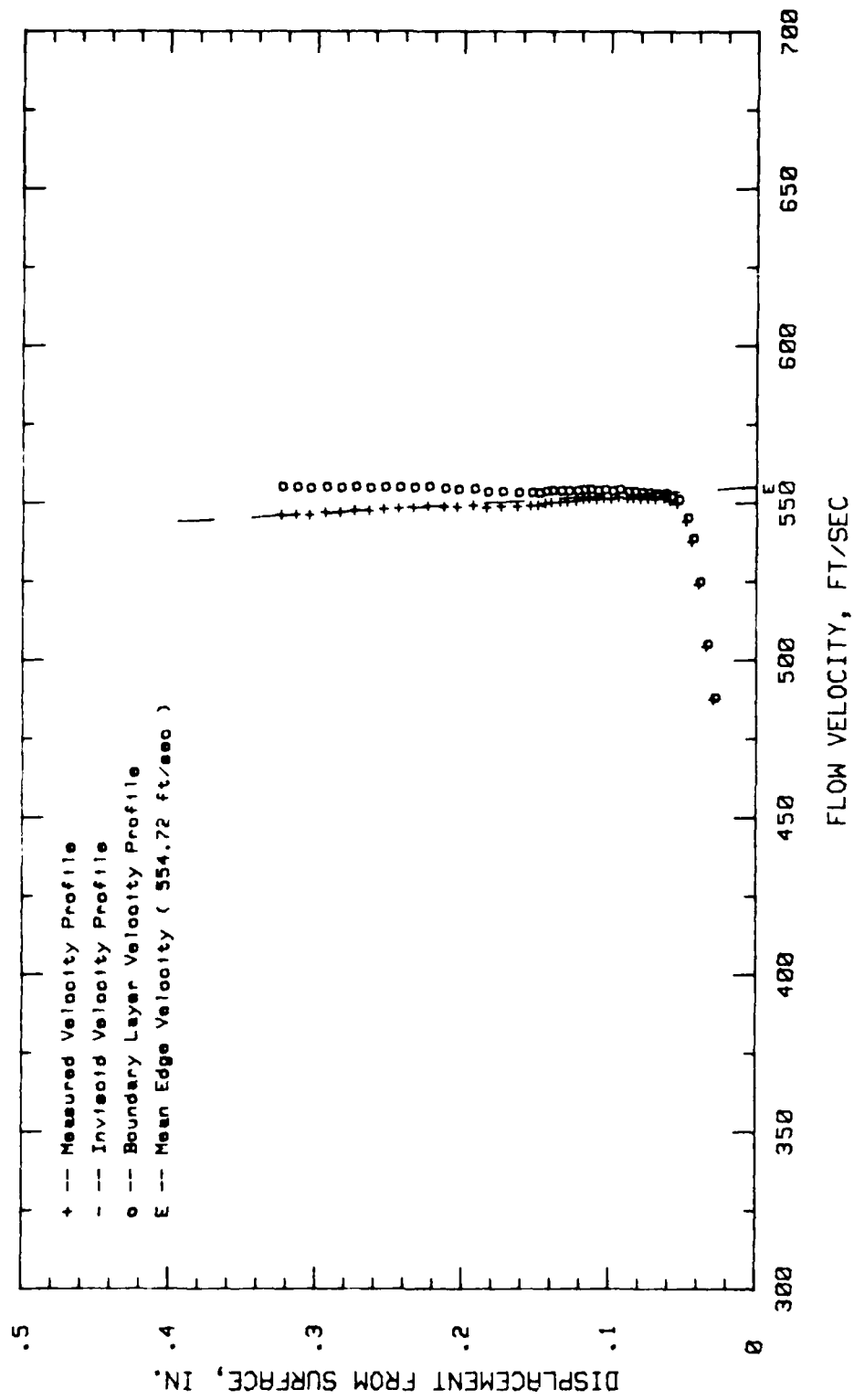


Fig.171. Boundary Layer Velocity Profiles, Conf.#3 at 65.62% Chord LOW TURB.

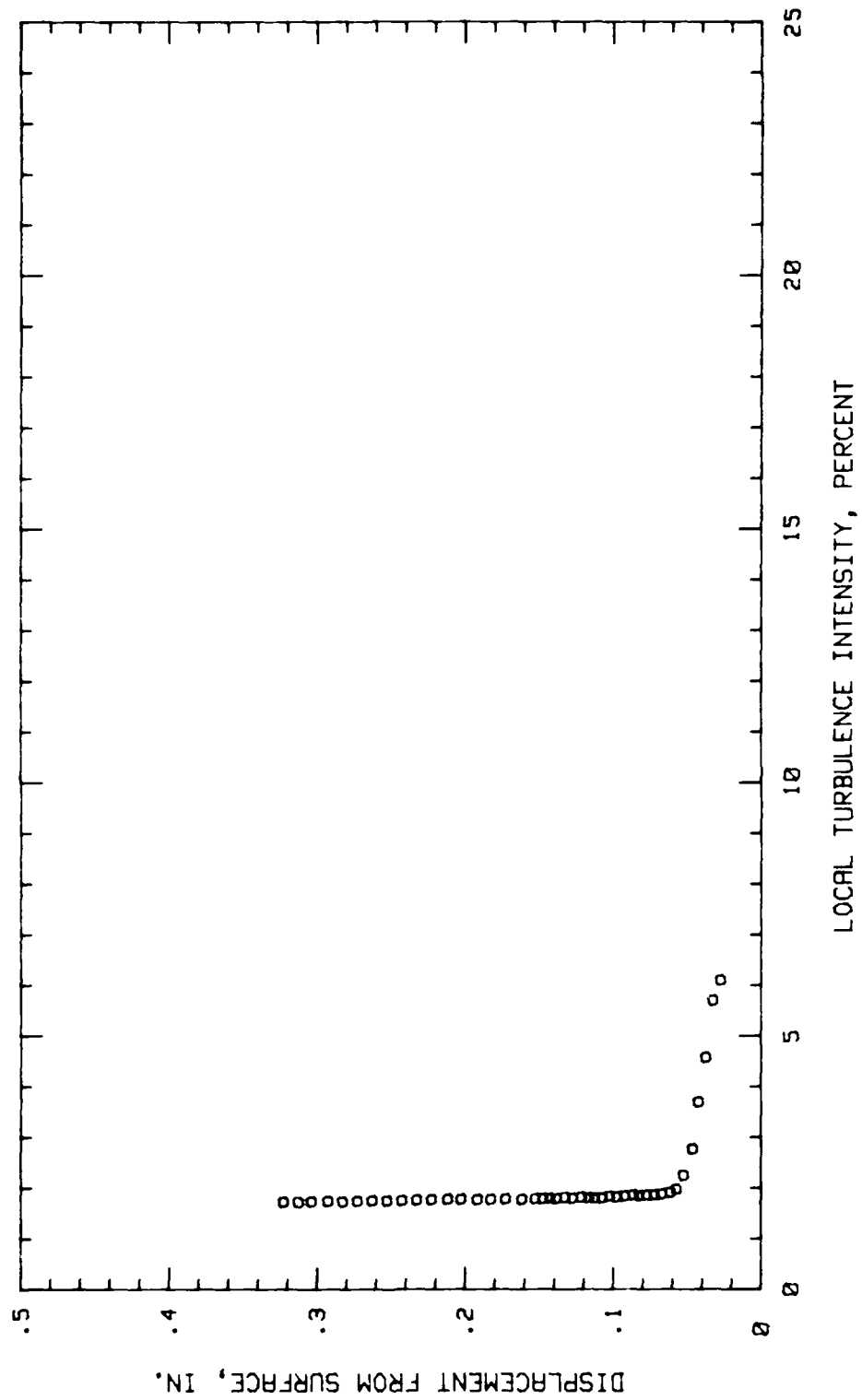


Fig.172.Boundary Layer Turb.Intensity Profile, Conf.#3 at 65.62% Chord LOW TURB.

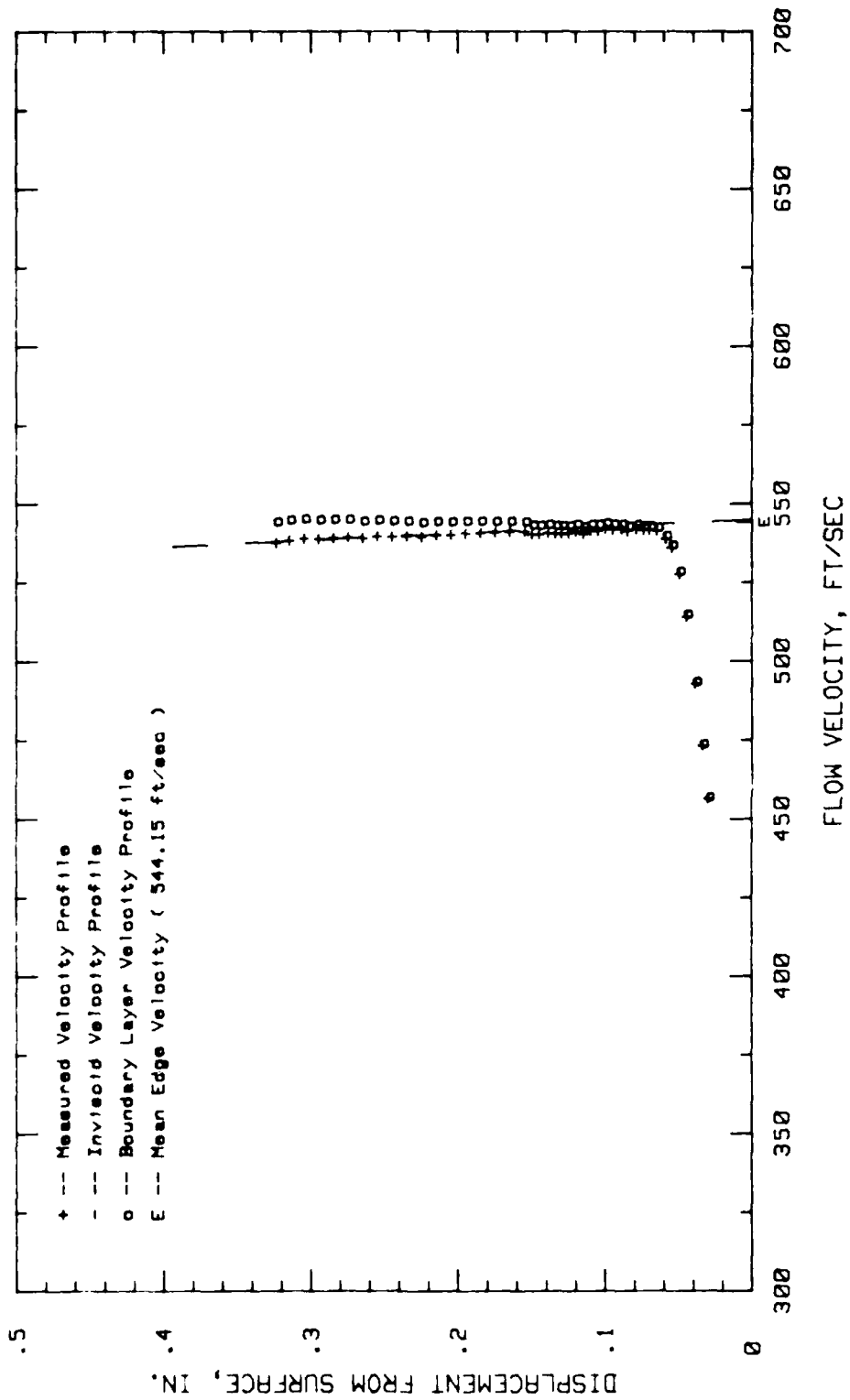


Fig.173.Boundary Layer Velocity Profiles, Conf.#3 at 70.31% Chord LOW TURB.

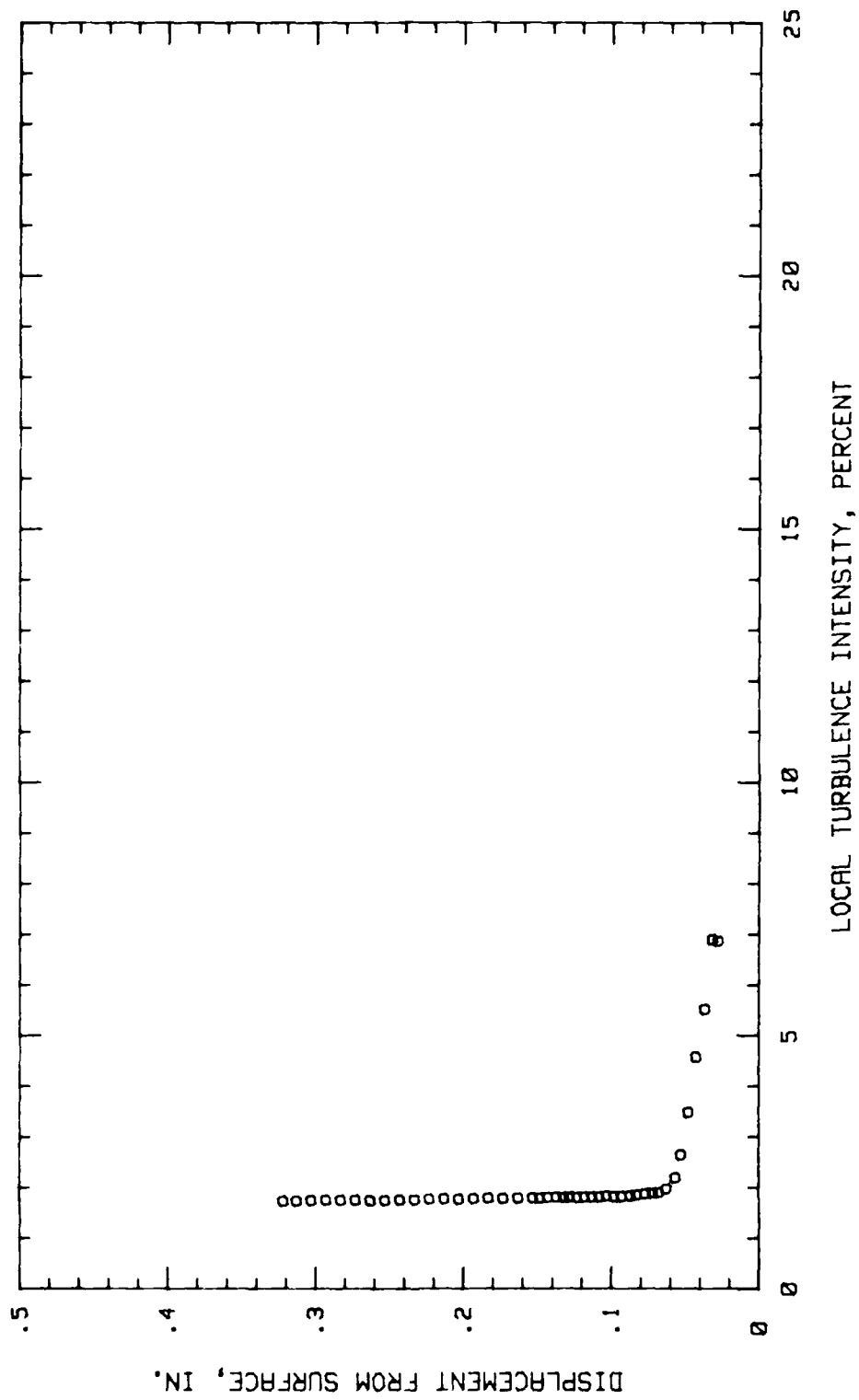


Fig.174.Boundary Layer Turb.Intensity Profile, Conf.#3 at 70.31% Chord LOW TURB.

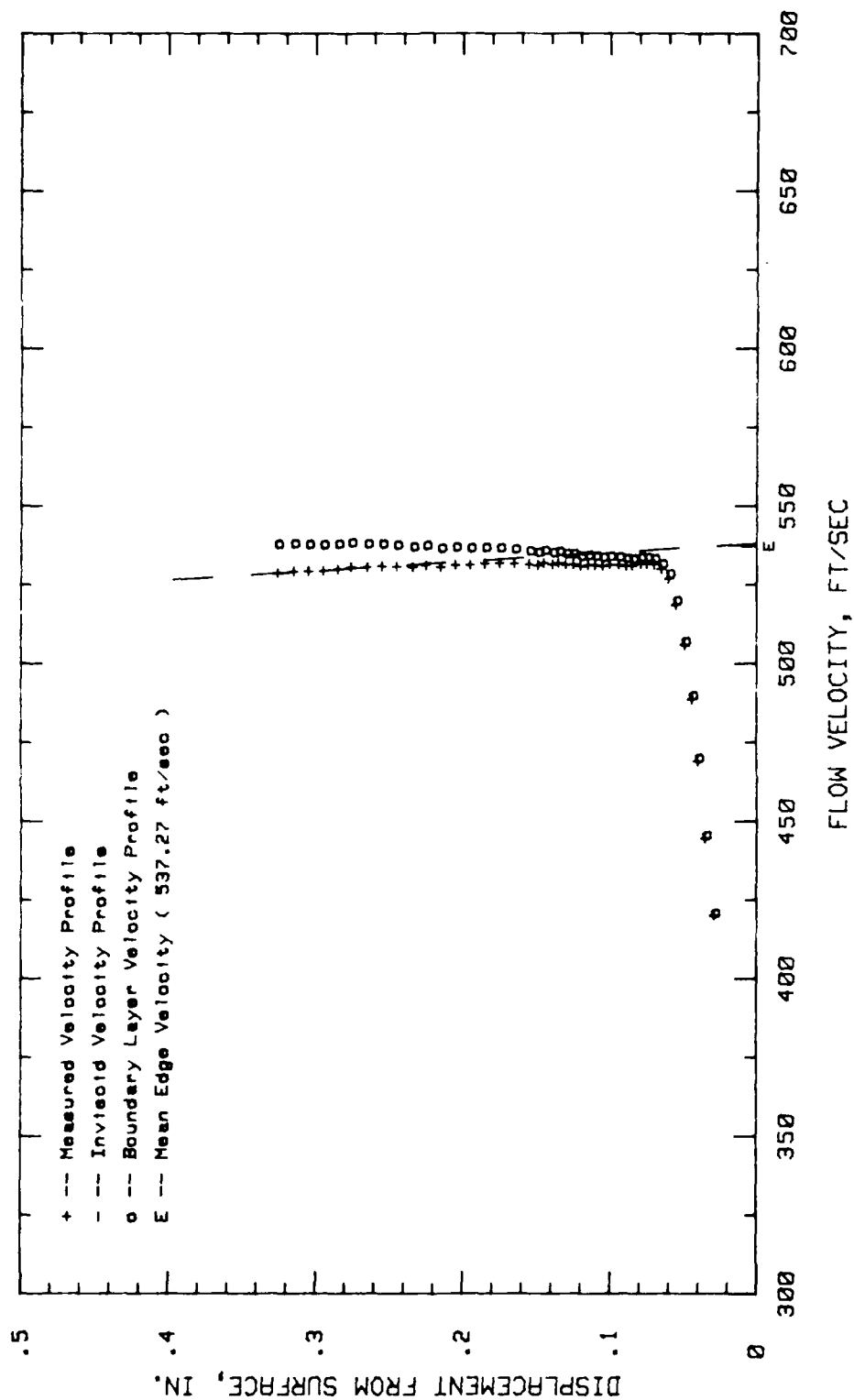


Fig.175. Boundary Layer Velocity Profiles, Conf.#3 at 75% Chord LOW TURB.

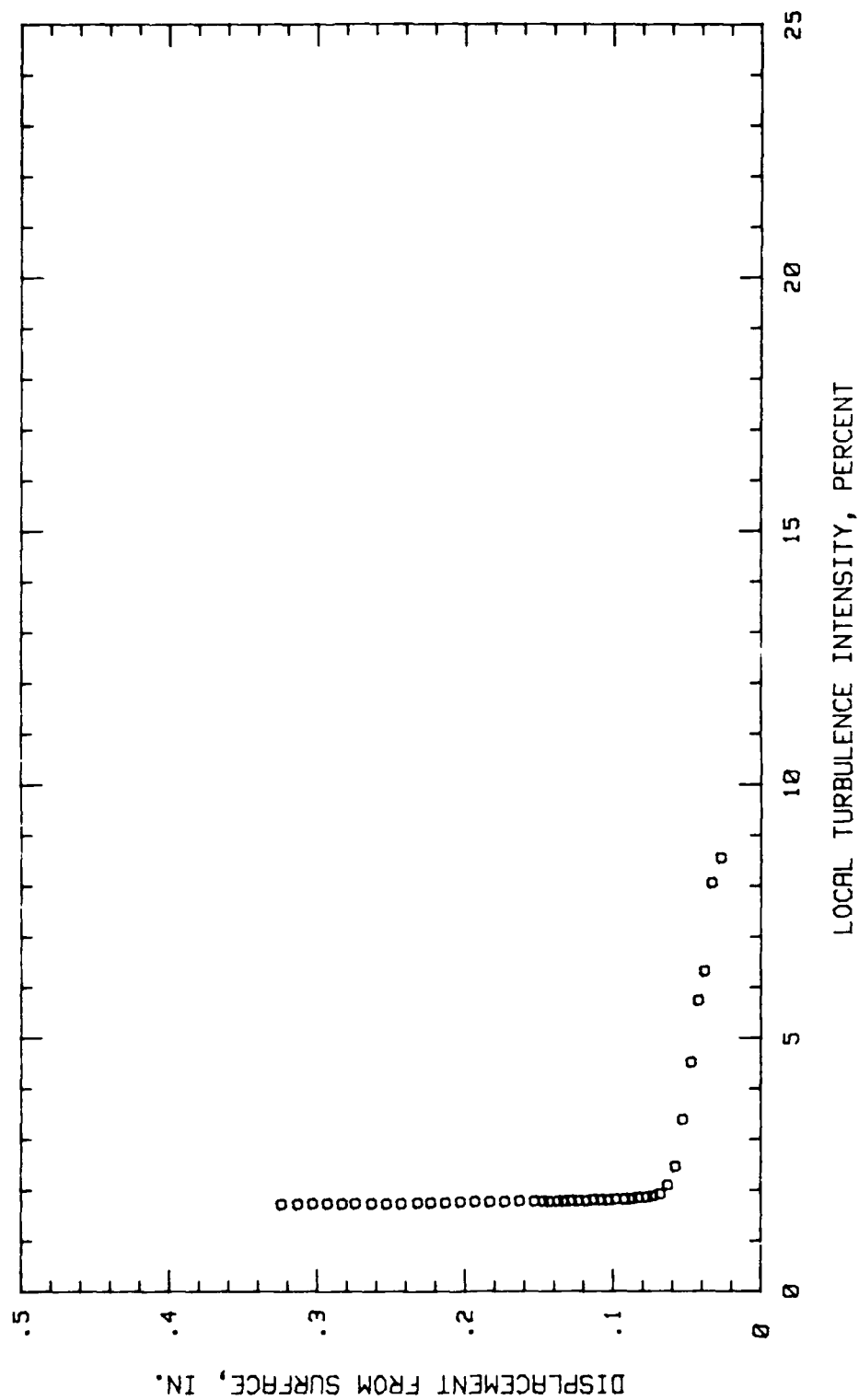


Fig.176. Boundary Layer Turb. Intensity Profile, Conf.#3 at 75% Chord LOW TURB.

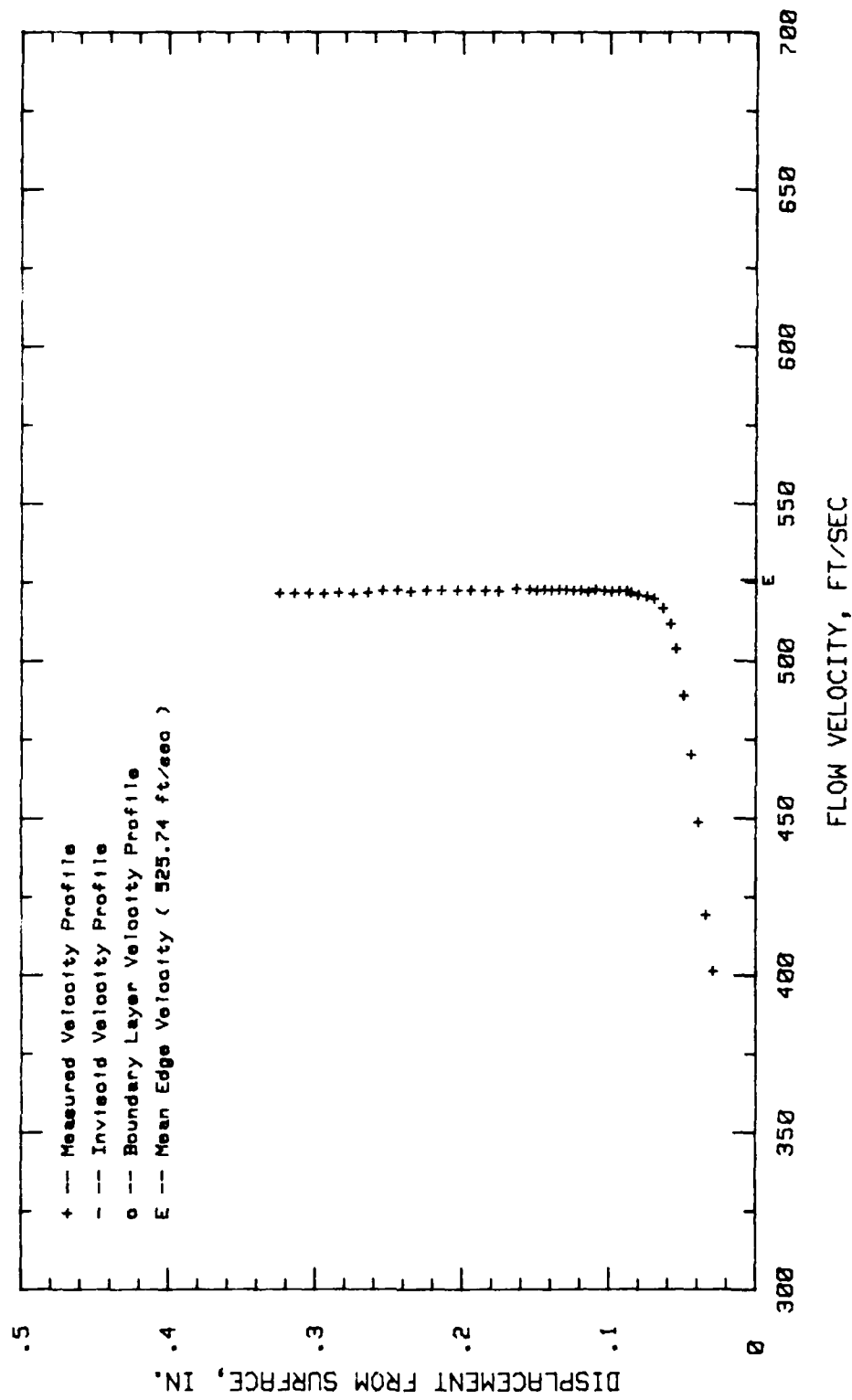


Fig.177. Boundary Layer Velocity Profiles, Conf.#3 at 79.68% Chord LOW TURB.

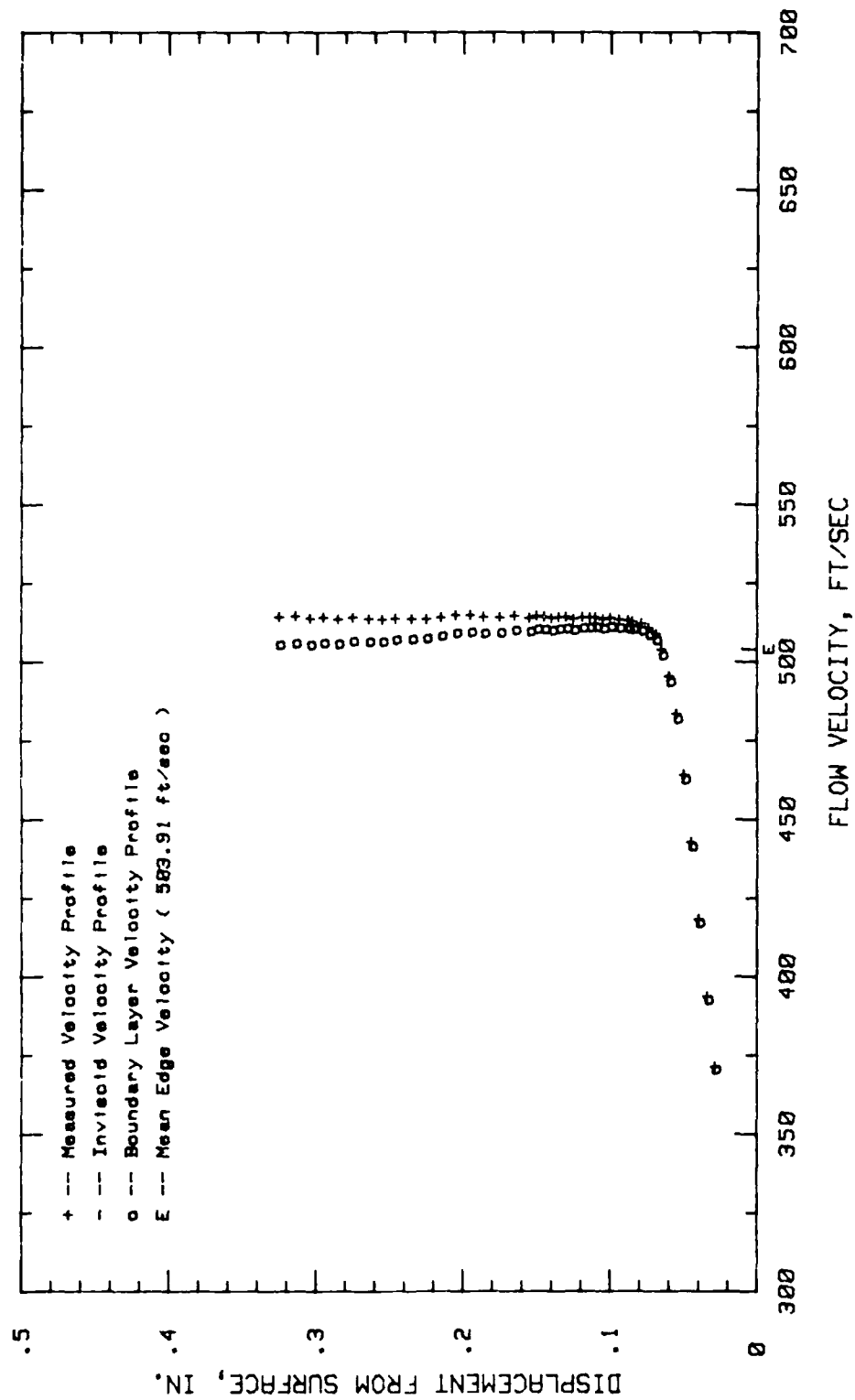


Fig.179. Boundary Layer Velocity Profiles, Conf.#3 at 84.37% Chord LOW TURB.

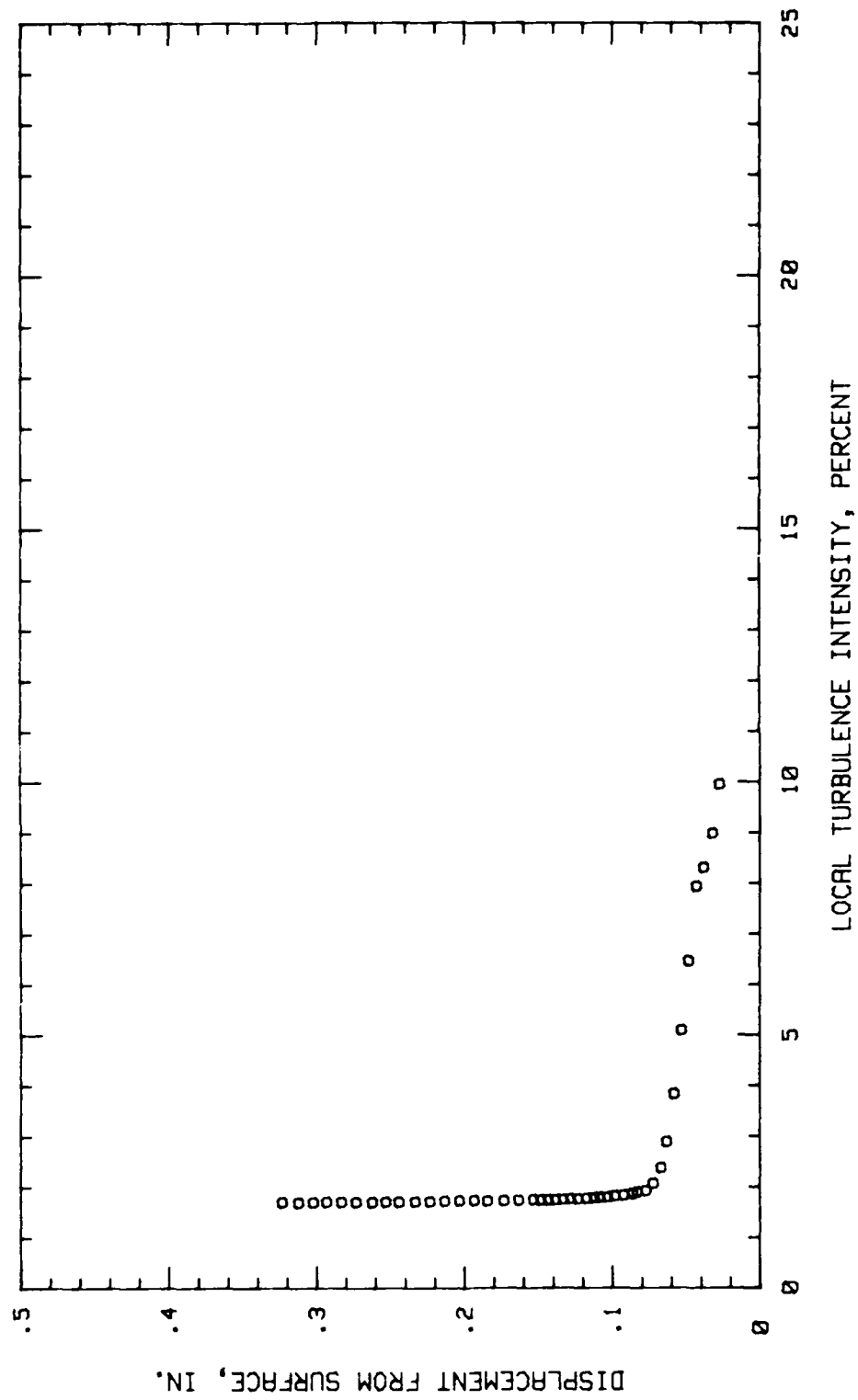


Fig.180.Boundary Layer Turb.Intensity Profile, Conf.#3 at 84.37% Chord LOW TURB.

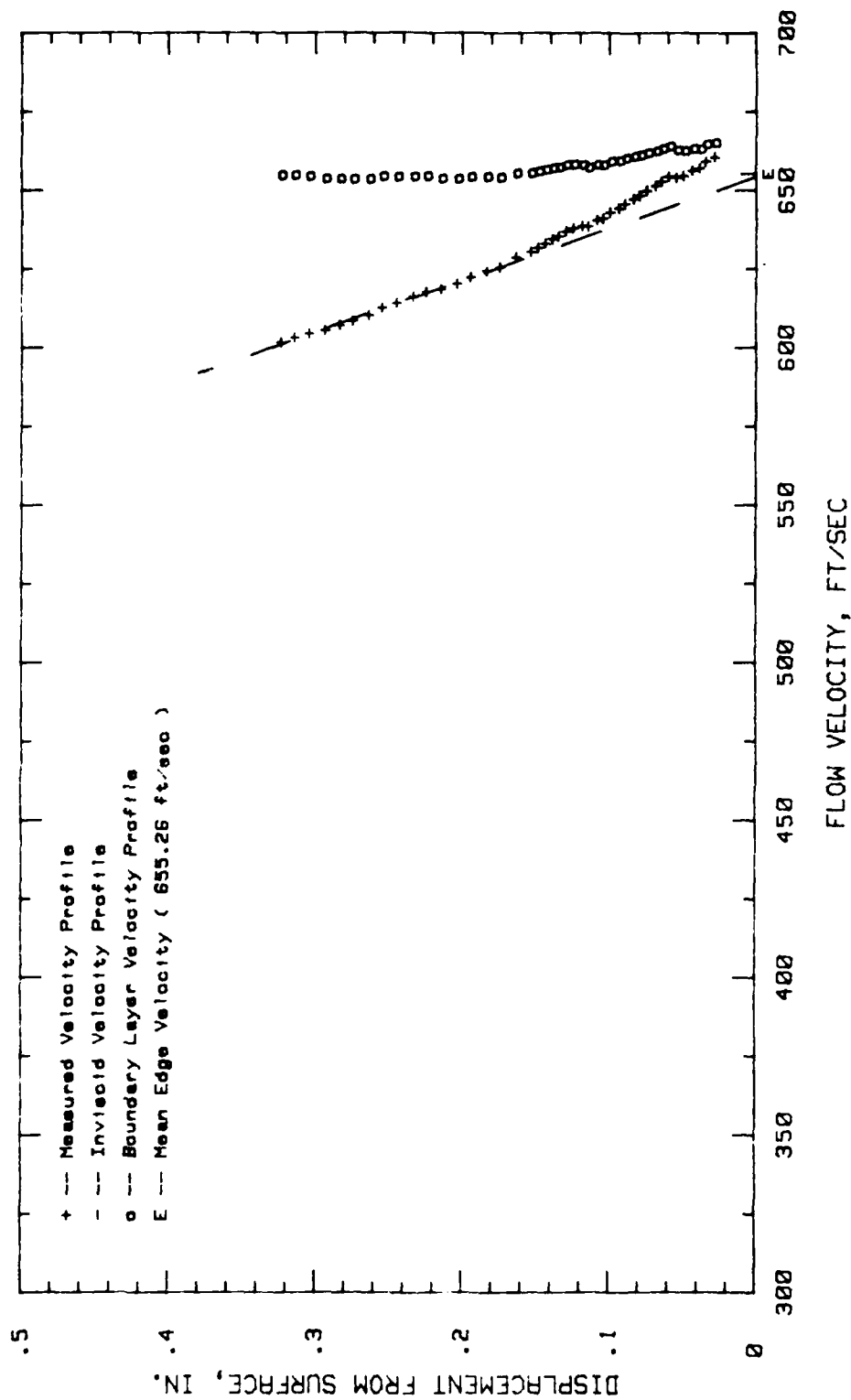


Fig.181. Boundary Layer Velocity Profiles, Conf.#3 at 4.68% Chord HIGH TURB.

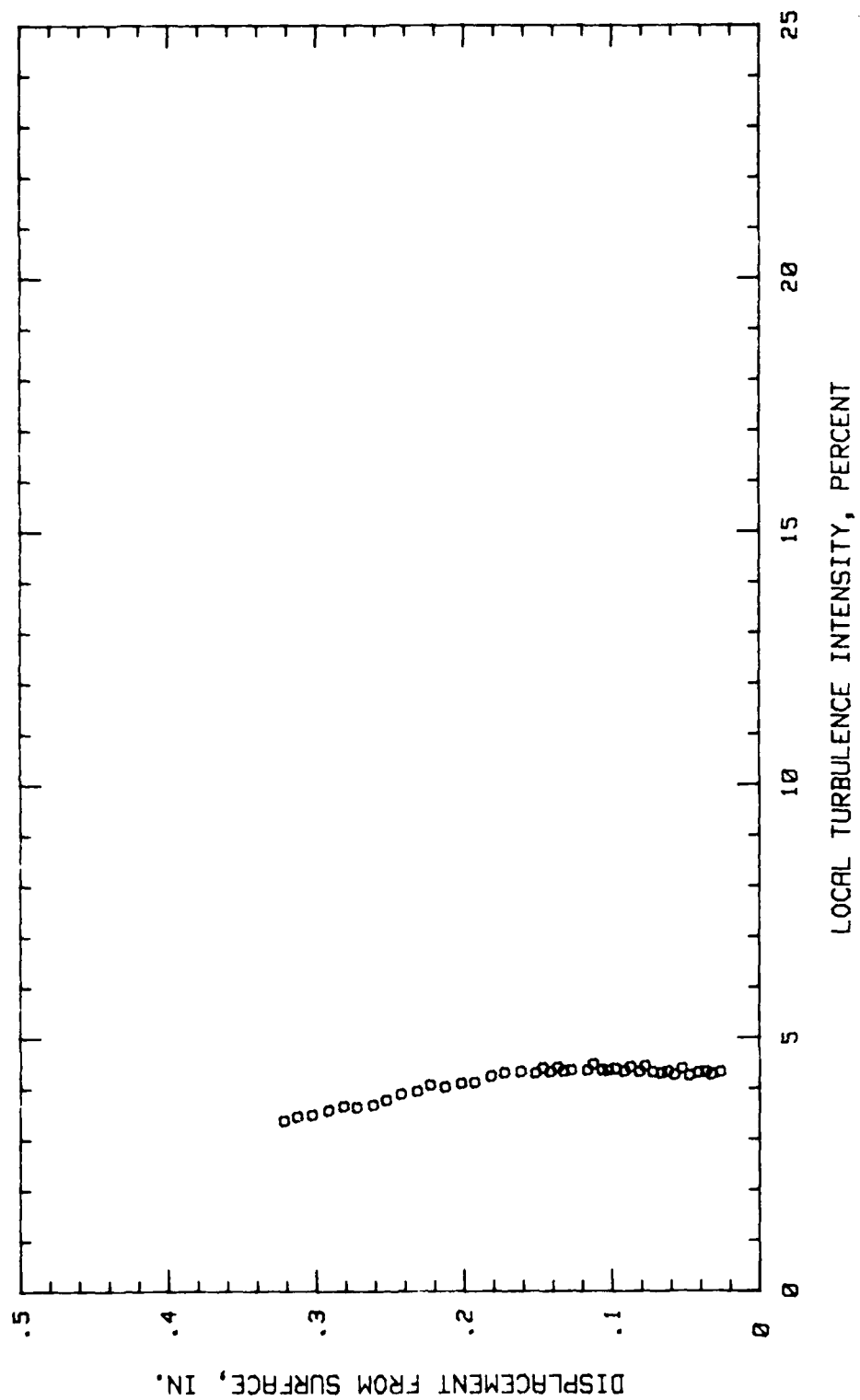


Fig.182. Boundary Layer Turb. Intensity Profile, Conf. #3 at 4.68% Chord HIGH TURB.

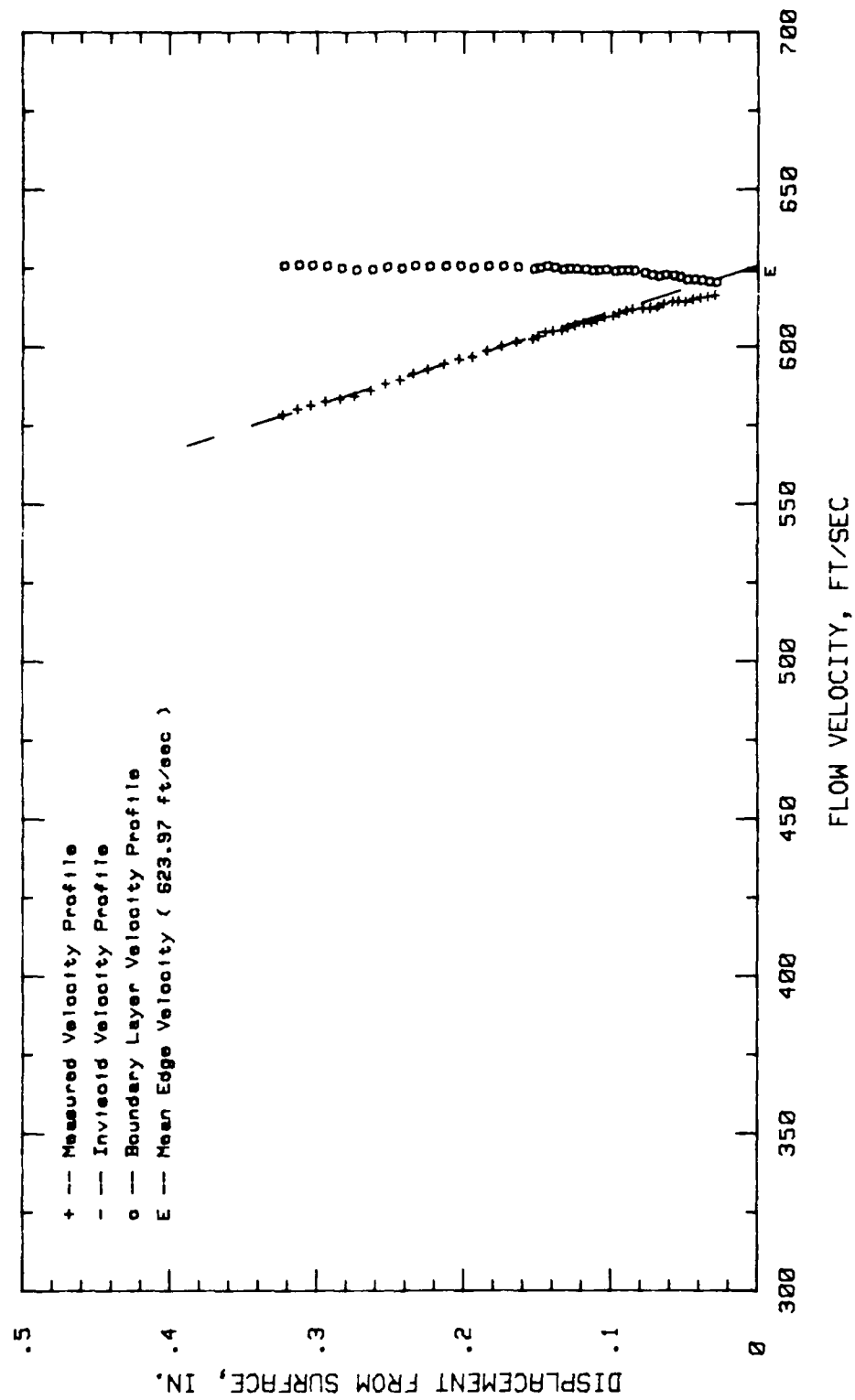


Fig.183. Boundary Layer Velocity Profiles, Conf.#3 at 9.37% Chord HIGH TURB.

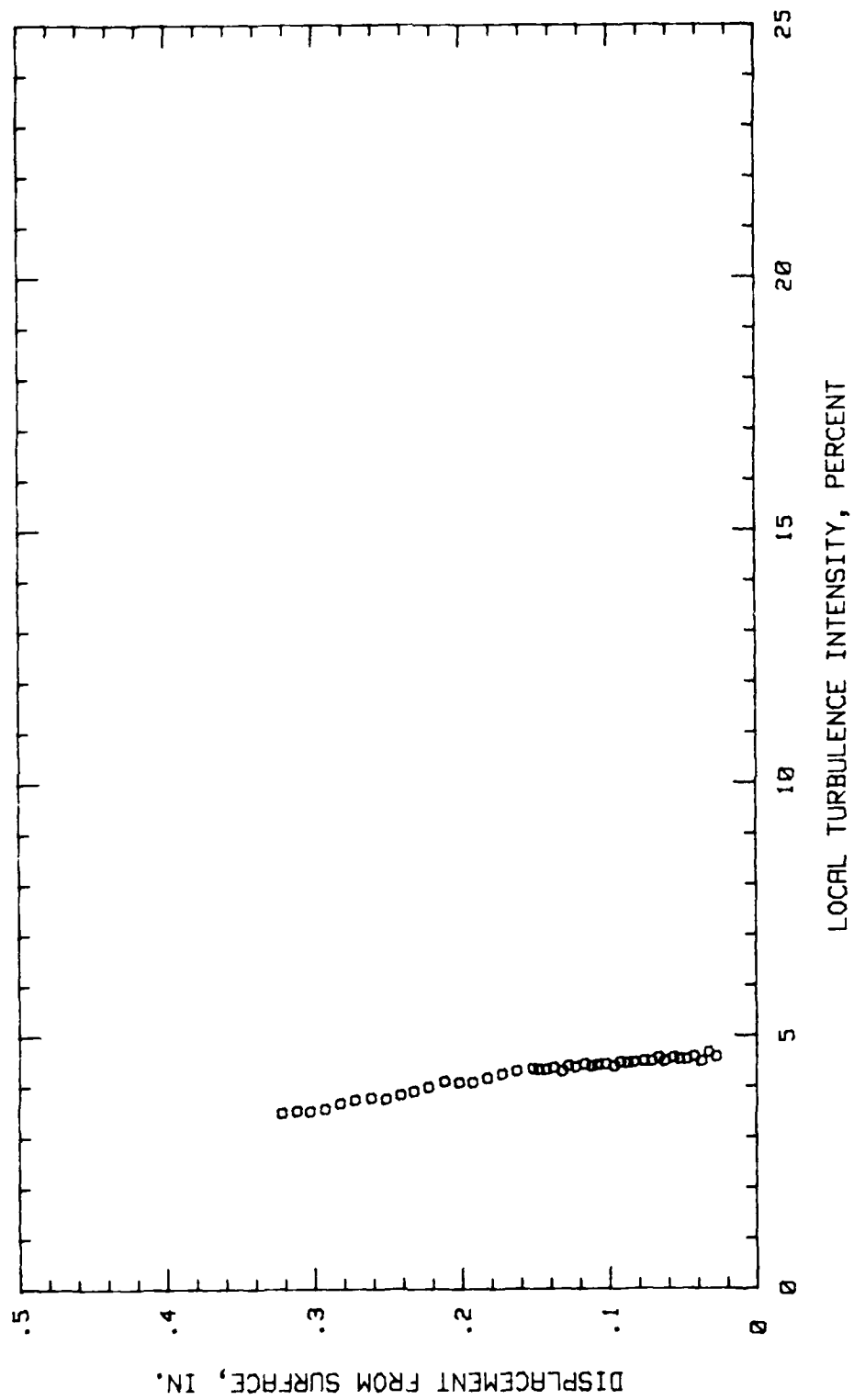


Fig. 184. Boundary Layer Turb. Intensity Profile, Conf. #3 at 9.37% Chord HIGH TURB.

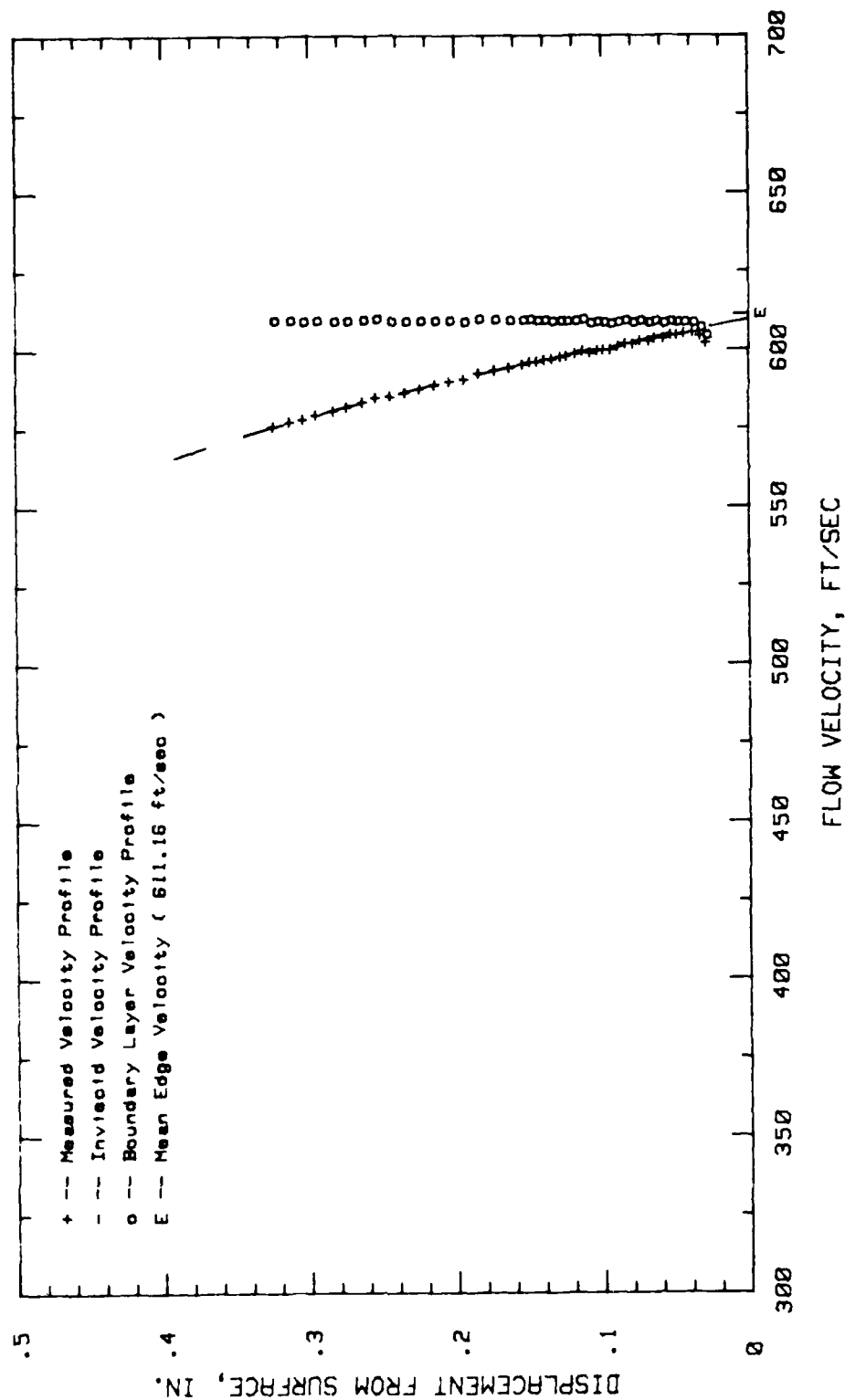


Fig.185.Boundary Layer Velocity Profiles, Conf.#3 at 25% Chord HIGH TURB.

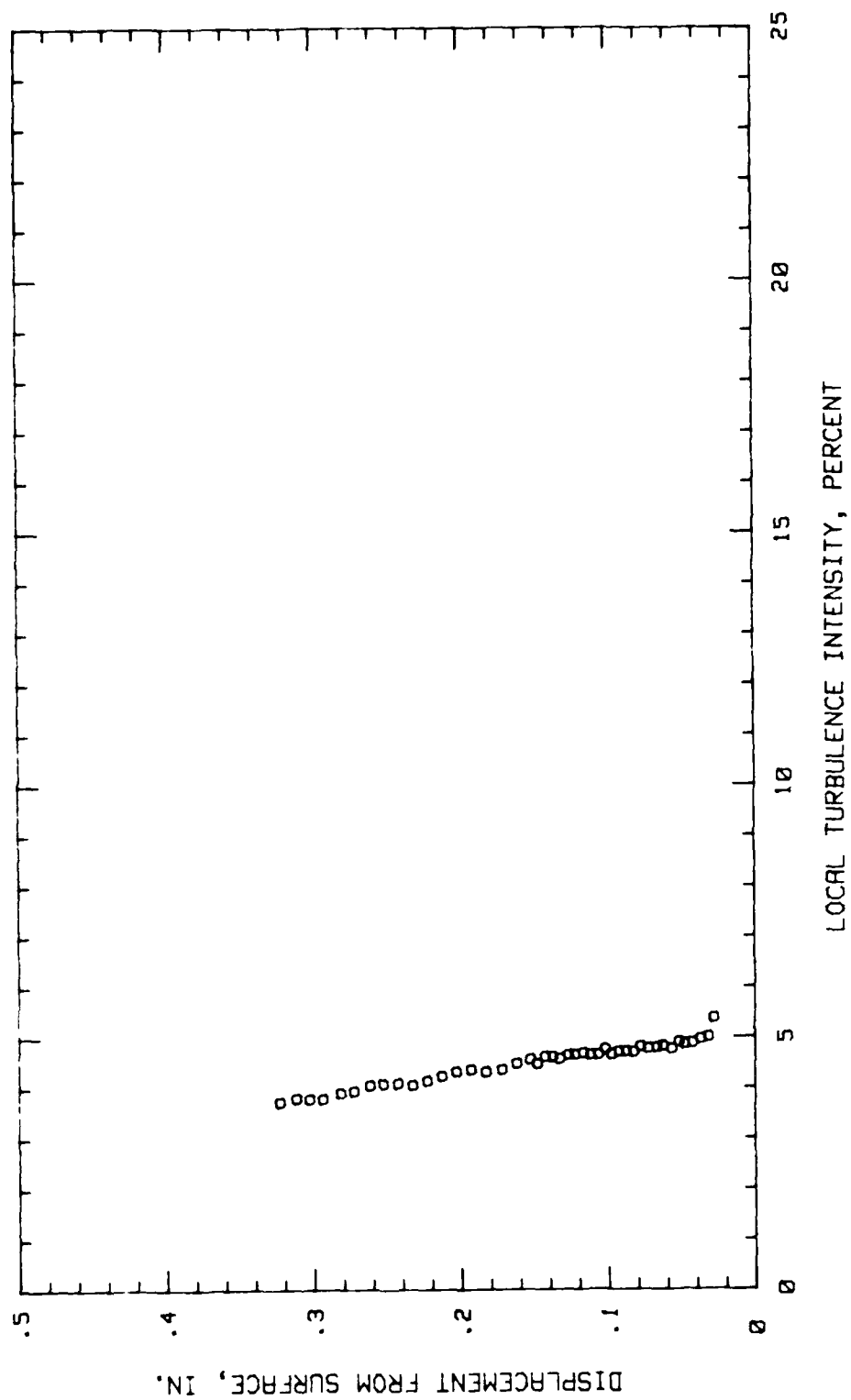


Fig.186.Boundary Layer Turb.Intensity Profile, Conf.#3 at 25% Chord HIGH TURB.

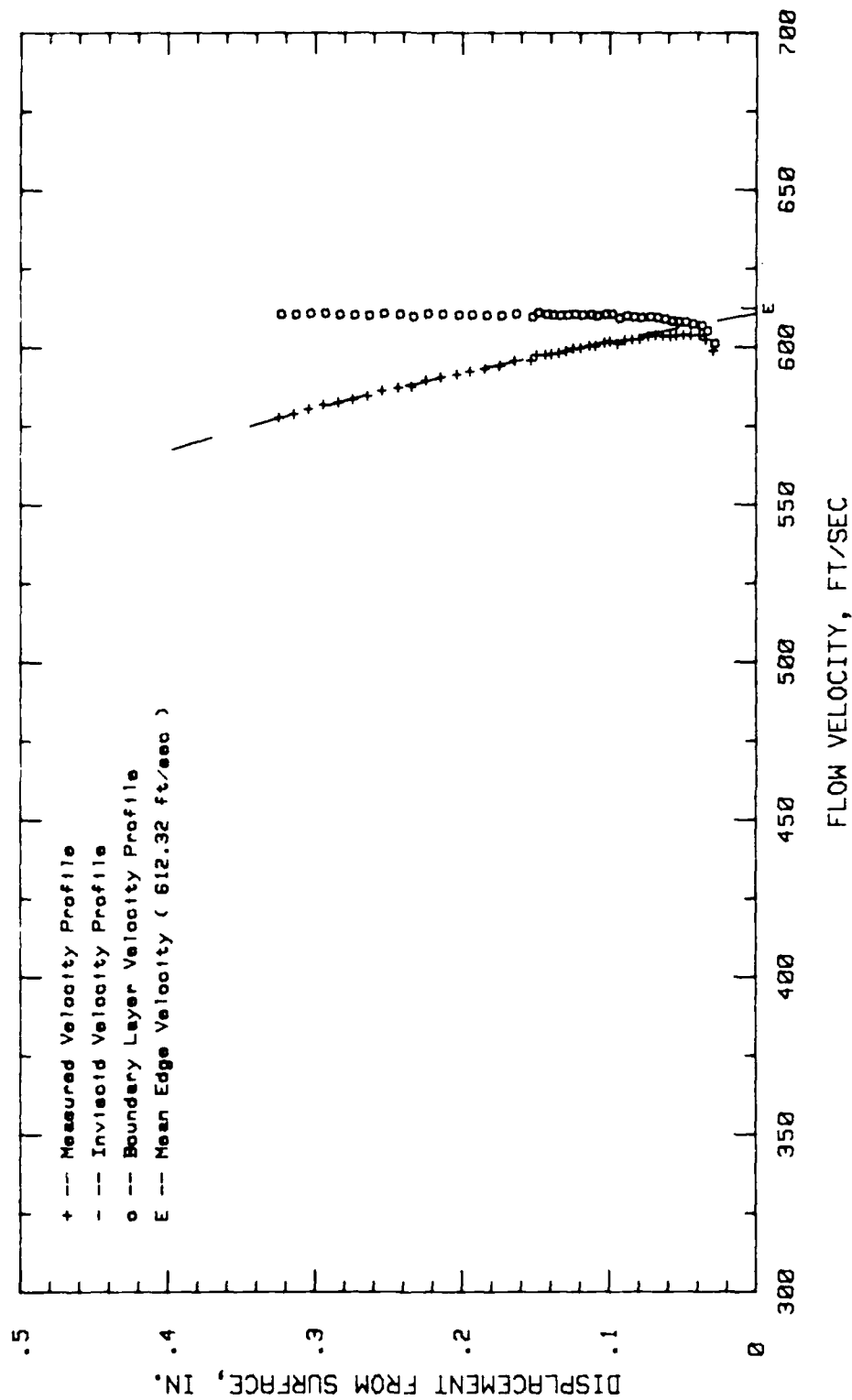


Fig.187. Boundary Layer Velocity Profiles, Conf.#3 at 29.68% Chord HIGH TURB.

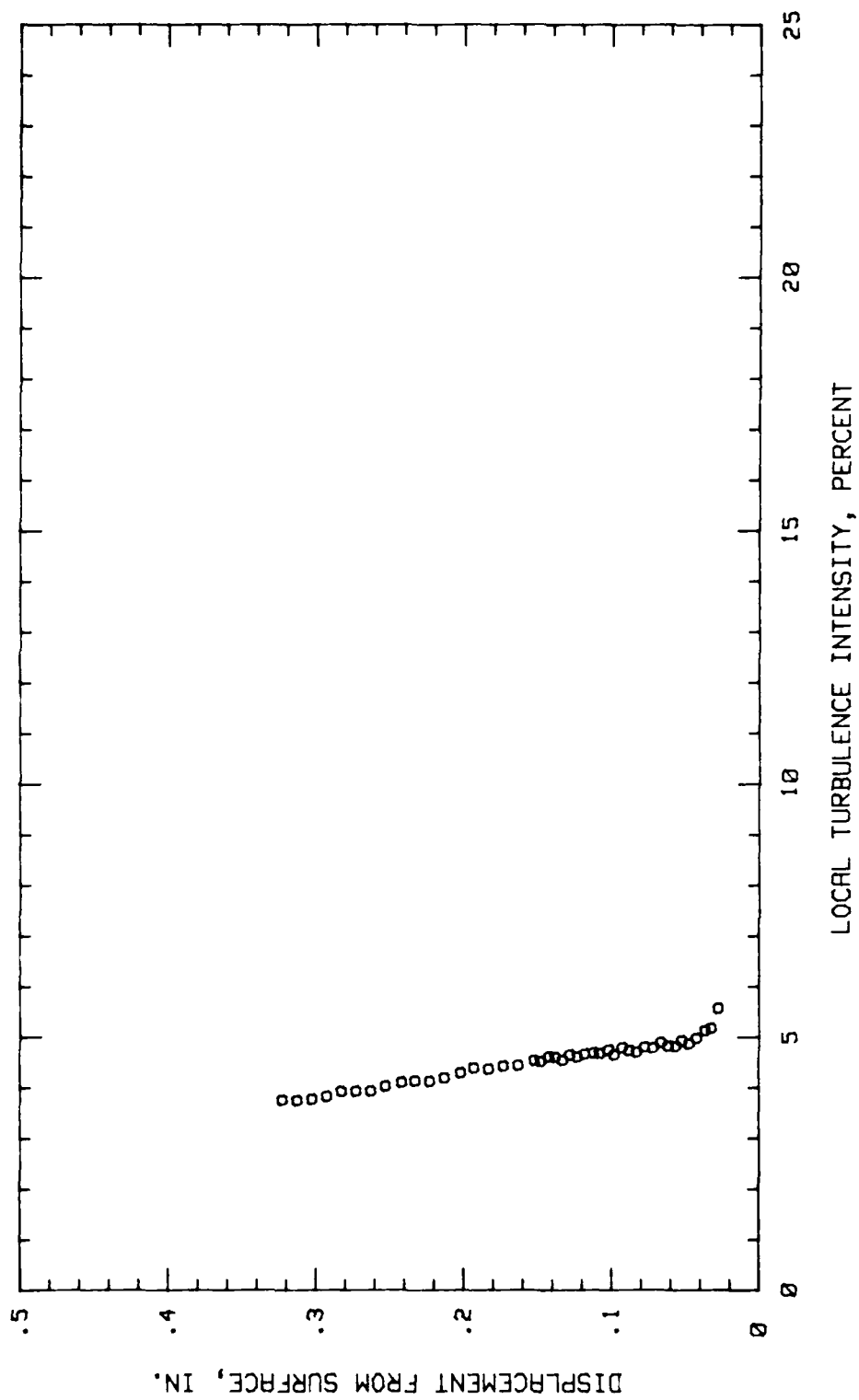


Fig. 188. Boundary Layer Turb. Intensity Profile, Conf. #3 at 29.68% Chord HIGH TURB

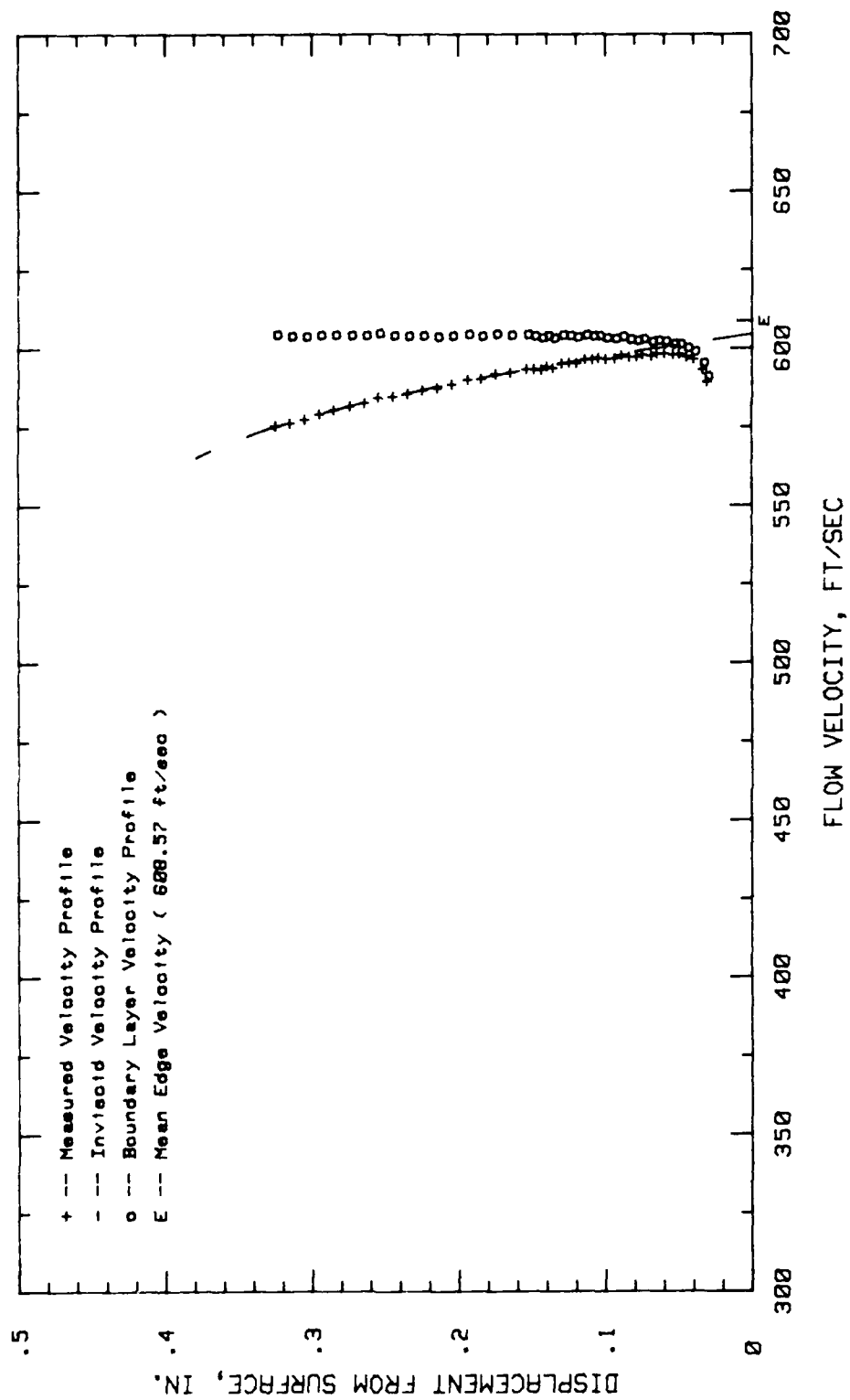


Fig.189. Boundary Layer Velocity Profiles, Conf.#3 at 34.37% Chord HIGH TURB.

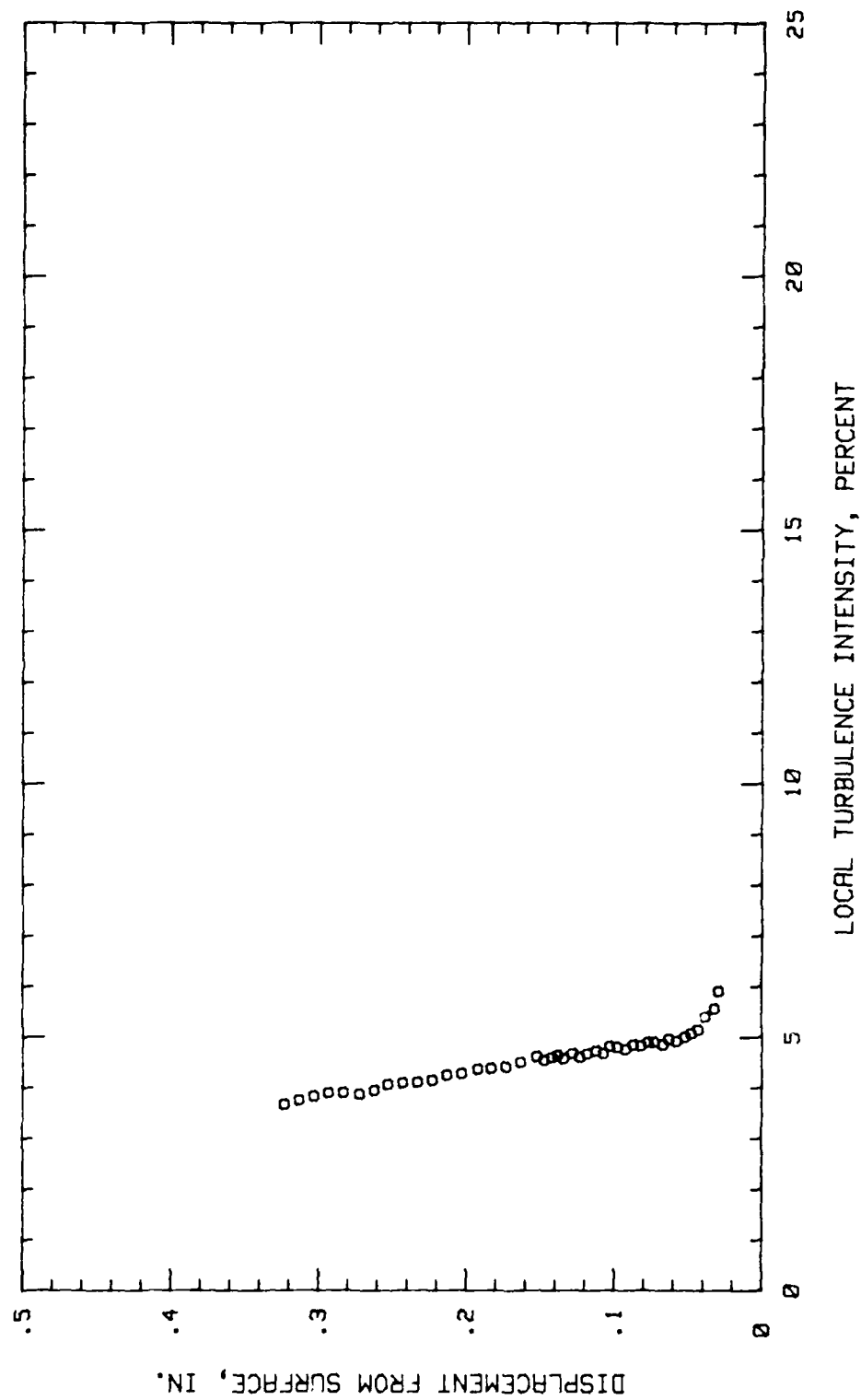


Fig. 190. Boundary Layer Turb. Intensity Profile, Conf. #3 at 34.37% Chord HIGH TURB

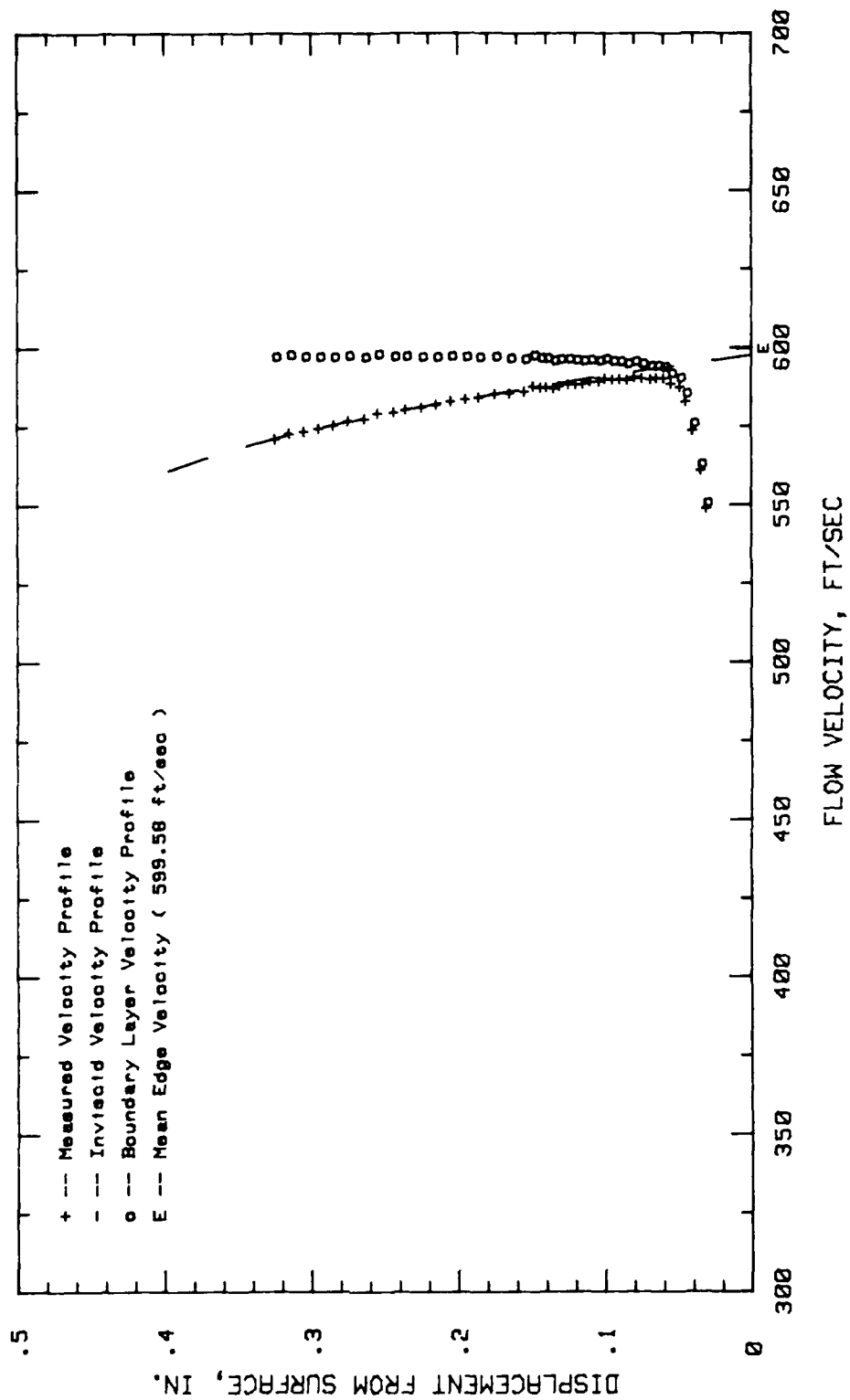


Fig.191. Boundary Layer Velocity Profiles, Conf.#3 at 40.62% Chord HIGH TURB.

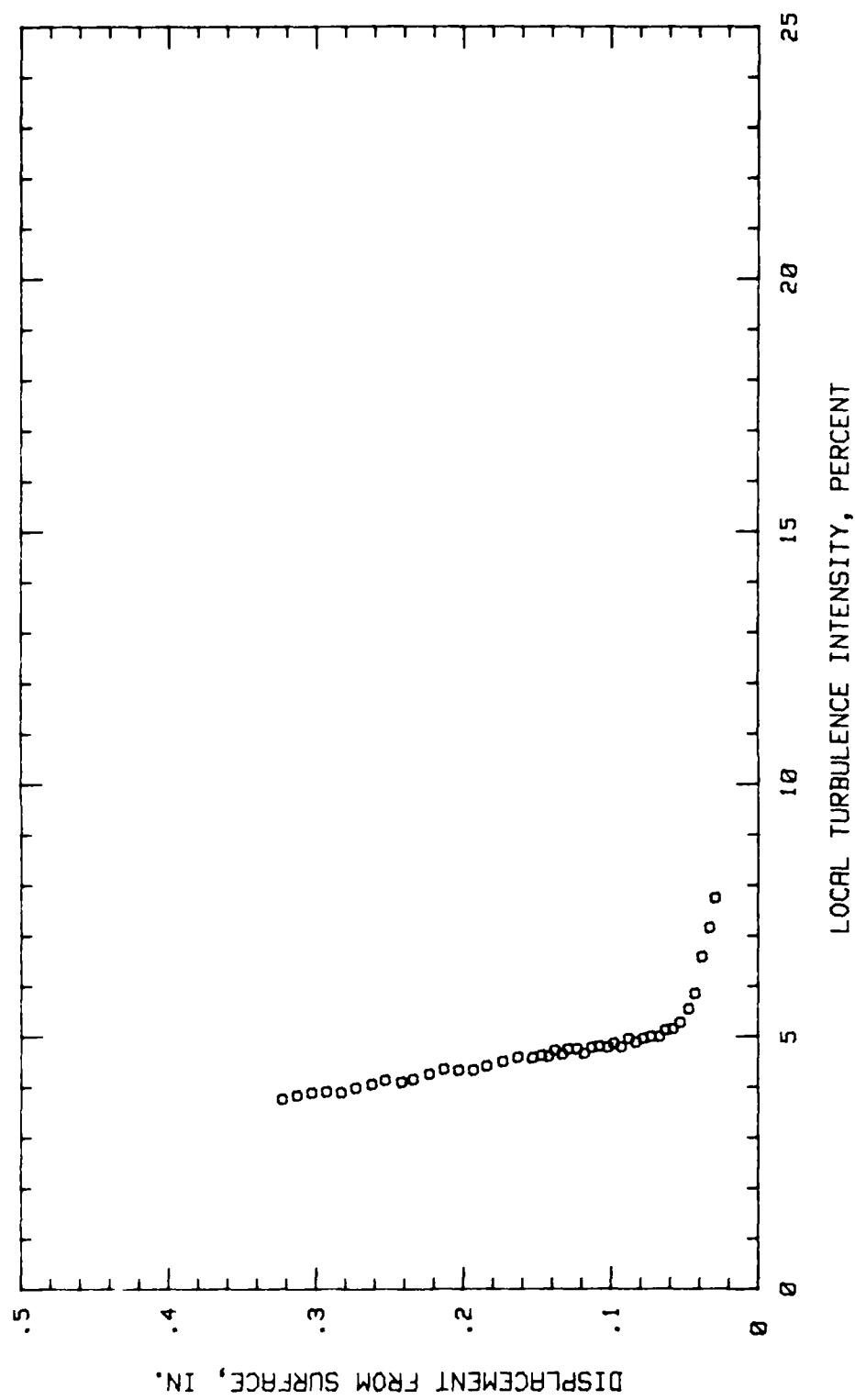


Fig. 192. Boundary Layer Turb. Intensity Profile, Conf. #3 at 40.62% Chord HIGH TURB

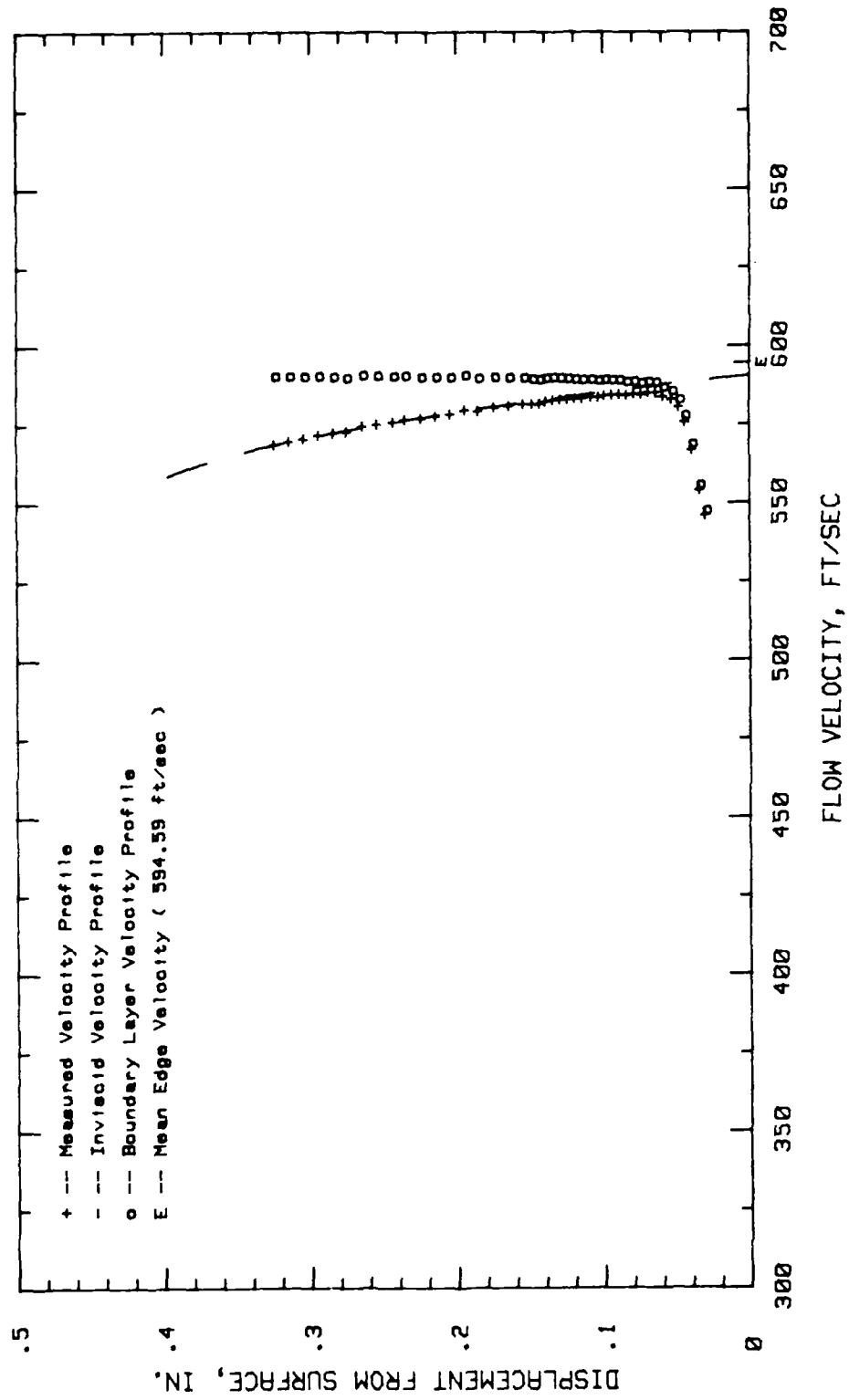


Fig.193.Boundary Layer Velocity Profiles, Conf.#3 at 45.31% Chord HIGH TURB.

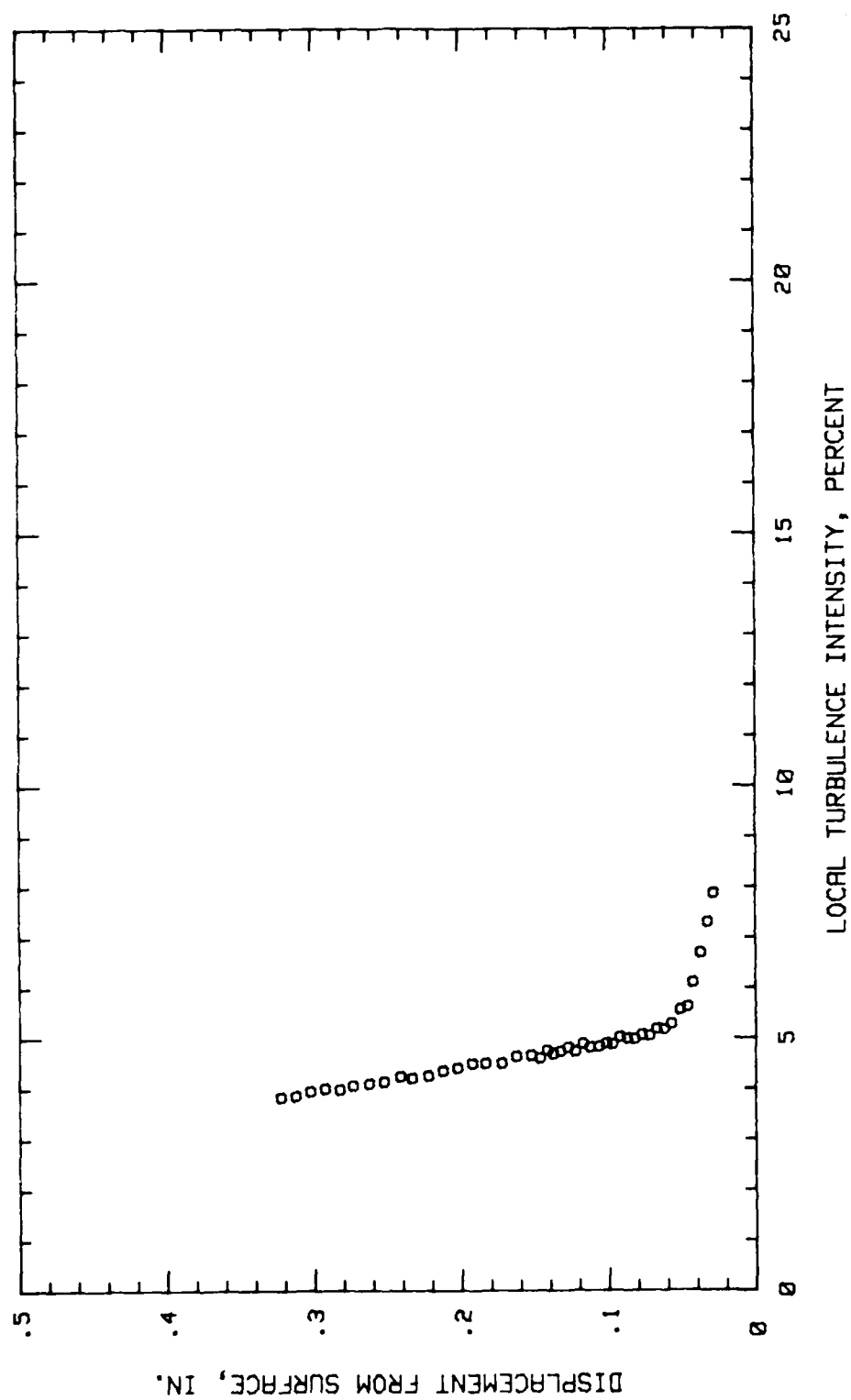


Fig.194. Boundary Layer Turb. Intensity Profile, Conf. #3 at 45.31% Chord HIGH TURB

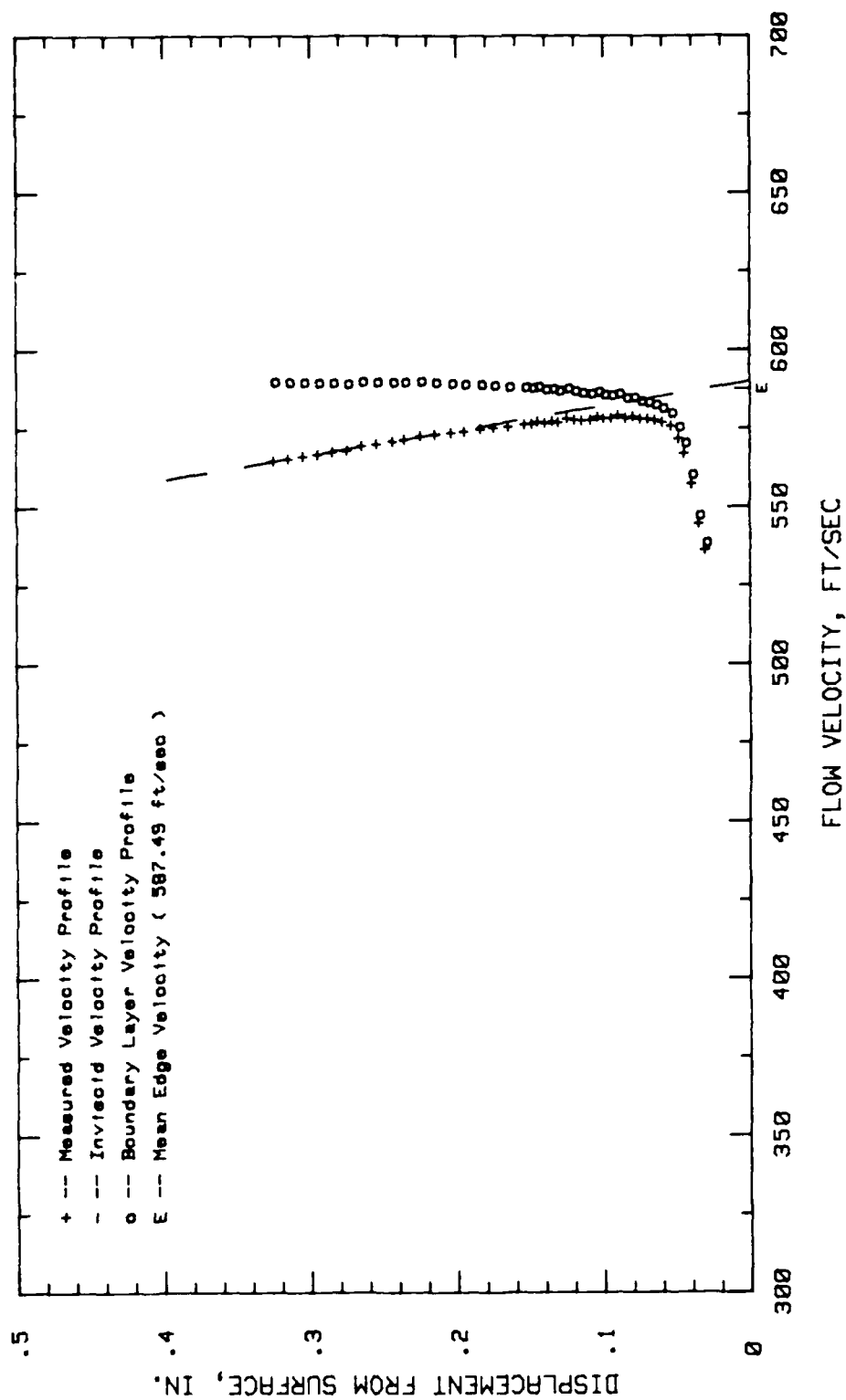


Fig.195.Boundary Layer Velocity Profiles, Conf.#3 at 50% Chord HIGH TURB.

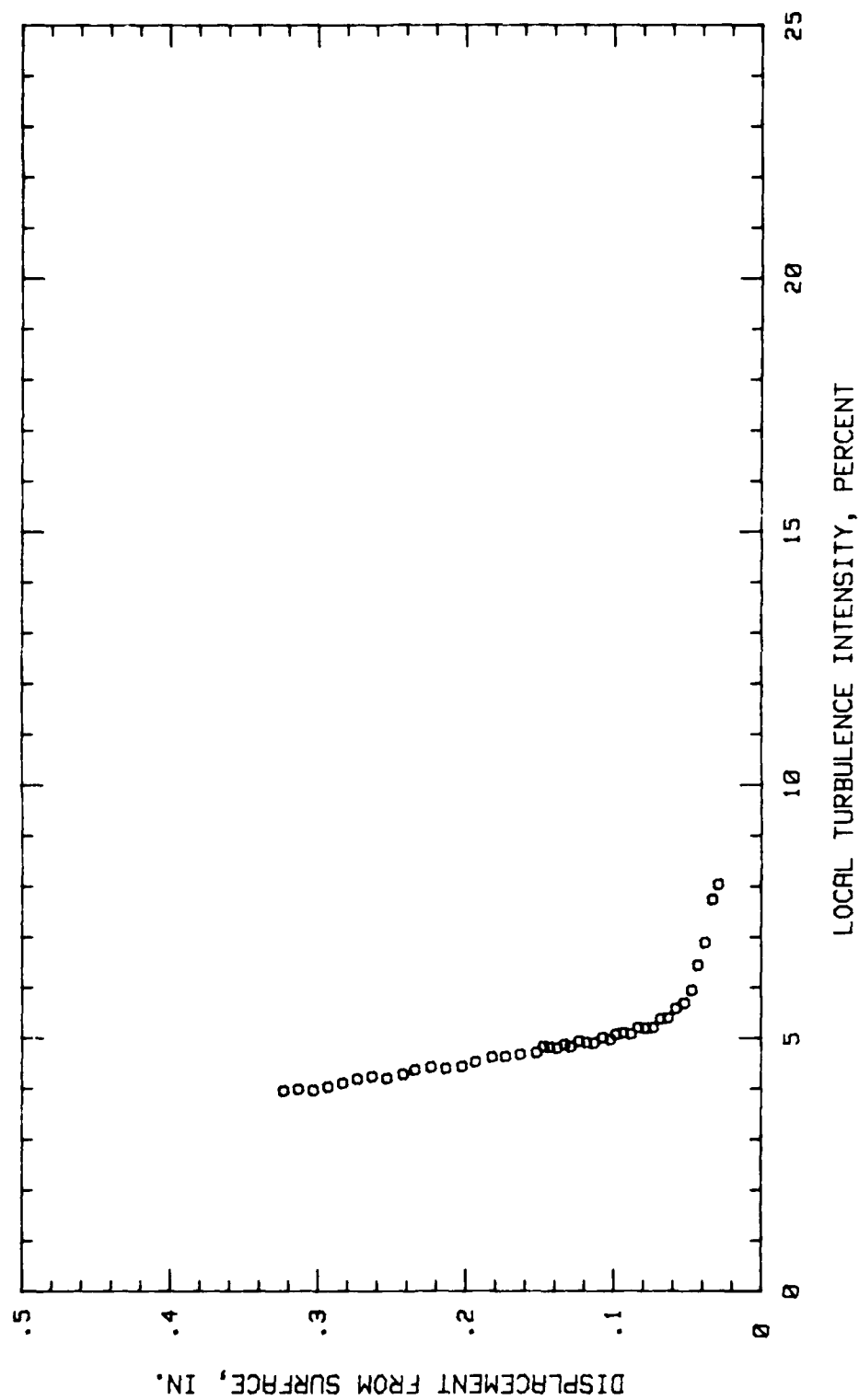


Fig.196.Boundary Layer Turb.Intensity Profile, Conf.#3 at 50% Chord HIGH TURB.

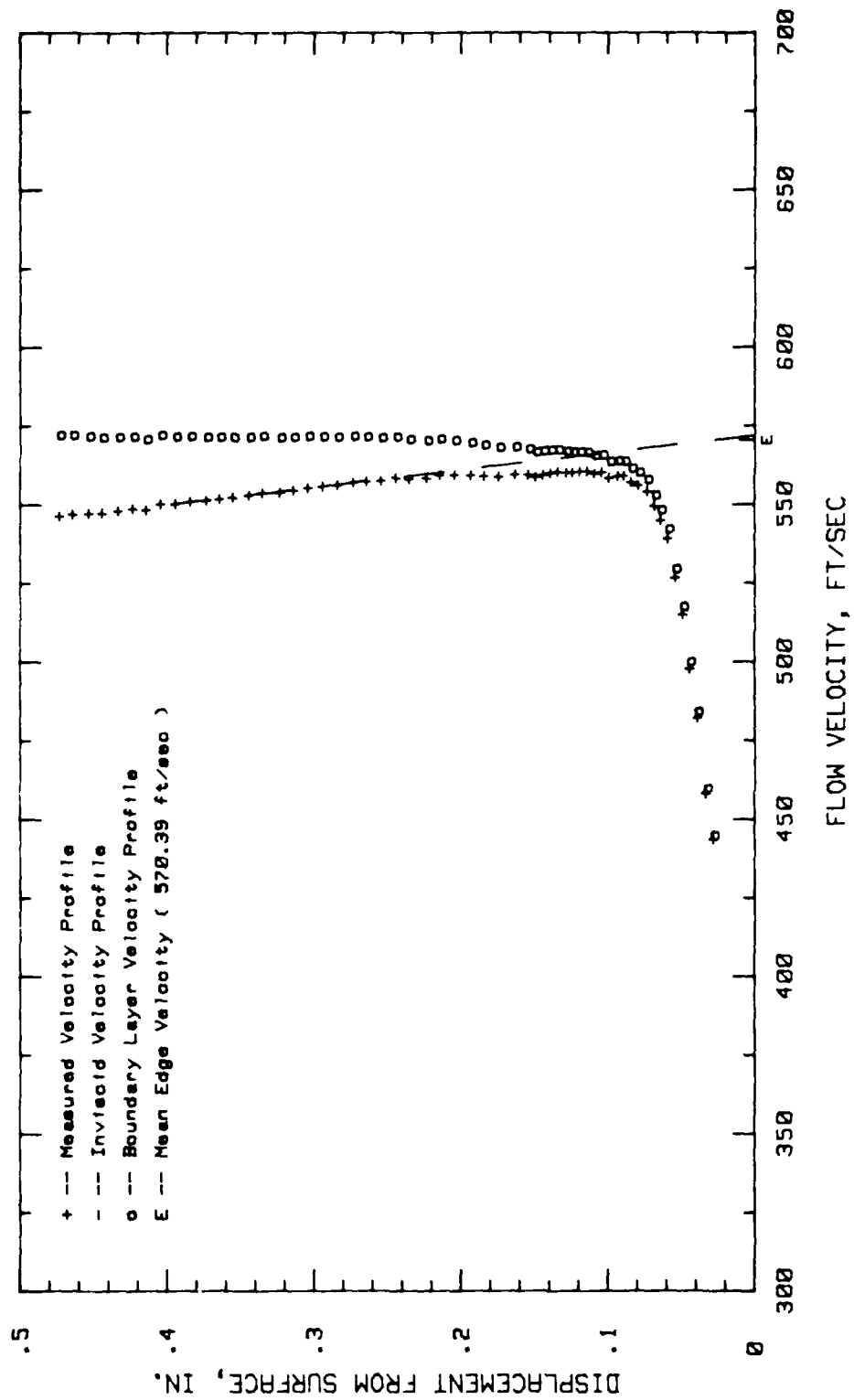


Fig.197. Boundary Layer Velocity Profiles, Conf.#3 at 65.62% Chord HIGH TURB.

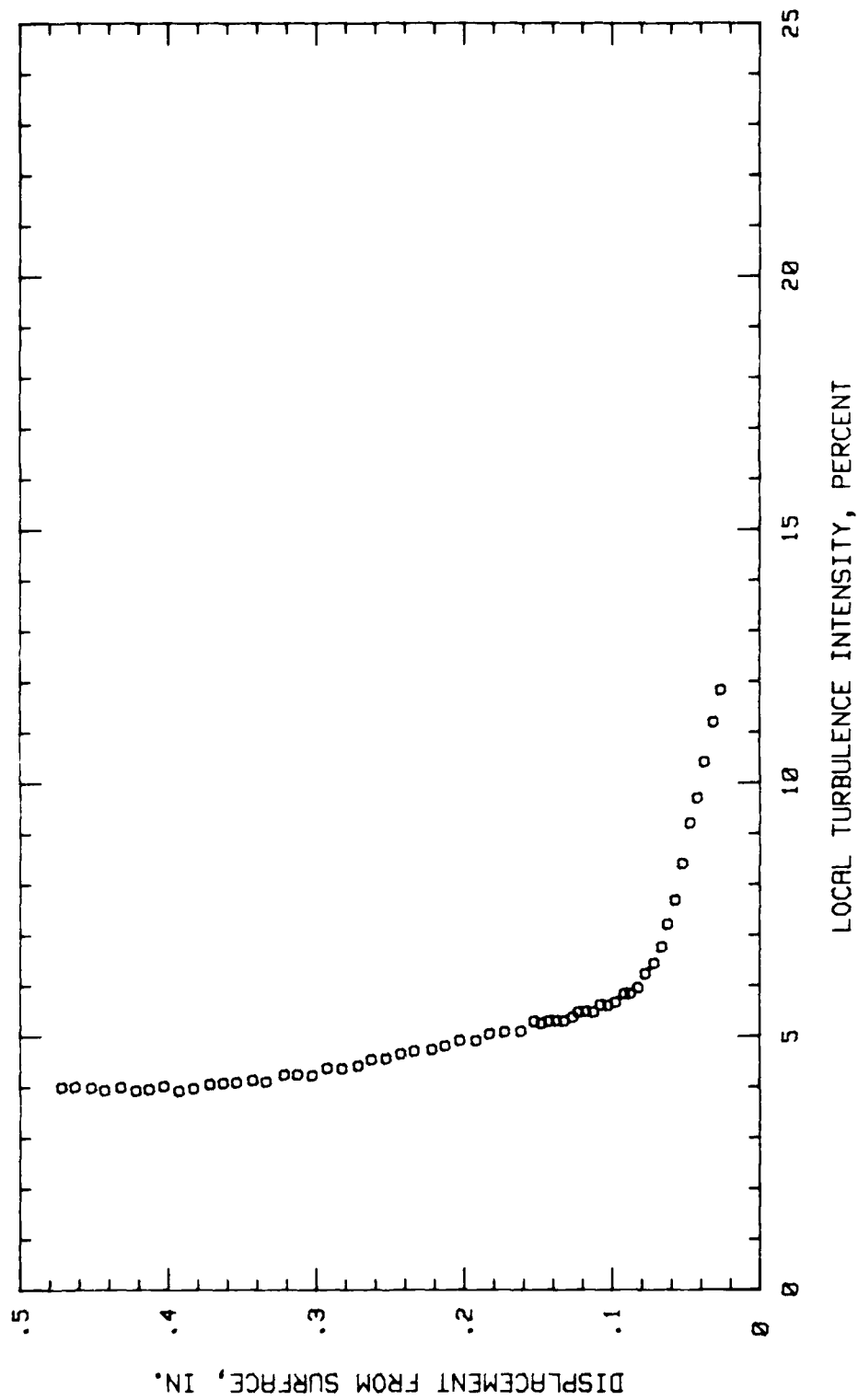


Fig.198.Boundary Layer Turb.Intensity Profile, Conf.#3 at 65.62% Chord HIGH TURB

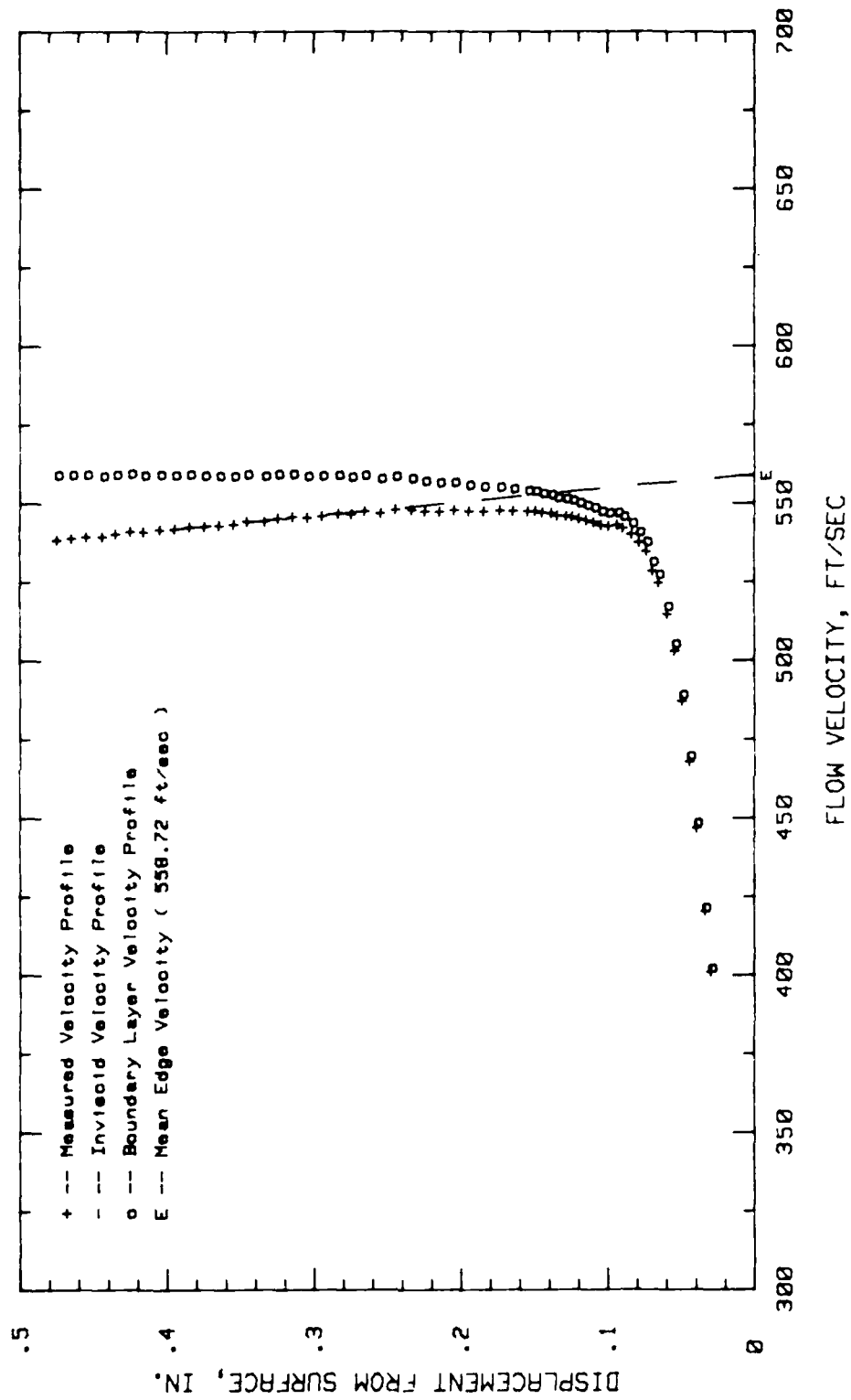


Fig.199. Boundary Layer Velocity Profiles, Conf.#3 at 70.31% Chord HIGH TURB.

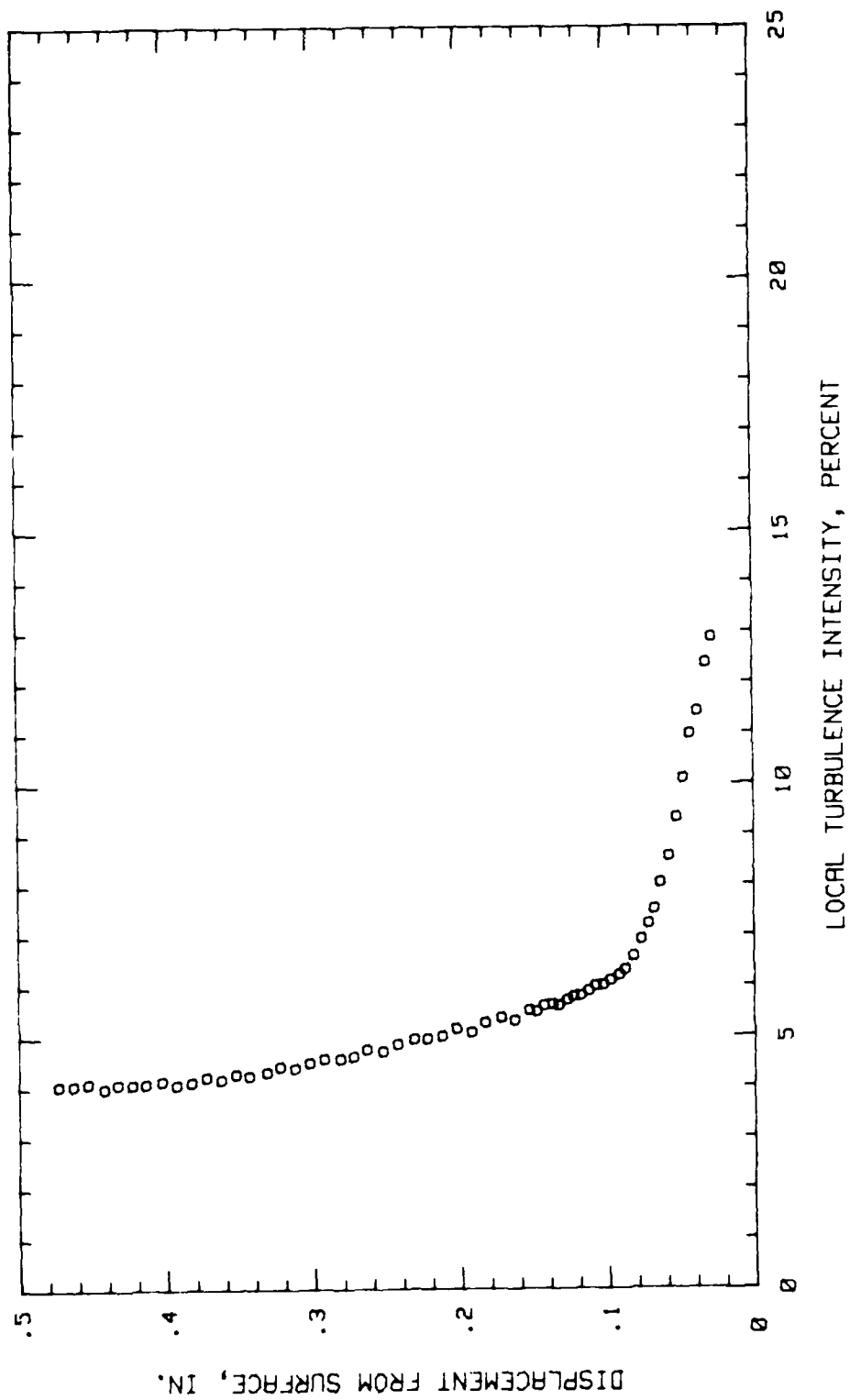


Fig.200.Boundary Layer Turb.Intensity Profile, Conf.#3 at 70.31% Chord HIGH TURB

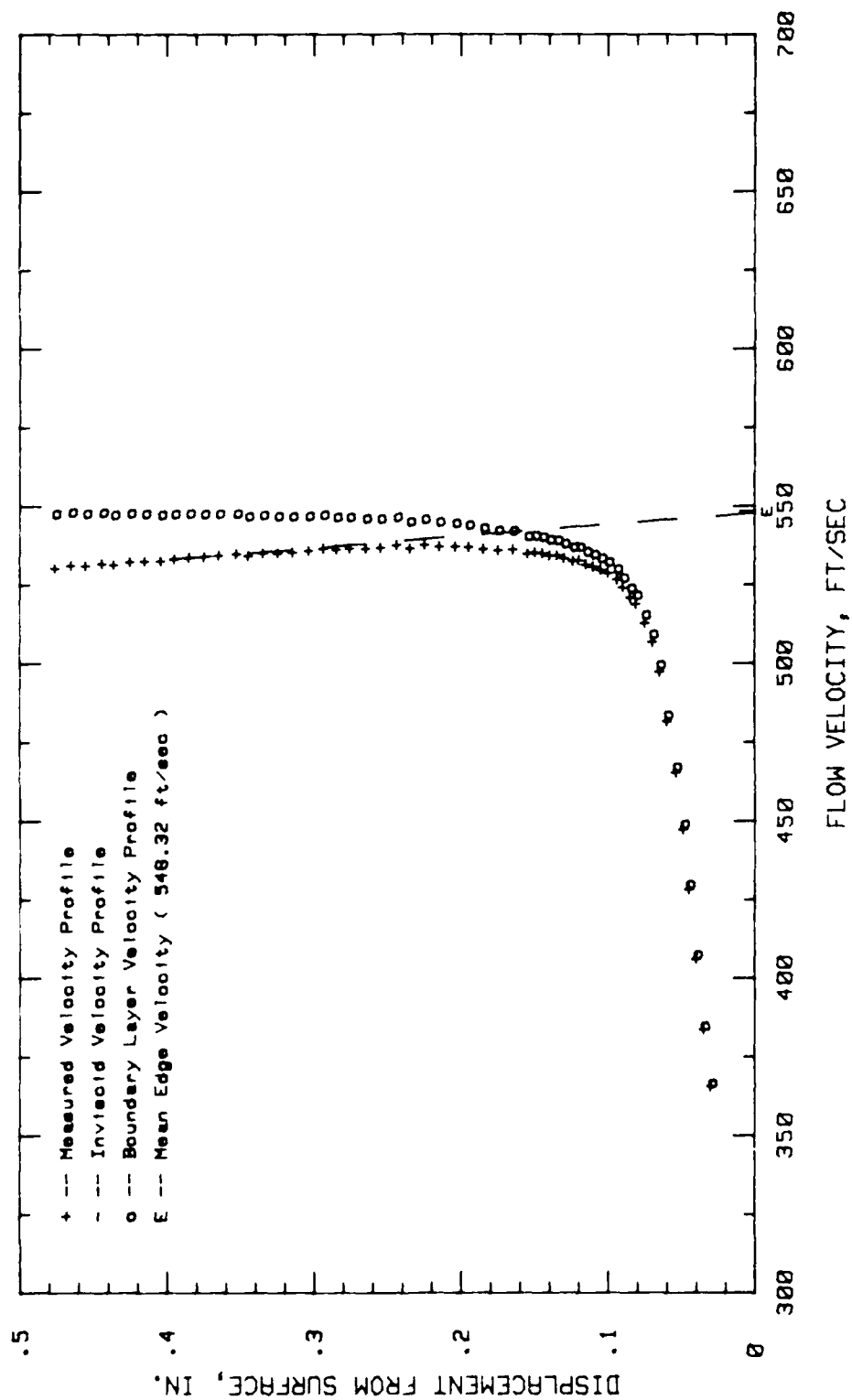


Fig.201. Boundary Layer Velocity Profiles, Conf.#3 at 75% Chord HIGH TURB.

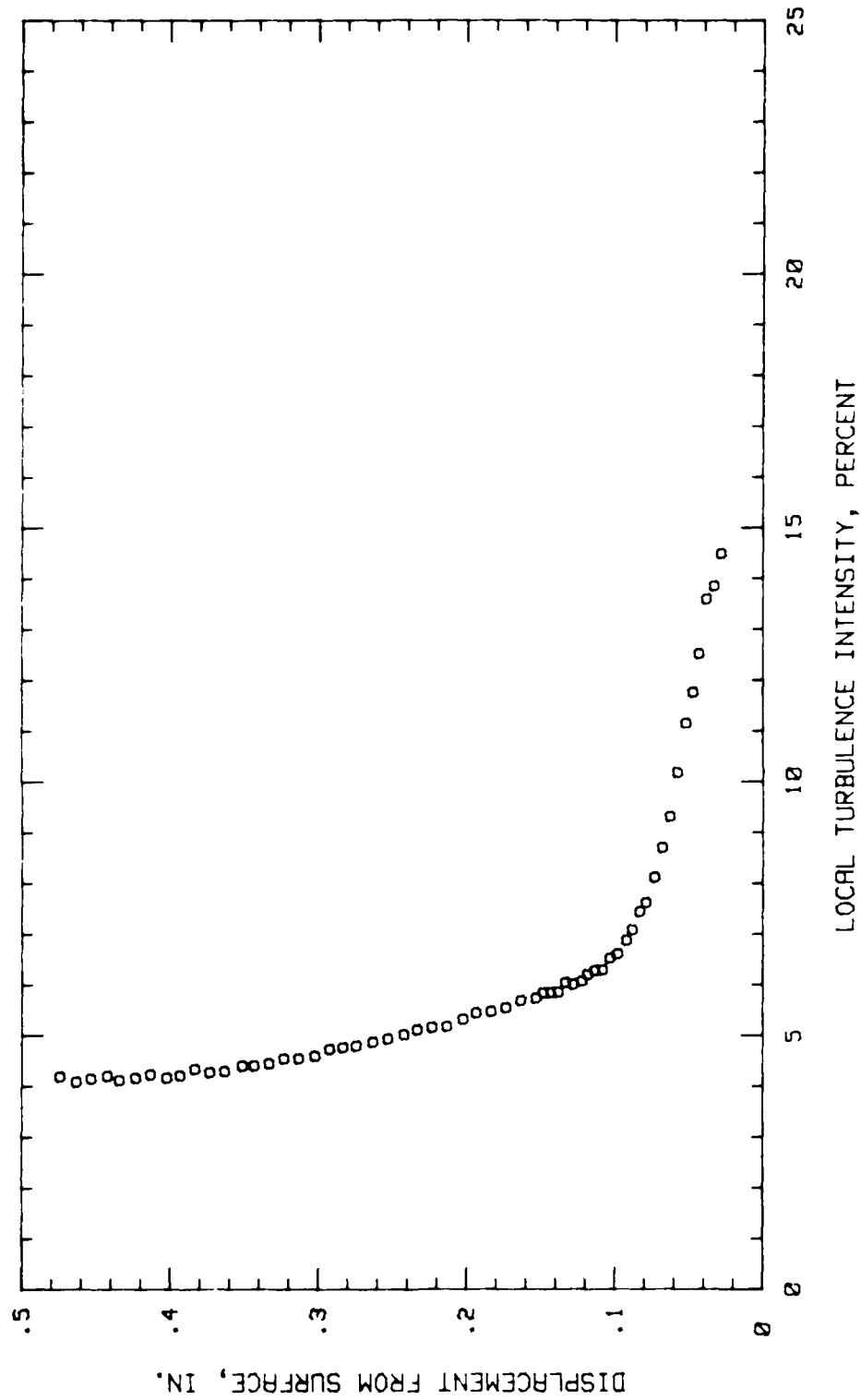


Fig.202.Boundary Layer Turb.Intensity Profile, Conf.#3 at 75% Chord HIGH TURB.

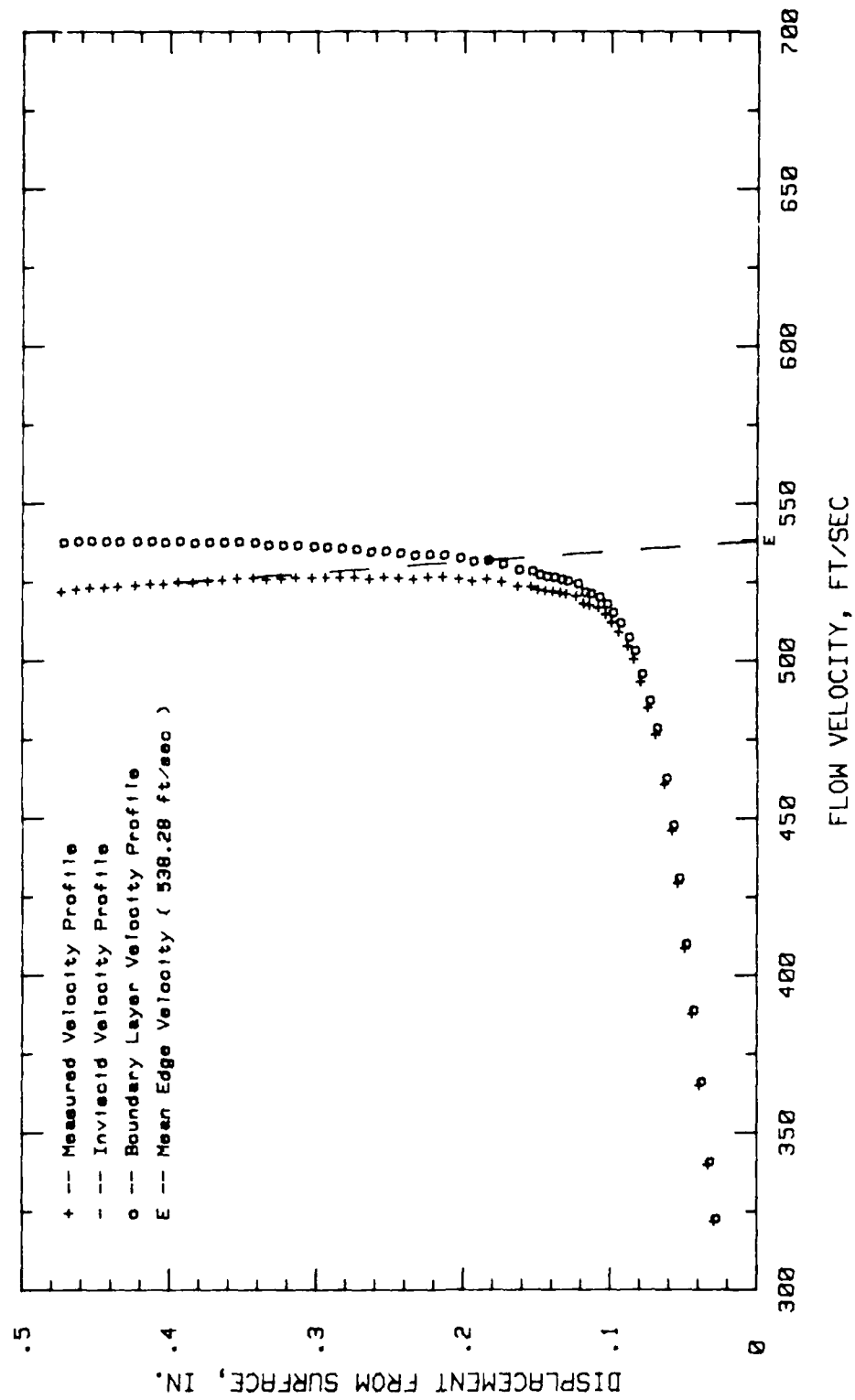


Fig.203. Boundary Layer Velocity Profiles, Conf.#3 at 79.68% Chord HIGH TURB.

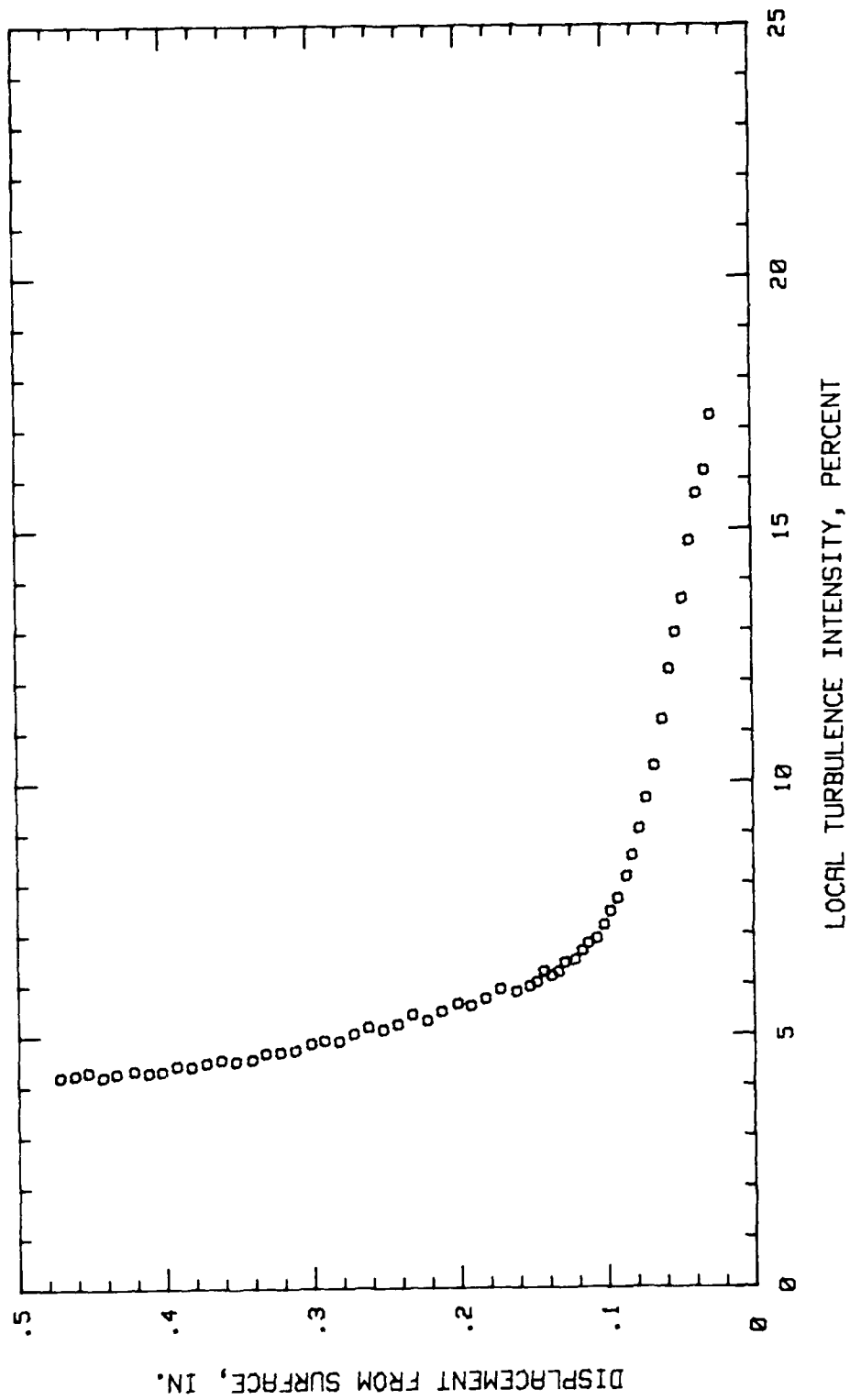


Fig.204. Boundary Layer Turb. Intensity Profile, Conf. #3 at 79.68% Chord HIGH TURB

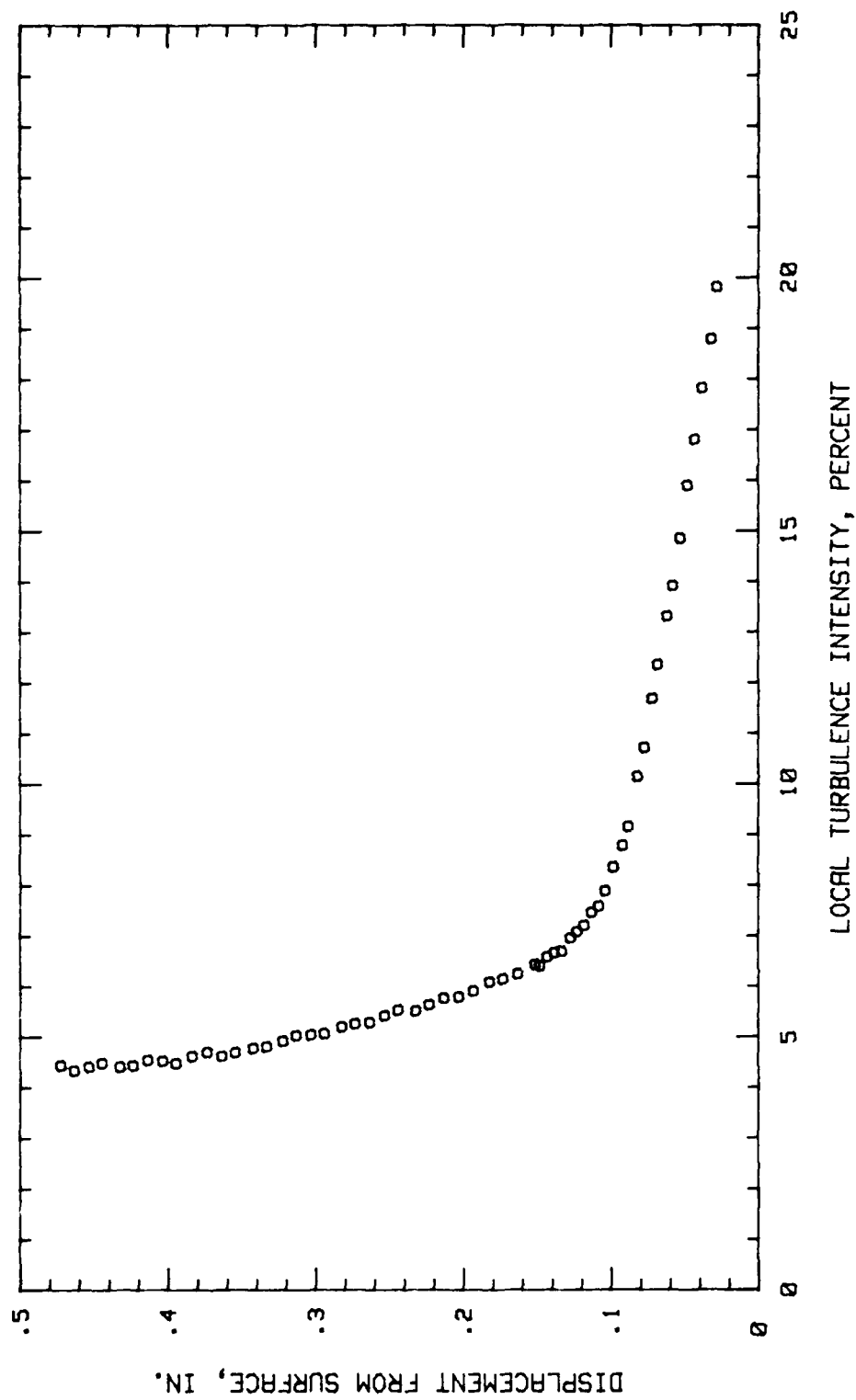


Fig.206.Boundary Layer Turb.Intensity Profile, Conf.#3 at 84.37% Chord HIGH TURB

Bibliography

1. Gostelow, J. P. Cascade Aerodynamics. New York: Pergamon Press, 1984.
2. Schlichting, H. and A. Das. "Flow Research On Blading," On the Influence of Turbulence Level on the Aerodynamic Losses of Axial Turbomachines. Edited by Lang S. Dzung. Baden, Switzerland: Brown, Boveri and Company Limited.
3. Poulin, Capt. J. Remy. Surface Roughness: Its Effects On The Performance Of A Two Dimensional Cascade. MS thesis, AFIT/GAE/AA/86D-13. School of Engineering, Air Force Institute of Technology (AU), Wright Patterson AFB OH, December 1986.
4. Williams, Capt. Larry D. Effects Of Surface Roughness On Pressure Distribution And Boundary Layer Over Compressor Blades At High Reynolds Number In A Two Dimensional Cascade. MS thesis, AFIT/GAE/AA/85D-17. School of Engineering, Air Force Institute of Technology (AU), Wright Patterson AFB OH, December 1985.
5. Tanis, 2Lt. Fredrick J., Jr. Roughness Effects On Compressor Blade Performance In Cascade At High Reynolds Number. MS thesis, GAE/AA/81D-2. School of Engineering, Air Force Institute of Technology (AU), Wright Patterson AFB OH, November 1983.
6. Lieblein, Seymour. "Experimental Flow In Two Dimensional Cascade," Aerodynamic Design Of Axial Flow Compressors (Revised), edited by Irving Johnson and Robert O. Bullock, Washington: NASA, 1965.
7. Lieblein, Seymour and William H. Roudebush. Low Speed Wake Characteristics Of Two Dimensional Cascade And Isolated Aerofoil Sections. Technical Note 3771, NACA, October 1956.
8. Scholz, Norbert. Aerodynamics Of Cascades, AG220. Neuilly sur seine, France: AGARD, 1977.
9. Deutsch, A. and N. Zierke. The Boundary Layer On Compressor Cascade Blades. NASA-CR-1735114: Semi-Annual Status Report, 1 December 1983 - June 1984.
10. Allison, Capt. Dennis M. Design And Evaluation Of A Cascade Test Facility. MS thesis GAE/AA/81D-2. School of Engineering, Air Force Institute of Technology (AU), Wright Patterson AFB OH, June 1982.

11. Moe, Capt. Gary P. Influence Of Surface Roughness On Compressor Blades At High Reynolds Number In A Two Dimensional Cascade. MS thesis GAE/AA/84D-19. School of Engineering, Air Force Institute of Technology, Wright Patterson AFB OH, December 1984.
12. Hewlett - Packard. 3052A Automatic Data Acquisition System Operating Instructions. Vol. 1A, undated.
13. Vincent, E. T. The Theory And Design Of Gas Turbines And Jet Engines. New York McGraw-Hill Book Company Incorporated, 1950.
14. Evans, R. L. The Effects Of Free Stream Turbulence On The Profile Boundary Layer and Losses In Compressor Cascade. New York: ASME, 1984.

VITA

Squadron Leader Salman Absar was born on 2nd December 1955 in Karachi, Pakistan. He received a Bachelor's degree in Aerospace Engineering from the University of Karachi in 1977. The same year, he was commissioned in the Pakistan Air Force. Since then, he has worked on various aircraft maintenance and management appointments in the Air Force and the Ministry of Defence. He is a member of the Pakistan Engineering Council.

Permanent address: FF3/31,
Sea View Township,
Defence Housing Authority,
KARACHI, PAKISTAN.

Unclassified

SECURITY CLASSIFICATION OF THIS PAGE

REPORT DOCUMENTATION PAGE

Form Approved
OMB No. 0704-0188

1a. REPORT SECURITY CLASSIFICATION Unclassified		1b. RESTRICTIVE MARKINGS	
2a. SECURITY CLASSIFICATION AUTHORITY		3. DISTRIBUTION/AVAILABILITY OF REPORT Approved for Public release; distribution unlimited.	
2b. DECLASSIFICATION/DOWNGRADING SCHEDULE			
4. PERFORMING ORGANIZATION REPORT NUMBER(S) AFIT/GAE/AA/88M-1		5. MONITORING ORGANIZATION REPORT NUMBER(S)	
6a. NAME OF PERFORMING ORGANIZATION School of Engineering.	6b. OFFICE SYMBOL (If applicable)	7a. NAME OF MONITORING ORGANIZATION	
6c. ADDRESS (City, State, and ZIP Code) Air Force Institute Of Technology, Wright Patterson AFB, Ohio 45433.		7b. ADDRESS (City, State, and ZIP Code)	
8a. NAME OF FUNDING/SPONSORING ORGANIZATION	8b. OFFICE SYMBOL (If applicable)	9. PROCUREMENT INSTRUMENT IDENTIFICATION NUMBER	
8c. ADDRESS (City, State, and ZIP Code)		10. SOURCE OF FUNDING NUMBERS	
		PROGRAM ELEMENT NO.	PROJECT NO.
		TASK NO.	WORK UNIT ACCESSION NO.
11. TITLE (Include Security Classification) See box 19 (Unclassified)			

12. PERSONAL AUTHOR(S)
Salman Absar, BEng. Sqn.Ldr.(Maj.), Pakistan Air Force.

13a. TYPE OF REPORT MS Thesis.	13b. TIME COVERED FROM _____ TO _____	14. DATE OF REPORT (Year, Month, Day) 1988, March	15. PAGE COUNT 280
-----------------------------------	--	--	-----------------------

16. SUPPLEMENTARY NOTATION

17. COSATI CODES			18. SUBJECT TERMS (Continue on reverse if necessary and identify by block number) Cascade Testing, Surface Roughness, Compressor blade pressure distribution, Boundary Layer, Turbulence.
FIELD	GROUP	SUB-GROUP	
21	05		

19. ABSTRACT (Continue on reverse if necessary and identify by block number)

Title: EFFECT OF FREESTREAM TURBULENCE ON A TWO DIMENSIONAL CASCADE, WITH AND WITHOUT SURFACE ROUGHNESS, AT HIGH REYNOLDS NUMBER.

Thesis Chairman: Dr. William C. Elrod.
Associate Professor of Aerospace Engineering.

Approved for public release; 18W AIR 280-17.
 Date of release: 21 May 88
 Distribution: unlimited
 Distribution Statement: Approved for public release; distribution unlimited.
 Work Unit: AFIT/ENY

20. DISTRIBUTION/AVAILABILITY OF ABSTRACT <input checked="" type="checkbox"/> UNCLASSIFIED/UNLIMITED <input type="checkbox"/> SAME AS RPT <input type="checkbox"/> DTIC USERS		21. ABSTRACT SECURITY CLASSIFICATION Unclassified	
22a. NAME OF RESPONSIBLE INDIVIDUAL Dr. William C. Elrod.		22b. TELEPHONE (Include Area Code) 513-255-3517	22c. OFFICE SYMBOL AFIT/ENY

DD Form 1473, JUN 86

Previous editions are obsolete.

SECURITY CLASSIFICATION OF THIS PAGE

Unclassified

Unclassified

The present study shows the effects of high freestream turbulence on the performance of a two dimensional cascade. The cascade consisted of seven NACA 65-A506 airfoils with two inches chord. Experiments were carried out at flow Reynolds number per foot in excess of two and a half million. Flow turbulence intensity of 7% was generated upstream of the cascade. Blades with three different categories of surface roughness were studied.

High freestream turbulence results in a decrease in total pressure loss coefficient in the cascade and an increase in the total pressure loss coefficient in the wake. The results also show an increase in pressure coefficient, over the suction surface, independent of the amount of surface roughness. The boundary layer thickness, after 50% chord, increases substantially, with an increase in freestream turbulence. This effect is aggravated with higher surface roughness. The effects of high freestream turbulence on boundary layer edge velocity are sensitive to local surface roughness. With low surface roughness, the boundary layer edge velocity increase with freestream turbulence. The results indicate an opposite effect when local surface roughness is increased.

Unclassified

END
DATE
FILMED

4-88
DTIC